# MOLECULAR INVESTIGATIONS INTO THE CATALYTIC MECHANISMS

# AND INHIBITION OF THE AMINOGLYCOSIDE RESISTANCE ENZYMES

# APH(3')-IIIa AND AAC(6')-APH(2")

David D. Boehr, B.Sc.

A Thesis

Submitted to the School of Graduate Studies

In Partial Fulfillment of the Requirements

For the Degree

Doctor of Philosophy

McMaster University

CATALYTIC MECHANISMS OF APH(3')-IIIa AND AAC(6')-APH(2")

DOCTOR OF PHILOSOPHY (2003)                    McMaster University
(Biochemistry)                                 Hamilton, Ontario


TITLE:              Molecular Investigations into the Catalytic Mechanisms
                    and Inhibition of the Aminoglycoside Antibiotic Resistance
                    Enzymes APH(3')-IIIa and AAC(6')-APH(2")

AUTHOR:             David Douglas Boehr, B.Sc. (University of Lethbridge)

SUPERVISOR:         Professor G.D. Wright

NUMBER OF PAGES:    214; i-xx

# Abstract

The golden age of antibiotics may be at an end. These compounds found clinical use in the 1940s, and their medical benefits were readily apparent, curing once fatal diseases and increasing life expectancy. However, bacteria have responded successfully to this threat by developing resistance to a multitude of antibiotics, and now, once treatable pathogens are again on the warpath. One of the classes of antibiotics to which resistance has arisen is the aminoglycoside aminocyclitols that specifically target the prokaryotic ribosome. The most clinically relevant form of aminoglycoside resistance is the expression of modifying enzymes, including APH(3')-IIIa and AAC(6')-APH(2") that catalyze the phosphorylation and/or acetylation of a wide range of aminoglycosides. Application of potent, specific inhibitors to these enzymes can provide a means of overcoming resistance, and a thorough understanding of these enzymes will aid in this endeavor. Towards this end, the molecular mechanisms of catalysis for aminoglycoside phosphorylation and acetylation have been investigated. Enzyme-catalyzed aminoglycoside phosphorylation likely operates through a dissociative-like mechanism where bond breakage predominates in the transition-state, similar to what is observed in the structurally similar serine/threonine protein kinase family, whereas aminoglycoside acetylation catalyzed by AAC(6')-APH(2") utilizes an active site base. Through these studies, a number of inhibitors have also been identified including wortmannin that specifically labels a highly conserved lysine in AAC(6')-APH(2"), 1-bromomethylphenanthrene that covalently modifies the acetyltransferase aspartate base in AAC(6')-APH(2"), and indolocidin, a peptide that inhibits a broad range of aminoglycoside resistance enzymes. The studies and molecules presented here will serve as the basis for the development of future inhibitors of these enzymes and the eventual triumph over aminoglycoside antibiotic resistance.

**Dedication**

I would like to dedicate this thesis to the loving memory of my parents, Margaret Rose (Oct 20, 1948 – June 24, 2000) and Douglas Wayne (August 23, 1946 – March 18, 2002). I am who I am because of them, because of their love, support and unwavering belief in me. My only hope is that I can be as good of a parent to my children as they were to me.

## Acknowledgements

First and foremost, I would like to thank my supervisor Gerry Wright for his patience, understanding and help during these past tumultuous five years. He let me have just enough space to explore my own ideas, however unconventional some of them may have been, while keeping me on task and my goals firmly set.

I would also like to thank the members of my lab, past and present, which have impacted both my science and my life. In particular, I would like to mention those people who most contributed to this thesis, including Denis Daigle, Kari-ann Draker, Steve Jenkins, Kalinka Koteva, Frank LaRonde and Paul Thompson. I would also especially like to thank Nicole Johnston for her friendship and support over the past few years. Furthermore, I would like to thank Raquel Epand for her technical support with ITC and CD, and Ricky Cox for the many discussions about APH(3')-IIIa and inhibitors. My time at McMaster would have been less successful without the input, support and critical analysis by my committee members: Eric Brown, Vettai Ananthanarayanan (Dr. Ananth) and Gerhard Gerber.

Finally, I would like to thank my beautiful wife (her name is Alyson) for all of her love and support. I could not have done any of this without her.

# Table of Contents

Aminoglycoside Resistance Enzymes

## Abbreviations

| | |
|---|---|
| **AAC** | - aminoglycoside acetyltransferase |
| **AANAT** | - arylalkylamine $N$-acetyltransferase |
| **ADP** | - adenosine diphosphate |
| **AGRP** | - aminoglycoside resistance profile |
| **AMP** | - aminoglycoside monophosphate |
| **AMPPNP** | - adenylyl imidodiphosphate |
| **ANT** | - aminoglycoside nucleotidyltransferase |
| **APH** | - aminoglycoside phosphotransferase |
| **ATP** | - adenosine triphosphate |
| **CD** | - circular dichroism (spectroscopy) |
| **CFU** | - colony forming units |
| **CoA** | - coenzyme A |
| **DMSO** | - dimethyl sulfoxide |
| **EDPI** | - energy dependent phase I (of aminoglycoside entry) |
| **EDPII** | - energy dependent phase II (of aminoglycoside entry) |
| **EDTA** | - $N, N, N', N'$- ethylenediaminetetraacetic acid |
| **ePKs** | - eukaryotic protein kinases |
| **Fmoc** | - $N$-(9-fluorenyl)methoxy carbonyl |
| **FPLC** | - fast performance liquid chromatography |
| **FSBA** | - 5'-[$p$-(fluorosulfonyl)benzoyl]adenosine |
| **HCK** | - hemopoietic cell kinase |

| | |
|---|---|
| **Gent$^R$** | - gentamicin resistance |
| **GNA1** | - glucosamine 6-phosphate *N*-acetyltransferase |
| **GNAT** | - GCN5-related N-acetyltransferases |
| **GTP** | - guanosine triphosphate |
| **H9** | - *N*-(2-aminoethyl)-5-isoquinonline sulfonamide |
| **HAT1** | - histone acetyltransferase 1 |
| **HEPES** | - *N*-(2-hydroxyethyl)piperazine-*N'*-2-ethanesulfonic acid |
| **HPLC** | - high performance liquid chromatography |
| **IC$_{50}$** | - concentration of inhibitor that gives 50% inhibition of activity |
| **ITC** | - isothermal titration calorimetry |
| **IPTG** | - isopropyl-β-D-thiogalactopyranoside |
| **Kan$^R$** | - kanamycin A resistance |
| **LB** | - Luria-Bertani (broth) |
| **MALDI-TOF** | - matrix assisted laser desorption time-of-flight(mass spectrometry) |
| **MES** | - 2-(*N*-morpholino)ethanesulfonic acid |
| **MIC** | - minimum inhibitory concentration |
| **MOPS** | - 3-(*N*-morpholino)-propanesulfonic acid |
| **MPLC** | - medium pressure liquid chromatography |
| **mRNA** | - messenger RNA |
| **MS** | - mass spectra |
| **mut** | - mutant |
| **NADH** | - nicotinamide adenine dinucleotide (reduced form) |

| | |
|---|---|
| **NMR** | - nuclear magnetic resonance |
| **NPL** | - nucleotide positioning loop |
| **OD** | - optical density |
| **OppA** | - oligopeptide binding protein A |
| **PCR** | - polymerase chain reaction |
| **PDB** | - protein data bank |
| **PG1** | - protegrin 1 |
| **PI 3-kinase** | - phosphatidylinositol 3-kinase |
| **PK/LDH** | - pyruvate kinase/ lactate dehydrogenase |
| **PMF** | - proton motive force |
| **RNA** | - ribonucleic acid |
| **rRNA** | - ribosomal RNA |
| **SDS-PAGE** | - sodium dodecyl sulfate- polyacrylamide gel electrophoresis |
| **SIE** | - solvent isotope effect |
| **SVE** | - solvent viscosity effect |
| **tRNA** | - transfer RNA |
| **WT** | - wild-type |

# List of Figures

xvi

# List of Tables

## Personal Publications

1. **Boehr, D.D., Draker, K.-a., Wright, G.D. 2003.** *Aminoglycoside and aminocyclitols* in <u>Antibiotic and Chemotherapy: Anti-infective agents and their use in therapy</u>. (Eds. Finch, R.G., Greenwood, D., Norrby, S.R. and Whitley, R.J.) Churchill Livingstone, Edingburgh, 155-184.

2. **Boehr, D.D., Jenkins, S.I. and Wright, G.D. 2003.** The molecular basis of the expansive substrate specificity of the antibiotic resistance enzyme AAC(6')-APH(2"): The role of Asp99 as an active site base important for acetyltransfer, *J. Biol. Chem.*, 278: 12873-12880.

3. **Boehr, D.D., Draker, K.-a., Koteva, K., Bains, M., Hancock, R.E. and Wright, G.D. 2003.** Broad-spectrum peptide inhibitors of aminoglycoside antibiotic resistance enzymes. *Chem. Biol.*, 10: 189-196.

4. **Draker, K.-a., Boehr, D.D., Elowe, N.H., Noga, T.J. and Wright, G.D. 2003.** Functional annotation of putative aminoglycoside antibiotic modifying proteins in *Mycobacterium tuberculosis H37Rv*. *J. Antibiotics*, 56: 135-142.

5. **Boehr, D.D., Farley, A.R., Wright, G.D. and Cox, J.R. 2002.** Analysis of the $\pi$–$\pi$ stacking interactions between the aminoglycoside antibiotic kinase APH(3')-IIIa and its nucleotide ligands. *Chem. Biol.*, 9: 1209-1217.

6. **Thompson, P.R., Boehr, D.D., Berghuis, A.M. and Wright, G.D. 2002.** Mechanism of aminoglycoside antibiotic kinase APH(3')-IIIa: role of the nucleotide positioning loop. *Biochemistry*, 41: 7001-7007.

7. **Boehr, D.D., Lane, W.S. and Wright, G.D. 2001.** Active site labeling of the gentamicin resistance enzyme AAC(6')-APH(2") by the lipid kinase inhibitor wortmannin. *Chem. Biol.*, 8: 791-800.

8. **Boehr, D.D., Thompson, P.R. and Wright, G.D. 2001.** Molecular mechanism of aminoglycoside antibiotic kinase APH(3')-IIIa: roles of conserved active site residues. *J. Biol. Chem.*, 276: 23929-23936.

9. **Sucheck, S.J., Wong, A.W., Koeller, K.M., Boehr, D.D., Draker, K.-a., Sears, P., Wright, G.D., Wong, C.-H. 2000.** Design of bifunctional antibiotics that target bacterial rRNA and inhibit resistance-causing enzymes. *J. Am. Chem. Soc.*, 122, 5230-5231.

10. **Weselake, R.J., Kazala, E.C., Cianflone, K., Boehr, D.D., Middleton, C.K., Rennie, C.D., Laroche, A. and Recnik, I. 2000.** Human acylation stimulating protein enhances triacylglycerol biosynthesis in plant microsomes. *FEBS Lett.*, 481, 189-192.

# Chapter 1.

# Introduction

## 1.1 The Biological Arms Race

The age of the Earth has been estimated to be 4.5 billion years, where animal life only appeared around 600 million years ago (Campbell, 1993). However, even prior to this time, the earth and the oceans were teeming with bacterial life. Cellular life is thought to have first arrived 3.5 billion years ago, and spread across the globe (Campbell, 1993). New species evolved in the midst of competition for limiting resources, developing more efficient methods to utilize their supplies, new ways to utilize novel nutrients, or abilities and attributes that allowed them to survive where other organisms could not. The introduction of multicellular plants and animals provided even more materials and environments for microbes to take advantage.

Competition among bacteria can take more aggressive forms. For example, some species synthesize and export chemicals that are toxic to other microbial organisms. These bacterially produced toxins, or 'antibiotics', are generally complex molecules that target essential cellular functions, including replication, DNA synthesis (e.g. novobiocin), transcription (e.g. rifampin), translation (e.g. aminoglycosides) and cellular integrity (e.g. β-lactams) (Table 1.1) (Walsh, 2003). It is important that the antibiotic-producers do not commit suicide while producing these toxic compounds, and so, they have developed a number of self-protection mechanisms (Walsh, 2003). Some of these defense mechanisms have been transferred and/or utilized by the bacterial targets of the antibiotics, essentially resulting in a 'biological arms race' among bacteria with the dual progression of preservation mechanisms and the introduction of newer antibiotics to overcome these mechanisms that has continued over many millennia.

**Table 1.1:** Antibiotics: Classes, Targets and Resistance Mechanisms[a]

| Class | Example | Target | Producing Organism | Resistance mechanism |
|---|---|---|---|---|
| Aminoglycosides | Gentamicin | Ribosome, initation complex/ translocation | *Micromonospora purpurea* | Aminoglycoside modifying enzymes |
| β-lactams | Penicillin G | Cell wall, transpeptidase | *Penicillium chrysogenum* | β-lactamases |
| Chloramphenicol | Chloramphenicol | Ribosome, peptidyl transferase | *Streptomyces venezualae* | Chloramphenicol acetyltransferase |
| Fusidanes | Fusidic acid | Ribosome, elongation factor G | *Fusidium coccineum* | EF G mutations, barrier |
| Glycopeptides | Vancomycin | Cell wall, acyl-D-alanyl-D-alanine | *Amycolatopsis orientalis* (*Streptomyces orientalis*) | Reprogramming of D-Ala-D-Ala to D-Ala-D-Lac |
| Lincosamides | Lincomycin | Ribosome | *Streptomyces lincolnensis* | Ribosomal mutation, inactivating enzyme |
| Macrolides | Erythromycin A | Ribosome, translocation | *Saccharopolyspora erythraea* | rRNA methylation, efflux |
| Oxazolidinones | Linezolid | Ribosome, 70S initiation complex | Synthetic | Ribosomal mutations |
| Quinolones | Ciprofloxacin | DNA gyrase | Synthetic | Gyrase mutations |
| Rifamycins | Rifampin | RNA polymerase | *Amycolatopsis mediterranei* | Polymerase mutation |
| Streptogramins | Pristinamycin | Ribosome | *Streptomyces pristinaespiralis* | Ribosomal modification, modifying enzymes |
| Sulfonamides | Sulfadiazine | Folate synthesis | Synthetic | Altered dihyrdopteroate synthetase |
| Tetracyclines | Tetracycline | Ribosome, A site | *Streptomyces aureofaciens* | Drug efflux |

[a] information compiled from (Greenwood *et al.*, 2003)

3

**1.2 The Antibiotic Era**

One of the great realizations of 19th century science encompassed the microbial theory of disease championed by Louis Pasteur, which held that many diseases were caused by microscopic living agents (Levy, 1992). The theory gave impetus to the discovery of bacterial species that gave rise to specific diseases, and later, this knowledge was utilized in the development of vaccines using attenuated pathogens (Miller, 2000). Paul Ehrlich's "magic bullet", Salvarsan, for syphilis, caused by the bacterium *Treponema pallidum*, demonstrated that a rational chemical approach could complement this biological tactic to treat bacterial infection and eventually led to the successful search for similarly capable synthetic compounds, including sulfanilamide (Levy, 1992).

With the new insight into bacterial disease and an early appreciation of the competitive pressures among microbes, the stage was set for the discovery of penicillin by Alexander Fleming in 1928 (Shnayerson and Plotkin, 2002). Fleming realized that yellow mold colonies on an agar plate of staphylococcus were killing the bacterial colonies, and afterward identified penicillin as the bacterial killing agent (Shnayerson and Plotkin, 2002). This study provided one of the first insights into the chemical warfare between microbial species and supported the search for additional antimicrobial agents among the microbes themselves.

There was subsequently a large cataloging of various microbiological samples, first performed by Rene Dubos and colleagues when they discovered the antibiotic tyrothricin (or gramicidin) that successfully treated mice infected with pneumococci (Levy, 1992). A talk by Dubos on his discovery drew his former supervisor Selman A.

Waksman towards searching the soil for more antimicrobial compounds, eventually leading to the isolation of the first aminoglycoside, streptomycin, from *Streptomyces griseus* in 1944 (Miller, 2000).

Streptomycin was the first antibiotic that could successfully treat *Mycobacterium tuberculosis*, the causative agent of tuberculosis, and was a major step forward in improving life expectancy and the quality of life (Miller, 2000). In fact, each new implementation of antibiotic chemotherapy has led to a decrease in mortality rates due to bacterial infection, and with the rapid growth of the antibiotic field, led some to believe that bacteria no longer posed a threat to human health (Levy, 1992; Shnayerson and Plotkin, 2002).

However, even Fleming himself cautioned against the imprudent use of antibiotics and demonstrated that resistance to the new miracle drug, penicillin, could arise (Levy, 1992), which led researchers such as Dubos to stop his own research into naturally occurring antimicrobials (Miller, 2000). Humans have stepped into the 'biological arms race' very late in its millennia-old progress, and so, it may not be surprising that under the intensive selection pressure of antibiotic use, the introduction of resistance mechanisms into once treatable pathogens has led to the resurgence of their threat to human life (Levy, 1992; Shnayerson and Plotkin, 2002). The threat has grown to epidemic proportions where even last resort drugs, such as vancomycin, fail to elicit their effect, in the case of serious enterococcal and staphylococcal infections (Shnayerson and Plotkin, 2002).

At present, we may be under-equipped to deal with the renewed microbial problem. The recent introduction of new antibiotic classes has even met with fear that it is only a matter of time before resistance surfaces to even these novel compounds (Shnayerson and Plotkin, 2002). A clearer understanding of antibiotics and resistance mechanisms, together with more prudent use of antibiotics, will help to ensure that we stay one step ahead of bacteria. This thesis deals specifically with aminoglycoside aminocyclitol antibiotics and associated resistance mechanisms, and addresses potential routes to overcoming aminoglycoside resistance.

## 1.3 Aminoglycosides

### 1.3.1   Aminoglycoside Structure

Waksman and colleagues were one of the initial groups that screened thousands of organic samples in hopes of "unearthing" the next penicillin, leading to the discovery of aminoglycosides such as streptomycin (Schatz *et al.*, 1944) and neomycin (Waksman and Lechevalier, 1949). Kanamycin was isolated from *Streptomyces kanamyceticus* in 1957 (Greenwood, 2003). These three antibiotics, streptomycin, neomycin and kanamycin, are representatives of the three structural classes of aminoglycosides (Figure 1.1). All of the aminoglycosides share a central aminocyclitol ring around which various positions are derivatized to produce distinct drugs. The kanamycin group is substituted at the 4- and 6-positions of a central 2-deoxystreptamine ring, whereas the neomycin group is substituted at the 4- and 5- positions of the same ring system (Figure 1.1). The third group includes streptomycin and is basically a loose collection of compounds that do not fit into the first

two groups. The modifying enzymes dealt with in this thesis only inactivate the first two

groups, so discussion will be limited to the kanamycin and neomycin groups. For these

two groups, the 6-aminohexose ring linked to position 4 of the 2-deoxystreptamine ring is

designated as the prime (') ring and the hexose or pentose attached to position 5 or 6 is

identified as the double prime (") ring (Figure 1.1).

Most of the important aminoglycosides are natural products purified from

producing organisms such as *Streptomyces*, *Micromonospora* and *Bacillus*, among others,

although a few, such as amikacin, netilmicin and isepamicin, are semi-synthetic

derivatives of other aminoglycoside antibiotics (Wright *et al.*, 1998).
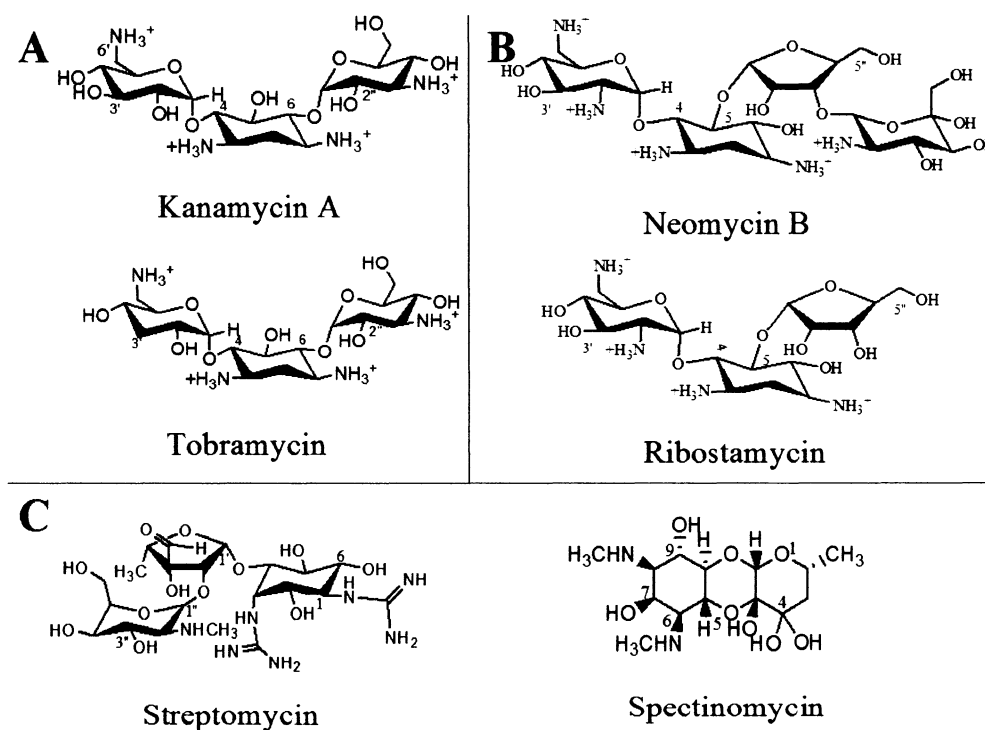


**Figure 1.1:** Structures of Representative Aminoglycosides from the 4,6-
Disubstituted/Kanamycin (A), 4,5- Disubstituted/Neomycin (B) and Miscellaneous (C)
Classes.

**1.3.2 Aminoglycoside Entry**

Aminoglycoside entry is a multi-phasic event, where firstly, the highly positively charged antibiotic crosses the outer membrane and periplasmic space in Gram negative organisms or the cell wall assembly of Gram positive organisms before it binds to the exterior of the cell membrane through electrostatic forces (Davis, 1987; Hancock, 1981; Wright *et al.*, 1998). After the very rapid initial binding, there appears to be at least two additional energy dependent phases (Hancock, 1981). The first phase (EDPI) is a much slower phase where a small amount of aminoglycoside gains entry to the cells. This phase appears to be highly dependent on the bacterial electron transport system (Bryan and Van den Elzen, 1976; Bryan and Van Den Elzen, 1977; Hancock, 1981; Miller *et al.*, 1980). The proton motive force (PMF) generated by the electron transport system also appears to be critical considering that uncouplers such as 2,4-dinitrophenol and carbonyl cyanide m-chlorophenol hydrazone that dissipate the PMF also inhibit aminoglycoside uptake (Bryan and Van den Elzen, 1976; Bryan and Van Den Elzen, 1977; Hancock, 1981; Miller *et al.*, 1980).

The second phase, termed energy dependent phase II (EDPII), is unique to aminoglycoside sensitive bacteria. Resistant bacteria continue to show a low level of aminoglycoside uptake according to EDPI, but do not show the much increased uptake characteristic of EDPII (Hancock, 1981).

Considering that aminoglycosides are highly positively charged compounds, there are questions regarding how such a chemical species could cross the hydrophobic component of the cell membrane. There is some evidence that, at least in *E. coli*, the

oligopeptide binding protein (OppA), the periplasmic component of the major oligopeptide transport system, may play an important role in aminoglycoside uptake as mutants with reduced OppA expression are resistant to aminoglycosides (Acosta *et al.*, 2000; Kashiwagi *et al.*, 1992; Kashiwagi *et al.*, 1998). However, although OppA may be involved in some capacity, it is not known whether it has a direct or indirect effect on aminoglycoside transport.

### 1.3.3   Mode of Action

Most of the aminoglycosides are bactericidal and bind similarly to the 30S prokaryotic ribosomal subunit, where they exert their major effect. The bacterial ribosome was first suggested to be the site of action through *in vivo* experiments demonstrating a marked decrease in protein synthesis following treatment of cells with aminoglycosides, and *in vitro* experiments on bacterial extracts showing that aminoglycoside treatment resulted in repression of both initiation and elongation in protein synthesis (Tai *et al.*, 1978; Tai *et al.*, 1973; Wallace *et al.*, 1973). Aminoglycosides can both slow elongation and cause mistranslation, while also interfering with the formation of initiation complexes to prevent free ribosomes from entering the chain elongation phase (Tai *et al.*, 1978; Tai *et al.*, 1973; Wallace *et al.*, 1973).

Chemical footprinting studies and careful correlation analysis of ribosomal mutation with aminoglycoside resistance implicated specific ribosomal proteins and the the tRNA binding site (A-site) of the 16S rRNA, as the most important determinants of aminoglycoside binding and action (Birge and Kurland, 1969; Leclerc *et al.*, 1991;

Moazed and Noller, 1987; Montandon *et al.*, 1986; Ozaki *et al.*, 1969; Schatz *et al.*, 1973;

Sigmund *et al.*, 1984; Woodcock *et al.*, 1991). Solution structures of aminoglycosides

and a 27-nucleotide portion of the 16S rRNA (Fourmy *et al.*, 1996; Fourmy *et al.*, 1998a;

Fourmy *et al.*, 1998b; Yoshizawa *et al.*, 1998) and more recently, X-ray crystal structures

of aminoglycosides bound to the 30S ribosomal subunit confirmed these interactions

(Carter *et al.*, 2000) (Figure 1.2). Aminoglycosides, belonging to the neomycin and

kanamycin classes, bind to the major groove of the 16S rRNA where they make

numerous contacts with the RNA, either directly or indirectly through intermediary water

molecules. Site-directed mutations of the nucleotides making important contacts with the

aminoglycoside leads to defective ribosomes (Recht *et al.*, 1996).
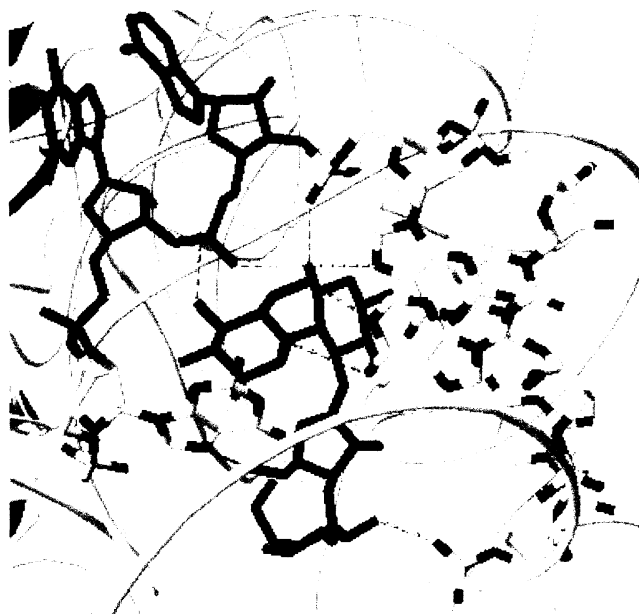


**Figure 1.2:** Structure of Paromomycin (black) Bound to the 30S Subunit of the Prokaryotic Ribosome from *Thermus thermophilus* (Carter *et al.*, 2000). H bonds are shown as dotted lines and the proof-reading bases adenine 1492 and adenine 1493 are shown in red (PDB 1IBK). This figure was generated using Deepview (Guex and Peitsch, 1997).

The direct target of aminoglycosides is thus well characterized, however, there is controversy how binding of aminoglycosides to prokaryotic ribosomes leads to cell death. Other antibiotics that target the ribosome are merely bacteriostatic agents (e.g. tetracycline) (Greenwood and Whitley, 2003). Early on in aminoglycoside research, it was shown that treatment of sensitive, but not resistant cells with antibiotic resulted in damaged cell membranes that allowed for nonspecific permeability to potassium ions, nucleotides and amino acids, suggesting cellular integrity as a secondary, or indirect, target of aminoglycoside action (Anand *et al.*, 1960; Anand and Davis, 1960; Hancock, 1964).

Davis has put forth a controversial proposal linking ribosome fidelity and membrane damage (Davis, 1987). According to Davis, following the rapid binding of positively charged aminoglycosides to the cell surface, small amounts of drug enter the cell (EDPI), bind to the ribosomes and cause the misreading of mRNA. Many of the gene products are normally targeted to the cytoplasmic membrane or the periplasm, but these mistranslated proteins embed themselves improperly into the cytoplasmic membrane to create membrane channels through which there is a greater influx of aminoglycosides (EDPII). Membrane damage and aminoglycoside saturation of the ribosomes together lead to cell death.

These are very exceptional events, but there is evidence to support Davis' hypothesis. Periplasmic pools of $^{35}$S labeled proteins decrease upon exposure of cells to aminoglycosides, and the secretory protein alkaline phosphatase, specifically, has been shown to partition in the membrane fraction and is no longer properly exported upon

aminoglycoside exposure (Davis *et al.*, 1986). Moreover, the crystal structure of aminoglycoside bound to the 30S ribosomal subunit has suggested a mechanism that could lead to mistranslation (Carter *et al.*, 2000). The 16S RNA has been suggested to be involved in the proof-reading mechanism of protein translation, where upon a correct match, the bases A1492 and A1493 "flip-out" to stabilize the interactions between the codon of the mRNA and anti-codon of the tRNA (Figure 1.2) (Carter *et al.*, 2000). Aminoglycosides, belonging to the kanamycin and neomycin classes, are also able to displace these adenines that interact with the codon-anticodon pairing and may lead to an increase in protein translation infidelity (Carter *et al.*, 2000). Antibiotics, including the aminoglycoside spectinomycin, that bind to a similar region on the 16S rRNA but do not interact with these bases are bacteriostatic, lending additional support to the hypothesis (Carter *et al.*, 2000). However, more work is required to verify these underlying mechanisms.

## 1.4 Aminoglycoside Resistance

Aminoglycosides quickly found clinical importance after their initial discovery in the mid 1940s, but reports of resistance were already apparent by the 1950s. Resistance can occur through either nonenzymatic or enzymatic means (Struelens, 2003). Although less common, nonenzymatic resistance, including mutations to the 30S ribosomal binding site or mutations to the electron transport system required for aminoglycoside entry (Struelens, 2003), is clinically important for *M. tuberculosis* and *M. leprae* (Musser, 1995). Enzymatic resistance, more common and generally more clinically relevant, can

occur via modification of the target, usually through the methylation of the ribosome, or the drug itself (Struelens, 2003). Methylation of the ribosome is generally only important for antibiotic-producing organisms (Struelens, 2003), although more recently, a plasmid-borne gene that encodes for a 16S rRNA $m^7G$ methyltransferase has been detected in *Klebsiella pneumoniae* that confers high-level aminoglycoside resistance (Galimand *et al.*, 2003). Modification of the antibiotic itself is by far the most clinically important mechanism of resistance (Struelens, 2003).

There are three major families of aminoglycoside modification enzymes: the aminoglycoside nucleotidyltransferases (ANTs), acetyltransferases (AACs) and phosphotransferases (APHs) that catalyze the transfer of AMP from ATP, an acetyl group from acetyl-CoA and the terminal phosphate of ATP, respectively, to aminoglycoside (Figure 1.3). All of these events serve to decorate the aminoglycoside in such a way that important contacts with the ribosome are disturbed leading to a loss of affinity between antibiotic and ribosome (Llano-Sotelo *et al.*, 2002).
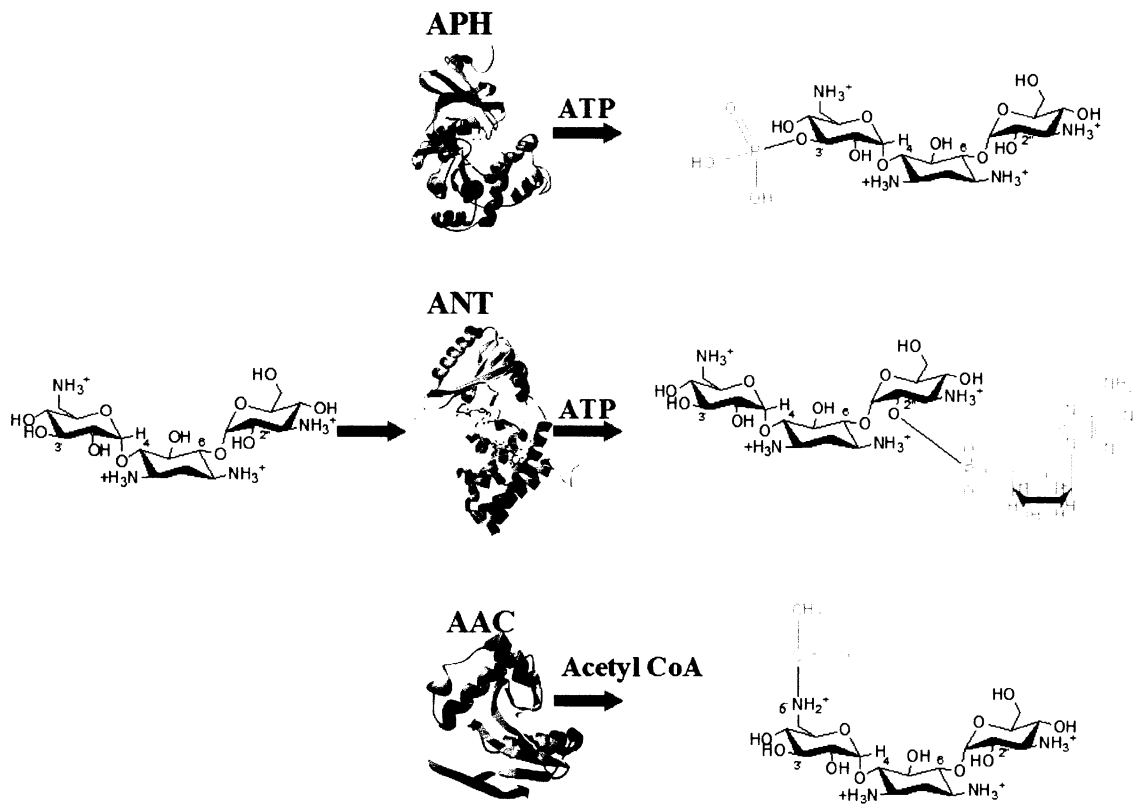
**Figure 1.3:** Structures of and Modifications Catalyzed by the Aminoglycoside Modifying Enzymes, including Aminoglycoside Phosphotransferases (APH), Aminoglycoside Nucleotidyltransferases (ANT) and Aminoglycoside Acetyltransferases (AAC).

### 1.4.1 Nomenclature

Shaw and colleagues have developed a systematic nomenclature for the aminoglycoside resistance enzymes (Shaw *et al.*, 1993). The enzyme is identified first by the type of reaction it catalyzes, whether it is an *N*-acetyltransferase (AAC), *O*-nucleotidytransferase (ANT) or an *O*-phosphotransferase (APH). This is then followed by the specific position it modifies in brackets, a roman numeral, identifying a unique aminoglycoside resistance profile (AGRP), and finally a lower cased letter, identifying distinct genes responsible for a particular AGRP. For example, APH(3')-IIIa is an

aminoglycoside phosphotransferase that modifies the 3' hydroxyl, has a distinct aminoglycoside modifying profile including kanamycin, amikacin, isepamicin, neomycin, butirosin, ribostamycin and lividomycin, and is the first gene identified with this particular AGRP.

### 1.4.2    Brief Overview of Aminoglycoside Resistance Enzymes

The resistance enzymes appear to be cytosolic proteins, considering the cofactor requirements of the enzymes, and given that there is no compelling evidence to suggest periplasmic localization in Gram-negative organisms (Wright *et al.*, 1998). The corresponding genetic determinants mostly reside on mobile genetic elements, either transposons or plasmids, although some appear to be chromosomal in origin (Wright *et al.*, 1998).

The local pattern of aminoglycoside usage significantly impacts the selection and maintenance of specific aminoglycoside resistance enzymes, although some general conclusions can be drawn (Miller *et al.*, 1997). In Gram-positive organisms, aminoglycoside resistance is usually attributable to *aac(6')-aph(2")*, encoding a bifunctional enzyme that is one of the foci of this thesis, *aph(3')-iiia*, the other focus of this thesis, and *ant(6)* (Miller *et al.*, 1997). Gram-negative organisms show a much more complicated resistance, where previously a high prevalence of *ant(2")* has ceded to a more elaborate pattern in which *aac(6')-I* genes are combined with other resistance determinants such as *aac(3)* and *ant(2")* (Miller *et al.*, 1997). This change in resistance pattern is likely attributable to the introduction of newer aminoglycosides such as

netilmicin, and a result of the constant evolving pressure on targeted pathogens (Miller *et al.*, 1997).

### 1.4.3 APH(3')-IIIa

APH(3')-IIIa is especially important in Gram-positive pathogens, but it has also been detected in the Gram-negative organism *Camplyobacter coli* (Papadopoulou and Courvalin, 1988; Taylor *et al.*, 1988). The gene has been cloned from *Streptococcus faecalis* (Trieu-Cuot and Courvalin, 1983) and *Staphylococcus aureus* (Gray and Fitch, 1983), and overexpressed in *E. coli* (McKay *et al.*, 1994). The protein purifies as a mixture of dimer and monomer, although the two forms of the enzyme are kinetically indistinguishable (McKay *et al.*, 1994).

The enzyme has a broad substrate profile, being able to efficiently modify both 4,5- and 4,6- disubstituted classes of aminoglycosides (McKay *et al.*, 1994). Nuclear magnetic resonance spectroscopy (NMR) has definitively assigned the site of modification for the kanamycin class as the 3' hydroxyl (McKay *et al.*, 1994), and has confirmed the ability of APH(3')-IIIa to dually modify many 4,5- disubstituted aminoglycosides as initially suggested by the biphasic progress curves seen for members of the neomycin class (Thompson *et al.*, 1996b). Double modification occurs on the 3' and 5" hydroxyls, where initial phosphotransfer is dependent on the individual aminoglycoside (Thompson *et al.*, 1996b).

A series of experiments have demonstrated that APH(3')-IIIa follows a Theorell-Chance kinetic mechanism (McKay and Wright, 1995; McKay and Wright, 1996). Theorell-Chance is a special case of an ordered BiBi kinetic mechanism where the

reaction occurring in the ternary complex (i.e. chemistry) does not contribute significantly to the overall rate of catalysis. For APH(3')-IIIa, ATP binds first, followed by the binding of aminoglycoside, phosphoryl transfer and immediate release of phosphorylated antibiotic. The release of ADP is the rate limiting step in catalysis (McKay and Wright, 1995; McKay and Wright, 1996).

The chemical mechanism has also been studied. The highly conserved residue His188 was initially thought to serve as a temporary docking site for a phosphate in a double displacement mechanisms, but site-directed mutagenesis of this residue to Ala did not greatly affect the enzyme's activity, and further work using positional isotope labeled ATP established that there is a direct attack of the aminoglycoside hydroxyl on to the $\gamma$-phosphate of ATP (Thompson et al., 1996a).

Additional mutagenesis work has been aided by the determination of the X-ray crystal structure of APH(3')-IIIa (Hon et al., 1997). The structure shows remarkable similarity to the eukaryotic protein kinase (ePK) family, with a smaller N-terminal lobe composed mostly of $\beta$-sheets and a larger C-terminal lobe composed mostly of $\alpha$-helices (Figure 2.1) (Hon et al., 1997). The ATP-binding pocket is formed by a deep cleft between the two lobes, and a putative aminoglycoside binding site has also been identified near the modeled terminal phosphate of ATP (Hon et al., 1997). The importance of this anionic depression in the binding of positively charged antibiotic has been confirmed with substrate modeling studies and directed mutagenesis of conserved residues in the region (Thompson et al., 1999). These studies have also illuminated the capacity of the enzyme to accept a wide range of antibiotic conformations, suggested by

17

its substrate profile and NMR studies modeling the bound conformations of the aminoglycoside butirosin A (Cox and Serpersu, 1997). More recently, structures of APH(3')-IIIa bound with kanamycin A and neomycin have been solved, further delineating the antibiotic binding pocket (Fong and Berghuis, 2002).

APH(3')-IIIa is not only structurally similar to ePKs, but it is also functionally similar. Certain ePK inhibitors can act on APH(3')-IIIa (Daigle *et al.*, 1997), and the enzyme demonstrates serine protein kinase activity (Daigle *et al.*, 1999b).

### 1.4.4   AAC(6')-APH(2")

AAC(6')-APH(2") was initially discovered in Gram-positive cocci such as *Enterococcus* and *Staphylococcus* (Hodel-Christian and Murray, 1991; Kaufhold *et al.*, 1992; Thal *et al.*, 1993), but more recently, has also been detected in Gram-negative bacteria (Miller *et al.*, 1997). The protein has both ATP-dependent phosphorylation and acetyl-CoA-dependent acetylation activities, and has the capacity to inactivate nearly all aminoglycoside antibiotics except for streptomycin and spectinomycin (Culebras and Martinez, 1999).

The gene has been cloned from *S. aureus* (Rouch *et al.*, 1987) and *E. faecalis* (Ferretti *et al.*, 1986), and the protein has been purified from *S. aureus* (Rouch *et al.*, 1987), *S. epidermidis* (Ubukata *et al.*, 1984) and from overexpressing constructs in *E. coli* (Azucena *et al.*, 1997) and *B. subtilis* (Daigle *et al.*, 1999a). Sequence homology studies and the construction of truncated proteins have demonstrated that the acetyltransferase (AAC(6')-Ie) and phosphotransferase (APH(2")-Ia) activities are associated with the N-terminal and C-terminal domains respectively (Ferretti *et al.*, 1986). These findings

suggest that the resistance gene may have arisen from a gene fusion event between an AAC and an APH (Ferretti *et al.*, 1986). In support of this hypothesis, homologues of both domains have been isolated, including APH(2")-Ic from *E. gallinarum* (Chow *et al.*, 1997) and APH(2")-Id from *E. casseflavus* (Tsai *et al.*, 1998) that show similarity to the APH domain, and AAC(6')-Im from *E. coli* and *E. faecalis* that shows similarity to the AAC domain (Chow *et al.*, 2001). Moreover, AAC(6')-Im can be detected together with APH(2")-Ib, where the genes are only 40 nucleotides apart and consequently, the genes can be transferred simultaneously (Chow *et al.*, 2001).

The two domains appear to be functionally distinct from one another, with each activity following a random rapid equilibrium steady-state kinetic mechanism independent from the other activity's required cofactor (Martel *et al.*, 1983). The predicted regiospecificity of modification for both phosphoryl (2"-OH) and acetyl (6-$NH_2$) modification of kanamycin A (Azucena *et al.*, 1997) and arbekacin (Kondo *et al.*, 1993) has been confirmed, and furthermore, bifunctionalization has been detected (Azucena *et al.*, 1997). The enzyme also has an even more startling array of activities, including alternate sites of phosphorylation for neomycin B (3' and 3") and lividomycin A (5'), as well as, *O*-acetylation of paramomycin (6'-OH) (Daigle *et al.*, 1999a). Thus, the APH(2")-Ia activity, especially, appears to be impervious to the structure of the aminoglycoside, and together with the unique AAC(6') domain, this enzyme may be the most threatening resistance enzyme known to date.

## 1.5 Project Goals

APH(3')-IIIa and AAC(6')-APH(2") are two very important aminoglycoside resistance enzymes. Both have been purified successfully to homogeneity and their assays are well developed (Daigle *et al.*, 1999a; McKay *et al.*, 1994). APH(3')-IIIa, especially, is a well characterized enzyme, already serving as the major topic of two PhD dissertations from Dr. G.D. Wright's laboratory, by Dr. Geoff McKay (McKay, 1999) and Dr. Paul Thompson (Thompson, 1999). The kinetic mechanism of APH(3')-IIIa has been worked out, necessary for an appreciation of what the steady-state kinetic parameters $k_{cat}$ and $K_M$ really represent, and is the first critical step towards understanding the chemical mechanism of aminoglycoside phosphorylation. Several structures of APH(3')-IIIa are available to help guide further exploration of important residues to APH function. With this large base of knowledge, APH(3')-IIIa continues to be studied as the model aminoglycoside kinase.

AAC(6')-APH(2") is less well characterized, but has also served as the major topic of another PhD dissertation, by Dr. Denis Daigle (Daigle, 2003). There are no available structures of this protein, but there are structures of APHs and AACs (Hon *et al.*, 1997; Wolf *et al.*, 1998; Wybenga-Groot *et al.*, 1999) and it is likely that the domains of the protein fold in a similar manner, although it is not known if the domains interact with one another and how this may affect function and/or structure. The clinical importance of AAC(6')-APH(2") (Miller *et al.*, 1997), and to a lesser extent APH(3')-IIIa, prompts further study of these proteins to understand the molecular mechanisms of aminoglycoside resistance with the goal in mind of using this knowledge to make rational

decisions concerning inhibitor design. The project can be divided into five chapters as follows:

### 1.5.1 Molecular Mechanism of Aminoglycoside Phosphorylation

Enzymes catalyze reactions by preferentially stabilizing transition-state species over that of substrates and so, compounds that mimic the transition-state should act as potent inhibitors of enzyme function (Schramm, 1998). An understanding of the chemical mechanism of catalysis will give insight into the nature of the transition-state, and hence, is an important step towards the design of enzyme inhibitors. Site-directed mutagenesis together with *in vitro* and *in vivo* analysis can provide information regarding the importance and roles of individual amino acid residues. This approach is applied in Chapter 2 to further define the molecular mechanism of APH(3')-IIIa. A comparison between APH(3')-IIIa and the kinase domain of AAC(6')-APH(2") (APH(2")-Ia) suggests that the molecular mechanisms are similar, although there are differences that may result in different inhibitor sensitivities.

### 1.5.2   Differential Sensitivities among APHs to Active-site Labeling Reagents

There are a number of APHs available to bacteria and treatment may require an understanding of the similarities and differences among the resistance enzymes, especially in terms of inhibitor sensitivities. The best-case scenario is the development of an inhibitor with broad efficacy across the APH class. However, initial evidence suggests that this may not be possible, where APH(3')-IIIa and APH(2")-Ia have different sensitivities to ePK inhibitors. In Chapter 3, further differences are found in inhibitor

sensitivities, in this case, the covalent modifiers wortmannin and FSBA can inactivate APH(2")-Ia and APH(3')-IIIa respectively but have no cross-reactivity with the other kinase. Thus, broad APH inhibitors directed against the ATP binding pocket may be an impossibility, but wortmannin can serve as a lead compound in the development of APH(2") inhibitors that will be able to overcome the devastating resistance associated with the bifunctional enzyme.

### 1.5.3    Molecular Mechanism of Aminoglycoside Acetylation and Inactivation of AAC(6')-Ie

The molecular mechanism of aminoglycoside phosphorylation was established in Chapter 2. However, AAC(6')-APH(2") is composed of both phosphotransferase and acetyltransferase domains, and a rational approach to overcoming resistance associated with this protein will also require an understanding of AAC function. In Chapter 4, the role of an active site base in AAC(6')-Ie catalysis is addressed through site-directed mutagenesis, solvent isotope, solvent viscosity and pH effect studies. The chapter also includes the results of a study with halomethyl aromatic compounds that can inactivate AAC(6')-Ie, likely through the modification of the active site base. Similar to wortmannin, these compounds can serve as leads in the development of irreversible inhibitors of AAC(6')-APH(2") function.

### 1.5.4    Domain Interactions in AAC(6')-APH(2")

The molecular mechanisms of aminoglycoside phosphorylation and acetylation are established in Chapters 2 and 4, respectively, in isolation. There is initial evidence

that the domains of AAC(6')-APH(2") do not functionally interact, however, to further probe potential domains interactions, N- and C-terminal truncated proteins were cloned and used in a variety of *in vitro* studies, including analysis of steady-state kinetic parameters, thermal inactivation experiments and analytic gel filtration experiments to assay association between the truncated proteins, and *in vivo* studies, including minimum inhibitory concentration (MIC) analysis of *E. coli* expressing constructs and the establishment of *Bacillus subtilis* integrants. These studies suggest that there are important contacts between the domains that are important for structure and stability of the resistance protein.

### 1.5.5    Broad-Spectrum Peptide Inhibitors of Aminoglycoside Resistance Enzymes

The work with wortmannin and FSBA presented in Chapter 3 suggested that the development of broad-spectrum inhibitors of aminoglycoside resistance is difficult. However, aminoglycoside resistance enzymes all share a common anionic depression that is used to bind positively charged aminoglycoside. We attempted to take advantage of this conserved structural feature by assaying positively charged peptides against a number of resistance activities, including APH(3')-IIIa, APH(2")-Ia, AAC(6')-Ie and AAC(6')-Ii. Indolicidin, an antimicrobial peptide isolated from bovine neutrophils, was successful in not only inhibiting APH(3')-IIIa and APH(2")-Ia, but it also demonstrated activity against AAC(6')-Ii. This molecule represents the first broad-range aminoglycoside resistance inhibitor.

## 1.6 References

**Acosta, M.B., Ferreira, R.C., Padilla, G., Ferreira, L.C. and Costa, S.O. 2000.** Altered expression of oligopeptide-binding protein (OppA) and aminoglycoside resistance in laboratory and clinical *Escherichia coli* strains. *J Med Microbiol.* 49: 409-413.

**Anand, M., Davis, B.D. and Armitage, A.K. 1960.** Uptake of streptomycin by *Escherichia coli. Nature.* 185: 23-24.

**Anand, N.B. and Davis, B.D. 1960.** Damage by streptomycin to the cell membrane of *Escherichia coli. Nature.* 185: 22-23.

**Azucena, E., Grapsas, I. and Mobashery, S. 1997.** Properties of a bifunctional bacterial antibiotic resistance enzyme that catalyzes ATP-dependent 2"-phosphorylation and acetyl-CoA dependent 6'-acetylation of aminoglycosides. *J Am Chem Soc.* 119: 2317 - 2318.

**Birge, E.A. and Kurland, C.G. 1969.** Altered ribosomal protein in streptomycin-dependent *Escherichia coli. Science.* 166: 1282-1284.

**Bryan, L.E. and Van den Elzen, H.M. 1976.** Streptomycin accumulation in susceptible and resistant strains of *Escherichia coli* and *Pseudomonas aeruginosa. Antimicrob Agents Chemother.* 9: 928-938.

**Bryan, L.E. and Van Den Elzen, H.M. 1977.** Effects of membrane-energy mutations and cations on streptomycin and gentamicin accumulation by bacteria: a model for entry of streptomycin and gentamicin in susceptible and resistant bacteria. *Antimicrob Agents Chemother.* 12: 163-177.

**Campbell, N.A. 1993.** Early Earth and the Origin of Life. *Biology* $3^{rd}$ *Ed.* The Benjamin/Cummings Publishing Company, Inc., Redwood City, pp. 504-514.

**Carter, A.P., Clemons, W.M., Brodersen, D.E., Morgan-Warren, R.J., Wimberly, B.T. and Ramakrishnan, V. 2000.** Functional insights from the structure of the 30S ribosomal subunit and its interactions with antibiotics. *Nature.* 407: 340-348.

**Chow, J.W., Kak, V., You, I., Kao, S.J., Petrin, J., Clewell, D.B., Lerner, S.A., Miller, G.H. and Shaw, K.J. 2001.** Aminoglycoside resistance genes aph(2")-Ib and aac(6')-Im detected together in strains of both *Escherichia coli* and *Enterococcus faecium. Antimicrob Agents Chemother.* 45: 2691-2694.

**Chow, J.W., Zervos, M.J., Lerner, S.A., Thal, L.A., Donabedian, S.M., Jaworski, D.D., Tsai, S., Shaw, K.J. and Clewell, D.B. 1997.** A novel gentamicin resistance gene in *Enterococcus*. *Antimicrob Agents Chemother*. 41: 511-514.

**Cox, J.R. and Serpersu, E.H. 1997.** Biologically important conformations of aminoglycoside antibiotics bound to an aminoglycoside 3'-phosphotransferase as determined by transferred nuclear Overhauser effect spectroscopy. *Biochemistry*. 36: 2353-2359.

**Culebras, E. and Martinez, J.L. 1999.** Aminoglycoside resistance mediated by the bifunctional enzyme 6'-N-aminoglycoside acetyltransferase-2"-O-aminoglycoside phosphotransferase. *Front Biosci*. 4: D1-8.

**Daigle, D.M. 2003. PhD Thesis.** *Biochemistry*. McMaster University, Hamilton, ON, Canada.

**Daigle, D.M., Hughes, D.W. and Wright, G.D. 1999a.** Prodigious substrate specificity of AAC(6')-APH(2"), an aminoglycoside antibiotic resistance determinant in enterococci and staphylococci. *Chem Biol*. 6: 99-110.

**Daigle, D.M., McKay, G.A., Thompson, P.R. and Wright, G.D. 1999b.** Aminoglycoside antibiotic phosphotransferases are also serine protein kinases. *Chem Biol*. 6: 11-18.

**Daigle, D.M., McKay, G.A. and Wright, G.D. 1997.** Inhibition of aminoglycoside antibiotic resistance enzymes by protein kinase inhibitors. *J Biol Chem*. 272: 24755-24758.

**Davis, B.D. 1987.** Mechanism of bactericidal action of aminoglycosides. *Microbiol Rev*. 51: 341-350.

**Davis, B.D., Chen, L.L. and Tai, P.C. 1986.** Misread protein creates membrane channels: an essential step in the bactericidal action of aminoglycosides. *Proc Natl Acad Sci U S A*. 83: 6164-6168.

**Ferretti, J.J., Gilmore, K.S. and Courvalin, P. 1986.** Nucleotide sequence analysis of the gene specifying the bifunctional 6'-aminoglycoside acetyltransferase 2"-aminoglycoside phosphotransferase enzyme in *Streptococcus faecalis* and identification and cloning of gene regions specifying the two activities. *J Bacteriol*. 167: 631-638.

**Fong, D.H. and Berghuis, A.M. 2002.** Substrate promiscuity of an aminoglycoside antibiotic resistance enzyme via target mimicry. *Embo J*. 21: 2323-2331.

Fourmy, D., Recht, M.I., Blanchard, S.C. and Puglisi, J.D. 1996. Structure of the A site of *Escherichia coli* 16S ribosomal RNA complexed with an aminoglycoside antibiotic. *Science*. 274: 1367-1371.

Fourmy, D., Recht, M.I. and Puglisi, J.D. 1998a. Binding of neomycin-class aminoglycoside antibiotics to the A-site of 16 S rRNA. *J Mol Biol*. 277: 347-362.

Fourmy, D., Yoshizawa, S. and Puglisi, J.D. 1998b. Paromomycin binding induces a local conformational change in the A-site of 16 S rRNA. *J Mol Biol*. 277: 333-345.

Galimand, M., Courvalin, P. and Lambert, T. 2003. Plasmid-mediated high-level resistance to aminoglycosides in Enterobacteriaceae due to 16S rRNA methylation. *Antimicrob Agents Chemother*. 47: 2565-2571.

Gray, G.S. and Fitch, W.M. 1983. Evolution of antibiotic resistance genes: the DNA sequence of a kanamycin resistance gene from *Staphylococcus aureus*. *Mol Biol Evol*. 1: 57-66.

Greenwood, D. 2003. Historical introduction. In Finch, R.G., Greenwood, D., Norrby, S.R. and Whitley, R.J. (eds.), *Antibiotic and Chemotherapy: Anti-infective agents and their use in therapy*. Churchill Livingstone, Edinburgh, pp. 3-10.

Greenwood, D. and Whitley, R. 2003. Modes of action. In Finch, R.G., Greenwood, D., Norrby, S.R. and Whitley, R.J. (eds.), *Antibiotic and chemotherapy*. Elsevier Science Limited, Edinburgh.

Greenwood, D., Whitley, R. and etc. 2003. In Finch, R.G., Greenwood, D., Norrby, S.R. and Whitley, R.J. (eds.), *Antibiotic and Chemotherapy: Anti-infective agents and their use in therapy*. Churchill Livingstone, Edinburgh, Vol. 8th.

Guex, N. and Peitsch, M.C. 1997. SWISS-MODEL and the Swiss-Pdbviewer. An environment for comparative protein modeling. *Electrophoresis*, 18: 2714-2723.

Hancock, R. 1964. Early effects of streptomycin on *Bacillus megaterium*. *J Bacteriol*. 88: 633-639.

Hancock, R.E. 1981. Aminoglycoside uptake and mode of action--with special reference to streptomycin and gentamicin. I. Antagonists and mutants. *J Antimicrob Chemother*. 8: 249-276.

Hodel-Christian, S.L. and Murray, B.E. 1991. Characterization of the gentamicin resistance transposon Tn5281 from *Enterococcus faecalis* and comparison to staphylococcal transposons Tn4001 and Tn4031. *Antimicrob Agents Chemother*. 35: 1147-1152.

**Hon, W.C., McKay, G.A., Thompson, P.R., Sweet, R.M., Yang, D.S., Wright, G.D. and Berghuis, A.M.** 1997. Structure of an enzyme required for aminoglycoside antibiotic resistance reveals homology to eukaryotic protein kinases. *Cell.* 89: 887-895.

**Kashiwagi, K., Miyaji, A., Ikeda, S., Tobe, T., Sasakawa, C. and Igarashi, K.** 1992. Increase of sensitivity to aminoglycoside antibiotics by polyamine-induced protein (oligopeptide-binding protein) in *Escherichia coli. J Bacteriol.* 174: 4331-4337.

**Kashiwagi, K., Tsuhako, M.H., Sakata, K., Saisho, T., Igarashi, A., da Costa, S.O. and Igarashi, K.** 1998. Relationship between spontaneous aminoglycoside resistance in *Escherichia coli* and a decrease in oligopeptide binding protein. *J Bacteriol.* 180: 5484-5488.

**Kaufhold, A., Podbielski, A., Horaud, T. and Ferrieri, P.** 1992. Identical genes confer high-level resistance to gentamicin upon *Enterococcus faecalis, Enterococcus faecium,* and *Streptococcus agalactiae. Antimicrob Agents Chemother.* 36: 1215-1218.

**Kondo, S., Tamura, A., Gomi, S., Ikeda, Y., Takeuchi, T. and Mitsuhashi, S.** 1993. Structures of enzymatically modified products of arbekacin by methicillin resistant *Staphylococcus aureus. J Antibiot.* 46: 310-315.

**Leclerc, D., Melancon, P. and Brakier-Gingras, L.** 1991. Mutations in the 915 region of *Escherichia coli* 16S ribosomal RNA reduce the binding of streptomycin to the ribosome. *Nucleic Acids Res.* 19: 3973-3977.

**Levy, S.B.** 1992. The Antibiotic Paradox: How miracle drugs are destroying the miracle. Plenum Press, New York.

**Llano-Sotelo, B., Azucena, E.F., Kotra, L.P., Mobashery, S. and Chow, C.S.** 2002. Aminoglycosides Modified by resistance enzymes display diminished binding to the bacterial ribosomal aminoacyl-tRNA site. *Chem Biol.* 9: 455-463.

**Martel, A., Masson, M., Moreau, N. and Le Goffic, F.** 1983. Kinetic studies of aminoglycoside acetyltransferase and phosphotransferase from *Staphylococcus aureus* RPAL. Relationship between the two activities. *Eur J Biochem.* 133: 515-521.

**McKay, G.A.** 1999. Characterization of Aminoglycoside Phosphotransferase APH(3')-IIIa: An enterococcal enzyme conferring resistance to aminoglycoside antibiotics. *Biochemistry.* McMaster University, Hamilton.

**McKay, G.A., Thompson, P.R. and Wright, G.D.** 1994. Broad spectrum aminoglycoside phosphotransferase type III from *Enterococcus*: overexpression, purification, and substrate specificity. *Biochemistry.* 33: 6936-6944.

**McKay, G.A. and Wright, G.D. 1995.** Kinetic mechanism of aminoglycoside phosphotransferase type IIIa. Evidence for a Theorell-Chance mechanism. *J Biol Chem.* 270: 24686-24692.

**McKay, G.A. and Wright, G.D. 1996.** Catalytic mechanism of enterococcal kanamycin kinase (APH(3')-IIIa): viscosity, thio, and solvent isotope effects support a Theorell-Chance mechanism. *Biochemistry.* 35: 8680-8685.

**Miller, G.H., Sabatelli, F.J., Hare, R.S., Glupczynski, Y., Mackey, P., Shlaes, D., Shimizu, K. and Shaw, K.J. 1997.** The most frequent aminoglycoside resistance mechanisms--changes with time and geographic area: a reflection of aminoglycoside usage patterns? Aminoglycoside Resistance Study Groups. *Clin Infect Dis.* 24 Suppl 1: S46-62.

**Miller, J. 2000.** Antibiotics and isotopes. In Ryan, J., Newman, A. and Jacobs, M. (eds.), *The Pharmaceutical Century: Ten decades of drug discovery*, ACS Publications, pp. 52-71.

**Miller, M.H., Edberg, S.C., Mandel, L.J., Behar, C.F. and Steigbigel, N.H. 1980.** Gentamicin uptake in wild-type and aminoglycoside-resistant small-colony mutants of *Staphylococcus aureus. Antimicrob Agents Chemother.* 18: 722-729.

**Moazed, D. and Noller, H.F. 1987.** Interaction of antibiotics with functional sites in 16S ribosomal RNA. *Nature.* 327: 389-394.

**Montandon, P.E., Wagner, R. and Stutz, E. 1986.** *E. coli* ribosomes with a C912 to U base change in the 16S rRNA are streptomycin resistant. *Embo J.* 5: 3705-3708.

**Musser, J.M. 1995.** Antimicrobial agent resistance in mycobacteria: molecular genetic insights. *Clin Microbiol Rev.* 8: 496-514.

**Ozaki, M., Mizushima, S. and Nomura, M. 1969.** Identification and functional characterization of the protein controlled by the streptomycin-resistant locus in *E. coli. Nature.* 222: 333-339.

**Papadopoulou, B. and Courvalin, P. 1988.** Dispersal in *Campylobacter spp.* of aphA-3, a kanamycin resistance determinant from gram-positive cocci. *Antimicrob Agents Chemother.* 32: 945-948.

**Recht, M.I., Fourmy, D., Blanchard, S.C., Dahlquist, K.D. and Puglisi, J.D. 1996.** RNA sequence determinants for aminoglycoside binding to an A-site rRNA model oligonucleotide. *J Mol Biol.* 262: 421-436.

**Rouch, D.A., Byrne, M.E., Kong, Y.C. and Skurray, R.A. 1987.** The aacA-aphD gentamicin and kanamycin resistance determinant of Tn4001 from *Staphylococcus aureus*: expression and nucleotide sequence analysis. *J Gen Microbiol.* 133: 3039-3052.

**Schatz, A., Bugie, E. and Waksman, S.A. 1944.** Streptomycin, a substance exhibiting antibiotic activity against Gram positive and Gram negative bacteria. *Proc Soc Exp Biol Med.* 55: 66-69.

**Schatz, A., Bugie, E. and Waksman, S.A. 1973.** Selman Abraham Waksman, Ph.D. 22 July 1888--16 August 1973. Streptomycin reported. *Ann Intern Med.* 79: 678.

**Schramm, V.L. 1998.** Enzymatic transition states and transition state analog design. *Annu Rev Biochem.* 67: 693-720.

**Shaw, K.J., Rather, P.N., Hare, R.S. and Miller, G.H. 1993.** Molecular genetics of aminoglycoside resistance genes and familial relationships of the aminoglycoside-modifying enzymes. *Microbiol Rev.* 57: 138-163.

**Shnayerson, M. and Plotkin, M.J. 2002.** The Killers Within: The deadly rise of drug-resistant bacteria. Little, Brown & Company, New York.

**Sigmund, C.D., Ettayebi, M. and Morgan, E.A. 1984.** Antibiotic resistance mutations in 16S and 23S ribosomal RNA genes of *Escherichia coli*. *Nucleic Acids Res.* 12: 4653-4663.

**Struelens, M.J. 2003.** The problem of resistance. In Finch, R.G., Greenwood, D., Norrby, S.R. and Whitley, R.J. (eds.), *Antibiotic and chemotherapy.* Churchill Livingstone, Edinburgh, Vol. 8th.

**Tai, P.C., Wallace, B.J. and Davis, B.D. 1978.** Streptomycin causes misreading of natural messenger by interacting with ribosomes after initiation. *Proc Natl Acad Sci U S A.* 75: 275-279.

**Tai, P.C., Wallace, B.J., Herzog, E.L. and Davis, B.D. 1973.** Properties of initiation-free polysomes of *Escherichia coli*. *Biochemistry.* 12: 609-615.

**Taylor, D.E., Yan, W., Ng, L.K., Manavathu, E.K. and Courvalin, P. 1988.** Genetic characterization of kanamycin resistance in *Campylobacter coli*. *Ann Inst Pasteur Microbiol.* 139: 665-676.

**Thal, L.A., Chow, J.W., Patterson, J.E., Perri, M.B., Donabedian, S., Clewell, D.B. and Zervos, M.J. 1993.** Molecular characterization of highly gentamicin-resistant *Enterococcus faecalis* isolates lacking high-level streptomycin resistance. *Antimicrob Agents Chemother.* 37: 134-137.

**Thompson, P.R. 1999.** Characterization of the catalytic mechanisms of two aminoglycoside phosphotransferases: APH(3')-IIIa from *Enterococcus faecalis* and APH(9)-Ia from *Legionella pneumophila.* *Biochemistry*. McMaster University, Hamilton, Ontario, pp. 1-305.

**Thompson, P.R., Hughes, D.W. and Wright, G.D. 1996a.** Mechanism of aminoglycoside 3'-phosphotransferase type IIIa: His188 is not a phosphate-accepting residue. *Chem Biol.* 3: 747-755.

**Thompson, P.R., Hughes, D.W. and Wright, G.D. 1996b.** Regiospecificity of aminoglycoside phosphotransferase from Enterococci and Staphylococci (APH(3')-IIIa). *Biochemistry*. 35: 8686-8695.

**Thompson, P.R., Schwartzenhauer, J., Hughes, D.W., Berghuis, A.M. and Wright, G.D. 1999.** The COOH terminus of aminoglycoside phosphotransferase (3')-IIIa is critical for antibiotic recognition and resistance. *J Biol Chem.* 274: 30697-30706.

**Trieu-Cuot, P. and Courvalin, P. 1983.** Nucleotide sequence of the *Streptococcus faecalis* plasmid gene encoding the 3'5"-aminoglycoside phosphotransferase type III. *Gene*. 23: 331-341.

**Tsai, S.F., Zervos, M.J., Clewell, D.B., Donabedian, S.M., Sahm, D.F. and Chow, J.W. 1998.** A new high-level gentamicin resistance gene, aph(2")-Id, in *Enterococcus spp. Antimicrob Agents Chemother.* 42: 1229-1232.

**Ubukata, K., Yamashita, N., Gotoh, A. and Konno, M. 1984.** Purification and characterization of aminoglycoside-modifying enzymes from *Staphylococcus aureus* and *Staphylococcus epidermidis. Antimicrob Agents Chemother.* 25: 754-759.

**Waksman, S.A. and Lechevalier, H.A. 1949.** Neomycin, a new antibiotic active against streptomycin-resistant bacteria, including tuberculosis organisms. *Science*. 109: 305-307.

**Wallace, B.J., Tai, P.C., Herzog, E.L. and Davis, B.D. 1973.** Partial inhibition of polysomal ribosomes of *Escherichia coli* by streptomycin. *Proc Natl Acad Sci U S A*. 70: 1234-1237.

**Walsh, C. 2003.** Validated targets and major antibiotic classes. *Antibiotics: Actions, origins, resistance*. ASM Press, Washington, DC.

**Wolf, E., Vassilev, A., Makino, Y., Sali, A., Nakatani, Y. and Burley, S.K. 1998.** Crystal structure of a GCN5-related N-acetyltransferase: Serratia marcescens aminoglycoside 3-N-acetyltransferase. *Cell*. 94: 439-449.

**Woodcock, J., Moazed, D., Cannon, M., Davies, J. and Noller, H.F. 1991.** Interaction of antibiotics with A- and P-site-specific bases in 16S ribosomal RNA. *Embo J.* 10: 3099-3103.

**Wright, G.D., Berghuis, A.M. and Mobashery, S. 1998.** Aminoglycoside antibiotics. Structures, functions, and resistance. *Adv Exp Med Biol.* 456: 27-69.

**Wybenga-Groot, L.E., Draker, K., Wright, G.D. and Berghuis, A.M. 1999.** Crystal structure of an aminoglycoside 6'-N-acetyltransferase: defining the GCN5-related N-acetyltransferase superfamily fold. *Structure Fold Des.* 7: 497-507.

**Yoshizawa, S., Fourmy, D. and Puglisi, J.D. 1998.** Structural origins of gentamicin antibiotic action. *Embo J.* 17: 6437-6448.

# Chapter 2.

# Molecular Mechanism of Aminoglycoside Phosphorylation

Reproduced in part from Boehr, D.D., Thompson, P.R and Wright, G.D. (2001). Molecular mechanism of aminoglycoside antibiotic kinase APH(3')-IIIa: roles of conserved active site residues. *J. Biol. Chem.*, 276, 23929-23936. Copyright 2001. The American Society for Biochemistry and Molecular Biology, Inc.

And Thompson, P.R., Boehr, D.D., Berghuis, A.M. and Wright, G.D. (2002). Mechanism of aminoglycoside antibiotic kinase APH(3')-IIIa: role of the nucleotide positioning loop. *Biochemistry*, 41, 7001-7007. Copyright 2002. American Chemical Society.

And Boehr, D.D., Farley, A.R., Wright, G.D. and Cox, J.R. (2002) Analysis of the $\pi-\pi$ stacking interactions between the aminoglycoside antibiotic kinase APH(3')-IIIa and its nucleotide ligands. *Chem. Biol.*, 9, 1209-1217. Copyright 2002. Elsevier Science Ltd.

Much of this work was conducted in collaboration with Dr. Paul R. Thompson and is a continuation of the work from his PhD thesis. Dr. P.R. Thompson generated and determined the steady-state kinetic parameters of the following mutants of APH(3')-IIIa: Glu60Ala, Asp190Asn, Asp190Glu, Asn195Ala, Ser27Ala and Ser27Pro. He also determined the solvent viscosity and solvent isotope effects for Asn195Ala and the metal ion effects for Ser27Ala and Ser27Pro. I generated and determined the steady-state kinetic parameters of the following mutants of APH(3')-IIIa: Asp208Asn, Asp208Glu, Met26Ala, Met26Pro, Tyr42Ala, Tyr42Val and Tyr42Phe. I also determined the solvent viscosity and solvent isotope effects of the following APH(3')-IIIa mutants: Glu60Ala, Ser27Ala, Met26Pro, and the metal ion effects for Met26Ala and Met26Pro. I also conducted the large scale proteolysis of APH(3')-IIIa to determine the subtilisin cut sites, and determined all of the reported minimum inhibitory concentrations. I completed the circular dichroism and the isothermal titration calorimetry work. Finally, I completed all the work on the phosphotransferase domain of AAC(6')-APH(2").

## 2.1 Introduction

Enzymes catalyze reactions primarily due to transition-state stabilization, that is, the active sites of enzymes have evolved to bind tightly to the transition-state structure, lasting only for a single bond vibration. Thus, compounds that mimic the transition-state structure will bind very tightly to the enzyme and act as very potent inhibitors. Understanding the molecular or chemical mechanism of enzyme catalysis is one means towards deciphering the transition-state structure, and hence, a steps towards the development of potent inhibitors of the enzyme.

APHs are structurally (Hon *et al.*, 1997) (Figure 2.1) and functionally (Daigle *et al.*, 1999b) similar to ePKs. As protein kinases are important pharmacological targets, many studies have been completed on this class of enzymes that lay the foundation for understanding the molecular mechanism of APHs.

Phosphoryl transfer is hypothesized to occur by either an associative or dissociative mechanism (Knowles, 1980) (Figure 2.2). Evidence to date suggests that the reactions in solution (Herschlag and Jencks, 1989a; Kirby and Varvoglis, 1967; Knowles, 1980) and the enzyme-catalyzed reaction (Hengge *et al.*, 1995; Hollfelder and Herschlag, 1995; Kim and Cole, 1997; Kim and Cole, 1998; Weiss and Cleland, 1989) follow dissociative-like mechanisms. However, the reaction does not appear to be fully dissociative but only partially dissociative, or they occur with stereochemical rigidity, as the phosphoryl transfer reactions studied have occurred with inversion of configuration (Buchwald *et al.*, 1982; Buchwald *et al.*, 1984). This suggests that there is partial bond formation in the transition state, and a true metaphosphate intermediate, characteristic of

a true dissociative mechanism, does not exist in aqueous solution reactions (Herschlag and Jencks, 1989b).

Between aminoglycoside phosphotransferases and Ser/Thr protein kinases, there are five absolutely conserved residues: Lys44, Glu60, Asp190, Asn195 and Asp208 (APH(3')-IIIa numbering), that line the catalytic core of these enzymes (Figure 2.3). The importance of some of these residues to APH function has already been demonstrated. For example, Lys44, which makes a H-bond interaction to the β-phosphate of ATP, has been shown to be important for ATP binding (Hon *et al.*, 1997). The importance of Asp190 and Asp208 to APH(3')-IIIa activity has also been demonstrated as mutation of either of these residues to Ala results in a significant decrease in activity (Daigle *et al.*, 1999b). Asp190 in APH(3')-IIIa aligns with Asp166 in protein kinase A, and based upon the positioning of this residue and its absolute conservation, it was originally hypothesized to act as a catalytic base that would deprotonate the incoming hydroxyl to generate a more potent nucleophile and result in an associative-like mechanism (Zheng *et al.*, 1993). However, more recent studies have suggested that general base catalysis is not important for protein kinase catalyzed phosphoryl transfer (Cole *et al.*, 1995; Zhou and Adams, 1997) suggesting an alternate role for this residue.
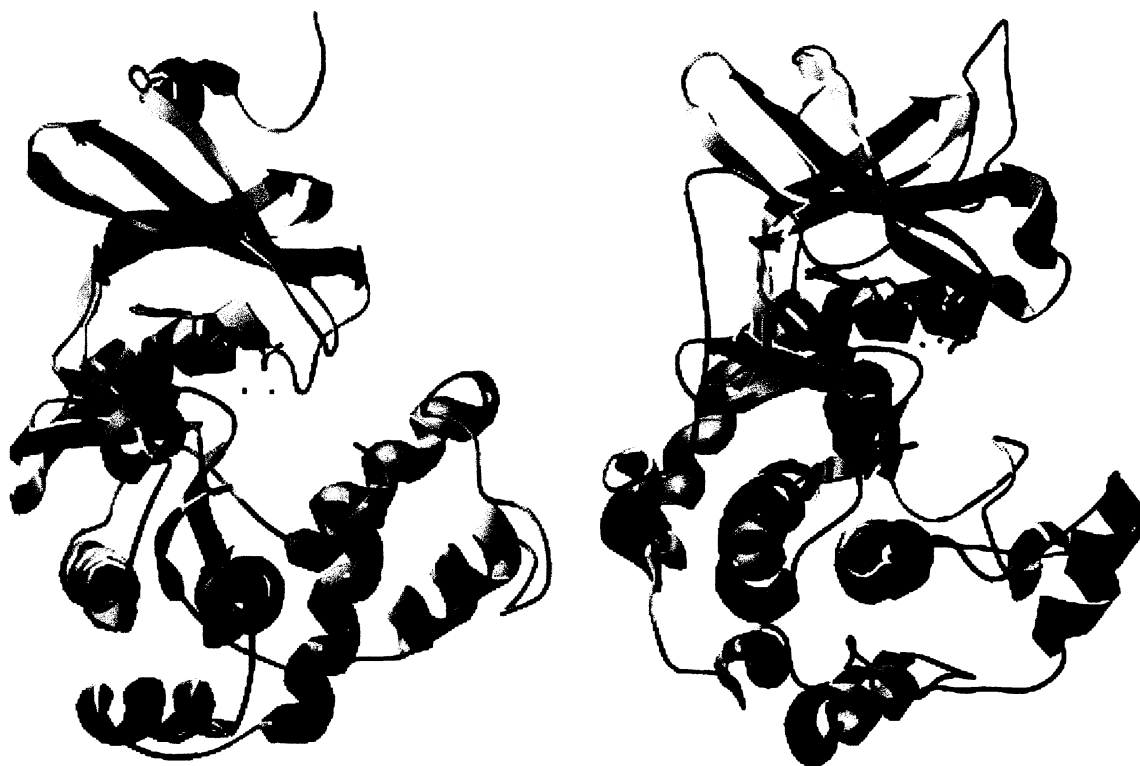
**Figure 2.1:** Structural Comparison between APH(3')-IIIa (left, PDB 1J7L) and Protein Kinase A (right, PDB 1ATP). Figures involving protein structures were all generated using DeepView (Guex and Peitsch, 1997) and POV-Ray (Cason *et al*, 2002).

## Associative
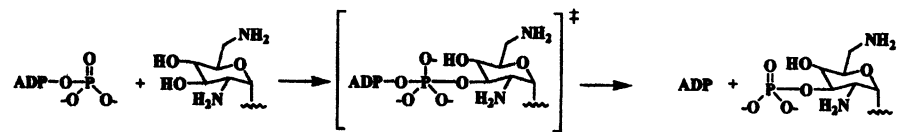


## Dissociative
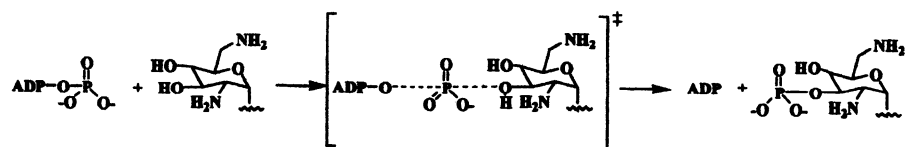


**Figure 2.2:** Associative and Dissociative Mechanisms of APH(3')-catalyzed Phosphoryl Transfer Reactions.

35

A



B
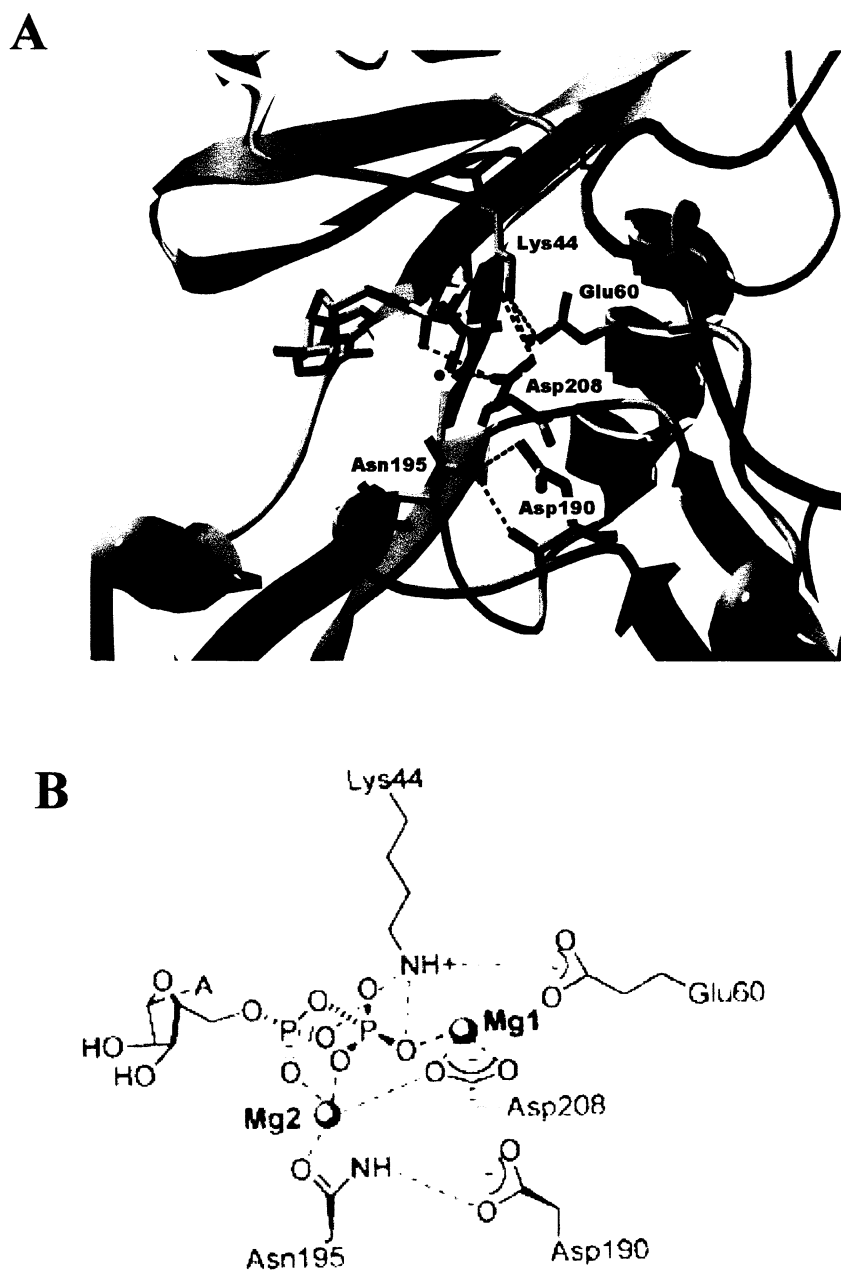


**Figure 2.3:** The Five Absolutely Conserved Residues Between the Aminoglycoside Phosphotransferases and Ser/Thr Protein Kinases Located in the Active Site of APH(3')-IIIa. (A) Residues shown in the structure of binary complex between APH(3')-IIIa and AMPPNP (PDB 1J7U). (B) A schematic representation of the residues showing important H-bond interactions in the APH(3')-IIIa.ADP binary complex.

In addition to these conserved active site residues, protein and aminoglycoside kinases share a Gly-rich loop that plays a role in ATP binding. This loop is located in the N-terminal domain between the first and second β-strands of the antiparallel β-sheet (Hon et al., 1997) (Figure 2.4). In protein kinases, the Gly-rich or nucleotide positioning loop (NPL) has the consensus sequence GXGXXG (where X is any other amino acid residue), and mutagenesis of these Gly residues to Ser or Ala is detrimental to enzymatic activity (Grant et al., 1998; Hemmer et al., 1997; Hirai et al., 2000). It has been postulated that the flexibility of the loop may be required for controlling the relative affinities for ATP and ADP (Hirai et al., 2000) and the loop may also be involved in the phosphoryl transfer step itself (Grant et al., 1998). Ser53, at the apex of the NPL in protein kinase A, has been suggested to interact with the γ-phosphate to aid in phosphoryl transfer (Aimes et al., 2000). The backbone amide of Ser53 forms a hydrogen bond with an axial oxygen of the γ-phosphate and, on the basis of the results for the Ser53Pro mutation, appears to be required for efficient catalysis, although the side chain hydroxymethyl group is not (Aimes et al., 2000).

Along with these active site similarities between APHs and Ser/Thr protein kinases, there are notable differences in their nucleotide binding sites (Burk et al., 2001). For example, Tyr42 in APH(3')-IIIa makes a π–π stacking interaction to ADP/ATP that is not present in Ser/Thr protein kinases where the equivalent residue is usually an Ala (Burk et al., 2001) (Figure 2.5). Considering that the π–π stacking arrangement is conserved in the APH(3') family of enzymes (either Tyr or Phe at this position) but is

lacking in protein kinases, taking advantage of this interaction in the design of inhibitors will provide some measure of specificity towards aminoglycoside kinases.

In this chapter, the molecular mechanism of APH(3')-IIIa has been investigated through characterization of important site-directed mutants. Much of this work was done in collaboration with Dr. Paul R. Thompson and I have included a number of his studies to provide a larger framework for these results. Complementary studies with the APH domain of AAC(6')-APH(2") have suggested that the chemical mechanisms of the two APHs are essentially identical.
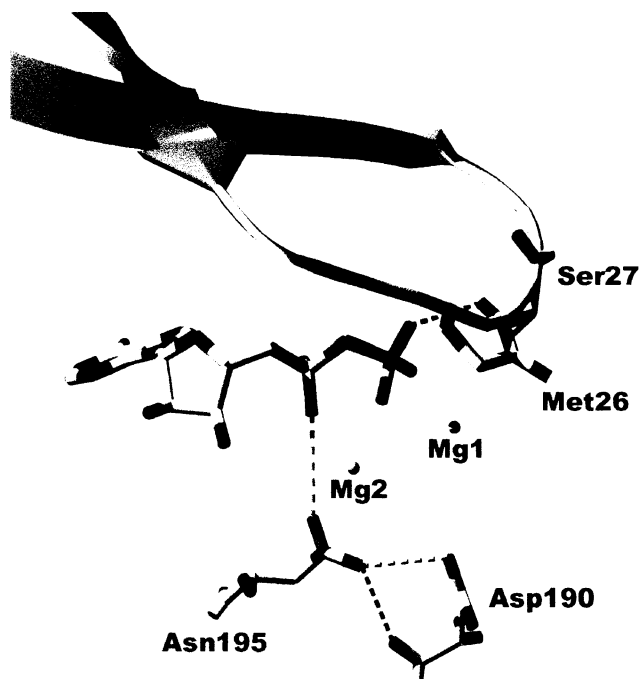
**Figure 2.4:** The Nucleotide Positioning Loop Region of APH(3')-IIIa. Met26 and Ser27 on the nucleotide positioning loop are highlighted. The structure shown is the binary complex between APH(3')-IIIa and ADP (PDB 1J7L).
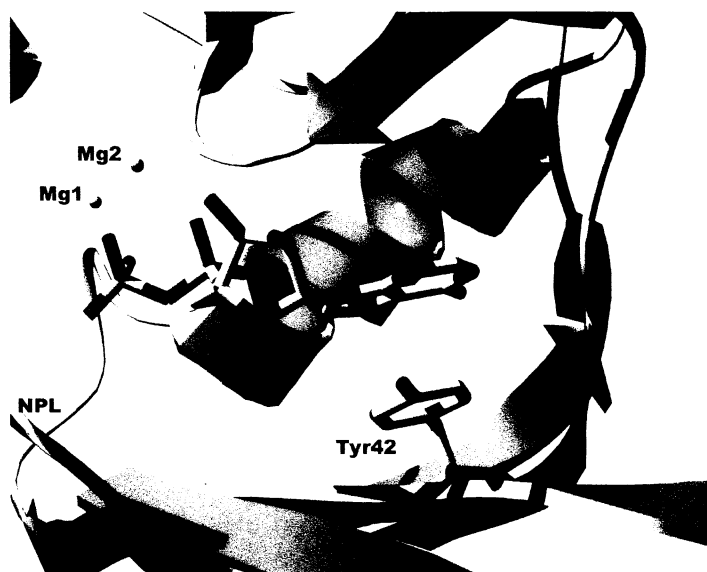


**Figure 2.5:** The π–π stacking interaction between Tyr42 in APH(3')-IIIa and ADP (PDB 1J7L).

39

## 2.2 Materials and Methods

### 2.2.1 Chemicals

ATP, ribostamycin, lividomycin, neomycin B, butirosin, amikacin, β-NADH, phosphoenolpyruvate, and PK/LDH enzymes were from Sigma (St. Louis, MO). Kanamycin A was from Bioshop (Burlington, Ontario, Canada). Oligonucleotide primers were purchased from the Central Facility of the Institute for Molecular Biology and Biotechnology, McMaster University.

### 2.2.2 Site-Directed Mutagenesis and Protein Purification

The Glu60Ala, Asp190Asn, and Asp190Glu site mutants were prepared by the "Megaprimer" methodology (Sarkar and Sommer, 1990). Primers were appropriately combined with primers p3'-PCR or p5'-PCR complimentary to ends of *aph(3')-IIIa* to generate the megaprimer by PCR using the plasmid pETSACG1 as a template, and this primer was used to amplify the complete gene containing the desired mutation. The remaining site-directed mutants were prepared according to the QuikChange method (Stratagene, LaJolla, CA). Positive clones were sequenced in their entirety at the Central Facility of the Institute for Molecular Biology and Biotechnology, McMaster University. The purification of APH(3')-IIIa has been described previously (McKay *et al.*, 1994), and the mutant enzymes were purified in an analogous manner. The purification of APH(2")-Ia is described in Chapter 3.

## 2.2.3 Protease Susceptibility of APH(3')-IIIa

A solution consisting of purified APH(3')-IIIa (12 µg) in 50 mM HEPES, pH 7.5, 40 mM KCl, 10 mM $MgCl_2$ in a final volume of 30 µL was incubated with 0.06 µg of subtilisin on ice for a time course up to 60 min. The reaction was quenched by the addition of 1 mM phenylmethylsulfonyl fluoride, and the products were separated by SDS-polyacrylamide gel electrophoresis (SDS PAGE). For large-scale production, APH(3')-IIIa (1 mg) was incubated with 2 mg subtilisin in a total volume of 1 mL 50 mM HEPES-NaOH pH 7.5, 40 mM KCl, 10 mM $MgCl_2$ for 1 hr at room temperature before stopping the reaction with 10 mL 100 mM phenylmethylsulfonyl fluoride. The reaction was desalted over a Superdex 75 size exclusion column at a flow rate of 0.25 mL/min water, before analyzed by matrix-assisted laser desorption time-of-flight mass spectrometry (MALDI-TOF) analysis at the Harvard Microchemistry Center (Boston, MA).

## 2.2.4 Aminoglycoside Phosphotransferase Assay

Aminoglycoside phosphotransferase activity was assayed by coupling ADP release to the activity of pyruvate kinase (PK) and lactate dehydrogenase (LDH) as previously described (Daigle *et al.*, 1999a; McKay *et al.*, 1994). Initial rates were fit using the nonlinear least-squares method contained with the Grafit 4.0 software package (Leatherbarrow, 2000) to either eq 2.1 or eq 2.2 if substrate inhibition was detected. A phosphocellulose binding assay (McKay *et al.*, 1994) was used for more sensitive detection. Values are reported +/- standard error.

$$v = (k_{cat}/E_t)[S]/(K_M + [S])$$                           (Eq. 2.1)

$$v = (k_{cat}/E_t)[S]/(K_M + [S]) (1 + [S]/K_i)$$             (Eq. 2.2)

## 2.2.5 Metal Ion Dependence

To measure the metal ion effect on initial rates, the concentrations of ATP (1 mM) and kanamycin (100 μM) were fixed, and the concentration of $MgCl_2$ varied between 0.1 and 10 mM. To ensure that the coupled assay system was active at such low concentrations of $Mg^{2+}$, ADP was added and the rate of reaction was determined. At all concentrations of $Mg^{2+}$ tested, the rate of ADP turnover was faster than the rate of aminoglycoside phosphorylation. The initial rates were fit to either Eq. 2.1 or Eq.2.2, depending on whether or not $Mg^{2+}$ inhibition was noted. The best fits of the data were obtained when the initial rates were plotted against the concentration of free $Mg^{2+}$ and not when plotted against the concentration of total $Mg^{2+}$. The concentration of free $Mg^{2+}$ was calculated using the parameters described previously (Fabiato and Fabiato, 1979).

## 2.2.6 Solvent Viscosity and Solvent Isotope Effects

Solvent viscosity effects and solvent isotope effects ($H_2O$ content $\leq 3.5\%$ (v/v)) were determined essentially as described (McKay and Wright, 1996). Glycerol was used as the microviscogen at concentrations from 0 to 30% (w/v), and the relative viscosity of the solutions was determined in quadruplicate using an Ostwald viscometer (McKay and Wright, 1996). Steady-state kinetic parameters were determined using the coupled assay described above. Macroviscogen controls were performed in all cases using PEG 8000.

## 2.2.7 Determination of Minimum Inhibitory Concentrations (MICs)

Bacterial cultures were streaked out over LB agar with ampicillin (50 µg/mL) as the selection marker and grown overnight at 37°C. Single colonies were selected and restreaked on LB agar with ampicillin and grown at 37°C for 18-24 h. A few colonies were picked and suspended in sterile 0.85% (w/v) NaCl to achieve an $OD_{625}$ of 0.08-0.1. These suspensions were then diluted to 1:10, and 5 µL of the diluted suspensions were added to 95 µL of Mueller-Hinton broth (Difco) in sterile microtiter plate wells containing serial dilutions of kanamycin A (0-512 µg/mL). The final dilution corresponds to ~5 × 10$^5$ colony forming units/mL. A sterile lid was placed over the microtiter plate, and it was allowed to incubate at 37°C for 16-20 h before being visually inspected for bacterial growth. It should be noted that the MIC results for *E. coli* expressing APH(3')-IIIa Glu60Ala, Asp190Ala, Asp190Asn, Asp190Glu, Asn195Ala, Asp208Ala, Asp208Asn, Asp208Glu were performed on polystyrene plates that bind positively charged compounds, such as aminoglycosides, and can cause an increase in the absolute values of MIC, whereas MIC results for *E. coli* expressing APH(3')-IIIa Met26Ala, Met26Pro, Ser27Ala, Ser27Pro were performed with polypropylene plates which do not suffer from this systematic error.

### 2.2.8 Circular Dichroism (CD) Spectra of APH(3')-IIIa WT and Tyr42Val

APH(3')-IIIa WT and Tyr42Val (5-10 mg/mL) were dialyzed extensively against 10 mM $Na_2HPO_4$ pH 8.0, and diluted to 10 µM with buffer. CD spectra were measured from 185 – 250 in a 1.0 mm-pathlength cell at 25°C using an Aviv Model 215 Circular

Dichroism Spectrophotometer (AVIV Instruments Inc, Lakewood, NJ). The buffer spectrum was subtracted from experimental spectra, and the resultants converted into molar ellipticity ($[\theta]$ deg cm$^2$ dmol$^{-1}$) using the packaged software.

### 2.2.9 Isothermal Titration Calorimetry (ITC)

All of the ITC experiments were performed on a VP-ITC instrument from Microcal Inc. (Northampton, MA). The experiments were conducted at 30°C in APH assay buffer that includes 50 mM HEPES-NaOH, pH 7.5, 40 mM KCl, and 10 mM MgCl$_2$. The proteins were dialyzed completely against buffer, and the buffer was used to dissolve ADP. The ADP solution was readjusted to pH 7.5 with a small amount of NaOH (1 M). The protein concentration in the sample cell of the calorimeter was 100–300 μM, and the ADP concentration in the syringe was 2 mM. The volume of the individual injection was 10 μL set at a syringe rate of 0.5 μL/s. A time period of 240 s was allowed between each injection for recovery back to baseline, and the stirring speed was set at 300 rpm. The experimental titrations were corrected for addition of buffer by subtracting the heat of dilution for ADP into buffer. The heat of dilution for the protein was found to be negligible. The binding data was then analyzed using Origin software (Wiseman *et al.*, 1989). The binding constant ($K$) and the enthalpy change ($\Delta H$) were used to calculate the free energy change ($\Delta G$), and the entropy change ($\Delta S$) according to the relations in Eq. 2.3.

$$-RT \ln K_{obs} = \Delta G_{obs} = \Delta H_{obs} - T\Delta S_{obs} \qquad \text{(Eq. 2.3)}$$

## 2.3 Results and Discussion

### 2.3.1 Partial Proteolysis of APH(3')-IIIa

With the many site-directed mutants of APH(3')-IIIa that were made, we were concerned to ensure that changes to steady-state kinetics parameters were an indication of important functions for those residues and not a reflection of gross structural changes to the protein which was of less interest. Protease susceptibility is a sensitive measure of changes in tertiary structure. Digestion of APH(3')-IIIa with subtilisin characteristically yields two N-terminal fragments, starting with His78 or Glu157 (Figure 2.6), as determined by MALDI–TOF mass spectrometry (Harvard Microchemistry Center, Boston, MA). All of the mutants described were assayed for changes in tertiary structure using subtilisin digestion and did not show any appreciable changes compared to wild-type. These results are consistent with no gross structural changes in APH(3')-IIIa upon site-directed mutation that would result in a difference in proteolysis patterns.



**Figure 2.6:** Positions of the Subtilisin Sites on APH(3')-IIIa.

### 2.3.2 Site-directed Mutagenesis of APH(3')-IIIa Residues Conserved with Ser/Thr/Tyr Protein Kinases

### 2.3.2.1 Glu60

Glu60 forms a salt bridge with Lys44 (Figure 2.3). This conserved residue does not appear to make a significant contribution to the catalytic power of APH(3')-IIIa as APH(3')-IIIa Glu60Ala mutant only showed slight changes in its ability to bind ATP and aminoglycoside, resulting in only minor changes to the specificity constants ($k_{cat}/K_M$) (Table 2.1).

### 2.3.2.2 Asn195

Asn195 coordinates to one of the magnesium ions present in the active site of APH(3')-IIIa. This magnesium ion (designated Mg2) in turn interacts with the $\beta$-phosphate of ATP (Figure 2.3). Mutation of this residue did not result in a significant change in $k_{cat}$ and only minor changes to $K_M$ values for a few of the aminoglycosides assayed (Table 2.1).

### 2.3.2.3 Asp190

The equivalent residue to Asp190 in Ser/Thr protein kinases (Asp166 in protein kinase A) has been hypothesized to act as an active site base as it is positioned in an appropriate position to deprotonate the incoming hydroxyl. Mutation of this residue to Ala (Daigle *et al.*, 1999b), Asn or Glu resulted in mutant enzymes with significant reductions in activity. However, if we estimate the p$K_a$ of the hydroxyl to be 15, and

bearing in mind that Asn would not act as an active site base having a $pK_a < 0$, the 140-fold decrease in activity seen with the Asp190Asn mutant is inconsistent with Asp190 acting as an active site base. Instead, Asp190 is more likely important for correctly orientating the incoming hydroxyl, and perhaps deprotonation following phosphoryl transfer, considering that the largest effects for APH(3')-IIIa Asp190Glu is an up to 1100-fold decrease in the specificity constants ($k_{cat}/K_M$) for aminoglycoside substrate (Table 2.1).

### 2.3.2.4 Asp208

Asp208 in APH(3')-IIIa coordinates both magnesium ions present in the active site of APH(3')-IIIa, along with making a H-bond interaction to Asn195 (Figure 2.3). The residue supplies two of the possible six coordinate interactions to Mg1, which is strategically positioned near the γ-phosphate and the incoming hydroxyl. The residue appears to be absolutely required as mutation to Ala (Daigle *et al.*, 1999b), Asn or Glu completely abolishes activity, having no detectable activity above the assay background even when conducted with a sensitive $^{32}P$ radioactive assay.

**Table 2.1:** Steady-state Kinetic Parameters for APH(3')-IIIa Wild-type and Site-Directed Mutants of Residues Conserved between Aminoglycoside and Protein Kinases.

| Substrate | | | | | |
|---|---|---|---|---|---|
| **APH(3')-IIIa WT** | $K_M$ ($\mu$M) | $k_{cat}$ (s$^{-1}$) | $k_{cat}/K_M$ (M$^{-1}$ s$^{-1}$) | $k_{cat}^{WT}/k_{cat}^{Mut}$ | $(k_{cat}/K_M)^{WT}/(k_{cat}/K_M)^{Mut}$ |
| ATP | 27.7 ± 3.7 | 1.76 ± 0.08 | 6.35 × 10$^4$ | | |
| Kanamycin A | 12.6 ± 2.6 | 1.79 ± 0.09 | 1.42 × 10$^5$ | | |
| Amikacin | 245 ± 27 | 2.46 ± 0.11 | 1.00 × 10$^4$ | | |
| Isepamicin | 198 ± 28.5 | 1.41 ± 0.35 | 0.71 × 10$^4$ | | |
| Neomycin B | 7.72 ± 0.9 | 2.08 ± 0.07 | 2.69 × 10$^5$ | | |
| Butirosin | 34.3 ± 3.1 | 2.02 ± 0.07 | 5.88 × 10$^4$ | | |
| Ribostamycin | 9.3 ± 1.8 | 1.89 ± 0.10 | 1.76 × 10$^5$ | | |
| Lividomycin A | 31.6 ± 5.1 | 3.97 ± 0.25 | 1.26 × 10$^5$ | | |
| **Glu60Ala** | | | | | |
| ATP | 12.5 ± 2.3 | 0.62 ± 0.02 | 4.96 × 10$^4$ | 2.8 | 1.4 |
| Kanamycin A | 7.8 ± 2.7 | 0.51 ± 0.02 | 6.54 × 10$^4$ | 3.5 | 2.2 |
| Amikacin | 57.6 ± 6.0 | 1.02 ± 0.03 | 1.77 × 10$^4$ | 2.4 | 0.6 |
| Neomycin B | 51.8 ± 11.5 | 2.60 ± 0.15 | 5.01 × 10$^4$ | 0.8 | 5.4 |
| **Asn195Ala** | | | | | |
| ATP | 113 ± 10 | 1.70 ± 0.06 | 1.50 × 10$^4$ | 1.0 | 5.8 |
| Kanamycin A | 15.6 ± 2.7 | 2.03 ± 0.07 | 1.30 × 10$^5$ | 0.9 | 1.1 |
| Amikacin | 1020 ± 260 | 0.83 ± 0.09 | 0.81 × 10$^3$ | 3.0 | 12.3 |
| Neomycin B | 4.1 ± 1.0 | 1.34 ± 0.05 | 3.27 × 10$^5$ | 1.6 | 0.8 |
| Isepamicin | 624 ± 149 | 0.86 ± .09 | 1.38 × 10$^3$ | 1.6 | 5.1 |
| Butirosin | 59.0 ± 17.0 | 0.53 ± 0.04 | 8.98 × 10$^3$ | 3.8 | 6.5 |
| Ribostamycin | 5.8 ± 1.0 | 1.86 ± 0.05 | 3.21 × 10$^5$ | 1.0 | 0.5 |
| Lividomycin A | 13.4 ± 3.2 | 3.05 ± 0.14 | 2.61 × 10$^5$ | 1.3 | 0.5 |
| **Asp190Asn** | | | | | |
| Kanamycin A | | 0.013 ± 0.001$^a$ | | 140 | |
| **Asp190Glu** | | | | | |
| ATP | 108 ± 11 | 0.047 ± 0.001 | 4.35 × 10$^2$ | 37 | 160 |
| Kanamycin A | 334 ± 37 | 0.043 ± 0.001 | 1.28 × 10$^2$ | 37 | 1100 |
| Amikacin | | ≤0.011 ± 0.0004$^a$ | | 220 | |
| Neomycin B | | ≤0.011 ± 0.0003$^a$ | | 190 | |

$^a$ The rates for the phosphorylation of amikacin and neomycin B were too slow to accurately measure the steady state kinetic parameters. Approximations for the $k_{cat}$ values are given.

## 2.3.3 Solvent Viscosity and Solvent Isotope Effects for Active Site Mutants

APH(3')-IIIa follows a Theorell-Chance like mechanism, where the rate determining step is not phosphoryl transfer itself, but rather the release of ADP (McKay and Wright, 1995; McKay and Wright, 1996). A similar case arises in protein kinase A, where pre-steady-state analysis has suggested that the phosphoryl transfer step is 25 times faster than ADP release (Grant and Adams, 1996). Thus, a change (or absence of a change) in the $k_{cat}$ for mutant APH(3')-IIIa may not reflect an alteration in the chemical rate of catalysis.

In the absence of pre-steady-state analysis, solvent viscosity effects give qualitative assessments of potential changes in the kinetic mechanisms of enzymes. In the case of APH(3')-IIIa, the solvent viscosity effect reaches a maximum of 1 (Brouwer and Kirsch, 1982) when ATP is used as the variable substrate (McKay and Wright, 1996) (Figure 2.7), reflecting rate-limiting ADP release. Solvent isotope effects can also be used to judge whether or not protonation/deprotonation plays any significant role in catalysis (Schowen and Schowen, 1982).

### 2.3.3.1 Glu60

Although there were not any significant differences in the activity for APH(3')-IIIa Glu60Ala compared to wild-type enzyme, it was possible that there were important changes to the molecular mechanism in the mutant that were not reflected in the steady-state kinetic parameters. However, this is unlikely to be the case as the solvent isotope

effects (SIE) for APH(3')-IIIa Glu60Ala closely matched that of the wild-type enzyme (Table 2.2). The effects are minor suggesting proton transfer makes a minimal contribution to catalysis, consistent with what is seen with C-terminal Src kinase (SIE = 1.2) (Cole *et al.*, 1994) and protein kinase A (SIE = 1.6) (Yoon and Cook, 1987). Any solvent isotope effect may be at least partially attributable to the higher viscosity of $D_2O$ compared to $H_2O$ (Schowen and Schowen, 1982), as both APH(3')-IIIa WT and Glu60Ala are diffusion controlled (Figure 2.7; Table 2.2).

**Table 2.2:** Solvent Isotope (SIE) and Solvent Viscosity Effects (SVE) for APH(3')-IIIa Wild-type and Glu60Ala and Asn195Ala Site-Directed Mutants.

| Enzyme | Varied substrate | SIE | | SVE |
| --- | --- | --- | --- | --- |
| | | $k_{cat}^{H}/k_{cat}^{D}$ | $(k_{cat}/K_M)^{H}/(k_{cat}/K_M)^{D}$ | $k_{cat}$ |
| WT | ATP | 1.79 ± 0.02 | 1.18 ± 0.09 | |
| | Kanamycin A | 1.67 ± 0.03 | 0.98 ± 0.07 | |
| Asn195Ala | ATP | 0.90 ± 0.03 | 0.60 ± 0.14 | 0.20 ± 0.06 |
| | Kanamycin A | 1.03 ± 0.04 | 0.64 ± 0.21 | |
| Glu60Ala | ATP | 1.79 ± 0.03 | 1.19 ± 0.09 | 2.89 ± 0.12 (glycerol) |
| | | | | 1.4 ± 0.2 (sucrose) |
| | Kanamycin A | 1.80 ± 0.04 | 1.11 ± 0.08 | |
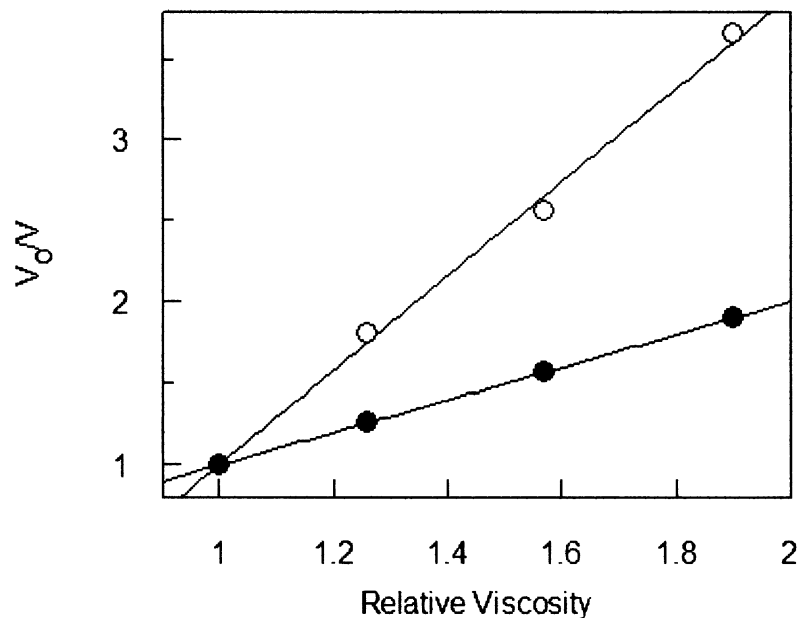
**Figure 2.7:** Solvent Viscosity Effects on the Maximal Rates of Wild-type (WT; ●) and Glu60Ala mutant (○) APH (3') IIIa-catalyzed Aminoglycoside Phosphorylation. Vo is the maximum rate without viscogen and V is the rate with the viscogen glycerol. Relative viscosities were determined using an Ostwald viscometer according to Section 2.2.

Viscosity experiments with APH(3')-IIIa yielded a SVE greater than 1, whether glycerol or sucrose was used as the microviscogen (Figure 2.7; Table 2.2). Glycerol and sucrose are unlikely to be inhibiting the mutant enzyme, considering that they do not have this effect on wild-type or the other site-directed mutants tested, and likely, there is more than one diffusion controlled rate limiting step(s) such as a diffusion controlled conformational change (Blacklow *et al.*, 1988; Simopoulos and Jencks, 1994). The mutant enzyme may need to undergo a larger diffusion-controlled conformational change in order to position Lys44 or other important residues prior to catalysis. Triosephosphate isomerase undergoes such a viscosity-dependent structural change (Sampson and Knowles, 1992), and it is well known from structural comparisons between active and

inactive protein kinases that in many of these kinases, including Hck (Sicheri *et al.*, 1997), the C-helix containing the conserved Glu must undergo a substantial conformational change upon activation (Johnson *et al.*, 1998). Although Glu60 may not be directly involved in catalysis, it is still important for the proper positioning of other catalytically important residues.

### 2.3.3.2 Asn195

APH(3')-IIIa Asn195Ala also did not show significant changes to the steady-state kinetic parameters. However, the solvent viscosity effect for APH(3')-IIIa Asn195Ala is significantly different from wild-type enzyme, as the activity of the mutant enzyme is completely independent of viscosity (Table 2.2). This result reflects a change in the rate-determining step, where ADP release is no longer rate limiting and catalysis likely makes a greater impact on the steady-state kinetic parameters. This is especially important in the light of the lack of any significant solvent isotope effect for Asn195Ala that suggests that proton mobilization plays no significant role in catalysis (Table 2.2).

### 2.3.4 Transition State Modeling of APH(3')-IIIa

The above studies have demonstrated that initial deprotonation of the aminoglycoside hydroxyl group to be phosphorylated is not essential for phosphate transfer (i.e. Asp190 is not acting as an active site base, lack of any significant solvent isotope effect). Phosphoryl transfer therefore likely proceeds through a dissociative-like mechanism with substantial P-O-P bond breakage prior to transfer to the incoming

hydroxyl, generating an electrophilic metaphosphate-like transition state, in agreement to what has been proposed for monophosphateester hydrolysis in solution (Herschlag and Jencks, 1989a; Kirby and Varvoglis, 1967; Knowles, 1980) and enzyme-catalyzed (Hengge *et al.*, 1995; Hollfelder and Herschlag, 1995; Kim and Cole, 1997; Kim and Cole, 1998; Weiss and Cleland, 1989) phosphoryl transfer reactions. With these results in mind, Dr. Albert Berghuis modeled in a dissociative-like transition state into the structure of APH(3')-IIIa to understand how other interactions in the enzyme may be involved in transition state stabilization. We were especially interested in interactions involving the 'nucleotide positioning loop' (NPL) which fits as a lid across the nucleotide binding site, changes conformation according to what is present at the active site (Burk *et al.*, 2001; Fong and Berghuis, 2002), and has been proposed to be directly involved in protein kinase A catalysis (Grant *et al.*, 1998).
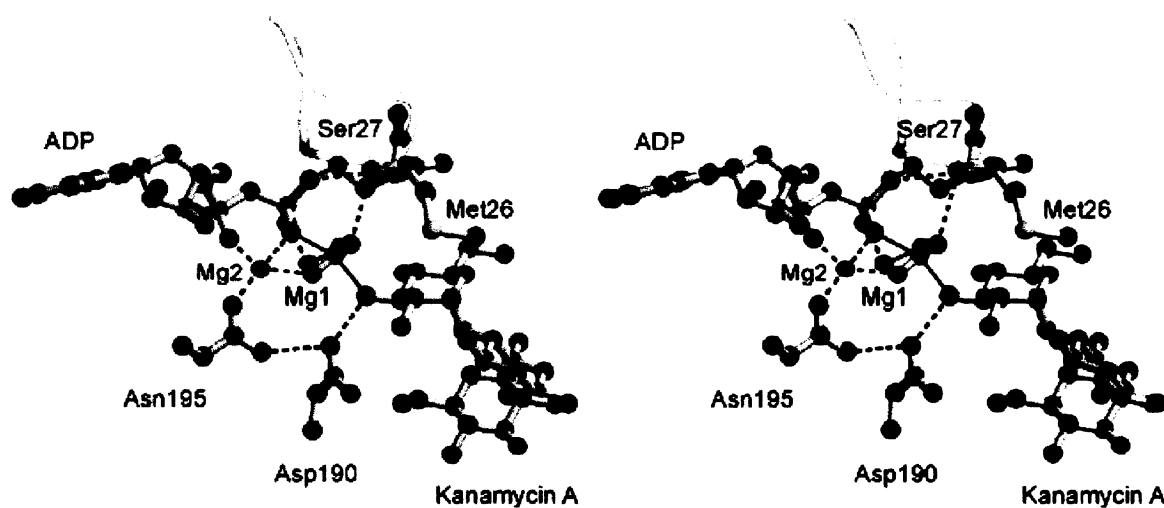


**Figure 2.8:** Modeling of a Dissociative-like Transition State in APH(3')-IIIa.

The constructed model predicts the presence of a hydrogen bond between the

Met26 backbone amide and one of the oxygens of the γ-phosphate/metaphosphate which

is not observed in any of the crystal structures. Ser27, on the NPL and completely

conserved in the APH(3') family of enzymes (Figure 2.9), is also interesting as the H-

bonds it donates to the β-phosphate changes depending on whether or not aminoglycoside

is bound to the structure. In the binary complexes (APH(3')-IIIa.AMPPNP and APH(3')-

IIIa.ADP), Ser27 donates a H-bond to a β-phosphate non-bridge oxygen through its

hydroxymethyl group (Burk *et al.*, 2001), whereas in complexes with nucleotide and

aminoglycoside, the backbone amide of Ser27 donates the H-bond (Fong and Berghuis,

2002). To validate the modeled transition-state structure and to learn more about the

potential roles the nucleotide positioning loop plays in the chemical mechanism of

APH(3')-IIIa, we characterized site-directed mutants of Met26 and Ser27.

```
APH(3')-VIIa    12 - - K C S - - - E  G  M  S  P A E V Y K C
APH(3')-Vc      11 H Y E W T S V N E  G  D  S  G A S V Y R L
APH(3')-IIa     22 - Y D W A Q Q T I  G  C  S  D A A V F R L
APH(3')-Ic      26 - Y R W A R D N V  G  Q  S  G A T I Y R L

APH(3')-IIIa    16 K Y R C V K D T E  G  M  S  P A K V Y K L
                        *  *  *  *  *  *  *  *
```

**Figure 2.9:** Sequence of the Nucleotide Positioning Loop Region of APH(3'). Sequence comparisons of the APH(3') family of enzymes. Asterisks indicate the nucleotide positioning loop region. Only Gly25 and Ser27 are absolutely conserved.

### 2.3.5 Site-directed Mutagenesis of APH(3')-IIIa Residues on the Nucleotide Positioning Loop (NPL)

#### 2.3.5.1 Ser27

The mutagenesis of Ser27 had a dramatic effect on the kinetic parameters for both ATP and a number of aminoglycoside substrates (Table 2.3). Both turnover rate ($k_{cat}$) and substrate capture ($k_{cat}/K_M$) were significantly depressed in the mutants, where the decrease in $k_{cat}$ was most responsible for the change in $k_{cat}/K_M$. The Ser27Pro mutation had the greatest effect, where it generally showed greater than a 10-fold further reduction in kinetic parameters compared to the Ser27Ala mutation (Table 2.3). These results are not due to misfolded enzymes as protease sensitivity assays that detect unfolded regions of the protein are consistent with WT results. Mutation of Ser27Pro (or Met26Pro; see below) has the potential to significantly disrupt local protein structure, either as a result of steric clashes due to the side chain or that appropriate $\psi$ and $\phi$ angles are unattainable for a Pro residue in this position. Close inspection of the structure in the NPL indicates that the Pro mutations will not cause significant perturbations in the protein structure. Furthermore, experimental protease sensitivity assays that detect unfolded regions of the protein are consistent with WT results.

The decrease in $k_{cat}$ suggested that for the Ser27Ala mutant ADP release is no longer fully rate-limiting, which is the case for the wild-type enzyme (McKay and Wright, 1995; McKay and Wright, 1996). Solvent viscosity effects on ATP-dependent steady-state kinetics for this mutant (Figure 2.10, $SVE_V$ = -0.25 ± 0.06) are consistent with a viscosity-independent rate-limiting step, most likely the chemical step.

As with the WT and other mutants of APH(3')-IIIa, the solvent isotope effects in D$_2$O for either ATP or kanamycin are not significant (Table 2.4), suggesting again that deprotonation of the substrate alcohol is not important for rate enhancement in this mutant.

On the basis of our earlier work on the Mg$^{2+}$ dependence of wild-type and mutant APH(3')-IIIa proteins, which indicated the importance of metal ions to catalysis, we also examined the metal ion dependence of the Ser27Ala and the Ser27Pro mutants (Figure 2.11). In contrast to the WT enzyme (Boehr *et al.*, 2001b), the Ser27 mutants do not demonstrate a dramatic decrease in rate with increasing Mg$^{2+}$ concentrations.

**Table 2.3:** Steady-State Kinetic Parameters for Nucleotide Positioning Loop Site-Directed Mutants of APH(3')-IIIa.

| substrate | $K_M$ (μM) | $k_{cat}$ (s$^{-1}$) | $k_{cat}/K_M$ (M$^{-1}$ s$^{-1}$) | $k_{cat}^{WT}/k_{cat}^{Mut}$ | $(k_{cat}/K_M)^{WT}/(k_{cat}/K_M)^{Mut}$ |
|---|---|---|---|---|---|
| **Ser27Ala** | | | | | |
| ATP | 54.4 ± 6.5 | 0.51 ± 0.02 | 9.4 × 10$^3$ | 3.5 | 6.8 |
| kanamycin A | 15.0 ± 3.7 | 0.61 ± 0.03 | 4.1 × 10$^4$ | 2.9 | 3.5 |
| neomycin B[a] | | 0.28 ± 0.02 | | 7.4 | |
| amikacin | 574 ± 162 | 0.32 ± 0.04 | 5.6 × 10$^2$ | 7.7 | 18 |
| Ribostamycin | 13.9 ± 3.8 | 0.68 ± 0.03 | 4.9 × 10$^4$ | 2.8 | 4.1 |
| **Ser27Pro** | | | | | |
| ATP[b] | 32.3 ± 3.9 | 0.056 ± 0.001 | 1.7 × 10$^3$ | 31 | 37 |
| kanamycin A | 11.9 ± 1.7 | 0.038 ± 0.001 | 3.2 × 10$^3$ | 47 | 45 |
| neomycin B[c] | | 0.0518 ± 0.0004 | | 40 | |
| amikacin[d] | | ≤0.009 ± 0.0004 | | 273 | |
| butirosin | 122.3 ± 33.4 | 0.021 ± 0.002 | 1.7 × 10$^2$ | 96 | 346 |
| ribostamycin | 5.0 ± 0.7 | 0.047 ± 0.001 | 9.4 × 10$^3$ | 40 | 22 |
| **Met26Ala** | | | | | |
| ATP | 4.89 ± 0.43 | 0.69 ± 0.01 | 1.4 × 10$^5$ | 2.6 | 0.45 |
| Kanamycin A | 22.4 ± 3.5 | 0.72 ± 0.01 | 3.2 × 10$^4$ | 2.5 | 4.4 |
| neomycin B | 7.91 ± 1.09 | 0.83 ± 0.02 | 1.1 × 10$^5$ | 2.5 | 2.4 |
| amikacin | 274 ± 18 | 0.70 ± 0.02 | 2.5 × 10$^3$ | 3.5 | 4 |
| butirosin | 12.9 ± 2.0 | 0.89 ± 0.03 | 6.9 × 10$^4$ | 2.3 | 0.85 |
| ribostamycin | 9.63 ± 1.01 | 0.69 ± 0.02 | 7.2 × 10$^4$ | 2.7 | 2.8 |
| **Met26Pro** | | | | | |
| ATP | 28.1 ± 4.4 | 0.12 ± 0.01 | 4.4 × 10$^3$ | 15 | 14 |
| Kanamycin A | 15.7 ± 2.8 | 0.15 ± 0.01 | 9.8 × 10$^3$ | 12 | 14 |
| neomycin B | 9.76 ± 2.22 | 0.21 ± 0.01 | 2.2 × 10$^4$ | 10 | 12 |
| amikacin | 424 ± 46 | 0.07 ± 0.00 | 1.8 × 10$^2$ | 35 | 56 |
| butirosin | 73.1 ± 7.8 | 0.20 ± 0.01 | 2.7 × 10$^3$ | 10 | 22 |
| ribostamycin | 13.4 ± 1.3 | 0.16 ± 0.01 | 1.2 × 10$^4$ | 12 | 17 |

[a] The $K_M$ for neomycin B could not be reliably determined, but we can estimate an upper limit of 3.5 μM. [b] Neomycin B was fixed at 100 μM. [c] $V_{max}$ occurred at the lowest substrate concentration tested. The $k_{cat}$ reported is an estimation using the data corresponding to 100 μM neomycin B and 1 mM ATP. [d] Amikacin was an exceptionally poor substrate for the Ser27Pro mutant. Thus an estimation of the $k_{cat}$ was made using the rate of reaction observed at 1.5 mM amikacin and 1 mM ATP.
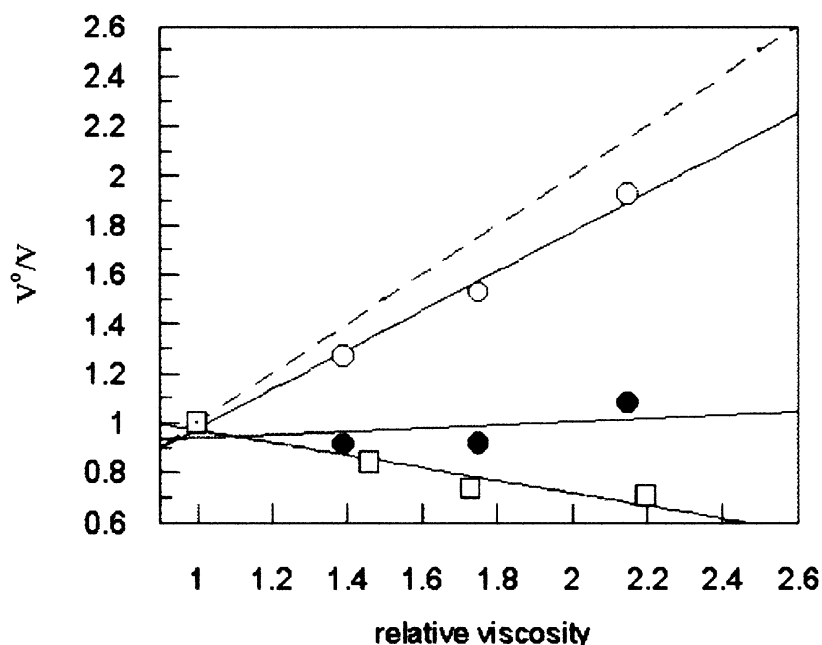


**Figure 2.10:** Solvent Viscosity Effect on the Steady-State Kinetics of ATP Utilization of APH(3')-IIIa Mutant Proteins: Ser27Ala (□), Met26Ala (O), and Met26Pro (●). The SVE for WT enzyme approaches the theoretical maximum effect of 1 (dashed line), indicative of a viscosity-dependent rate-limiting step.

**Table 2.4:** Solvent Isotope Effects for APH(3')-IIIa NPL Site-Directed Mutants Met26Pro and Ser27Ala.

| Enzyme | $^H V / ^D V$ | | $^H (V/K) / ^D (V/K)$ | |
|---|---|---|---|---|
| | ATP | Kanamycin A | ATP | Kanamycin A |
| Ser27Ala | 0.93+/-0.04 | 0.90+/-0.04 | 0.73 +/- 0.11 | 0.98 +/- 0.14 |
| Met26Pro | 1.24 +/- 0.08 | 0.883 +/- 0.079 | 1.21 +/- 0.27 | 1.19 +/- 0.34 |
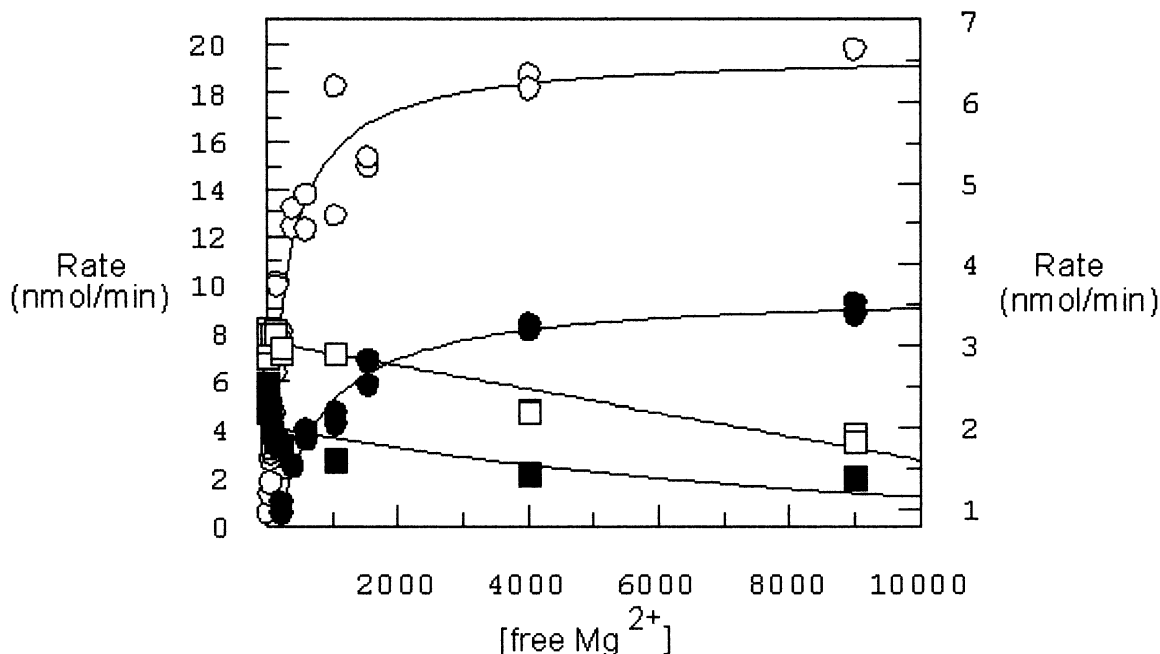
**Figure 2.11:** Magnesium Ion Dependence of APH(3')-IIIa Ser27 and Met26 Mutant Proteins. The initial rates obtained for Ser27Ala (O) and Met26Ala (■) were plotted using the left $Y$-axis whereas the initial rates obtained for the Ser27Pro (●) and Met26Pro (□) were plotted using the right $Y$-axis. The concentrations of ATP (1 mM) and kanamycin (100 μM) were fixed at 1 and 0.1 mM, respectively.

## 2.3.5.2 Met26

Structural modeling of APH(3')-IIIa-catalyzed phosphoryl transfer indicated that a hydrogen bond between the backbone amide of Met26 to a metaphosphate-like intermediate or transition-state could occur. Consequently, we generated the Met26Ala and Met26Pro mutant proteins for *in vitro* and *in vivo* analyses to test this hypothesis. Met26 is not conserved among the APH(3') family of enzymes (Figure 2.9), and it was therefore not unexpected that mutation of this residue to Ala had little effect on enzyme activity (Table 2.3; only a modest decrease in $k_{cat}$ of 2.3-3.5-fold). Recall that the wild-type enzyme follows a Theorell-Chance kinetic mechanism (McKay and Wright, 1995;

McKay and Wright, 1996), and hence $K_M$ for ATP closely approximates $K_d$ for this substrate. Upon mutation of Met26 to Ala, the $K_M$ for ATP decreases significantly (5.7-fold, Table 2.3), and the affinity for ADP may likewise decrease, resulting in a lowered rate for ADP release and a decreased $k_{cat}$. Indeed, comparable to the WT enzyme, $k_{cat}$ for this mutant is largely viscosity dependent (Figure 2.10, $SVE_V = 0.80 \pm 0.05$), indicating that there is not a significant change to the contributions that govern $k_{cat}$.

APH(3')-IIIa Met26Pro mutant is significantly impaired in its ability to phosphorylate aminoglycosides (Table 2.3), where the majority of the effect is associated with a decrease in $k_{cat}$ (10-35-fold). Unlike the Met26Ala mutant, the activity of Met26Pro is not affected by increases in viscosity (Figure 2.10) and likely suggests that, analogous to the Ser27 mutations, the phosphoryl transfer step makes an important contribution to $k_{cat}$ in this mutant. APH(3')-IIIa Met26Pro also does not display a significant solvent isotope effect (Table 2.4), paralleling the wild-type and Ser27Ala results.

The magnesium dependence of Met26Ala is similar to WT where activity decreases with increasing metal ion concentration, whereas Met26Pro shows a pattern similar to the Ser27 mutations (Figure 2.11). The change in the magnesium dependence patterns in the Ser27 and Met26Pro mutants, alongside the lack of a solvent viscosity effect for these mutants, strongly suggests a change to the factors governing the turnover rate. The results for the Met26 mutants are unlikely to be due to misfolded enzyme as protease sensitivity patterns for these mutants were identical to wild-type patterns.

## 2.3.6 Biological Assessment of APH(3')-IIIa Site-Directed Mutants

For a comparison to the *in vitro* kinetic data, minimum inhibitory concentrations (MICs) for *Escherichia coli* carrying the WT and mutated resistance determinants were compared to the MICs for *E. coli* without an aminoglycoside resistance determinant. It should be noted that the MICs for the Glu60, Asp190, Asn195 and Asp208 mutants were conducted on polystyrene plates, whereas the MICs for the Met26 and Ser27 mutants were conducted on polypropylene plates. Polystyrene can bind positively charged compounds like aminoglycosides and cause a systematic increase in the MIC value, however, what is most important in these assays is the relative comparison between *E. coli* expressing and not expressing resistance protein.

The MIC results agree with the *in vitro* assays (Table 2.5). For example, resistance is completely abrogated with the Asp208 mutants, again arguing for a critical role for this residue. Although there was not a significant change with respect to the steady-state kinetic parameters for the Glu60Ala or Asn195Ala mutants, there was a much greater impact on biological resistance, especially with the Asn195Ala mutant (Table 2.5). These results are in agreement with the solvent viscosity effects for these mutants that suggest that although the steady-state kinetic parameters did not change, there are important changes to enzyme function upon mutation of these absolutely conserved residues.

**Table 2.5:** Minimum Inhibitory Concentration (MIC) Determinations for APH(3')-IIIa Mutants.

| Protein | MIC of Kanamycin A (µg/mL) |
|---|---|
| *Polystyrene Microtitre Plates* | |
| BL21(DE3)/pET22b(+) control | 8 |
| WT | >512 |
| Glu60Ala | 512 |
| Asp190Ala | 16 |
| Asp190Asn | 16 |
| Asp190Glu | 16 |
| Asn195Ala | 64 |
| Asp208Ala | 8 |
| Asp208Asn | 8 |
| Asp208Glu | 8 |
| *Polypropylene Microtitre Plates* | |
| BL21(DE3)/pET22b(+) control | 2 |
| WT | 1024 |
| Met26Ala | 512 |
| Met26Pro | 128 |
| Ser27Ala | 64 |
| Ser27Pro | 4 |

With respect to the nucleotide positioning loop mutants, consistent with the *in vitro* effects, mutation of Met26 to Ala appeared to have little effect, whereas there were significant decreases in MICs for the Ser27 and Met26Pro mutants (Table 2.5). Mutation of Ser27 to Pro had the largest effect, where the MIC was nearly indistinguishable from *E. coli* without an aminoglycoside resistance determinant.

### 2.3.7 Model for the Molecular Mechanism of APH(3')-IIIa

The results obtained are consistent with a model of phosphoryl transfer where nucleotide positioning residues Ser27 and Met26 play important roles (Figure 2.12). Upon Mg-ATP binding, the nucleotide positioning loop undergoes a conformation

change permitting the formation of a hydrogen bond between the hydroxymethyl group of Ser27 and a β-phosphate nonbridge oxygen; the other nonbridge oxygen on the β-phosphate acts as a ligand to Mg1. Mg1 also interacts with the γ-phosphate of ATP and is linked to the enzyme via the invariant and essential Asp208; thus this magnesium ion is positioned as a fulcrum from which phosphoryl transfer occurs. In a dissociative mechanism, the γ-PO bond must lengthen to generate the elongated transition state, and it follows that the interaction between Mg1 and the β-phosphate must be weakened so that the γ-phosphate can be transferred. Upon binding aminoglycoside, APH(3')-IIIa undergoes a conformational change in the NPL such that the side chain of Ser27 begins to translate away and the amide backbone of Ser27 is pressed toward the β-phosphate. These events help to turn the β-phosphate on its axis, and as the nonbridge oxygens of the γ- and β-phosphates begin to eclipse, the repulsion between the two phosphates will increase and the γ-PO bond will weaken. The structure of APH(3')-IIIa in complex with ADP and kanamycin A reveals an additional hydrogen bond to the β-phosphate nonbridge oxygen by the Ser27 backbone amide (Fong and Berghuis, 2002). Therefore, during group transfer, this addition must occur along with bond breakage between the β- and γ-phosphate, resulting in a net increase in distance between Mg1 and its β-phosphate oxygen ligand. The importance of the amide of Met26 would lie in stabilization of the metaphosphate, possibly through a direct interaction (Figure 2.12). The nucleotide positioning loop therefore serves as a lever working with Mg1 to facilitate the requisite β-

γ phosphate bond breakage necessary for generation of the metaphosphate-like transition-state.

Asp190, in this model, would be important in positioning the incoming hydroxyl and may act after or during the late stages of phosphoryl transfer as an active site base. Lys44 and Asn195 act as important ATP-binding residues to both efficiently capture ATP and to help regulate substrate/product flux through the enzyme. Additionally, Lys44 may be involved in drawing and stabilizing additional electron density into the β-phosphate non-bridge oxygen to accommodate the proposed mechanism, where Glu60 plays a critical role in positioning this residue.
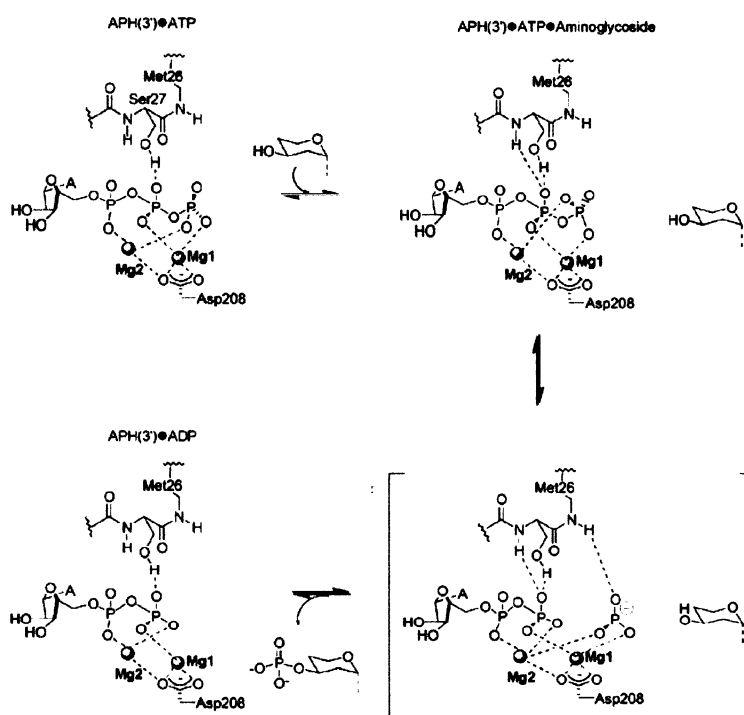


**Figure 2.12:** Proposed Role of the Nucleotide Positioning Loop in APH(3')-IIIa-catalyzed Phosphoryl Transfer.

### 2.3.8 Analysis of the π–π Stacking Interaction Between APH(3')-IIIa Tyr42 and ATP/ADP

Although the catalytic mechanism for APHs and ePKs are likely to be similar, there are many differences in the active sites between these classes of enzymes, including a π–π stacking interaction in the APH(3') family of enzymes that is lacking in the protein kinases (Figure 2.5). This site thus serves as a site of discrimination between APHs and protein kinases that can anchor specific inhibitors to the APH(3') family of enzymes.

To investigate the nature of the π–π interaction in the nucleotide binding site of APH(3')-IIIa, I produced mutant proteins Tyr42Ala, Tyr42Phe, and Tyr42Val. APH(3')-IIIa Tyr42Ala was insoluble and could not be used in the study. This indicates that Tyr42 may be important in the proper folding of the enzyme. Proteolysis studies of the mutant Tyr42Val and Tyr42Phe proteins with subtilisin yielded the same fragment pattern as APH(3')-IIIa WT protein, suggesting that there are no gross alterations in protein structure with these mutant proteins. Furthermore, the far-UV circular dichroism (CD) spectra for APH(3')-IIIa WT and APH(3')-IIIa Tyr42Val (Figure 2.13) are essentially identical, verifying that proper secondary structure is maintained upon mutation of Tyr42. Together, these results suggest that there are no significant structural differences between APH(3')-IIIa WT and Tyr42Phe and Tyr42Val proteins.
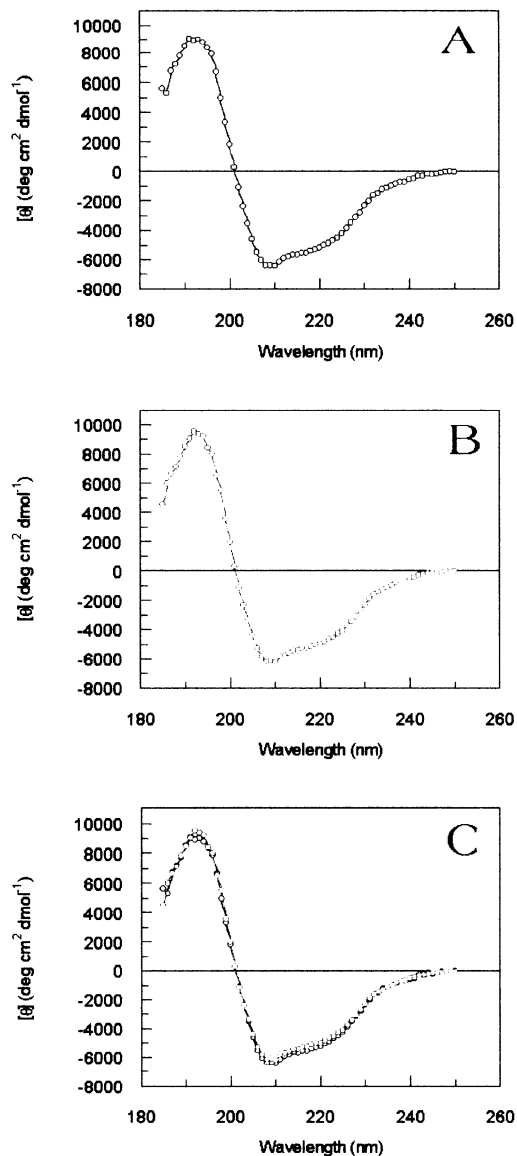
**Figure 2.13:** Secondary Structure Comparisons of APH(3')-IIIa WT (A) and Tyr42Val (B) Proteins using Circular Dichroism. CD spectra of 10 µM protein solutions in 10 mM Na₂HPO₄ pH 8.0 were determined using an Aviv Model 215 CD spectrophotometer with a 1.0 mm-pathlength cell set at 25°C. The overlap of WT and Tyr42Val spectra is pictured in C.

## 2.3.8.1 Kinetic Analyses of Tyr42 Mutants

For APH(3')-IIIa, $K_M$ for ATP gives a true dissociation constant and can be used as a measure of nucleotide affinity for the protein. Furthermore, ADP departure is rate limiting, and so, tighter binding of nucleotide may result in a slower release of ADP and a decrease in the overall rate ($k_{cat}$). APH(3')-IIIa Tyr42Phe appeared to bind ATP more tightly than wild-type enzyme, where $K_M$ for ATP decreased 4-fold compared to WT enzyme (Table 2.6). The apparent affinities for the aminoglycosides kanamycin A and neomycin B were less affected by the mutation, where the changes in $K_M$ were less than two-fold. The tighter binding of nucleotide (ATP/ADP) is reflected in the decrease in $k_{cat}$ (1.4- to 5.2-fold; Table 2.6).

The mutation of Tyr42Val had a much more dramatic effect on the affinity for ATP, where $K_M$ for ATP increased nearly 10-fold (Table 2.6). The affinity for ADP was likely decreased as well considering the modest increase in $k_{cat}$ (2-fold), despite an overall decrease in the catalytic efficiency ($k_{cat}/K_M$; 5.9-fold). The $K_M$ values for the 4,6-disubstituted aminoglycoside kanamycin A, but not the 4,5-disubstituted neomycin, is reduced modestly in the Tyr42Val mutant compared to the WT and Tyr42Phe enzymes. Unlike ATP, the $K_M$ for aminoglycosides is a complex function of several rate constants, and this slight change in value is not likely attributable to a change in $K_d$, especially as the amino acid is remote from the aminoglycoside binding site and there is no comparable effect on neomycin $K_M$.

**Table 2.6:** Steady-State Kinetic Parameters for APH(3')-IIIa Tyr42 Mutants.

| | $K_M$ ($\mu$M) | $k_{cat}$ (s$^{-1}$) | $k_{cat}/K_M$ (M$^{-1}$s$^{-1}$) | $K_M^{Mut}/ K_M^{WT}$ | $k_{cat}^{WT}/ k_{cat}^{Mut}$ | $(k_{cat}/K_M)^{WT}/ (k_{cat}/K_M)^{Mut}$ |
|---|---|---|---|---|---|---|
| **Tyr42Phe** | | | | | | |
| ATP | 6.31 +/- 0.57 | 0.34 +/- 0.01 | 5.32 x 10$^4$ | 0.23 | 5.2 | 1.2 |
| Kanamycin A | 8.74 +/- 2.6 | 0.36 +/- 0.02 | 4.08 x 10$^4$ | 0.69 | 5.0 | 3.5 |
| Neomycin B | 13.8 +/- 1.6 | 1.54 +/- 0.05 | 1.11 x 10$^5$ | 1.8 | 1.4 | 2.4 |
| **Tyr42Val** | | | | | | |
| ATP | 272 +/- 23 | 2.93 +/- 0.07 | 1.08 x 10$^4$ | 9.8 | 0.60 | 5.9 |
| Kanamycin A[a] | 3.56 +/- 1.29 | 2.70 +/- 0.14 | 7.59 x 10$^5$ | 0.28 | 0.66 | 0.19 |
| Neomycin B[a] | 6.93 +/- 1.68 | 1.87 +/- 0.10 | 2.70 x 10$^5$ | 0.90 | 1.1 | 1.0 |

[a] parameters determined in the presence of 3 mM ATP.

### 2.3.8.2 Thermodynamic Analyses of Tyr42 Mutants

The thermodynamics of the interaction between APH(3')-IIIa and nucleotide ligand can be investigated directly through isothermal titration calorimetry (ITC). ITC measures the heat exchanged with the environment upon association between a receptor and a ligand. Thus, ITC directly measures the enthalpy of binding ($\Delta$H), and a titration of the binding sites will yield an association constant ($K_a$). Using these two values, we can obtain a complete thermodynamic profile of the interaction using the formula:

$$-RT \ln K_{a,obs} = \Delta G_{obs} = \Delta H_{obs} - T\Delta S_{obs}$$

As $K_M$ for ATP closely approximates $K_d$ for ATP for APH(3')-IIIa, we can get an estimate of the Gibbs free energy of ATP binding (Table 2.7). These values are very

comparable to those values for the Gibbs free energy of ADP binding using ITC (Figure 2.14; Table 2.7). From the ITC experiments, it can be seen that ADP binding to APH(3')-IIIa WT is dominated by enthalpic forces, whereas the entropic contribution is unfavorable (Table 2.7). Similarly, binding of ADP to APH(3')-IIIa Tyr42Phe is governed by enthalpy and entropy is unfavorable; however, enthalpy is slightly less favorable and entropy is slightly more favorable with the Tyr42Phe mutant protein compared to WT (Figure 2.15).

**Table 2.7:** Thermodynamic Parameters for Nucleotide Binding to APH(3')-IIIa WT and Tyr42 Mutants[a].

| | ATP[b] | | ADP[c] | | | |
|---|---|---|---|---|---|---|
| | $K_d$ ($\mu$M) | $\Delta G_{obs}$ (kcal/mol) | $K_{d,obs}$ ($\mu$M) | $\Delta H_{obs}$ (kcal/mol) | $-T\Delta S_{obs}$ (kcal/mol) | $\Delta G_{obs}$ (kcal/mol) |
| WT | 27.7 +/- 3.7 | - 6.46 | 17.0 +/- 2.6 | -11.5 +/- 0.5 | + 4.90 | - 6.62 |
| Tyr42Phe | 6.31 +/- 0.57 | - 7.38 | 6.46 +/- 0.28 | -10.2 +/- 0.2 | + 3.00 | - 7.20 |
| Tyr42Val | 272 +/- 23 | - 5.06 | 187 +/- 26 | -1.95 +/- 0.2 | - 3.22 | - 5.17 |

[a] the values determined in 50 mM HEPES-NaOH pH 7.5, 40 mM KCl, 10 mM $MgCl_2$. [b] in APH(3')-IIIa, the $K_M$ for ATP approximates $K_d$ for ATP, so $\Delta G$ was calculated according to $\Delta G = -RT \ln (1/K_d)$, where T= 310 K in the kinetic assays. [c] parameters for ADP were determined using ITC at 303 K as described in Section 2.2.
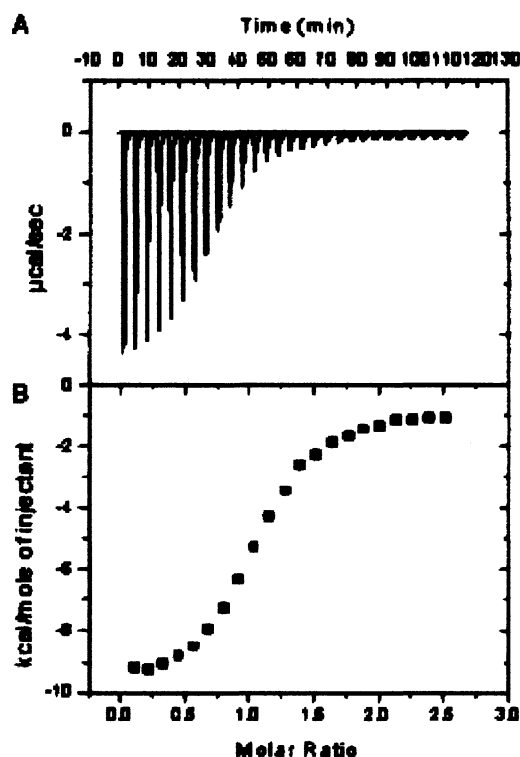
**Figure 2.14:** Isothermal Calorimetric Titration for the Interaction between ADP and APH(3')-IIIa. A. Raw data for 22 10-μL injections of ADP (2.0 mM stock) into the isothermal cell containing 100 μM APH(3')-IIIa WT at 4 min intervals and 30°C. Both the protein and ADP were in 50 mM HEPES-NaOH pH 7.5, 40 mM KCl, 10 mM MgCl$_2$. B. Experimental points were obtained by the integration of the above peaks and plotted against the molar ratio of ADP to protein in the reaction cell.

In contrast to the results for APH(3')-IIIa WT and Tyr42Phe, the entropy contribution is favorable for Tyr42Val and is most responsible for the interaction with ADP, although enthalpy still makes an important contribution (Table 2.7; Figure 2.15). Molecular modeling by Dr. J.R. Cox on the nucleotide binding site of APH(3')-IIIa has revealed that replacing Tyr with Val at position 42 should not hinder the nucleotide from entering the adenine binding region. In addition, the mutation to Val makes the adenine binding region more hydrophobic, an environment common to the binding of the adenine ring in other protein complexes (Chakrabarti and Samanta, 1995). Our results with the

Tyr42Val mutant suggest that the binding of ADP is entropically driven, which is to be

expected when binding is mostly hydrophobic or dispersive in nature (Dill, 1990).

However, in the case of APH(3')-IIIa, having a more hydrophobic nucleotide binding

pocket (as in the Tyr42Val mutant) compromises nucleotide affinity. This result

highlights the importance of polar interactions in the association of an aromatic amino

acid in position 42 and the adenine ring and the difference between the nucleotide

binding pocket of APH(3')-IIIa and those of other similar ATP binding proteins,

including Ser/Thr protein kinases. These discrete requirements for high-affinity binding

to APH(3')-IIIa and the conservation of the Tyr residue among six of the APH-class

enzymes (Shaw *et al.*, 1993) provides the structural and energetic leverage for the

development of ATP-site-directed inhibitors specific for APH enzymes.
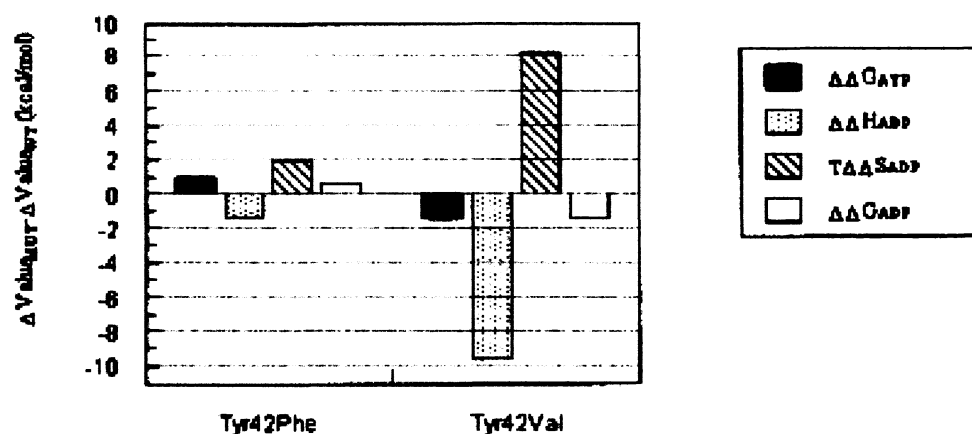


**Figure 2.15:** Changes in the Thermodynamic Contributions to Nucleotide Binding upon Mutation of APH(3')-IIIa Tyr42. Plotted values are relative to WT (i.e. $\Delta\Delta$Value = $\Delta$Value$_{MUT}$ − $\Delta$Value$_{WT}$), thus, positive values indicate that the thermodynamic parameter is more favorable in the mutant compared to WT.

### 2.3.9 Comparison of the Molecular Mechanism of APH(3')-IIIa to Other Aminoglycoside Phosphotransferases

### 2.3.9.1 Phosphotransferase Domain of AAC(6')-APH(2")

Although less studies have been undertaken to study the molecular mechanism of the phosphotransferase domain of the bifunctional enzyme (APH(2")-Ia), the results are consistent with those for APH(3')-IIIa. For example, the mutagenesis of the APH(3')-IIIa-equivalent residues of Lys44 (Boehr *et al.*, 2001a) (Chapter 3) and Asp190 (Daigle *et al.*, 1999b) in APH(2")-Ia yielded consistent results with those seen above and have further underscore the importance of these residues to enzyme-catalyzed aminoglycoside phosphorylation. To further compare the molecular mechanisms of APH(2")-Ia and APH(3')-IIIa, I determined the effects of solvent viscosity, solvent isotope and metal ion concentration on the activity of APH(2")-Ia.

Unlike APH(3')-IIIa, APH(2")-Ia does not display a significant solvent viscosity effect with respect to the $k_{cat}$ for ATP (Figure 2.16), higher magnesium concentrations do not inhibit the enzyme (Figure 2.17) and manganese can be effectively used as the divalent metal ion (Figure 2.17). These results suggest that unlike APH(3')-IIIa, ADP release is not the rate-determining step and the chemical step likely makes an important contribution to the turnover rate.
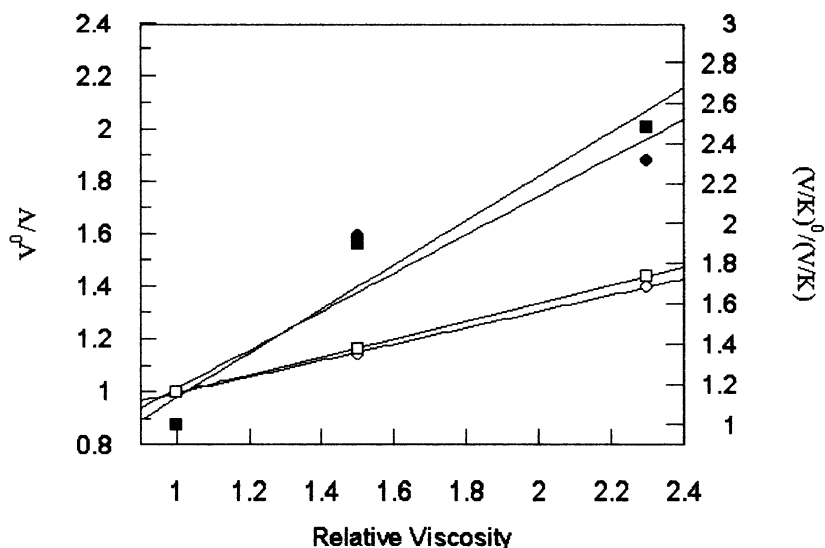
**Figure 2.16:** Solvent Viscosity Effects for APH(2")-Ia using ATP (V -O; V/K - ●) or Kanamycin A (V- □; V/K- ■) as the Variable Substrate.

APH(2")-Ia does not display any significant solvent isotope effects (Table 2.8), and so, similar to APH(3')-IIIa, substrate deprotonation does not contribute significantly to substrate turnover. These initial results are in agreement with those seen with APH(3')-IIIa, suggesting both enzymes operate through dissociative-like mechanisms. However, the differences seen in the solvent viscosity and metal ion dependence studies suggest that although the overall mechanism may be similar, the microscopic rate constants contributing to the steady-state kinetic parameters are significantly different. Moreover, residues such as Ser27 and Tyr42 are not conserved in APH(2")-Ia suggesting subtle differences in mechanism and potential differences in ligand binding. As will be seen in Chapter 3, these differences result in distinct inhibitor sensitivities, which

does not augur well for the development of inhibitors cross-reactive to a broad-range of APH enzymes.

**A**



**B**
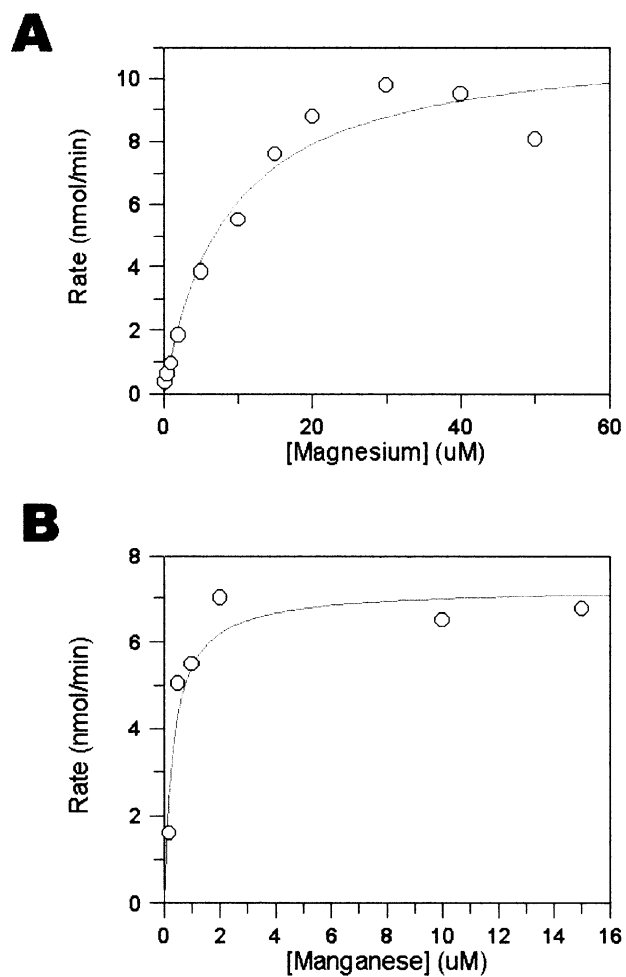


**Figure 2.17**: Effect of Metal Ion Concentration on the Activity of APH(2")-Ia using Magnesium (A) and Manganese (B) as the Divalent Cation.

**Table 2.8:** Solvent Isotope Effects for APH(2")-Ia.

| $^H V/^D V$ | | $^H(V/K)/^D(V/K)$ | |
|---|---|---|---|
| ATP | Kanamycin A | ATP | Kanamycin A |
| 1.16 +/- 0.15 | 1.03 +/- 0.10 | 1.47 +/- 0.24 | 0.922 +/- 0.351 |

## 2.3.9.2 Other Aminoglycoside Phosphotransferases

The importance of the APH(3')-IIIa equivalent residues of Asp190 and Asp208 have been confirmed in APH(3')-IIa by biological assays of site-directed mutants (Kocabiyik and Perlin, 1992), and the solving of the crystal structure of APH(3')-IIa (Nurizzo *et al.*, 2003) will provide the structural support for the further investigation of this enzyme. The spectinomycin kinase APH(9)-Ia has also been investigated and the importance of APH(3')-IIIa equivalent residues of Asp190 and Lys44 have been validated through *in vitro* characterization of site-directed mutants (Thompson *et al.*, 1998). APH(9)-Ia also demonstrates a low solvent isotope effect (2.5 – 2.7), suggesting aminoglycoside deprotonation plays a minor role in catalysis (Thompson *et al.*, 1998). These values are more significant than the ones seen with APH(3')-IIIa or APH(2")-Ia, and it should be noted that 'associative' and 'dissociative' only represent two extremes of a continuum of mechanisms. It is more likely that enzyme-catalyzed phosphoryl transfer is not a fully dissociative mechanism, and the degree to which the mechanism is dissociative or associative will depend on the system being assayed.

## 2.4 References

**Aimes, R.T., Hemmer, W. and Taylor, S.S. 2000.** Serine-53 at the tip of the glycine-rich loop of cAMP-dependent protein kinase: role in catalysis, P-site specificity, and interaction with inhibitors. *Biochemistry.* 39: 8325-8332.

**Blacklow, S.C., Raines, R.T., Lim, W.A., Zamore, P.D. and Knowles, J.R. 1988.** Triosephosphate isomerase catalysis is diffusion controlled. Appendix: Analysis of triose phosphate equilibria in aqueous solution by 31P NMR. *Biochemistry.* 27: 1158-1167.

**Boehr, D.D., Lane, W.S. and Wright, G.D. 2001a.** Active site labeling of the gentamicin resistance enzyme AAC(6')- APH(2") by the lipid kinase inhibitor wortmannin. *Chem Biol.* 8: 791-800.

**Boehr, D.D., Thompson, P.R. and Wright, G.D. 2001b.** Molecular mechanism of aminoglycoside antibiotic kinase APH(3')-IIIa: roles of conserved active site residues. *J Biol Chem.* 276: 23929-23936.

**Brouwer, A.C. and Kirsch, J.F. 1982.** Investigation of diffusion-limited rates of chymotrypsin reactions by viscosity variation. *Biochemistry.* 21: 1302-1307.

**Buchwald, S.L., Hansen, D.E., Hassett, A. and Knowles, J.R. 1982.** Chiral [16O, 17O, 18O]phosphoric monoesters as stereochemical probes of phosphotransferases. *Methods Enzymol.* 87: 279-301.

**Buchwald, S.L., Saini, M.S., Knowles, J.R. and Van Etten, R.L. 1984.** Stereochemical course of phospho group transfer by human prostatic acid phosphatase. *J Biol Chem.* 259: 2208-2213.

**Burk, D.L., Hon, W.C., Leung, A.K. and Berghuis, A.M. 2001.** Structural analyses of nucleotide binding to an aminoglycoside phosphotransferase. *Biochemistry.* 40: 8756-8764.

**Cason, C.J., Froechlick, T., Kopp, N., et al. 2002.** Persistence of Vision POV-Ray v 3.5. POV Team, Williamstown, Australia.

**Chakrabarti, P. and Samanta, U. 1995.** CH/pi interaction in the packing of the adenine ring in protein structures. *J Mol Biol.* 251: 9-14.

**Cole, P.A., Burn, P., Takacs, B. and Walsh, C.T. 1994.** Evaluation of the catalytic mechanism of recombinant human Csk (C- terminal Src kinase) using nucleotide analogs and viscosity effects. *J Biol Chem.* 269: 30880-30887.

Cole, P.A., Grace, M.R., Phillips, R.S., Burn, P. and Walsh, C.T. 1995. The role of the catalytic base in the protein tyrosine kinase Csk. *J Biol Chem*. 270: 22105-22108.

Daigle, D.M., Hughes, D.W. and Wright, G.D. 1999a. Prodigious substrate specificity of AAC(6')-APH(2"), an aminoglycoside antibiotic resistance determinant in enterococci and staphylococci. *Chem Biol*. 6: 99-110.

Daigle, D.M., McKay, G.A., Thompson, P.R. and Wright, G.D. 1999b. Aminoglycoside antibiotic phosphotransferases are also serine protein kinases. *Chem Biol*. 6: 11-18.

Dill, K.A. 1990. Dominant forces in protein folding. *Biochemistry*. 29: 7133-7155.

Fabiato, A. and Fabiato, F. 1979. Calculator programs for computing the composition of the solutions containing multiple metals and ligands used for experiments in skinned muscle cells. *J Physiol (Paris)*. 75: 463-505.

Fong, D.H. and Berghuis, A.M. 2002. Substrate promiscuity of an aminoglycoside antibiotic resistance enzyme via target mimicry. *Embo J*. 21: 2323-2331.

Grant, B.D. and Adams, J.A. 1996. Pre-steady-state kinetic analysis of cAMP-dependent protein kinase using rapid quench flow techniques. *Biochemistry*. 35: 2022-2029.

Grant, B.D., Hemmer, W., Tsigelny, I., Adams, J.A. and Taylor, S.S. 1998. Kinetic analyses of mutations in the glycine-rich loop of cAMP- dependent protein kinase. *Biochemistry*. 37: 7708-7715.

Guex, N. and Peitsch, M.C. 1997. SWISS-MODEL and the Swiss-Pdbviewer. An environment for comparative protein modeling. *Electrophoresis*, 18: 2714-2723.

Hemmer, W., McGlone, M., Tsigelny, I. and Taylor, S.S. 1997. Role of the glycine triad in the ATP-binding site of cAMP-dependent protein kinase. *J Biol Chem*. 272: 16946-16954.

Hengge, A.C., Sowa, G.A., Wu, L. and Zhang, Z.Y. 1995. Nature of the transition state of the protein-tyrosine phosphatase- catalyzed reaction. *Biochemistry*. 34: 13982-7.

Herschlag, D. and Jencks, M.P. 1989a. Phosphoryl transfer to anionic oxygen nucleophiles. Nature of the transition state and electrostatic repulsions. *J. Am. Chem. Soc.* 111: 7587-7596.

Herschlag, D. and Jencks, W.P. 1989b. Evidence that metaphosphate monoanion is not an intermediate in solvolysis reactions in aqueous solution. *J. Am. Chem. Soc.* 111: 7679-7586.

Hirai, T.J., Tsigelny, I. and Adams, J.A. 2000. Catalytic assessment of the glycine-rich loop of the v-Fps oncoprotein using site-directed mutagenesis. *Biochemistry.* 39: 13276-13284.

Hollfelder, F. and Herschlag, D. 1995. The nature of the transition state for enzyme-catalyzed phosphoryl transfer. Hydrolysis of O-aryl phosphorothioates by alkaline phosphatase. *Biochemistry.* 34: 12255-12264.

Hon, W.C., McKay, G.A., Thompson, P.R., Sweet, R.M., Yang, D.S., Wright, G.D. and Berghuis, A.M. 1997. Structure of an enzyme required for aminoglycoside antibiotic resistance reveals homology to eukaryotic protein kinases. *Cell.* 89: 887-895.

Johnson, L.N., Lowe, E.D., Noble, M.E. and Owen, D.J. 1998. The Eleventh Datta Lecture. The structural basis for substrate recognition and control by protein kinases. *FEBS Lett.* 430: 1-11.

Kim, K. and Cole, P.A. 1997. Measurement of a Bronsted nucleophilic coefficient and insights into the transition state for a protein tyrosine kinase. *J. Am. Chem. Soc.* 119: 11096-11097.

Kim, K. and Cole, P.A. 1998. Kinetic analysis of a protein tyrosine reaction transition state in the forward and reverse directions. *J. Am. Chem. Soc.* 120: 6851-6858.

Kirby, A.J. and Varvoglis, A.G. 1967. The reactivity of phosphate esters. Monoester hydrolysis. *J. Am. Chem. Soc.* 89: 415-423.

Knowles, J.R. 1980. Enzyme-catalyzed phosphoryl transfer reactions. *Annu Rev Biochem.* 49: 877-919.

Kocabiyik, S. and Perlin, M.H. 1992. Site-specific mutations of conserved C-terminal residues in aminoglycoside 3'-phosphotransferase II: phenotypic and structural analysis of mutant enzymes. *Biochem Biophys Res Commun.* 185: 925-931.

Leatherbarrow, R.J. 2000. Grafit. . Erithacus Software, Staines.

McKay, G.A., Thompson, P.R. and Wright, G.D. 1994. Broad spectrum aminoglycoside phosphotransferase type III from *Enterococcus*: overexpression, purification, and substrate specificity. *Biochemistry.* 33: 6936-6944.

McKay, G.A. and Wright, G.D. 1995. Kinetic mechanism of aminoglycoside phosphotransferase type IIIa. Evidence for a Theorell-Chance mechanism. *J Biol Chem*. 270: 24686-24692.

McKay, G.A. and Wright, G.D. 1996. Catalytic mechanism of enterococcal kanamycin kinase (APH(3')-IIIa): viscosity, thio, and solvent isotope effects support a Theorell-Chance mechanism. *Biochemistry*. 35: 8680-8685.

Nurizzo, D., Shewry, S.C., Perlin, M.H., Brown, S.A., Dholakia, J.N., Fuchs, R.L., Deva, T., Baker, E.N. and Smith, C.A. 2003. The Crystal Structure of Aminoglycoside-3'-Phosphotransferase-IIa, an Enzyme Responsible for Antibiotic Resistance. *J Mol Biol*. 327: 491-506.

Sampson, N.S. and Knowles, J.R. 1992. Segmental motion in catalysis: investigation of a hydrogen bond critical for loop closure in the reaction of triosephosphate isomerase. *Biochemistry*. 31: 8488-8494.

Sarkar, G. and Sommer, S.S. 1990. The "megaprimer" method of site-directed mutagenesis. *Biotechniques*. 8: 404-407.

Schowen, K.B. and Schowen, R.L. 1982. Solvent isotope effects of enzyme systems. *Methods Enzymol*. 87: 551-606.

Shaw, K.J., Rather, P.N., Hare, R.S. and Miller, G.H. 1993. Molecular genetics of aminoglycoside resistance genes and familial relationships of the aminoglycoside-modifying enzymes. *Microbiol Rev*. 57: 138-163.

Sicheri, F., Moarefi, I. and Kuriyan, J. 1997. Crystal structure of the Src family tyrosine kinase Hck. *Nature*. 385: 602-609.

Simopoulos, T.T. and Jencks, W.P. 1994. Alkaline phosphatase is an almost perfect enzyme. *Biochemistry*. 33: 10375-10380.

Thompson, P.R., Hughes, D.W., Cianciotto, N.P. and Wright, G.D. 1998. Spectinomycin kinase from *Legionella pneumophila*. Characterization of substrate specificity and identification of catalytically important residues. *J Biol Chem*. 273: 14788-14795.

Weiss, P.M. and Cleland, W.W. 1989. Alkaline phosphatase catalyzes the hydrolysis of glucose-6-phosphate. *J. Am. Chem. Soc.* 111: 1928-1929.

Wiseman, T., Williston, S., Brandts, J.F. and Lin, L.N. 1989. Rapid measurement of binding constants and heats of binding using a new titration calorimeter. *Anal Biochem*. 179: 131-137.

**Yoon, M.Y. and Cook, P.F. 1987.** Chemical mechanism of the adenosine cyclic 3',5'-monophosphate dependent protein kinase from pH studies. *Biochemistry.* 26: 4118-4125.

**Zheng, J., Knighton, D.R., ten Eyck, L.F., Karlsson, R., Xuong, N., Taylor, S.S. and Sowadski, J.M. 1993.** Crystal structure of the catalytic subunit of cAMP-dependent protein kinase complexed with MgATP and peptide inhibitor. *Biochemistry.* 32: 2154-2161.

**Zhou, J. and Adams, J.A. 1997.** Is there a catalytic base in the active site of cAMP-dependent protein kinase? *Biochemistry.* 36: 2977-2984.

# Chapter 3.

# Inactivation of the Aminoglycoside Phosphotransferase AAC(6')-APH(2") by the Lipid Kinase Inhibitor Wortmannin

Mass spectral analysis of the labeled protein fragments was performed and analyzed by W.S. Lane. All other work reported in this chapter was performed by myself.

## 3.1 Introduction

The chemical mechanism of APH(3')-IIIa was elucidated in Chapter 2, and initial results suggest that the phosphotransferase domain of AAC(6')-APH(2") operates through a similar mechanism. However, there are differences between APH(3')-IIIa and APH(2")-Ia, including differential sensitivity to protein kinase inhibitors (Daigle *et al.*, 1997), indicating that the kinase active sites have important geometrical differences. This is consistent with the fact that the enzymes also have different aminoglycoside substrate profiles (Daigle *et al.*, 1999a; McKay *et al.*, 1994b), with the kinase domain of AAC(6')-APH(2") (referred to as APH(2")-Ia herein) having a broader substrate specificity than APH(3')-IIIa; an observation that implies that APH(2")-Ia has a greater ability to accept more diverse structures into its active site. In addition to a broader aminoglycoside specificity, APH(2")-Ia has a more expansive kinase regiospecificity with the capacity to phosphorylate a number of hydroxyl groups around the aminoglycoside core, including positions 3', 5", 2" and 3'" depending on the aminoglycoside (Azucena *et al.*, 1997; Daigle *et al.*, 1999a). APH(3')-IIIa, in contrast, phosphorylates either 3'- and/or 5"-hydroxyls (McKay *et al.*, 1994b; Thompson *et al.*, 1996) (Figure 3.1). The kinetic mechanisms of the two enzymes are also different: APH(3')-IIIa follows a Theorell–Chance mechanism where ADP release is solely rate limiting (McKay and Wright, 1995; McKay and Wright, 1996), while APH(2")-Ia proceeds through a random rapid equilibrium mechanism (Martel *et al.*, 1983) with the catalytic step making an important contribution to the turnover              rate              (see              Chapter              2).
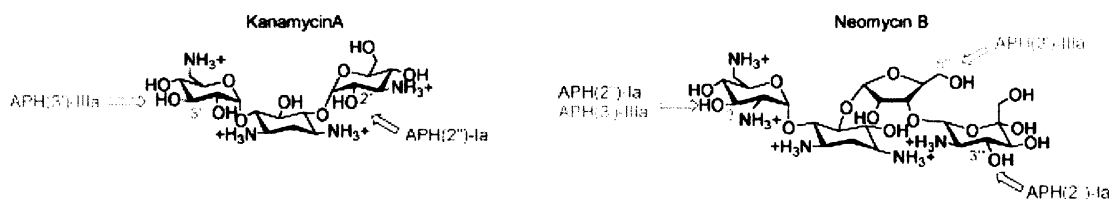
**Figure 3.1:** Regiospecificities of Phosphoryl Transfer by APH(3')-IIIa and APH(2")-Ia, the Phosphotransferase Domain of AAC(6')-APH(2"). APH(3')-IIIa catalyzes phosphoryl transfer onto 4,6-disubstituted aminoglycosides exclusively on 3'-OHs, whereas it can bisphosphorylate 3'-OHs and 5'-OHs on 4,5-disubstituted aminoglycosides (McKay *et al.*, 1994b; Thompson *et al.*, 1996). Phosphorylation by APH(2")-Ia is highly dependent upon the individual aminoglycoside, where the enzyme can phosphorylate similar and different sites than APH(3')-IIIa (Azucena *et al.*, 1997; Daigle *et al.*, 1999a).

Rational design of selective inhibitors of aminoglycoside kinases requires a structural understanding of the differences between these enzymes, however while much information has been gleaned from the structural determination of APH(3')-IIIa, similar information is lacking for APH(2")-Ia. As a first step in elaborating the structural differences between these enzymes, we elected to explore active site labeling techniques.

One candidate active site label is the electrophilic ATP analogue 5'-[*p*-(fluorosulfonyl)benzoyl]adenosine (FSBA), which was previously shown to inactivate APH(3')-IIIa by modifying the invariant Lys44 in the ATP binding pocket (McKay *et al.*, 1994a). Another candidate is the lipid kinase inhibitor wortmannin (see Figure 3.2 for structures). Lipid kinases also share a similar fold with aminoglycoside and protein kinases, as seen with the three-dimensional structure of phosphatidylinositol phosphate kinase type IIB (Rao *et al.*, 1998), and therefore, lipid kinase inhibitors have the potential to inhibit aminoglycoside kinases as well. Wortmannin was originally discovered to be an

inhibitor of myosin light chain kinase with an $IC_{50}$~0.2 µM (Nakanishi *et al.*, 1992).

Later studies showed wortmannin to be a 100-fold more potent irreversible inhibitor of

phosphatidylinositol 3-kinase (PI 3-kinase) with an $IC_{50}$~2 nM (Powis *et al.*, 1994), and

is now commonly used to study the role of PI 3-kinase in signal transduction cascades

(Fruman *et al.*, 1998). Wortmannin acts by covalently binding Lys802 in the ATP

binding pocket of PI 3-kinase (Wymann *et al.*, 1996). A study of a series of structural

analogues of wortmannin concluded that PI 3-kinase is irreversibly inactivated through

nucleophilic attack of the Lys amino group at the C21 position of wortmannin generating

the substituted α–β unsaturated lactone (Figure 3.2) (Norman *et al.*, 1996).

In the present Chapter, we show that wortmannin is an inactivator of APH(2")-Ia

but not APH(3')-IIIa. This contrasts with the ATP analogue FSBA which did not

inactivate APH(2")-Ia, but was previously shown to covalently modify APH(3')-IIIa and

the spectinomycin kinase APH(9)-Ia (McKay *et al.*, 1994a; Thompson *et al.*, 1998).

These different active site labeling sensitivities provide a chemical means of

discriminating between aminoglycoside kinases and highlight the geometrical differences

in the active sites of the two enzymes.

A. FSBA Inactivation



B. Wortmannin Inactivation
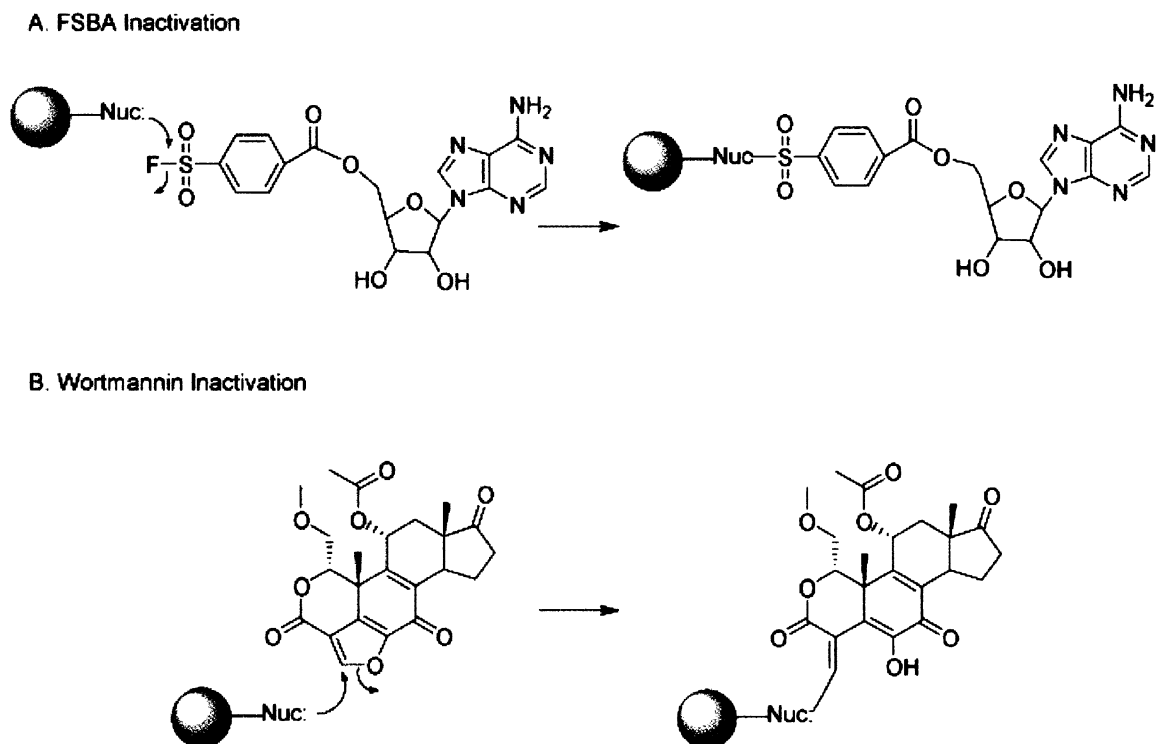


**Figure 3.2:** Structure and Reactivity of Kinase Active Site Labeling Compounds FSBA (A) and Wortmannin (B). A nucleophile in the active site, generally a lysine, attacks the electrophilic position on the respective compound as indicated resulting in an inactivated enzyme.

## 3.2 Materials and Methods

### 3.2.1 Chemicals

Acetyl-CoA, dithiodipyridine and wortmannin were from Sigma (St. Louis, MO, USA). Kanamycin A, gentamicin and IPTG (isopropyl-β-D-thiogalactopyranoside) were from Bioshop (Burlington, ON, Canada). Restriction endonucleases were from MBI Fermentas (Hamilton, ON, Canada). All oligonucleotide primers were synthesized at the Central Facility of the Institute for Molecular Biology and Biotechnology, McMaster University.

### 3.2.2. Subcloning of *aph(2")-Ia* into pET22b(+) and *aac(6')-aph(2")* into pET15b(+)

Plasmid pETBFAPH was constructed by the ligation of a 1 kb *aph(2")-Ia* fragment of the bifunctional *aac(6')-aph(2")* gene beginning at position 525 of the gene, corresponding to Met175 (D. Daigle and G. Wright, unpublished) digested with *Nde*I and *Hin*dIII into pET22b(+), and likewise, plasmid pET15AACAPH was constructed by the ligation of the 1.5 kb *aac(6')-aph(2")* insert from pBF9 (Daigle *et al.*, 1999a) digested with *Nde*I and *Bam*HI into pET15b(+), which generates the N-terminal 6-His-tagged enzyme. The new constructs were transformed into $CaCl_2$-competent *E. coli* BL21(DE3) for subsequent overexpression and purification.

### 3.2.3. Purification of Enzymes

APH(3')-IIIa was purified by previously described methods (McKay *et al.*, 1994b). Overexpression of APH(2")-Ia and the N-terminal His-tagged AAC(6')-APH(2") was similar to that for APH(3')-IIIa, where 1 L of Luria Bertani broth supplemented with 50 μg/mL kanamycin A was inoculated with 10 mL of an overnight culture of *E. coli* BL21(DE3) containing the appropriate constructs and grown at 37°C for 3 h until $OD_{600}$~0.6. Enzyme production was induced by the addition of 1 mM IPTG and grown for a further 3 h at 37°C. The cells were collected by centrifugation at 5000×*g* for 10 min, resuspended and washed with 0.85% NaCl, before storing them overnight at -20°C.

The purification of APH(2")-Ia followed the same procedure as that used to purify the full length, non-His-tagged enzyme as outlined in (Daigle *et al.*, 1999a). For the purification of the N-terminal His-tagged version of AAC(6')-APH(2"), the cells were

resuspended in 15 mL 50 mM $Na_2HPO_4$ pH 8.0, 300 mM NaCl, 10 mM imidazole, lysed

using a French pressure cell at 20000 psi and the supernatant cleared by centrifugation

(10000×$g$ for 20 min). The 15 mL of crude lysate was gently mixed with 5 mL Ni NTA

agarose for 1 h at 4°C, and then loaded onto a column (9×3 cm). The resin was washed

with 20 mL 50 mM $Na_2HPO_4$ pH 8.0, 300 mM NaCl, 20 mM imidazole and 20 mL 50

mM $Na_2HPO_4$ pH 8.0, 300 mM NaCl, 40 mM imidazole. The protein was eluted with 25

mL 50 mM $Na_2HPO_4$ pH 8.0, 300 mM NaCl, 250 mM imidazole. The fractions

containing purified AAC(6')-APH(2") were pooled, concentrated over an Amicon PM30

membrane and dialyzed against 50 mM HEPES pH 7.5, 1 mM EDTA. Approximately 50

mg of His-tagged AAC(6')-APH(2") was purified from a 1 L cell culture. Protein

concentrations were determined using the Bradford method (Bradford, 1976).

### 3.2.4. APH and AAC Kinetic Assays

The assays used to measure aminoglycoside phosphotransferase and acetyltransferase

activities were previously described in (Daigle *et al.*, 1999a). However, most assays were

scaled down from 1 mL to 250 μL volumes, so they could be conducted in 96 well

microtiter plates using a Molecular Devices SpectraMax Plus microtiter plate reader. For

Michaelis–Menten kinetic determinations, initial rates were fit by non-linear least

squares to Eq. 3.1, using Grafit version 4.0 (Leatherbarrow, 2000). Results are reported

+/- standard error.

$v=(k_{cat}/E_t)[S]/(K_M+[S])$                                    (Eq. 3.1)

### 3.2.5. Inactivation of AAC(6')-APH(2″) by Wortmannin

Wortmannin inactivation experiments were conducted in 50 mM HEPES-NaOH

pH 7.5 at room temperature with various concentrations of wortmannin dissolved in

dimethyl sulfoxide (DMSO; 5% v/v for all wortmannin concentrations including

controls) in a total volume of 20 μL. Reactions were initiated by the addition of enzyme

(0.3–0.5 nmol) and 5 μL aliquots were removed, added to 37°C temperature-equilibrated

assay broth and assayed for kanamycin kinase or acetyltransferase activity.

### 3.2.6. Large-scale Affinity Labeling of APH(2″)-Ia to Determine the Site(s) of Modification

APH(2″)-Ia (100 nmol) was inactivated by the addition of several aliquots of

wortmannin (1 μmol every 2 h for a total of 6 h) to the inactivation buffer consisting of

50 mM HEPES-NaOH pH 7.5 and 10 mM MgCl$_2$ in a total volume of 0.5 mL. The

control incubation, without wortmannin but with an equivalent amount of DMSO, was

carried out simultaneously. Inactivation was deemed complete when <2% of the

kanamycin phosphotransferase activity remained.

The volume of the reactions was increased to 1.5 mL, and the solutions were

dialyzed against 2 L 25 mM NH$_4$HCO$_3$ pH 8.3 at 4°C. One volume of 200 mM Tris–HCl

pH 8.3, 2 mM EDTA, 8 M urea and 4 mM dithiothreitol was then added and the solutions

stirred for 1 h under nitrogen at room temperature. To cap cysteine residues, 1.1

equivalents iodoacetic acid per cysteine residue (550 nmol) were added to the reaction

mixture and stirred for an additional 60 min in the dark. The reactions were subsequently

dialyzed overnight against 20 mM $NH_4HCO_3$ pH 8.3 at 4°C. The solutions were then

evaporated using a SpeedVac, before resuspension in 100 μL 100 mM $NH_4HCO_3$ pH 8.3,

8 M urea. The reactions were incubated at room temperature for 30 min prior to the

addition of 45.5 μL 100 mM $NH_4HCO_3$ pH 8.3 and 5.5 μL of trypsin solution (2 mg

trypsin in 50 mL 1.2 M HCl). The trypsin digestion was allowed to proceed for 24 h at

room temperature in the dark before freezing and storing the reactions at -80°C.

### 3.2.7. Trypsin Digest Analysis

Multiple peptide sequences were determined in a single run by microcapillary

reverse-phase chromatography directly coupled to a Finnigan LCQ quadrupole ion trap

mass spectrometer equipped with a custom nanoelectrospray source. The column was

packed in-house with 10 cm of POROS 10R2 into a New Objective one-piece 75 μm in

diameter column terminating in an 8.5 μm tip. Flow rate was nominally 200 nL/min. The

ion trap repetitively surveyed MS (395–1400 *m/z*), executing data-dependent scans on the

three most abundant ions in the survey scan, allowing high resolution (zoom) scans to

determine charge state and exact mass, and MS/MS spectra for peptide sequence

information. MS/MS spectra were acquired with a relative collision energy of 30% and

an isolation width of 2.5 Da. Recurring ions were dynamically excluded. After database

correlation with SEQUEST, modified peptides were confirmed by manual interpretation

of the MS/MS spectra using FuzzyIons (Chittum *et al.*, 1998; Eng *et al.*, 1994).

### 3.2.8. Site-Directed Mutagenesis of Selected Lysine Residues to Alanine

Peptide mapping results identified four potential Lys residues that were being modified by wortmannin. To determine the role of each Lys in the activity of APH(2")-Ia, they were individually mutated to Ala using the Quik-Change mutagenesis method (Stratagene, La Jolla, CA, USA). Briefly, the appropriate mutagenic oligonucleotides (Table 3.1) and their reverse complements were used in combination with 10 ng template DNA (pETBFAPH) in *Pfu* DNA polymerase (Stratagene, La Jolla, CA, USA)-catalyzed PCR reactions. Parental DNA was digested with *Dpn*I, before the mutant plasmid DNA was transformed into CaCl$_2$-competent *E. coli* XL1-Blue. Positive clones were sequenced in their entirety before transformation into *E. coli* BL21(DE3) and subsequent protein purification.

**Table 3.1:** Oligonucleotide Primers used in this Study to Generate Appropriate APH(2")-Ia Mutants

| Mutant | Mutagenic Primer (5' to 3') |
|---|---|
| Lys13Ala | GCCACAAATGTTGCGGCAATGAAATATTTAATTGAGC |
| Lys52Ala | GGCATATTTAGTTAATAATGAATACATTTTTGCAACAAAATTTAG |
| Lys125Ala | GTCAGAAGAAGAACAAAATTTGTTAGCACGAGATATTGCC |
| Lys287Ala | GGAATTAAAAATATTGCACAGGAATTTATCGAAAATGGTAGAAAAG |

### 3.2.9. Absorbance Spectrum of HisAAC(6')-APH(2") Inactivated with Wortmannin

The course of the reaction between HisAAC(6')-APH(2") (17 nmol) and wortmannin (250 nmol) in 0.5 mL 50 mM HEPES-NaOH pH 7.5 at room temperature was followed by taking absorbance scans from 200 nm to 600 nm every 10 min using a Cary             3E             UV/Vis             spectrophotometer.

## 3.3. Results

### 3.3.1. Kinetic Analysis of APH(2")-Ia Domain and N-terminal 6-histidine (6-His)-tagged AAC(6')-APH(2")

We have previously reported the purification of the aminoglycoside resistance determinant AAC(6')-APH(2") in *Bacillus subtilis* using an expression plasmid under the control of the constitutive *vegII* promoter (Daigle *et al.*, 1999a). In this study, we created *E. coli* expression constructs that introduce an N-terminal hexa His tag on AAC(6')-APH(2") (HisAAC(6')-APH(2")) for ease in purification and a construct that expresses a C-terminal truncated version that encodes only the APH(2")-Ia domain of the bifunctional enzyme (Figure 3.3).
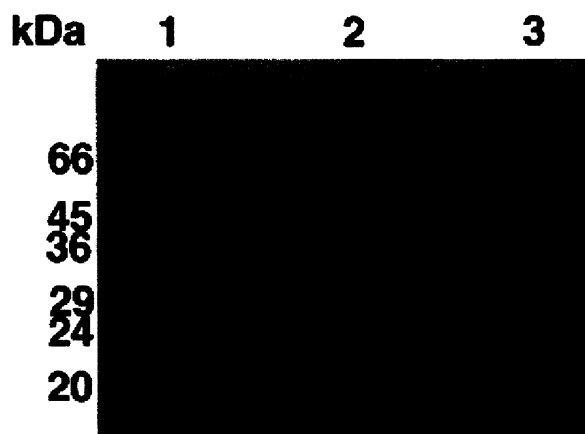


**Figure 3.3:** Purity of APH(2") Enzymes. The sodium dodecyl sulfate–polyacrylamide gel was stained with Coomassie blue. Lane 1, molecular mass standards; lane 2, APH(2")-Ia fragment beginning at Met175 of AAC(6')-APH(2"); lane 3, His6-AAC(6')-APH(2").

The N-terminal His tag did not have a significant effect on the activity of AAC(6')-APH(2"). Although there were modest changes to $K_M$ and $k_{cat}$ for some substrates, the catalytic efficiencies ($k_{cat}/K_M$) for these substrates remained comparable to

those determined for the *B. subtilis*-expressed enzyme (Table 3.2). Likewise, the C-terminal truncated version encoding only the APH(2") domain did not display significantly different aminoglycoside modification properties (Table 3.2).

Most of the subsequent studies utilized the C-terminal truncated version of APH(2"), except where indicated. The *B. subtilis*-expressed AAC(6')-APH(2"), HisAAC(6')-APH(2") and the truncated APH(2")-Ia domain all showed identical sensitivities to the active site labeling compounds FSBA and wortmannin (data not shown).

### 3.3.2. APH(2")-Ia and APH(3')-IIIa have Different Sensitivities to the Covalent Modifiers FSBA and Wortmannin

FSBA, an inactivator of APH(3')-IIIa (McKay *et al.*, 1994a), did not have an effect on either the acetyltransferase or phosphotransferase activity of HisAAC(6')-APH(2") at concentrations of 2 mM (data not shown). In contrast, wortmannin did not affect the activity of APH(3')-IIIa up to a concentration of 2 mM, but did efficiently inactivate the phosphotransferase domain of HisAAC(6')-APH(2") (Figure 3.4). The reaction appeared to be irreversible as extensive dialysis or gel filtration could not restore APH activity. The acetyltransferase activity of the bifunctional enzyme was not affected (Figure 3.4). Thus, FSBA is a specific inactivator of APH(3')-IIIa, whereas wortmannin is specific to APH(2")-Ia.

**Table 3.2:** Enzymatic Properties of Aminoglycoside Modifying Enzymes

| Construct | APH activity | | | | | | AAC activity | | | | | |
| --- | --- | --- | --- | --- | --- | --- | --- | --- | --- | --- | --- | --- |
| | Kanamycin A[a] | | | ATP[b] | | | Kanamycin A[c] | | | Acetyl CoA[d] | | |
| | $K_M$ ($\mu$M) | $k_{cat}$ (sec$^{-1}$) | $k_{cat}/K_M$ (M$^{-1}$s$^{-1}$) | $K_M$ ($\mu$M) | $k_{cat}$ (sec$^{-1}$) | $k_{cat}/K_M$ (M$^{-1}$s$^{-1}$) | $K_M$ ($\mu$M) | $k_{cat}$ (sec$^{-1}$) | $k_{cat}/K_M$ (M$^{-1}$s$^{-1}$) | $K_M$ ($\mu$M) | $k_{cat}$ (sec$^{-1}$) | $k_{cat}/K_M$ (M$^{-1}$s$^{-1}$) |
| *B.subtilis* expressed AAC(6')-APH(2") | 7.0 ± 0.9 | 0.41± 0.02 | 5.8 x 10$^4$ | 64 ± 9 | 0.17 ± 0.02 | 2.7 x 10$^3$ | 11 ± 1 | 0.69 ± 0.02 | 6.3 x 10$^4$ | 7.2 ± 1.4 | 0.24 ± 0.04 | 3.4 x 10$^4$ |
| HisAAC(6')-APH(2") | 4.7 ± 0.5 | 0.32 ± 0.03 | 6.8 x 10$^4$ | 135 ± 9 | 0.32 ± 0.03 | 2.4 x 10$^3$ | 31 ± 3 | 1.7 ± 0.2 | 5.6 x 10$^4$ | 38 ± 5 | 1.2 +/- 0.3 | 3.1 x 10$^4$ |
| C-terminal truncate APH(2")-Ia domain | 6.0 ± 1.1 | 0.24 ± 0.01 | 4.0 x 10$^4$ | 90 ± 3 | 0.21± 0.01 | 2.3 x 10$^3$ | -- | -- | -- | -- | -- | -- |

a- ATP held at 1 mM

b- kanamycin A held at 100 $\mu$M

c- acetyl-CoA held at 100 $\mu$M for *B. subtilis* expressed AAC(6')-APH(2") and 300 $\mu$M for HisAAC(6')-APH(2")

d- kanamycin A held at 100 $\mu$M for *B. subtilis* expressed enzyme AAC(6')-APH(2") and 300 $\mu$M for HisAAC(6')-APH(2")
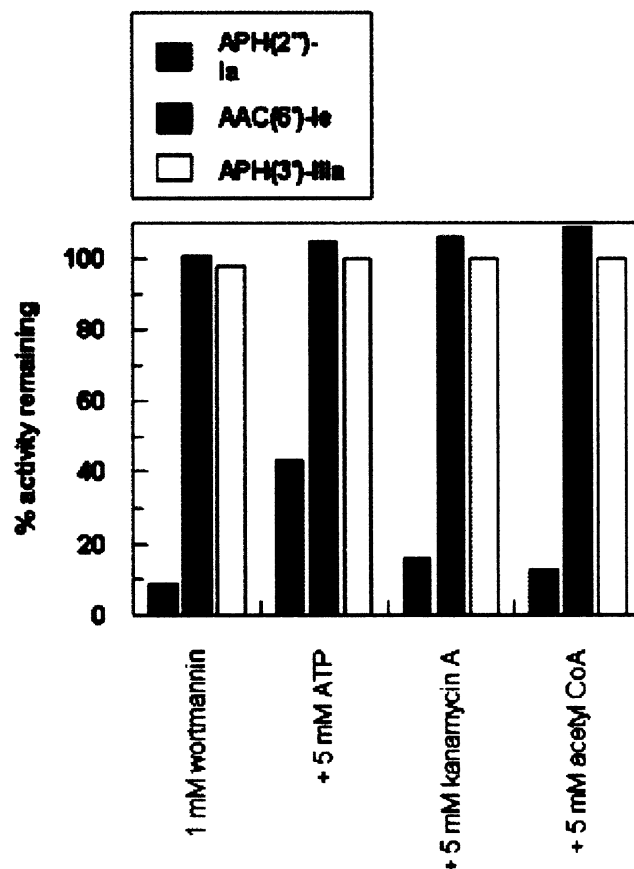
**Figure 3.4:** Wortmannin Inactivates the Aminoglycoside Kinase (APH(2")) Activity of AAC(6')-APH(2"). Inactivation assays were performed as described in Section 3.2.5. following a 60 min incubation at 22°C.

Wortmannin inactivation of APH(2") was accompanied by a marked change in color of the reaction mixture from colorless to yellow, which permitted ready monitoring of enzyme inactivation by monitoring of the increase in absorbance at 440 nm (Figure 3.5). The presence of an isosbestic point is consistent with formation of a single wortmannin species.
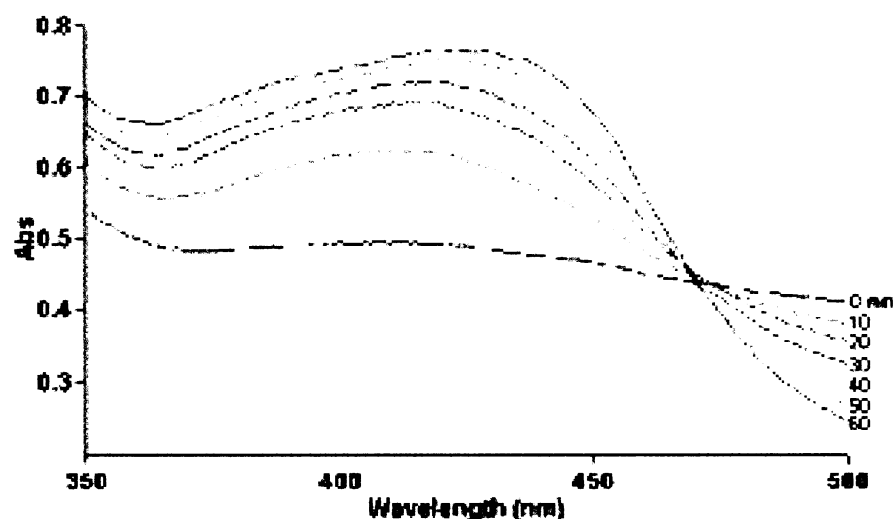
**Figure 3.5:** Reaction of Wortmannin with HisAAC(6')-APH(2") as Followed by Absorbance Spectrum Scans with a Cary 3E UV/Vis Spectrophotometer.

### 3.3.3. ATP Protection of APH(2")-Ia Activity from Inactivation by Wortmannin

To validate the specificity of the reaction and to localize the site of modification, substrate protection experiments were performed. Neither kanamycin A nor acetyl-CoA afforded any protection to APH(2")-Ia, however, ATP was able to protect APH(2")-Ia from inactivation (Figure 3.4), suggesting that wortmannin binds at or near the ATP binding pocket of APH(2")-Ia and interacts with an important active site residue.

### 3.3.4. Kinetics of Inactivation of APH(2")-Ia by Wortmannin

Wortmannin inactivated APH(2")-Ia in both a concentration- and time-dependent manner following pseudo first order kinetics (Figure 3.6A), consistent with the following model:

$$E + I \; \underset{}{\overset{K_i}{\rightleftharpoons}} \; EI \; \overset{k_{max}}{\longrightarrow} \; EI^*$$
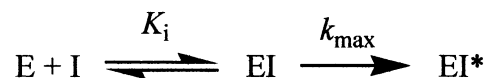
where $K_i$ is the apparent binding constant, $k_{max}$ is the rate of inactivation at saturating

inactivator (I), and EI* is the modified enzyme. Replot of the pseudo first order

constants, $k_{obs}$, versus wortmannin concentration to determine $K_i$ and $k_{max}$ revealed the

predicted saturation kinetics typical of enzyme affinity reagents (Figure 3.6B). The

dissociation constant, $K_i$, and the maximal rate of inactivation, $k_{max}$, were calculated to be

$1.05 \pm 0.1$ mM and $1.51 \pm 0.07 \times 10^{-2}$ min$^{-1}$ respectively. Thus wortmannin was shown to be

a specific inactivator of APH(2")-Ia likely functioning by covalently labeling the enzyme

in a region adjacent or overlapping the ATP binding site.
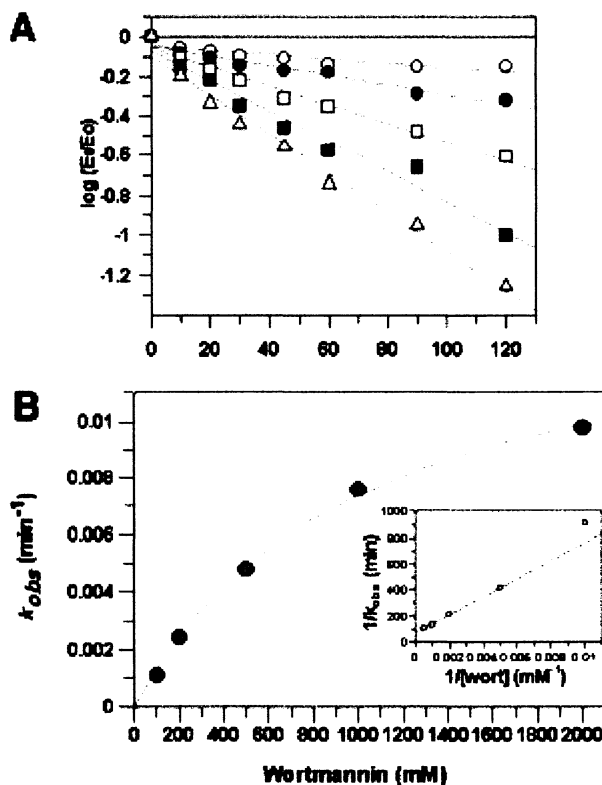
**Figure 3.6:** Time- and Concentration-Dependent Inactivation of APH(2")-Ia by Wortmannin. (A) APH(2")-Ia (0.4 nmol) in 50 mM HEPES-NaOH pH 7.5 and DMSO (5% v/v) inactivated with wortmannin at a final concentration of 100 (o), 200 (●), 500 (□ ), 1000 (■) and 2000 (△) μM. (B) Plot of first order rates of inactivation ($k_{obs}$) vs. inactivator concentration. The inset is a double reciprocal replot to determine $K_i$ and $k_{max}$, which were calculated to be 1.05±0.1 mM and 1.51±0.07×10⁻² min⁻¹ respectively.

## 3.3.5. Wortmannin Labels Lys Residues in APH(2")-Ia

Identification of covalently labeled amino acids was accomplished using a combination of tryptic peptide mapping and mass spectral analysis. Four Lys residues (Lys13, Lys52, Lys125 and Lys287) were tentatively identified as being modified under the conditions used to perform the experiment (Table 3.3). Efforts to establish stoichiometry of labeling using mass spectrometry (MS) failed.

**Table 3.3:** Peptides Labeled by Wortmannin as Identified by Mass Spectral Analysis of Trypsin-Digested and Inactivated APH(2")-Ia

| Peptide | Predicted Modified Residue |
|---|---|
| YDDNATVK*AMK | Lys13 |
| LVNNEYIFK*TK | Lys52 |
| STMSEEEQNLLK*R | Lys125 |
| NIK*QEFIENGR | Lys287 |

The role of each of the identified Lys residues in the aminoglycoside modifying activity of APH(2")-Ia was probed by mutating each Lys to Ala separately and characterizing the mutant enzymes. Mutagenesis of Lys13, Lys125 and Lys287 had little to no effect on the activity of APH(2")-Ia (Table 3.4). However, mutagenesis of Lys52 had a dramatic effect on the aminoglycoside modifying ability of APH(2")-Ia with significant changes on both the ATP and kanamycin A kinetic parameters (Table 3.4). The effect was most pronounced with respect to ATP where there was a 35-fold decrease in the catalytic efficiency (Table 3.4) which is consistent with this residue having a role in ATP capture, and demonstrates that this residue is homologous to Lys44 in APH(3')-IIIa as suggested by the primary sequence alignment (Figure 3.7). An equivalent Lys44Ala mutation in APH(3')-IIIa had a similar 31-fold effect on catalytic efficiency (Hon et al., 1997).

**Table 3.4:** Kinetic Analysis of APH(2")-Ia Lys to Ala Mutants

| | $K_M$ ($\mu$M) | $k_{cat}$ (s$^{-1}$) | $k_{cat}/K_M$ (M$^{-1}$s$^{-1}$) | $k_{cat}^{WT}$ /$k_{cat}^{mut}$ | $k_{cat}/K_M^{WT}$ /$k_{cat}/K_M^{mut}$ |
|---|---|---|---|---|---|
| **Lys13Ala** | | | | | |
| kanamycin A$^a$ | $10.6 \pm 2.0$ | $0.28 \pm 0.02$ | $2.6 \times 10^4$ | 0.86 | 1.5 |
| ATP$^b$ | $113 \pm 12$ | $0.33 \pm 0.02$ | $2.9 \times 10^3$ | 0.64 | 0.79 |
| **Lys52Ala** | | | | | |
| kanamycin A$^c$ | $2.07 \pm 0.86$ | $0.017 \pm 0.001$ | $8.2 \times 10^3$ | 14 | 4.9 |
| ATP$^b$ | $227 \pm 36$ | $0.015 \pm 0.001$ | $6.6 \times 10^1$ | 14 | 35 |
| **Lys125Ala** | | | | | |
| kanamycin A$^a$ | $6.53 +/- 1.13$ | $0.20 +/- 0.01$ | $3.1 \times 10^4$ | 1.2 | 1.3 |
| ATP$^b$ | $100 +/- 12$ | $0.24 +/- 0.02$ | $2.4 \times 10^3$ | 0.88 | 0.96 |
| **Lys287Ala** | | | | | |
| kanamycin A$^a$ | $8.80 +/- 1.03$ | $0.30 +/- 0.01$ | $3.4 \times 10^4$ | 0.80 | 1.2 |
| ATP$^b$ | $94 +/- 13$ | $0.23 +/- 0.02$ | $2.4 \times 10^3$ | 0.88 | 0.96 |

a- ATP held at 1 mM; b- kanamycin A held at 100 $\mu$M; c-  ATP held at 2 mM

The impact of mutating Lys52 on ATP capture is consistent with the conclusion that wortmannin inactivates APH(2")-Ia by covalently modifying this residue. Additional support for this conclusion comes from the observation that wortmannin did not efficiently inactivate the Lys52Ala mutant (>90% activity remaining) under conditions where the wild type enzyme was completely inactivated (<1% activity remaining) (Figure 3.8). The other Lys mutants remained susceptible to wortmannin inactivation (Figure 3.8).

APH(2")-Ia (1)    M E Y R Y D D N A I  N V K A    M K   (16) - (44) L V N M E " " " Y I F " K T K (54) - -

APH(3')-Ia (1)    M G H I Q R E T S G R P R L    N G   (16) - (44) Y G N P D " A P E L F L K " N (56) - -

APH(3')-IIa (1)   " " " " M I E Q D G L H A G    S P   (12) - (40) S A Q G R " " P V L F V K " T (51) - -

APH(3')-IIIa (1)  " " " " " " " " " M A K M R    I S   (7) - (36) V G E M E " " " N L Y L K " M (45) - -


APH(2")-Ia (114)  S T M S E E E Q N L L K R (120) - (283) M  I K  Q E F I E N G R K E I Y K R T Y  K D

APH(3')-Ia (112)  E Y P D S G " " E N I V D (123) - (284)

APH(3')-IIa (108) A P A E K " " " " " " V S (114) - (284)

APH(3')-IIIa (104) D E Q S P " " " E K I L E (113) - (262)

**Figure 3.7:** Primary Sequence Alignment of Aminoglycoside Phosphotransferases. Lysines modified in APH(2")-Ia by wortmannin are highlighted. Only Lys52 is conserved among the APHs and is homologous to Lys44 in APH(3')-IIIa which is known to interact with the α- and β-phosphates of ATP.
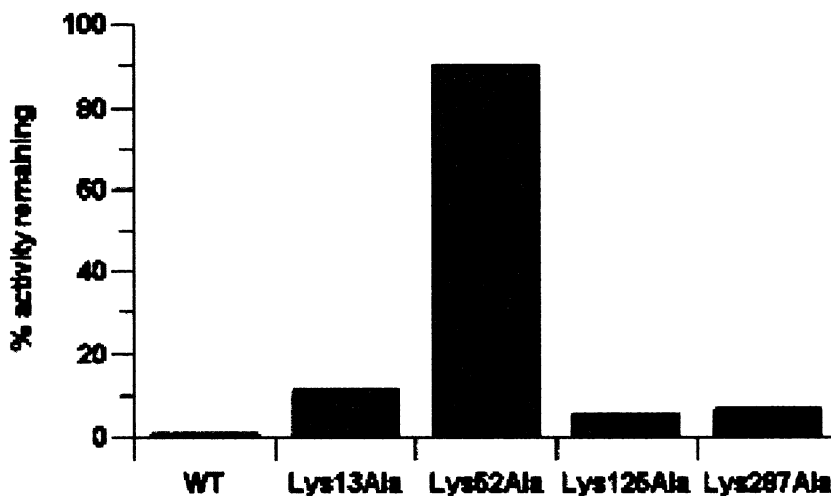
**Figure 3.8:** Wortmannin Inactivation of Lys——→Ala Mutants of APH(2")-Ia. Only the Lys52Ala mutant is protected against inactivation.

## 3.4. Discussion

AAC(6')-APH(2") and APH(3')-IIIa are major aminoglycoside antibiotic resistance determinants in Gram-positive pathogens such as *Enterococcus* and *Staphylococcus* (Wright *et al.*, 1998). The two enzymes share a common active site motif, which is similar to that of protein and lipid kinases. The structure of APH(3')-IIIa confirmed the similarity with protein and lipid kinases (Hon *et al.*, 1997), and further functional studies showed that both AAC(6')-APH(2") and APH(3')-IIIa have serine protein kinase activity (Daigle *et al.*, 1999b) and are sensitive to protein kinase inhibitors (Daigle *et al.*, 1997). Although the phosphotransferase domain of the bifunctional enzyme is likely to be structurally homologous to APH(3')-IIIa, APH(3')-IIIa and APH(2")-Ia have important functional differences, including different aminoglycoside substrate specificities (Daigle *et al.*, 1999a; McKay *et al.*, 1994b), phosphoryl transfer regiospecificities (Azucena *et al.*, 1997; Daigle *et al.*, 1999a; McKay *et al.*, 1994b;

Thompson *et al.*, 1996), kinetic mechanisms (Martel *et al.*, 1983; McKay and Wright, 1995; McKay and Wright, 1996), and inhibitor sensitivities (Daigle *et al.*, 1997). The structure of APH(3')-IIIa has provided much valuable information that has directed our search for inhibitors of aminoglycoside kinases, but considering the important differences with APH(2")-Ia, we also sought structural information concerning this important aminoglycoside resistance determinant.

### 3.4.1. Inactivation of AAC(6')-APH(2") with Wortmannin

FSBA had previously been shown to inactivate APH(3')-IIIa by covalently modifying a conserved lysine that is important in binding ATP (McKay *et al.*, 1994a), but this compound had no effect on APH(2")-Ia. In contrast, wortmannin, a potent PI 3-kinase inactivator, was able to inhibit APH(2")-Ia but had no effect on APH(3')-IIIa. Peptide mapping of APH(2")-Ia following inactivation by wortmannin under saturating conditions and after prolonged incubation identified four candidate peptides containing Lys residues, which have the potential to react with the compound. Mutagenesis of only Lys52 substantially altered the aminoglycoside modifying ability of APH(2")-Ia and wortmannin did not inactivate the Lys52Ala mutant but was still able to inactivate the other Lys to Ala mutants, demonstrating that wortmannin inactivation of APH(2")-Ia requires Lys52 but not the other lysines identified in the mapping experiment. ATP protection of APH(2")-Ia is consistent with modification of Lys52, where primary sequence alignment has shown this residue to be homologous to Lys44 in APH(3')-IIIa (Figure 3.7), a residue known to interact with the $\alpha$- and $\beta$-phosphates of ATP (Hon *et al.*, 1997). We conclude that wortmannin inactivates APH(2")-Ia by covalently modifying

Lys52 in the ATP binding pocket. This conclusion is consistent with experiments on PI

3-kinase where wortmannin was shown to inactivate this lipid kinase by covalent

modification of Lys802 (Wymann *et al.*, 1996), a residue homologous to Lys52 and

Lys44 in APH(2")-Ia and APH(3')-IIIa respectively. Modification of the three other

lysines in APH(2")-Ia was likely an artifact of the prolonged incubation conditions used

and to the non-specific reactivity of this electrophilic compound.

### 3.4.2. Differences in the ATP Binding Pockets of Aminoglycoside Phosphotransferases and Implications for Inhibitor Design

It is intriguing that FSBA and wortmannin modify the homologous residue in the

aminoglycoside phosphotransferases, and yet FSBA is specific for APH(3')-IIIa and

wortmannin is specific for APH(2")-Ia. This suggests that there are fundamental

differences in the ATP binding pockets of these two enzymes, in agreement with our

previous studies showing that the enzymes have different sensitivities to certain protein

kinase inhibitors that are generally targeted towards the ATP binding pocket (Daigle *et

al.*, 1997). Even among very similar protein kinases, there are differences in inhibitor

sensitivities, and many potent and specific inhibitors have been directed against the ATP

binding pocket of important pharmacological targets (Toledo *et al.*, 1999). However, in

the case of aminoglycoside kinases, it would be more desirable to develop broad range

inhibitors that could inhibit a number of enzymes. The results of this study suggest that it

might be challenging to develop broad range and potent inhibitors of aminoglycoside

kinases by directing compounds against the ATP binding pocket, although more

information about these ATP binding pockets is required. A broad range inhibitor would

likely need to take advantage of other features common to the APHs such as the aminoglycoside binding pocket, but even then, design would be difficult considering that APHs show a diverse range of aminoglycoside substrate profiles and regiospecificities.

More potent and specific inactivators of APH(2")-Ia based on the wortmannin structure would likely require modifications around the C and D rings, as studies with PI 3-kinase have identified these rings as critical in initial binding efficiency (Creemer et al., 1996; Norman et al., 1996). In the case of APH(2")-Ia, positively charged substitutions might be favored as a negatively charged active site is a common motif in the structures of aminoglycoside modifying enzymes (Hon et al., 1997; Sakon et al., 1993; Wolf et al., 1998; Wybenga-Groot et al., 1999).

## 3.5. References

**Azucena, E., Grapsas, I. and Mobashery, S. 1997.** Properties of a bifunctional bacterial antibiotic resistance enzyme that catalyzes ATP-dependent 2"-phosphorylation and acetyl-CoA dependent 6'-acetylation of aminoglycosides. *J Am Chem Soc.* 119: 2317 - 2318.

**Bradford, M.M. 1976.** A rapid and sensitive method for the quantitation of microgram quantities of protein utilizing the principle of protein-dye binding. *Anal Biochem.* 72: 248-254.

**Chittum, H.S., Lane, W.S., Carlson, B.A., Roller, P.P., Lung, F.D., Lee, B.J. and Hatfield, D.L. 1998.** Rabbit beta-globin is extended beyond its UGA stop codon by multiple suppressions and translational reading gaps. *Biochemistry.* 37: 10866-10870.

**Creemer, L.C., Kirst, H.A., Vlahos, C.J. and Schultz, R.M. 1996.** Synthesis and in vitro evaluation of new wortmannin esters: potent inhibitors of phosphatidylinositol 3-kinase. *J Med Chem.* 39: 5021-5024.

**Daigle, D.M., Hughes, D.W. and Wright, G.D. 1999a.** Prodigious substrate specificity of AAC(6')-APH(2"), an aminoglycoside antibiotic resistance determinant in enterococci and staphylococci. *Chem Biol.* 6: 99-110.

**Daigle, D.M., McKay, G.A., Thompson, P.R. and Wright, G.D. 1999b.** Aminoglycoside antibiotic phosphotransferases are also serine protein kinases. *Chem Biol.* 6: 11-18.

**Daigle, D.M., McKay, G.A. and Wright, G.D. 1997.** Inhibition of aminoglycoside antibiotic resistance enzymes by protein kinase inhibitors. *J Biol Chem.* 272: 24755-24758.

**Eng, J.K., McCormick, A.L. and Yates, J.R.I. 1994.** An approach to correlate tandem mass spectral data of peptides with amino acid sequences in a protein database. *J. Am. Soc. Mass Spectrom.* 5: 976.

**Fruman, D.A., Meyers, R.E. and Cantley, L.C. 1998.** Phosphoinositide kinases. *Annu Rev Biochem.* 67: 481-507.

**Hon, W.C., McKay, G.A., Thompson, P.R., Sweet, R.M., Yang, D.S., Wright, G.D. and Berghuis, A.M. 1997.** Structure of an enzyme required for aminoglycoside antibiotic resistance reveals homology to eukaryotic protein kinases. *Cell.* 89: 887-895.

**Leatherbarrow, R.J. 2000.** Grafit. . Erithacus Software, Staines.

**Martel, A., Masson, M., Moreau, N. and Le Goffic, F. 1983.** Kinetic studies of aminoglycoside acetyltransferase and phosphotransferase from *Staphylococcus aureus* RPAL. Relationship between the two activities. *Eur J Biochem.* 133: 515-521.

**McKay, G.A., Robinson, R.A., Lane, W.S. and Wright, G.D. 1994a.** Active-site labeling of an aminoglycoside antibiotic phosphotransferase (APH(3')-IIIa). *Biochemistry.* 33: 14115-14120.

**McKay, G.A., Thompson, P.R. and Wright, G.D. 1994b.** Broad spectrum aminoglycoside phosphotransferase type III from *Enterococcus*: overexpression, purification, and substrate specificity. *Biochemistry.* 33: 6936-6944.

**McKay, G.A. and Wright, G.D. 1995.** Kinetic mechanism of aminoglycoside phosphotransferase type IIIa. Evidence for a Theorell-Chance mechanism. *J Biol Chem.* 270: 24686-24692.

**McKay, G.A. and Wright, G.D. 1996.** Catalytic mechanism of enterococcal kanamycin kinase (APH(3')-IIIa): viscosity, thio, and solvent isotope effects support a Theorell-Chance mechanism. *Biochemistry.* 35: 8680-8685.

**Nakanishi, S., Kakita, S., Takahashi, I., Kawahara, K., Tsukuda, E., Sano, T., Yamada, K., Yoshida, M., Kase, H., Matsuda, Y. and et al. 1992.** Wortmannin, a microbial product inhibitor of myosin light chain kinase. *J Biol Chem.* 267: 2157-2163.

105

Norman, B.H., Shih, C., Toth, J.E., Ray, J.E., Dodge, J.A., Johnson, D.W., Rutherford, P.G., Schultz, R.M., Worzalla, J.F. and Vlahos, C.J. 1996. Studies on the mechanism of phosphatidylinositol 3-kinase inhibition by wortmannin and related analogs. *J Med Chem*. 39: 1106-1111.

Powis, G., Bonjouklian, R., Berggren, M.M., Gallegos, A., Abraham, R., Ashendel, C., Zalkow, L., Matter, W.F., Dodge, J., Grindey, G. and et al. 1994. Wortmannin, a potent and selective inhibitor of phosphatidylinositol-3- kinase. *Cancer Res*. 54: 2419-2423.

Rao, V.D., Misra, S., Boronenkov, I.V., Anderson, R.A. and Hurley, J.H. 1998. Structure of type IIbeta phosphatidylinositol phosphate kinase: a protein kinase fold flattened for interfacial phosphorylation. *Cell*. 94: 829-839.

Sakon, J., Liao, H.H., Kanikula, A.M., Benning, M.M., Rayment, I. and Holden, H.M. 1993. Molecular structure of kanamycin nucleotidyltransferase determined to 3.0-A resolution. *Biochemistry*. 32: 11977-11984.

Thompson, P.R., Hughes, D.W., Cianciotto, N.P. and Wright, G.D. 1998. Spectinomycin kinase from *Legionella pneumophila*. Characterization of substrate specificity and identification of catalytically important residues. *J Biol Chem*. 273: 14788-14795.

Thompson, P.R., Hughes, D.W. and Wright, G.D. 1996. Regiospecificity of aminoglycoside phosphotransferase from Enterococci and Staphylococci (APH(3')-IIIa). *Biochemistry*. 35: 8686-8695.

Toledo, L.M., Lydon, N.B. and Elbaum, D. 1999. The structure-based design of ATP-site directed protein kinase inhibitors. *Curr Med Chem*. 6: 775-805.

Wolf, E., Vassilev, A., Makino, Y., Sali, A., Nakatani, Y. and Burley, S.K. 1998. Crystal structure of a GCN5-related N-acetyltransferase: *Serratia marcescens* aminoglycoside 3-N-acetyltransferase. *Cell*. 94: 439-449.

Wright, G.D., Berghuis, A.M. and Mobashery, S. 1998. Aminoglycoside antibiotics: Structures, function and resistance. In Rosen, B.P. and Mobashery, S. (eds.), *Resolving the Antibiotic Paradox: Progress in Drug Design and Resistance*. Plenum Press, pp. 27-69.

Wybenga-Groot, L.E., Draker, K., Wright, G.D. and Berghuis, A.M. 1999. Crystal structure of an aminoglycoside 6'-N-acetyltransferase: defining the GCN5-related N-acetyltransferase superfamily fold. *Structure Fold Des*. 7: 497-507.

**Wymann, M.P., Bulgarelli-Leva, G., Zvelebil, M.J., Pirola, L., Vanhaesebroeck, B., Waterfield, M.D. and Panayotou, G. 1996.** Wortmannin inactivates phosphoinositide 3-kinase by covalent modification of Lys-802, a residue involved in the phosphate transfer reaction. *Mol Cell Biol.* 16: 1722-1733.

# Chapter 4.

# Molecular Mechanism and Inactivation of the Acetyltransferase Domain of AAC(6')-APH(2")

S.I. Jenkens guided the synthesis of (halomethyl)napthalene and (halomethyl)phenanthrene compounds, and prepared and characterized the compounds in terms of NMR. All other work described in this chapter was performed by myself.

## 4.1 Introduction

The bifunctional enzyme AAC(6')-APH(2") contains both an N-terminal acetyltransferase and C-terminal phosphotransferase domains. In Chapters 2 and 3, the mechanism of phosphorylation by APH(2")-Ia has been discussed. The acetyltransferase activity, AAC(6')-Ie, also has unique properties. For example, AAC(6')-Ie is the sole member of the very large AAC(6') subclass known to acetylate the antibiotic fortimicin A (Shaw *et al.*, 1993), and moreover, in addition to *N*-acetylation activity, this enzyme has been shown to have *O*-acetylation capabilities (Daigle *et al.*, 1999) (Figure 4.1). The unusual activities of AAC(6')-Ie may be related to residues that can bind fortimicin A and 6'-OH aminoglycosides, or to unique residues that are required to catalyze the acetylation of these antibiotics.
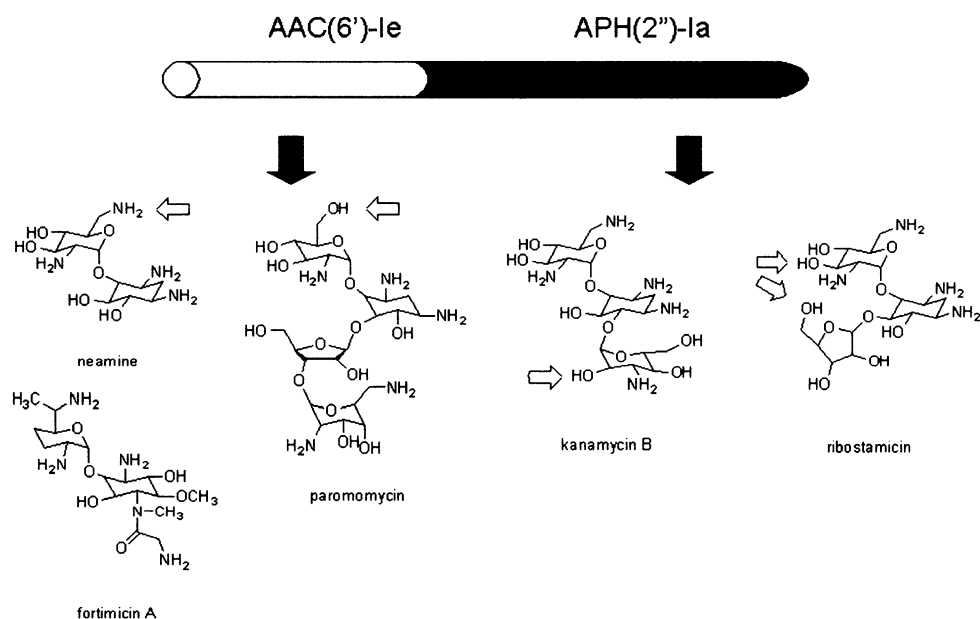


**Figure 4.1:** Regiospecificity of Acetyl and Phosphoryl Modification of Aminoglycosides Catalyzed by AAC(6')-APH(2"). Arrows indicate sites of modification.

109

The APH class of enzyme is relatively well characterized (Wright and Thompson, 1999), mostly owing to structural and functional studies on APH(3')-IIIa (Chapter 2 and references therein). Our mechanistic studies on APH(2")-Ia (Chapters 2 and 3) are consistent with results obtained with APH(3')-IIIa. On the other hand, the molecular mechanisms of AACs are comparatively less understood, despite the fact that crystal structures for AAC(3')-Ia (Wolf *et al.*, 1998), AAC(2')-Ic (Vetting *et al.*, 2002), and AAC(6')-Ii (Wybenga-Groot *et al.*, 1999) are known. The clinical importance of AAC(6')-APH(2") and the substrate specificity differences between AAC(6')-Ie and other aminoglycoside acetyltransferases warrant a more thorough study of the acetyltransferase domain of AAC(6')-APH(2") to understand the distinct properties of this enzyme.

Structural studies on AACs have demonstrated that the aminoglycoside acetyltransferases belong to the GNAT (GCN-5 related N-acetyltransferases) superfamily (Dyda *et al.*, 2000). The kinetic mechanisms of characterized superfamily members (De Angelis *et al.*, 1998; Magnet *et al.*, 2001; Radika and Northrop, 1984; Tanner *et al.*, 1999), including AAC(6')-Ie (Martel *et al.*, 1983), are sequential BiBi suggesting that acetyl transfer occurs directly from acetyl-CoA to acceptor substrate via the formation of a ternary enzyme·acetyl-CoA·aminoglycoside complex. Crystal structures of *Tetrahymena* GCN5 (tGCN5) histone acetyltransferase bound with acetyl-CoA and histone H3 (Rojas *et al.*, 1999) and serotonin N-acetyltransferase (also known as arylalkylamine N-acetyltransferase or AANAT) bound with a bisubstrate analog (Hickman *et al.*, 1999a; Hickman *et al.*, 1999b; Khalil *et al.*, 1999; Wolf *et al.*, 2002), further argue for a direct acetyl transfer mechanism. For such a transfer to occur, the

amine of the acceptor substrate must react with the carbonyl carbon of acetyl-CoA. However, at physiological pH, amines tend to be fully protonated and, hence, are not in a chemically competent state to accept the acetyl group. Consequently, an active site base has been proposed to deprotonate the amine to generate a more potent nucleophile capable of being acetylated.

Structural and functional analyses of AANAT (Hickman *et al.*, 1999a; Hickman *et al.*, 1999b; Scheibner *et al.*, 2002) and tGCN5 (Langer *et al.*, 2001; Rojas *et al.*, 1999; Tanner *et al.*, 1999) have implicated His122 and Glu173, respectively, as the catalytic base in these enzymes, and mutation of Glu173 to Gln results in an ~1000-fold decrease in GCN5 acetyltransferase activity (Langer *et al.*, 2001; Tanner *et al.*, 1999). However, studies with AANAT have been less enlightening, as mutation of His122 to Gln only results in a 6-fold decrease in activity (Scheibner *et al.*, 2002). It has been suggested that substrate deprotonation does not occur directly, but through a series of well-ordered water molecules, or "proton wire," connecting the substrate amine and the catalytic base (Dyda *et al.*, 2000). In such a scenario, other residues in the active site that are capable of accepting hydrogen from these water molecules may compensate in part for the loss of the normal proton acceptor. Indeed, His120 in AANAT appears to play this role and only when both His122 and His120 are mutated to Gln is there a much more substantial effect consistent with base catalysis (Scheibner *et al.*, 2002).

In contrast to either tGCN5 or AANAT, glucosamine 6-phosphate *N*-acetyltransferase (GNA1) appears to lack an active site base since mutational analysis of

Glu-98, which is at the same geometrical position as His120 in AANAT, is inconsistent with base catalysis (Mio *et al.*, 1999). In this case, an active site base may not be required considering that the p$K_a$ of its substrate (~7.75) is sufficiently low that a significant proportion will be in the chemically competent form at physiological pH (Peneff *et al.*, 2001). A very complex picture of catalysis emerges from these findings where the molecular details of acetyl transfer in the GNAT family depend on the specific enzyme and/or substrate. This is not surprising, taking into account the limited sequence similarity shared between these proteins where the conserved GNAT core is mostly involved in providing a binding site for acetyl-CoA and not in providing common scaffolding for catalysis.

Here we have addressed the role of an active site base in the catalytic mechanism of AAC(6')-Ie. We demonstrate through solvent isotope effects, pH studies, and mutational analysis that Asp99 fulfills the role of an active site base and is responsible for the ability of AAC(6')-Ie to catalyze *O*-acetyl transfer. Although Asp99 provides the enzyme with an enhanced detoxification profile, we further demonstrate that compounds such as 1-(bromomethyl)phenanthrene can inactivate AAC(6')-Ie by covalently modifying this residue. These compounds have the potential to be further developed as potent inhibitors of AAC(6')-APH(2") to overcome aminoglycoside resistance *in vivo*.

## 4.2 Materials and Methods

### 4.2.1 Reagents

The purification of N-terminal hexahistidine-tagged AAC(6')-APH(2") has been described in Chapter 3, and mutant enzymes were purified similarly.

### 4.2.2 AAC(6')-Ie Kinetic Assays

Most AAC assays were conducted according to Chapter 3 and Daigle *et al.*( 1999). For more sensitive assays, acetyltransferase activity was determined using [1-$^{14}$C]acetyl-CoA and a phosphocellulose binding assay described previously (Wybenga-Groot *et al.*, 1999). Reaction mixtures typically contained 25 mM HEPES-NaOH, pH 7.5, 0.1 μCi of [1-$^{14}$C]AcCoA (200 μM final concentration), 1 mM aminoglycoside substrate, and 0.3 nmol of pure AAC(6')-Ie, and were allowed to proceed for 10 min at 37°C.

Initial rates were fit to the Michaelis-Menten equation (Equation 4.1) using Grafit 4.0 (Leatherbarrow, 2000),

$$v = (k_{cat}/E_t)[S]/(K_M + [S])  \qquad\qquad \text{(Eq. 4.1)}$$

where $v$ is the initial velocity, $E_t$ is the total amount of enzyme in the assay and [S] is the concentration of substrate. The concentrations of acetyl-CoA and kanamycin A were held at 300 μM when measuring the steady-state kinetic parameters for aminoglycoside substrate and acetyl-CoA, respectively. Results are reported +/- standard error.

**4.2.3 Solvent Viscosity, Solvent Isotope, and pH Effects for AAC(6')-Ie**

The solvent viscosity, solvent isotope, and pH effects for AAC(6')-Ie were determined by varying the buffer conditions of the standard assay. For the solvent viscosity effect experiments, steady-state kinetic parameters were determined with varying concentrations of the microviscosogen glycerol (0, 15, 22.5, and 30% (w/v)). The viscosity of the solutions was determined using an Ostwald viscometer in triplicate, and the slope of a plot of relative viscosity *versus* $rate_o/rate_{viscogen}$ reveals the solvent viscosity effect (SVE). Steady-state kinetic parameters were also performed in the macroviscosogen polyethylene glycol 8000 (6.7% w/v) and were not found to have a significant effect on the rate constants.

Solvent isotope effects were measured by conducting kinetic analyses in $D_2O$ (99.9% from Isotec), where the final amount of $H_2O$ was not more than 5%. pD values were determined by measuring pH and adding 0.4 unit ($pD = pH + 0.4$). The proton inventory study was conducted by adding ratios of buffer in $H_2O$ and $D_2O$ and making appropriate corrections for the addition of enzyme and substrates to calculate the final amount of $D_2O$ in the enzyme assay solution.

Buffers with overlapping pH ranges were used to investigate the effect of pH on enzyme activity. Buffers used were: 25 mM MOPS-NaOH (pH 6.0-6.5), 25 mM MES-NaOH (pH 6.5-7.5), 25 mM HEPES-NaOH (pH 7.0-8.0), and 25 mM glycylglycine (pH 8.0-9.5). None of the buffers gave any significant nonspecific effects. The data were

analyzed using Grafit 4 (Leatherbarrow, 2000). For AAC(6')-Ie WT, which displays two

ionizations, the data can be fit to the following equation through nonlinear regression,

$$\log v = \log (C / (1 + [H^+]/K_a + K_b/[H^+]))$$
<div align="right">(Eq. 4.2)</div>

For single ionization analysis with AAC(6')-Ie Asp99Ala, the data can be fit using

nonlinear regression analysis of the following equation,

$$\log v = \log (C / (1 + K_b/[H^+]))$$
<div align="right">(Eq. 4.3)</div>

where $v$ is the first-order ($k_{cat}$) or second-order ($k_{cat}/K_M$) rate constant, $K_a$ and $K_b$ are the

acid and base equilibrium constants, respectively, $C$ is the pH-independent value, and

$[H^+]$ is the proton concentration.

## 4.2.4 Site-Directed Mutagenesis

Site-directed mutagenesis was performed using the QuikChange method

(Stratagene, La Jolla, CA). The appropriate mutagenic primers

(Tyr96Phe,                GAGATAGTCTTTGGTATGGATCAATTTATAGGAGAGCC;

Asp99Ala,                 GAGATAGTCTATGGTATGGCTCAATTTATAGGAGAGCC;

Asp99Asn,    GAGATAGTCTATGGTATGGAACAATTTATAGGAGAGCC;    and

Asp99Glu, GAGATAGTCTATGGTATGAATCAATTTATAGGAGAGCC) and their

reverse complements were used in combination with 20 ng of template DNA

(pET15AACAPH (Boehr *et al.*, 2001)) in *Pfu* DNA polymerase (Stratagene, La Jolla, CA)-catalyzed PCR reactions. After parental DNA was digested with *Dpn*I, mutant plasmid DNA was transformed into $CaCl_2$-competent *E. coli* XL-1 Blue. Positive clones were sequenced in their entirety and then used to transform into *E. coli* BL21(DE3) for subsequent protein purification.

### 4.2.5 Minimum Inhibitory Concentration Determinations with Fortimicin A

Minimum inhibitory concentration (MIC) determinations were performed as described in Chapter 2, where the MICs for *E. coli* BL21(DE3) carrying control plasmid pET15b(+) were compared with *E. coli* BL21(DE3) carrying pET15AACAPH and appropriate plasmids with site mutants in the *aac(6')-aph(2")* gene.

### 4.2.6 Synthesis of 1-(Bromomethyl)phenanthrene, 1-(Bromomethyl)naphthalene, and 9-(Chloromethyl)phenanthrene

The preparation of 1-(bromomethyl)phenanthrene and 9-(chloromethyl)phenanthrene using *N*-bromo- and *N*-chlorosuccinimide, respectively, has been previously reported (Wright *et al.*, 1990). 1-(Bromomethyl)naphthalene was prepared in an analogous manner using *N*-bromosuccinimide: thin-layer chromatography, $R_f$ ($SiO_2$, 2% (v/v) ethylacetate in hexanes), 0.42; $^1H$ NMR (200 MHz, $CDCl_3$): δ 8.21 (d, J = 8.57 Hz, 1H, CH), 7.90 (t, J = 9.18 Hz, 2H, CH), 7.43-7.67 (m, 4 H, CH), 4.99 (s, 2H, $CH_2Br$); $^{13}C$ NMR (50 MHz, $CDCl_3$): δ 133.9, 133.2, 131.0, 129.7, 128.8, 127.7, 126.5, 126.1, 125.3, 123.6, and 31.7.

**4.2.7 Inactivation of AAC(6')-Ie by (Halomethyl)phenanthrenes and (Halomethyl)naphthalenes**

Inactivation experiments were carried out by incubating enzyme (0.2-2 μM) with compound (0-200 μM) dissolved in dimethylsulfoxide (0.04% v/v total) in 240 μL of 25 mM HEPES-NaOH, pH 7.5, and 2 mM 4,4'-dithiodipyridine at 37°C for 10-40 min, prior to the addition of kanamycin A and acetyl-CoA (300 μM final concentrations) to measure acetyltransferase activity. For the substrate protection experiments, kanamycin A (500 μM) and/or desulfo-CoA (100 μM) were incubated with the inactivation mixture for 10 min before the addition of acetyl-CoA (500 μM final). The concentration of desulfo-CoA used in these experiments (100 μM) was in the range of the $IC_{50}$ for desulfo-CoA using 300 μM kanamycin A and 300 μM acetyl-CoA. The effect of pH on inactivation was determined by conducting inactivation experiments in the following buffers: 25 mM MOPS-NaOH (pH 6.5), 25 mM HEPES-NaOH (pH 7.0-8.0), and 25 mM glycylglycine (pH                                                                                                    8.5).


**4.3 Results and Discussion**

**4.3.1 AAC(6')-Ie Can Acetylate Aminoglycoside 6'-OH and 6'- NH$_2$**

AAC(6')-Ie is unique in that it is the only known member of the AAC(6') subclass that can acetylate fortimicin A, and it also has the ability to $O$-acetylate aminoglycosides at the 6' position as represented by paromomycin (Daigle et al., 1999) (Figure 4.1 and Table 4.1). The $pK_a$ of the 6'-NH$_3^+$ of aminoglycosides related to neamine (Botto and Coxon, 1983), and kanamycin A (Dorman et al., 1976) has previously been determined to

be 8.6. As such, a significant proportion of the aminoglycoside will be in the fully protonated state at physiological pH, and a catalytic base would be predicted to increase the efficiency of the reaction, although there is no absolute requirement for an active site base. An active site base would be predicted to be more critical with 6'-OH aminoglycosides, because the p$K_a$ of the hydroxyl will be in the range of 14-16.

### 4.3.2 Solvent Viscosity and Solvent Isotope Effects for AAC(6')-Ie

AAC(6')-Ie has previously been shown to follow a random order BiBi kinetic mechanism (Martel *et al.*, 1983). To further define the kinetic mechanism, we performed solvent viscosity effect (SVE) experiments with glycerol as the microviscosogen to identify the rate-determining step(s) in the catalytic cycle. A significant SVE indicates that one or more rate-determining steps are diffusion-controlled, with either substrate coming to the enzyme, product leaving the enzyme, or a diffusion-controlled conformational change, whereas the lack of a significant SVE effect indicates a diffusion-independent rate-determining step, such as a viscosity-independent conformational change or chemistry at the active site.

There was a minor solvent viscosity effect for both $k_{cat}$ and $k_{cat}/K_M$ with acetyl-CoA as the variable substrate, but there was not a significant SVE for either $k_{cat}$ or $k_{cat}/K_M$ with kanamycin A as the variable substrate (Table 4.2). The lack of a SVE is consistent with the chemical step(s) being rate-limiting.

**Table 4.1:** Steady-State Kinetic Parameters of Wild-Type and Mutant AAC(6')-Ie

| Substrate | $K_M$ (μM) | $k_{cat}$ (s$^{-1}$) | $k_{cat}/K_M$ (M$^{-1}$s$^{-1}$) | | |
|---|---|---|---|---|---|
| **WT** | | | | | |
| acetyl-CoA[a] | 38 +/- 5 | 1.2 +/- 0.3 | 3.1 x 10$^4$ | | |
| kanamycin A[a] | 31 +/- 3 | 1.7 +/- 0.2 | 5.6 x 10$^4$ | | |
| neamine | 78.3 +/- 15.7 | 0.43 +/- 0.02 | 5.6 x 10$^3$ | | |
| fortimicin A | 25.4 +/- 5.5 | 0.28 +/- 0.04 | 1.1 x 10$^4$ | | |
| paromomycin | 324 +/- 45 | 0.059 +/- 0.003 | 1.8 x 10$^2$ | | |
| Substrate | $K_M$ (μM) | $k_{cat}$ (s$^{-1}$) | $k_{cat}/K_M$ (M$^{-1}$s$^{-1}$) | $k_{cat}^{WT}/$ $k_{cat}^{MUT}$ | $(k_{cat}/K_M)^{WT}/$ $(k_{cat}/K_M)^{MUT}$ |
| **Tyr96Phe** | | | | | |
| acetyl-CoA | 73.6 +/- 12.2 | 1.3 +/- 0.1 | 1.8 x 10$^4$ | 0.92 | 1.7 |
| kanamycin A | 79.0 +/- 11.1 | 1.1 +/- 0.1 | 1.3 x 10$^4$ | 1.6 | 4.2 |
| neamine | 326 +/- 35 | 1.3 +/- 0.1 | 3.9 x 10$^3$ | 0.34 | 1.4 |
| fortimicin A | 43.5 +/- 12.1 | 0.45 +/- 0.04 | 1.0 x 10$^4$ | 0.62 | 1.1 |
| paromomycin | 771 +/- 310 | 0.026 +/- 0.006 | 3.3 x 10$^1$ | 2.3 | 5.5 |
| **Asp99Ala** | | | | | |
| acetyl-CoA | 45.3 +/- 9.0 | 0.035 +/- 0.002 | 7.9 x 10$^2$ | 34 | 39 |
| kanamycin A | 126 +/- 28 | 0.033 +/- 0.003 | 2.6 x 10$^2$ | 52 | 215 |
| keamine | 443 +/- 89 | 0.029 +/- 0.001 | 6.5 x 10$^1$ | 15 | 85 |
| fortimicin A[b] | n.d. | 2 x 10$^{-4}$ | n.d. | 1400 | n.d. |
| paromomycin[b] | n.d. | <2 x 10$^{-5}$ | n.d. | >2500 | n.d. |
| **Asp99Asn** | | | | | |
| acetyl-CoA | 39.9 +/- 9.0 | 0.17 +/- 0.01 | 4.4 x 10$^3$ | 6.9 | 7.1 |
| kanamycin A | 90.2 +/- 33 | 0.038 +/- 0.005 | 4.3 x10$^2$ | 45 | 131 |
| neamine | 509 +/- 114 | 0.028 +/- 0.003 | 5.5 x 10$^1$ | 16 | 101 |
| fortimicin A[b] | n.d. | 8 x 10$^{-4}$ | n.d. | 350 | n.d. |
| paromomycin[b] | n.d. | <1 x 10$^{-5}$ | n.d. | >2500 | n.d. |
| **Asp99Glu** | | | | | |
| acetyl-CoA | 17.0 +/- 6.3 | 0.11 +/- 0.01 | 6.5 x 10$^3$ | 11 | 4.8 |
| kanamycin A | 102 +/- 23 | 0.19 +/- 0.02 | 1.8 x 10$^3$ | 9.1 | 30 |

| neamine | 229 +/- 30 | 0.066 +/- 0.005 | $2.9 \times 10^2$ | 6.6 | 19 |
|---|---|---|---|---|---|
| fortimicin A | 70.0 +/- 26.1 | 0.006 +/- 0.001 | $8.2 \times 10^1$ | 49 | 134 |
| paromomycin[b] | n.d. | $4 \times 10^{-4}$ | n.d. | 140 | n.d. |

[a] values taken from (Boehr et al., 2001).

[b] due to the low activities in the mutant proteins associated with these substrates, only an estimate of $k_{cat}$ could be determined where aminoglycoside was held at 1 mM and [$^{14}$C]-acetyl-CoA was held at 200 μM.

**Table 4.2:** Solvent Viscosity and Solvent Isotope Effects for AAC(6')-Ie.

| Varied Substrate | Solvent Viscosity Effect | | Solvent Isotope Effect | |
|---|---|---|---|---|
| | $^n(k_{cat})$ | $^n(k_{cat}/K_M)$ | $^H k_{cat}/ ^D k_{cat}$ | $^H(k_{cat}/K_M) / ^D(k_{cat}/K_M)$ |
| Acetyl-CoA | 0.42 +/- 0.10 | 0.44 +/- 0.15 | 1.18 +/- 0.04 | 1.23 +/- 0.15 |
| Kanamycin A | 0.22 +/- 0.10 | 0.08 +/- 0.03 | 1.52 +/- 0.05 | 3.27 +/- 0.39 |

The importance of proton extraction in the chemical step(s) was investigated by determining solvent isotope effects (SIEs) ($^H k_{cat}/^D k_{cat}$). The only significant SIE determined for AAC(6')-Ie was for the second order rate constant ($k_{cat}/K_M$) with respect to kanamycin A (Table 4.2). As solvent isotope effects may be related to one or multiple exchangeable hydrogens, we further defined the solvent isotope effect for kanamycin A by performing a proton inventory study, where the steady-state kinetic parameters are determined in varying ratios of $H_2O$ to $D_2O$ (Figure 4.2). The linearity of the curve is consistent with the SIE being due to mobilization of only one hydrogen (Schowen and Schowen, 1982), likely a hydrogen extracted from the 6'-$NH_3^+$ position of kanamycin A. Thus, these results are consistent with deprotonation of kanamycin A being important in productive aminoglycoside capture.
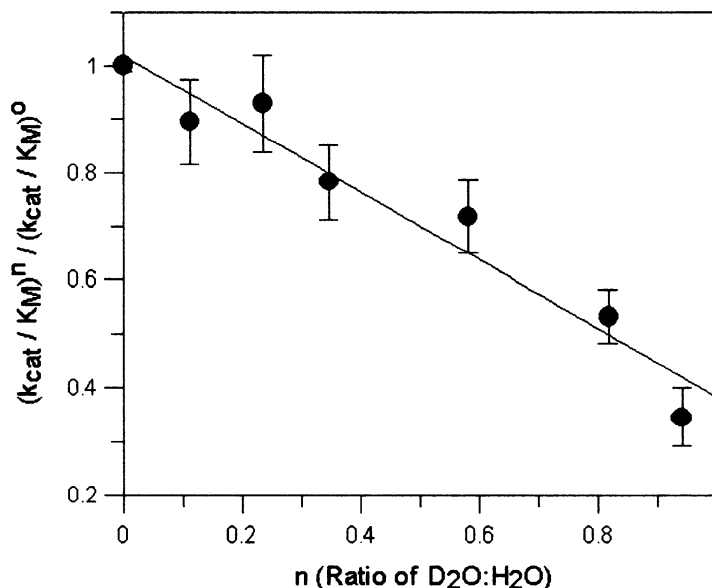
**Figure 4.2:** Proton Inventory Study of AAC(6')-Ie Action using Kanamycin A as the Variable Substrate. The steady-state parameters for kanamycin A were determined in varying ratios of $D_2O:H_2O$ in the presence of 300 μM acetyl-CoA.

## 4.3.3 pH Effects for AAC(6')-Ie

The effects of pH on steady-state kinetic parameters can give insight into the required ionization state of important enzyme active site residues. The pH effects for AAC(6')-Ie showed two important ionizations whether acetyl-CoA or neamine was the variable substrate (Figure 4.3 A and B, and Table 4.3). These $pK_a$ values may be related to the required ionization states of enzymatically important residues. Thus, for example, the acidic limb of the pH curve ($pK_a$ = 7.2-7.3) could be associated with a residue that needs to be deprotonated for maximum enzyme activity. The putative active site base required to deprotonate the antibiotic would normally need to be deprotonated to accept a hydrogen from the aminoglycoside substrate. Thus, the pH profiles are consistent with a

chemical mechanism employing an active site base and an active site acid, and we can

tentatively assign the first $pK_a$ to the active site base.

**Table 4.3:** Summary of the Dependence of AAC(6')-Ie WT and Asp99Ala Steady-state Kinetics on pH.

| | $k_{cat}$ | | $k_{cat}/K_M$ | |
|---|---|---|---|---|
| | $pK_{a1}$ | $pK_{a2}$ | $pK_{a1}$ | $pK_{a2}$ |
| **WT** | | | | |
| - neamine | 7.2 +/- 0.2 | 7.6 +/- 0.2 | 7.3 +/- 0.2 | 7.8 +/- 0.2 |
| - acetyl-CoA | 7.2 +/- 0.1 | 7.5 +/- 0.1 | 7.3 +/- 0.2 | 7.6 +/- 0.3 |
| **Asp99Ala** | | | | |
| - neamine | -[a] | 8.0 +/- 0.2 | -[a] | -[b] |
| - acetyl-CoA | -[a] | 8.5 +/- 0.2 | -[a] | 7.9 +/- 0.2 |

[a] pH dependence curves only indicated one ionization, associated with $pK_{a2}$ in AAC(6')-Ie WT

[b] the pH dependence curve for $k_{cat}/K_M$ for neamine did not reveal a distinct ionization

### 4.3.4 Mutational Analyses of AAC(6')-Ie Tyr96 and Asp99

These results suggest that AAC(6')-Ie employs an active site base that acts to

deprotonate the aminoglycoside substrate, thereby generating a more potent nucleophile

to facilitate acetyl transfer from acetyl-CoA. In members of the GNAT superfamily, there

are two amino acid positions that have been suggested to act as the active site base. In the

histone acetyltransferase tGCN5, Glu173 has been suggested to fulfill this role (Langer *et*

*al.*, 2001; Tanner *et al.*, 1999), whereas in AANAT, the active site base appears to be

His122 (Scheibner *et al.*, 2002). The three-dimensional structure of AAC(6')-APH(2'')

has not been determined, so we used available sequence alignments (Shmara *et al.*, 2001;

Wybenga-Groot *et al.*, 1999) to generate a partial alignment of GNAT family members

that could aid in identifying the putative active site base in AAC(6')-Ie (Figure 4.4).
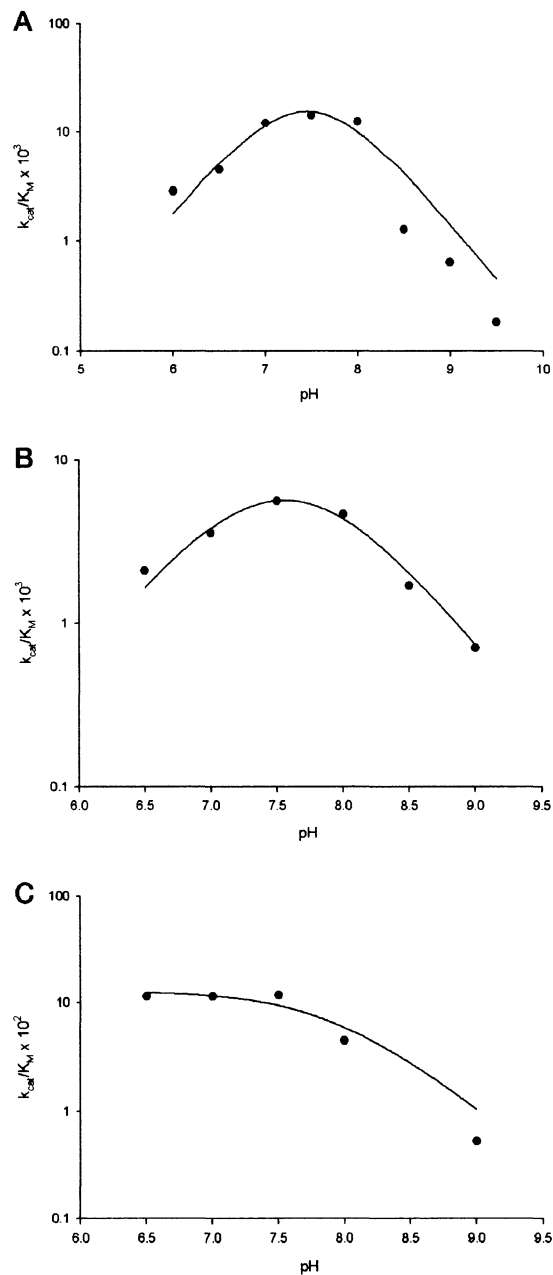
**Figure 4.3:** pH Dependence of AAC(6')-Ie WT with Variable Substrate Acetyl-CoA (*A*) or Neamine (*B*) and AAC(6')-Ie Asp99Ala Activity with the Variable Substrate Acetyl-CoA (*C*). The other substrate was held at 300 μM. Steady-state kinetic parameters were determined at various pH levels with the following buffers: 25 mM MES-NaOH (pH 6.0), 25 mM MOPS-NaOH (pH 6.5), 25 mM HEPES-NaOH (pH 7.0-8.0), and 25 mM glycylglycine                                    (pH                                    8.5-9.5).

```
AANAT       105- L  T  Q  S  L  A  L  H  R  P  R  G  H  S  A  H  L  H  -  A  L  A  V -126
tGCN5       171- F  A  E  -  -  -  -  -  -  -  -  -  -  -  -  -  -  -  V  A  -  F  L  A  V -179
AAC(3)-la   98-  -  -  -  -  -  -  -  -  E  Q  P  R  S  E  I  Y  I  Y  -  D  L  A  V -111
AAC(6')-li  70-  G  W  E  -  -  -  -  -  -  -  -  -  -  -  -  -  L  H  -  P  L  V  V -78
AAC(6')-lb  95-  G  V  R  -  -  -  -  -  -  -  -  -  -  -  -  -  G  I  D  Q  S  L  A  N -105
AAC(6')-le  94-  I  V  Y  -  -  -  -  -  -  -  -  -  -  -  -  -  G  M  D  Q  -  F  I  G -103
                    *                                                    *
```

**Figure 4.4:** Alignment of β-strand 4 Segments of Motif A from Selected GNAT Family Members. *Shaded text* indicates conserved hydrophobic regions, and *asterisks* indicate positions of residues suggested to play the role of an active site base in different family members. The alignment is based on previous structure-based alignments (Shmara *et al.*, 2001; Wybenga-Groot *et al.*, 1999).

The residues in AAC(6')-Ie that align with known or predicted active site bases in GNAT family members are Tyr96 and Asp99 (Figure 4.4). To test the possibility that these residues could act as the active site base, we generated the following mutant proteins: AAC(6')-Ie Tyr96Phe, AAC(6')-Ie Asp99Ala, AAC(6')-Ie Asp99Asn, and AAC(6')-Ie Asp99Glu. The mutation of Asp99 to Ala is a more drastic change, whereas mutation to Asn conserves R group length but not the proton extracting carboxylate moiety and mutation to Glu conserves the carboxylate moiety but extends R group length by one methylene unit.

There were only minor effects on the steady state kinetic parameters when Tyr96 was mutated to Phe (Table 4.1). The largest effects were seen for paromomycin (*e.g.* change in $k_{cat}/K_M$ compared with WT was 5.5-fold). These results are not consistent with Tyr96 acting as an active site base, although it may have a minor effect on substrate binding with some aminoglycosides.

The changes in steady-state parameters for AAC(6')-Ie Asp99Ala and AAC(6')-Ie Asp99Asn were similar (Table 4.1). For kanamycin A, there were significant decreases in both $k_{cat}$ (45- to 52-fold) and $k_{cat}/K_M$ (131- to 215-fold) parameters. The changes for neamine were smaller but still significant for both $k_{cat}$ (15- to 16-fold) and $k_{cat}/K_M$ (85- to 101-fold). In contrast, there were more drastic changes for $k_{cat}$ with fortimicin A (350- to 1400-fold) and paromomycin (>2500).

The decreases in activity determined with AAC(6')-Ie Asp99Glu were generally less than for either Ala or Asn mutations (Table 4.1). This result suggests that the carboxylate moiety of Asp99 is most critical for WT enzyme activity. This would be expected if Asp99 acts as the active site base, because it would require the ability to ionize and accept a hydrogen from the aminoglycoside substrate. A Glu at this position would have a similar capacity, although it would not likely be optimally positioned for such a task, whereas Asn or Ala could not fulfill this role. Moreover, the fact that AAC(6')-Ie Asp99Ala and AAC(6')-Ie Asp99Asn become increasingly impaired in their ability to catalyze acetyl transfer with paromomycin is consistent with Asp99 acting as the active site base. It will become exceedingly important to have an active site base to deprotonate the aminoglycoside when the $pK_a$ of the acceptor group increases and a greater proportion of the substrate will be in a noncompetent form for efficient acetyl group transfer at physiological pH.

To correlate *in vitro* effects to biological impact, we performed minimum inhibitory concentration (MIC) determinations for *E. coli* expressing AAC(6')-APH(2")

WT or Asp99 mutant enzymes (Table 4.4). Because APH(2")-Ia cannot phosphorylate

fortimicin A, protection of bacteria from this particular antibiotic is solely the

responsibility of the AAC(6')-Ie activity in the bifunctional enzyme. The MIC

determinations were consistent with the kinetic data, where *E. coli* carrying

pET15AACAPH Asp99Ala and pET15AACAPH Asp99Asn provided no protection

against fortimicin A (Table 4.4). This finding further underscores the importance of

Asp99 in the acetylation and detoxification of fortimicin A.

**Table 4.4:** Minimum Inhibitory Concentration (MIC) Determinations with Fortimicin A for *Escherichia coli* BL21(DE3) Expressing HisAAC(6')-APH(2") Wild-Type and Asp99 Mutants.

| Construct | MIC ($\mu$g/mL) |
|---|---|
| BL21(DE3) control[a] | 2 |
| Wild type | 512 |
| Asp99Ala | 2 |
| Asp99Asn | 2 |
| Asp99Glu | 16 |

a- carrying pET15b(+)

### 4.3.5 pH Effects for AAC(6')-Ie Asp99Ala

We have previously assigned the first ionization in the pH profile of AAC(6')-Ie

to the putative active site base. To further test this hypothesis and more fully develop the

role of Asp99 in the catalytic mechanism of AAC(6')-Ie, we determined the effects of pH

on $k_{cat}$ and $k_{cat}/K_M$ for AAC(6')-Ie Asp99Ala (Figure 4.3C and Table 4.3). The results do

not show the double ionization curves as seen in AAC(6')-Ie WT. The pH curves for $k_{cat}$

with either neamine or acetyl-CoA as the variable substrate and for $k_{cat}/K_M$ with acetyl-

CoA as the variable substrate show only a single ionization associated with the second

$pK_a$ in AAC(6')-Ie (Table 4.3). Thus, these results are consistent with Asp99 serving as

the active site base, and we can assign the first $pK_a$ in the pH profile of AAC(6')-Ie WT to

Asp99.

When neamine is the variable substrate, there is not a distinct ionization (Table

4.3). This is likely related to the form of neamine that preferentially binds to AAC(6')-Ie

WT compared with AAC(6')-Ie Asp99Ala. With AAC(6')-Ie WT, neamine is bound as the

fully protonated form, however, as AAC(6')-Ie Asp99Ala lacks an active site base to

deprotonate the incoming aminoglycoside, neamine likely binds in the unprotonated form

in order to be chemically active. This effect complicates analysis and essentially conceals

the basic limb of the pH profile.


## 4.3.6    Inhibition    of    AAC(6')-Ie    by    (Halomethyl)naphthalene    and (Halomethyl)phenanthrene Derivatives

A library screen of small planar molecules against AAC(6')-Ie identified 1-

(bromomethyl)phenanthrene and 9-(chloromethyl)phenanthrene as inhibitors of AAC(6')-

Ie, where 1-(bromomethyl)phenanthrene gave much more significant inhibition than 9-

(chloromethyl)phenanthrene (Figure 4.5). This difference may be related to either the

position or nature of the halogen group. We also assayed 1-(bromomethyl)naphthalene

and 1-(chloromethyl)naphthalene to assess the importance of the halo-group and the

additional    benzene    ring    to    inhibition    by    1-(bromomethyl)phenanthrene.    The

bromomethyl- derivative demonstrated more significant inhibition of AAC(6')-Ie activity

than did the chloromethyl- derivative, however, 1-(bromomethyl)naphthalene was a much

poorer inhibitor than was 1-(bromomethyl)phenanthrene (Fig. 4.5), highlighting the

importance of both the bromo- group and the additional benzene ring in inhibition.
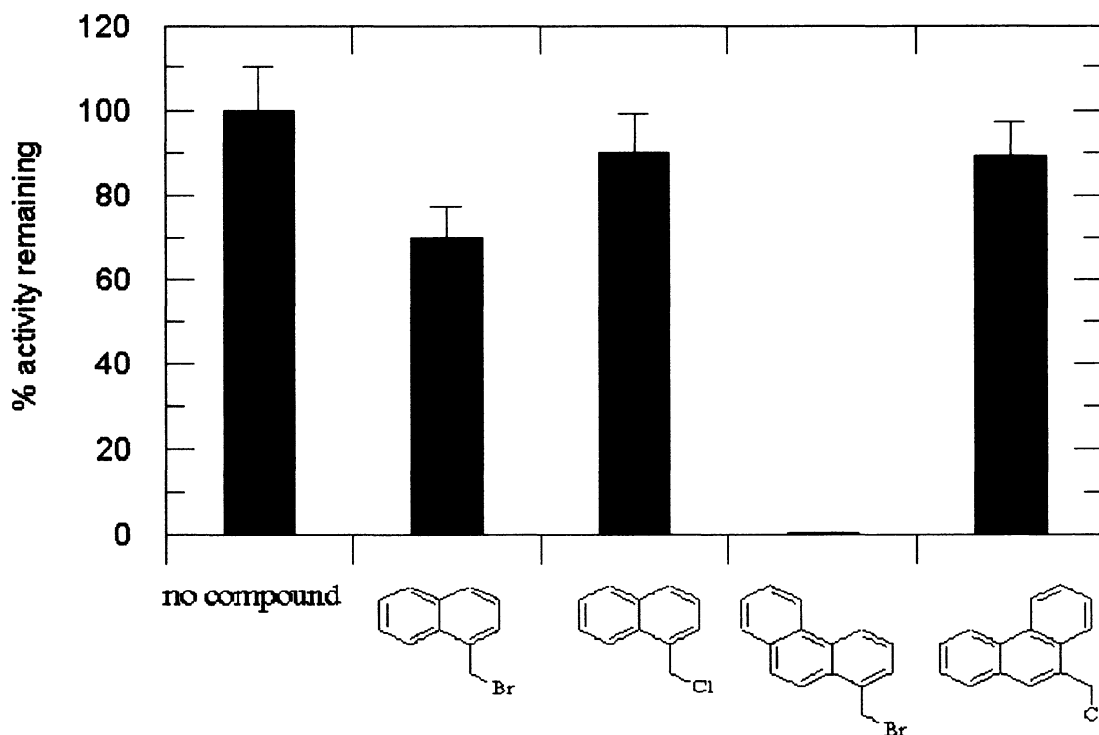


**Figure 4.5:** Inhibition of AAC(6')-Ie by 1-(Bromomethyl)naphthalene, 1-(Chloromethyl)naphthalene, 1-(Bromomethyl)phenanthrene, and 9-(Chloromethyl)phenanthrene (*left* to *right*). Enzyme (0.2 μM) was incubated with 25 μM compound at 37 °C for 20 min before assaying for acetyltransferase activity with the addition of acetyl-CoA and kanamycin A to final concentrations of 300 μM.

### 4.3.7 1-(Bromomethyl)phenanthrene is a Potent Irreversible Inhibitor of AAC(6')-Ie

The increased potency of the bromo- derivatives compared with the equivalent

chloro- compounds suggested that these molecules can act as covalent modifiers of

AAC(6')-Ie. One hallmark of an irreversible inhibitor is time-dependent inhibition of

enzyme activity, where there is typically an initial enzyme·inhibitor complex described by

the dissociation constant $K_i$ before covalent modification of an active site residue with a first order rate constant $k_{max}$, according to the following reaction,

$$E + I \underset{}{\overset{K_i}{\rightleftharpoons}} EI \xrightarrow{k_{max}} EI^*$$
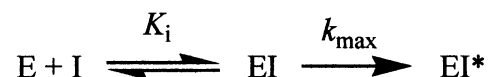
Both 1-(bromomethyl)phenanthrene (Figure 4.6A) and 1-(bromomethyl)naphthalene (not shown) showed time-dependent inhibition of AAC(6')-Ie. Unfortunately, due to the reactivities and relative insolubilities of these compounds, a complete kinetic profile of the inactivation reactions could not be achieved, and so, $K_i$ and $k_{max}$ values could not be determined. However, a linear plot of the first order rate constants *versus* time yields a slope that estimates $k_{max}/K_i$. For 1-(bromomethyl)phenanthrene (Figure 4.6B) and 1-(bromomethyl)naphthalene (not shown), this gives approximate $k_{max}/K_i$ values of $11.7 \pm 1.0\ M^{-1}s^{-1}$ and $1.82 \pm 0.17\ M^{-1}s^{-1}$, respectively. Because the leaving group is identical in both compounds, the difference in reactivities is likely related to the initial binding event. Thus, 1-(bromomethyl)phenanthrene binds to the enzyme 6.4-fold more efficiently than 1-(bromomethyl)naphthalene, indicating the importance of the third benzene ring in ligand recognition.
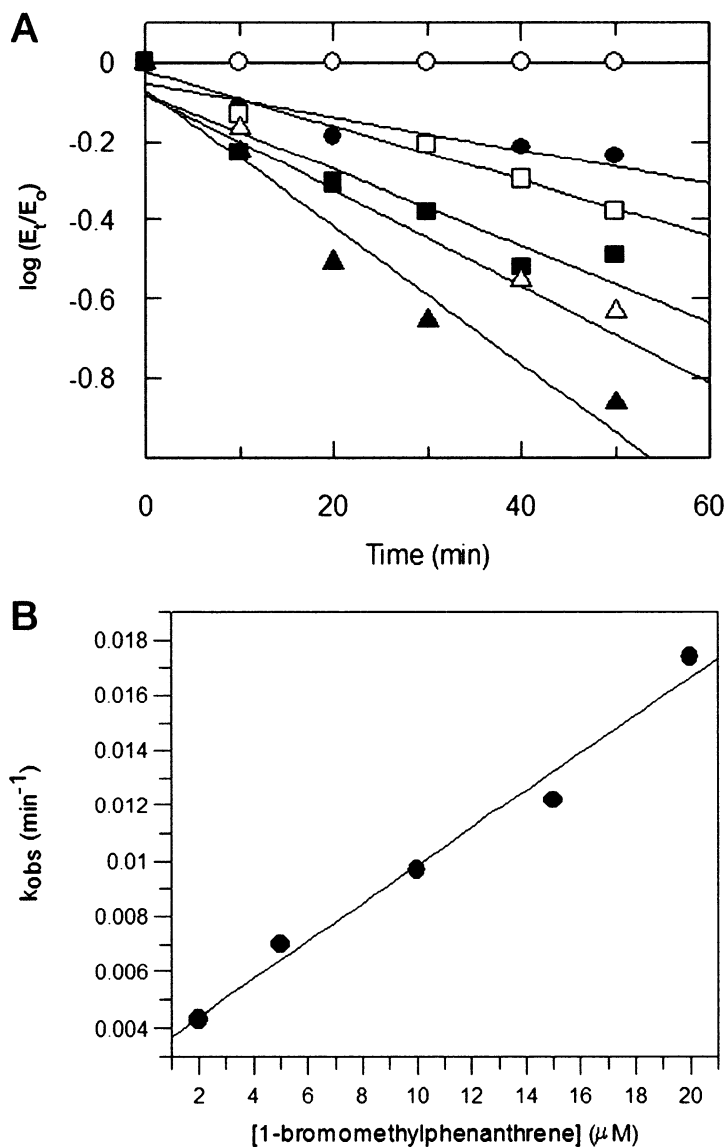
**Figure 4.6:** Time- and Concentration-Dependent Inhibition of AAC(6')-Ie by 1-(Bromomethyl)phenanthrene. To determine the kinetics of inactivation for 1-(bromomethyl)phenanthrene (*A*), enzyme (0.2 μM) was incubated with 0 (O), 2 (●), 5 (□), 10 (■), 15 (△), or 20 (▲) μM compound prior to assaying acetyltransferase activity with the addition of acetyl-CoA and kanamycin A to final concentrations of 300 μM. The first order rate constants determined from *A* were used to construct the curves in *B*.

Neither extensive dialysis nor gel filtration could return enzyme activity following

inactivation by 1-(bromomethyl)phenanthrene, again consistent with 1-

(bromomethyl)phenanthrene acting as a covalent modifier of AAC(6')-Ie. Moreover, MALDI-TOF was consistent with covalent modification of the enzyme by 1-(bromomethyl)phenanthrene (data not shown). These results suggest that 1-(bromomethyl)phenanthrene inactivates AAC(6')-Ie by covalently modifying an important residue in the enzyme.

### 4.3.8   1-(Bromomethyl)phenanthrene   Inactivates   AAC(6')-Ie   by   Covalently Modifying Asp99

To gain insight into which residue or residues are modified by 1-(bromomethyl)phenanthrene, we performed substrate/inhibitor protection experiments, where the enzyme was incubated with 1-(bromomethyl)phenanthrene and kanamycin A and/or desulfo-CoA prior to measurement of acetyl transfer activity with the addition of acetyl-CoA. Kanamycin A and desulfo-CoA both weakly protected AAC(6')-Ie from inactivation by 1-(bromomethyl)phenanthrene (Figure 4.7A). Moreover, when the enzyme was incubated with both kanamycin A and desulfo-CoA, protection was much more substantial and was additive with respect to the single compound protection experiments (Figure 4.7A). This result is consistent with 1-(bromomethyl)phenanthrene having a binding site that overlaps that of both the kanamycin A and desulfo-CoA/acetyl-CoA                                             binding                                             sites.
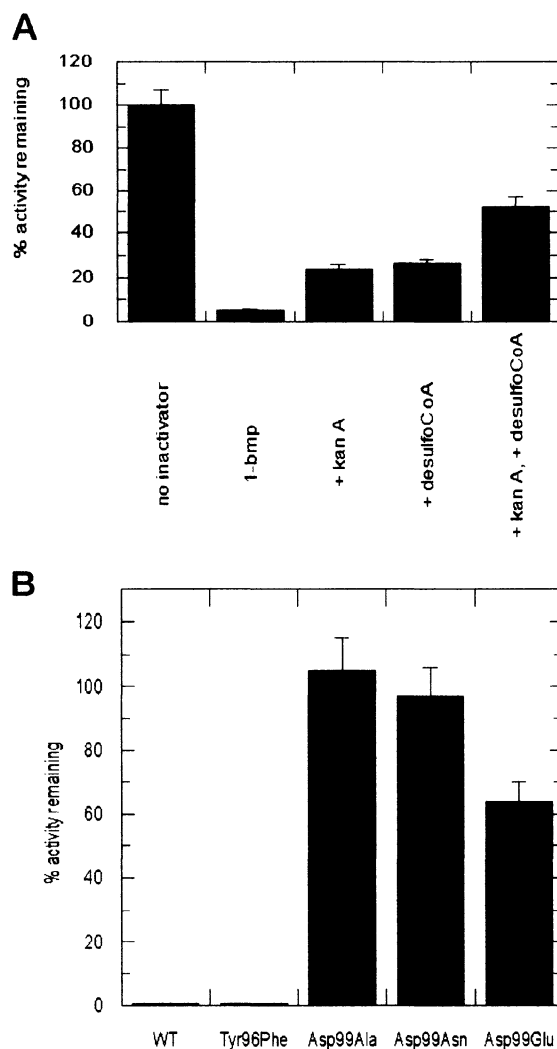
**Figure 4.7:** Characterization of 1-(Bromomethyl)phenanthrene Inactivation of AAC(6')-Ie. *A*, protection of AAC(6')-Ie from inactivation by 1-(bromomethyl)phenanthrene. Enzyme (0.2 µM) was incubated in the presence of 20 µM 1-(bromomethyl)phenanthrene (1-bmp) in the presence or absence of kanamycin A (500 µM) and desulfo-CoA (100 µM) for 10 min at 37°C before the addition of acetyl-CoA (500 µM) to measure the acetyltransferase activity. Activities were compared with incubations without 1-(bromomethyl)phenanthrene. *B*, susceptibility of AAC(6')-Ie and mutants to inactivation by 1-(bromomethyl)phenanthrene. Enzyme (0.2-2 µM) was incubated with 40 µM 1-(bromomethyl)phenanthrene for 10 min at 37°C before the addition of acetyl-CoA and kanamycin A to final concentrations of 300 µM to assay for acetyltransferase activity.

Taking into account the results of the protection experiments, only a few select residues in AAC(6')-Ie could be potential candidates to serve as the active site nucleophile in the reaction. Because our attempts to identify the residue through a series of experiments involving large-scale enzyme inactivation, proteolysis of the complex, and mass spectral analysis of the proteolytic fragments failed due to relative insolubility of 1-(bromomethyl)phenanthrene and nonspecific protein losses during work-up, we opted to use an alternative approach. We previously determined that, although 1-(bromomethyl)phenanthrene can inactivate AAC(6')-Ie, it cannot inactivate AAC(6')-Ii (Draker, K.-a. and Wright, G.D., unpublished observations). Its inability to inactivate AAC(6')-Ii could be because 1-(bromomethyl)phenanthrene can not efficiently bind to AAC(6')-Ii or because AAC(6')-Ii lacks an appropriate active site residue to serve as the nucleophile in the reaction.

Close inspection of the active site of AAC(6')-Ii, together with the alignment between AAC(6')-Ii and AAC(6')-Ie (Figure 4.4), suggested that Asp99 in AAC(6')-Ie could be responsible for the different reactivities of the enzymes. The equivalent residue in AAC(6')-Ii (His74) would not likely act as a nucleophile in the reaction with 1-(bromomethyl)phenanthrene, and there does not appear to be any other candidate residues in the vicinity. To test this hypothesis, we determined the sensitivities of Tyr96 and Asp99 mutant proteins to 1-(bromomethyl)phenanthrene. AAC(6')-Ie Tyr96Phe was just as sensitive as wild type enzyme to inactivation by 1-(bromomethyl)phenanthrene, indicating that the hydroxyl group of Tyr96 is not required for inactivation (Figure 4.7B). However, AAC(6')-Ie Asp99Ala and AAC(6')-Ie Asp99Asn were completely resistant to

inactivation by 1-(bromomethyl)phenanthrene (Figure 4.7B). This suggested that either Asp99 is the active site residue that is modified by 1-(bromomethyl)phenanthrene or Asp99 is important in the initial binding event between compound and enzyme. Consistent with the former hypothesis, AAC(6')-Ie Asp99Glu is sensitive to inactivation, albeit less sensitive than AAC(6')-Ie WT (Figure 4.7B). This result suggests that the carboxylate moiety provided by Asp99 (or Asp99Glu) is most critical to the inactivation reaction and implicates Asp99 as the active site residue that is covalently modified by 1-(bromomethyl)phenanthrene.

To further validate this conclusion, we determined the effect that pH has on the inactivation of AAC(6')-Ie by 1-(bromomethyl)phenanthrene. AAC(6')-Ie was most sensitive to inactivation at lower pH, whereas it became more resistant as the assay pH increased (Figure 4.8). This result yielded a $pK_a$ for the inactivation reaction of 7.2. We have previously assigned a $pK_a$ of 7.2 to Asp99, thus, together these results are consistent with Asp99 serving as the active site nucleophile that is covalently modified by 1-(bromomethyl)phenanthrene. Therefore, although the presence of Asp99 in AAC(6')-Ie leads to a wider resistance profile by enabling AAC(6')-APH(2") to acetylate fortimicin A and paromomycin, it also makes the enzyme sensitive to inactivation by 1-(bromomethyl)phenanthrene.
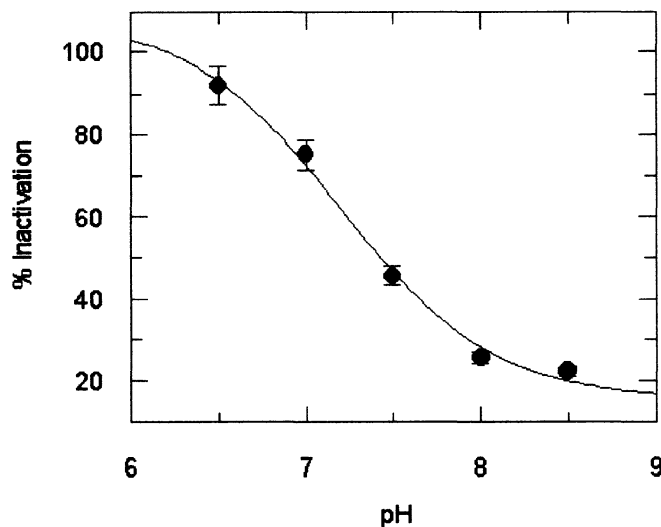
**Figure 4.8:** pH Dependence of the Inactivation of AAC(6')-Ie WT by 1-(Bromomethyl)phenanthrene. Enzyme (0.2 μM) was incubated with 20 μM 1-(bromomethyl)phenanthrene for 10 min at 37°C before the addition of acetyl-CoA and kanamycin A to final concentrations of 300 μM to assay for acetyltransferase activity. These inactivation reactions were conducted at different pH levels using the following buffers: 25 mM MOPS-NaOH (pH 6.5), 25 mM HEPES-NaOH (pH 7.0-8.0), and 25 mM glycylglycine                                (pH                                8.5).

## 4.3.9 Molecular Mechanism of AAC(6')-Ie and Comparison to Other GNAT Family Members

Because there is no available crystal structure for AAC(6')-APH(2"), it is not known if Asp99 acts directly upon aminoglycoside substrate or if base catalysis is mediated through a chain of water molecules similar to that proposed for both tGCN5 histone acetyltransferase and AANAT (Dyda *et al.*, 2000). However, recently the structure of AAC(2')-Ic from *Mycobacterium tuberculosis*, an aminoglycoside acetyltransferase also known to catalyze $O$-acetylation, has been solved (Vetting *et al.*, 2002). As with other GNAT superfamily members, there is not a direct interaction with the substrate 2'-NH₂ and a potential active site base, but rather, a series of water

135

molecules that connects the amine to Glu82, the residue that aligns with Asp99 in AAC(6')-Ie. This suggests that with a sufficiently potent active site base, *O*-acetylation may be catalyzed through a "proton-wire" of appropriately positioned water molecules.

These studies identify Asp99 as an active site base required for *O*-acetylation of aminoglycoside substrates and *N*-acetylation of fortimicin A and provides the molecular basis for these unique properties in an AAC(6'). It also identifies this residue as sensitive to modification by small molecule inhibitors. This provides a unique anchoring site for the development of specific inhibitors of AAC(6')-Ie that could find use as leads in the development of anti-resistance molecules.

## 4.4 References

**Boehr, D.D., Lane, W.S. and Wright, G.D. 2001.** Active site labeling of the gentamicin resistance enzyme AAC(6')- APH(2") by the lipid kinase inhibitor wortmannin. *Chem Biol.* 8: 791-800.

**Botto, R.E. and Coxon, B. 1983.** Nitrogen-15 nuclear magnetic resonance spectroscopy of neomycin B and related aminoglycosides. *J. Am. Chem. Soc.* 105: 1021-1028.

**Daigle, D.M., Hughes, D.W. and Wright, G.D. 1999.** Prodigious substrate specificity of AAC(6')-APH(2"), an aminoglycoside antibiotic resistance determinant in enterococci and staphylococci. *Chem Biol.* 6: 99-110.

**De Angelis, J., Gastel, J., Klein, D.C. and Cole, P.A. 1998.** Kinetic analysis of the catalytic mechanism of serotonin N-acetyltransferase (EC 2.3.1.87). *J Biol Chem.* 273: 3045-3050.

**Dorman, D.E., Paschal, J.W. and Merkel, K.E. 1976.** 15N nuclear magnetic resonance spectroscopy. The nebramycin aminoglycosides. *J. Am. Chem. Soc.* 98: 6885-6888.

**Dyda, F., Klein, D.C. and Hickman, A.B. 2000.** GCN5-related N-acetyltransferases: a structural overview. *Annu Rev Biophys Biomol Struct.* 29: 81-103.

Hickman, A.B., Klein, D.C. and Dyda, F. 1999a. Melatonin biosynthesis: the structure of serotonin N-acetyltransferase at 2.5 A resolution suggests a catalytic mechanism. *Mol Cell.* 3: 23-32.

Hickman, A.B., Namboodiri, M.A., Klein, D.C. and Dyda, F. 1999b. The structural basis of ordered substrate binding by serotonin N-acetyltransferase: enzyme complex at 1.8 A resolution with a bisubstrate analog. *Cell.* 97: 361-369.

Khalil, E.M., De Angelis, J., Ishii, M. and Cole, P.A. 1999. Mechanism-based inhibition of the melatonin rhythm enzyme: pharmacologic exploitation of active site functional plasticity. *Proc Natl Acad Sci U S A.* 96: 12418-12423.

Langer, M.R., Tanner, K.G. and Denu, J.M. 2001. Mutational analysis of conserved residues in the GCN5 family of histone acetyltransferases. *J Biol Chem.* 276: 31321-31331.

Leatherbarrow, R.J. 2000. Grafit. . Erithacus Software, Staines.

Magnet, S., Lambert, T., Courvalin, P. and Blanchard, J.S. 2001. Kinetic and mutagenic characterization of the chromosomally encoded *Salmonella enterica* AAC(6')-Iy aminoglycoside N-acetyltransferase. *Biochemistry.* 40: 3700-3709.

Martel, A., Masson, M., Moreau, N. and Le Goffic, F. 1983. Kinetic studies of aminoglycoside acetyltransferase and phosphotransferase from *Staphylococcus aureus* RPAL. Relationship between the two activities. *Eur J Biochem.* 133: 515-521.

Mio, T., Yamada-Okabe, T., Arisawa, M. and Yamada-Okabe, H. 1999. *Saccharomyces cerevisiae* GNA1, an essential gene encoding a novel acetyltransferase involved in UDP-N-acetylglucosamine synthesis. *J Biol Chem.* 274: 424-9.

Peneff, C., Mengin-Lecreulx, D. and Bourne, Y. 2001. The crystal structures of Apo and complexed *Saccharomyces cerevisiae* GNA1 shed light on the catalytic mechanism of an amino-sugar N-acetyltransferase. *J Biol Chem.* 276: 16328-16334.

Radika, K. and Northrop, D.B. 1984. The kinetic mechanism of kanamycin acetyltransferase derived from the use of alternative antibiotics and coenzymes. *J Biol Chem.* 259: 12543-12546.

Rojas, J.R., Trievel, R.C., Zhou, J., Mo, Y., Li, X., Berger, S.L., Allis, C.D. and Marmorstein, R. 1999. Structure of *Tetrahymena* GCN5 bound to coenzyme A and a histone H3 peptide. *Nature.* 401: 93-98.

**Scheibner, K.A., De Angelis, J., Burley, S.K. and Cole, P.A. 2002.** Investigation of the roles of catalytic residues in serotonin N-acetyltransferase. *J Biol Chem.* 277: 18118-18126.

**Schowen, K.B. and Schowen, R.L. 1982.** Solvent isotope effects of enzyme systems. *Methods Enzymol.* 87: 551-606.

**Shaw, K.J., Rather, P.N., Hare, R.S. and Miller, G.H. 1993.** Molecular genetics of aminoglycoside resistance genes and familial relationships of the aminoglycoside-modifying enzymes. *Microbiol Rev.* 57: 138-163.

**Shmara, A., Weinsetel, N., Dery, K.J., Chavideh, R. and Tolmasky, M.E. 2001.** Systematic analysis of a conserved region of the aminoglycoside 6'-N-acetyltransferase type Ib. *Antimicrob Agents Chemother.* 45: 3287-3292.

**Tanner, K.G., Trievel, R.C., Kuo, M.H., Howard, R.M., Berger, S.L., Allis, C.D., Marmorstein, R. and Denu, J.M. 1999.** Catalytic mechanism and function of invariant glutamic acid 173 from the histone acetyltransferase GCN5 transcriptional coactivator. *J Biol Chem.* 274: 18157-18160.

**Vetting, M.W., Hegde, S.S., Javid-Majd, F., Blanchard, J.S. and Roderick, S.L. 2002.** Aminoglycoside 2'-N-acetyltransferase from *Mycobacterium tuberculosis* in complex with coenzyme A and aminoglycoside substrates. *Nat Struct Biol.* 9: 653-658.

**Wolf, E., De Angelis, J., Khalil, E.M., Cole, P.A. and Burley, S.K. 2002.** X-ray crystallographic studies of serotonin N-acetyltransferase catalysis and inhibition. *J Mol Biol.* 317: 215-224.

**Wolf, E., Vassilev, A., Makino, Y., Sali, A., Nakatani, Y. and Burley, S.K. 1998.** Crystal structure of a GCN5-related N-acetyltransferase: *Serratia marcescens* aminoglycoside 3-N-acetyltransferase. *Cell.* 94: 439-449.

**Wright, G.D., Parent, T. and Honek, J.F. 1990.** Non-sterol structural probes of the lanosterol 14 alpha-demethylase from *Saccharomyces cerevisiae*. *Biochim Biophys Acta.* 1040: 95-101.

**Wright, G.D. and Thompson, P.R. 1999.** Aminoglycoside phosphotransferases: proteins, structure, and mechanism. *Front Biosci.* 4: D9-21.

**Wybenga-Groot, L.E., Draker, K., Wright, G.D. and Berghuis, A.M. 1999.** Crystal structure of an aminoglycoside 6'-N-acetyltransferase: defining the GCN5-related N-acetyltransferase superfamily fold. *Structure Fold Des.* 7: 497-507.

# Chapter 5.

# Interactions Between the Acetyltransferase and Phosphotransferase Domains of AAC(6')-APH(2")

Dr. Denis Daigle generated the plasmid pDRTF. All other work was performed by myself.

## 5.1 Introduction

The bifunctional enzyme AAC(6')-APH(2"), possessing both acetyl CoA-dependent acetylation and ATP-dependent phosphorylation activities (Culebras and Martinez, 1999) is arguably the most important, yet most difficult, aminoglycoside resistance enzyme to overcome. The protein is the most common determinant in Gram-positive pathogens such as *Enterococcus* and *Staphylococcus*, where it confers incredibly high protection with MICs over 2000 μg/mL, and has shown a growing importance in the resistance profiles of Gram-negative organisms (Miller *et al.*, 1997).

Initial sequence alignments first suggested, and a series of truncation experiments later confirmed, that there are two distinct active sites, where the acetyltransferase and phosphotransferase activities reside in the N-terminal and C-terminal portions of the protein respectively (Ferretti *et al.*, 1986; Rouch *et al.*, 1987). Chapters 2 – 4 focused on the elucidation of the chemical mechanisms of aminoglycoside phosphorylation and acetylation. It is also necessary to understand how the domains interact functionally and/or structurally. This may aid in the identification of compounds that can negatively affect both domains, and hence, simplify treatment of this resistance determinant, and may help in delineating the molecular reason behind the very high antibiotic protection that it confers upon the host bacteria. In the absence of a high resolution structure of this enzyme, we have explored the domain-domain interactions in AAC(6')-APH(2") by further refining and characterizing the minimal domain sequences of the acetyltransferase and phosphotransferase activities in terms of both *in vitro* and *in vivo* activities. Our studies have suggested that although the domains do not functionally interact, they have

intimate structural linkages that are important for conformation and stability, and disruption of these domain-domain contacts negatively affects both activities.

## 5.2 Materials and Methods

### 5.2.1 Reagents

DNA polymerases (Taq, Vent, T4), together with HindIII and PstI restriction endonucleases were purchased from MBI Fermentas (Burlington, ON, Canada). Remaining restriction endonucleases were purchased from New England Biolabs (Mississauga, ON, Canada). Ni NTA agarose was purchased from Qiagen (Mississauga, ON, Canada), and all other chromatography resins were purchased from Amersham Pharmacia. All other chemicals were purchased from Sigma (St. Louis, MO) unless otherwise noted. All oligonucleotide primers were synthesized at the Central Facility of the Institute for Molecular Biology and Biotechnology, McMaster University.

### 5.2.2 Construction of Plasmids Expressing N-terminal and C-terminal Truncated Proteins

A list of plasmids used in this study can be found in Table 5.1. The construction of pBF9 (Daigle *et al.*, 1999), pBF16 and pET22BFAPH (Chapter 3) has been previously described. The construction of the other pKK223-3** based plasmids, followed similar procedures, where sequences were amplified using Vent or Taq DNA polymerase from plasmid pBF9 using appropriate primers (Table 5.1) that incorporate unique NdeI and HindIII restriction sites and ligated into pK223-3**, following digestion of both DNA fragment and plasmid with NdeI and HindIII. pET15BFAAC and pET22BFAAC were

constructed by ligating the *Nde*I-*Hind*III digested insert from pKKBFAAC into similarly

digested pET15b(+) or pET22b(+) (Novagen, Madison, WI) respectively. The pKK223-

3** and pET based plasmids were transformed into CaCl$_2$-competent *E. coli* XL1 Blue

and BL21(DE3) cells respectively.

### 5.2.3 Purification of Proteins

The purification of N-terminal hexahistidine tagged AAC(6')-APH(2") was

described in Chapter 3, and mutant enzymes were purified similarly. N-terminal and C-

terminal truncated proteins were expressed using the pET15b(+) or pET22b(+) system,

where 1-2 L of Luria Bertani (LB) broth supplemented with ampicillin (100 μg/mL) was

inoculated with 10-20 mL of overnight culture and grown to an OD$_{600}$ of 0.6 at 37°C,

prior to inducing with 10 mL 100 μM isopropyl-β-D-thiogalactopyranoside. For non-His

tagged N-terminal truncated protein, cells were grown for an additional six hours at 30°C

following induction, whereas for the remaining truncated proteins, cells were grown for

an additional three hours at 37°C. Cells were collected by centrifugation at 10 000x*g*,

washed with 0.85% NaCl, and stored at –20°C. The N-terminal truncated His tagged

protein was purified similarly to the full-length hexahistidine tagged protein (Boehr *et al.*,

2001).

The non-His tagged proteins were purified following a similar method used for *B.*

*subtilis*-expressed, non-His-tagged AAC(6')-APH(2") according to (Daigle *et al.*, 1999).

After resuspending the cells in lysis buffer (50 mM HEPES-NaOH pH 7.5, 1 mM EDTA,

1 mM phenylmethanesulfonyl fluoride), cells were lysed by three passes through a

French pressure cell at 20 000 psi. The cell debris was removed by centrifugation at 10

000x*g* for 20 minutes. The lysate was applied to a Q sepharose FF anion exchange column (50 mL bed volume), washed with three column volumes of buffer A (50 mM HEPES-NaOH pH 7.5, 1 mM EDTA) and eluted with a gradient of buffer B (50 mM HEPES-NaOH pH 7.5, 1 mM EDTA, 1 M NaCl) which included the following steps: linear gradient from 0 to 20% buffer B over one column volume, held at 20% buffer B for one column, linear gradient of 20% to 50% buffer B over 4 column volumes, held at 50% buffer B for one column volume and a linear gradient of 50% to 100% buffer B over 1 column volume. Fractions were analyzed using SDS PAGE, where the proteins generally eluted between 200 mM and 500 mM NaCl. Fractions were pooled and concentrated to a final volume of 5 mL over an Amicon PM10 ultrafiltration membrane, before being applied to a Sepharose S200 gel filtration column (4 cm x 110 cm) and eluted with buffer A + 200 mM NaCl at a flow rate of 0.5 mL/min. Following analysis by SDS PAGE, the proteins were concentrated over PM10 membrane and dialyzed against 25 mM HEPES-NaOH pH 7.5.

**5.2.4 Enzyme Kinetic Assays**

The assays were described in Chapter 3. For measuring kinetic parameters for APH activity, GTP and kanamycin were fixed at 100 μM when measuring the steady-state kinetic parameters for aminoglycoside substrate and GTP, respectively. For the acetyltransferase assays, acetyl-CoA and kanamycin A were held at 300 μM when measuring the steady state kinetic parameters for aminoglycoside substrate and acetyl-CoA, respectively. The results reported are +/- standard error.

## 5.2.5 Circular Dichroism

The CD spectra of 10 μM protein solutions in 10 mM $Na_2HPO_4/NaH_2PO_4$ pH 8.0 were taken using an AVIV 215 spectrophotometer at 25°C and a 1-mm pathlength quartz cell. Secondary structure of the constructs was compared using the program CDNN ver. 2.1 (Bohm *et al.*, 1992; Dalmas *et al.*, 1994). The neural network was trained to an appropriate level with the following proteins: cytochrome C, hemoglobin, lactate dehydrogenase, myoglobin, ribonuclease, flavodoxin, subtilisin, triosephosphate isomerase, thermolysin and hemerythrin.

## 5.2.6 Site-Directed Mutagenesis

Site-directed mutagenesis was performed using the Quick-Change method (Stratagene, La Jolla, CA, USA). The appropriate mutagenic primers and their reverse complements were used in combination with 20 ng template DNA (pET15AACAPH (Boehr *et al.*, 2001)) in *Pfu* DNA polymerase (Stratagene, La Jolla, CA, USA)-catalyzed PCR reactions. After parental DNA was digested with *Dpn*I, mutant plasmid DNA was transformed into $CaCl_2$-competent *E. coli* XL-1 Blue. Positive clones were sequenced in their entirety, and then used to transform into *E. coli* BL21(DE3) for subsequent protein purification.

## 5.2.7 Thermal Inactivation Assays

Proteins (2-3 mg/mL) were incubated at 50°C, in the presence or absence of substrate, for various time intervals before being transferred to appropriate, thermally equilibrated (37°C) assay buffer and assayed for acetyltransferase and/or

phosphotransferase activities, according to the previously described procedures. Assays typically contained 2-10 ng of protein. Assays were initiated with the addition of both substrates. For AAC assays, kanamycin A and acetyl CoA had final concentrations of 300 μM, and for APH assays, kanamycin A and ATP had final concentrations of 100 μM and 2000 μM, respectively. Thermal inactivation of enzyme activity follows first-order kinetics and rates were analyzed accordingly using Grafit 4.0 (Leatherbarrow, 2000).

### 5.2.8 Analytical Gel Filtration

Analytical gel filtration experiments were performed on an AKTA FPLC (Amersham Pharmacia) using a Superdex 200 column (10 x 30 mm, 24 mL bed volume) with 50 mM Tris-HCl pH 7.5, 100 mM KCl as elution buffer. The column was standardized using β-amylase ($M_r$= 200 000), alcohol dehydrogenase (150 000), bovine albumin (66 000), carbonic anhydrase (29 000), cytochrome C (12 400) and blue dextran for calculation of void volume, using appropriate concentrations (2 – 10 mg/mL, 100 μL injections) according to supplier instructions (Sigma MW-GF-200). Experimental protein samples (2 - 6 mg/mL, 100 μL injections) were run similarly, and the linear relationship between the logarithm of $M_r$ and elution volume for the standard proteins was used to calculate the apparent $M_r$ for the various AAC(6')-APH(2") constructs.

### 5.2.9 Construction of *B. subtilis* Integrants

Sequences were amplified using *Taq* DNA polymerase from plasmid pBF9 using appropriate primers (Table 5.1). The fragments were purified, treated with T4 DNA polymerase to ensure blunt ends and cloned into pCR4-Blunt, according to the

instructions supplied with the Zero Blunt TOPO PCR cloning kit (Invitrogen, Carlsbad, CA). The original primers generated *Pac*I and *Bam*HI restriction sites flanking the desired sequences, and so, were subsequently used to subclone the fragments into *Pac*I-*Bam*HI treated pSWEET-bgaB (Bhavsar *et al.*, 2001). Following transformation and selection into CaCl$_2$-competent *E. coli* XL1 Blue, the plasmids were purified, linearized by restriction digest with *Pst*I and used to transform *B. subtilis* 1A717, according to previous procedures (Bhavsar *et al.*, 2001). *B. subtilis* 1A717 contains an erythromycin resistant cassette in place of the α-amylase gene locus, and so, positive integrants were initially selected by growth on LB agar containing chloramphenicol (10 μg/mL) and the absence of growth with erythromycin (1 μg/mL). Integrants were confirmed by PCR-amplification of the appropriately sized inserts and protein expression was determined through Western blot analysis as described below.

### 5.2.10 MIC Determinations

MIC determinations for the *E. coli* constructs were performed as described in Chapter 2. For the *B. subtilis* constructs, the procedure was modified to account for the more tightly regulated *xyl* promoter of the pSWEET system (Bhavsar *et al.*, 2001). A single colony from a LB agar plate supplemented with 10 μg/mL chloramphenicol, was used to inoculate a culture of LB broth supplemented with 10 μg/mL chloroamphenicol and 2% (w/v) xylose. This culture (1 μL) was added to a 96-well polypropylene microtitre plate containing LB broth supplemented with 2% (w/v) xylose along with increasing concentrations of antibiotic (99 μL) and incubated at 30°C for 20-24 hours.

MICs were determined by visual inspection for bacterial growth. All of the MIC
determinations were performed in at least duplicate.

### 5.2.11 Quantitation of Protein Expression Copy Number using Western Blot Analyses

For *E. coli* constructs, LB broth (100 mL) supplemented with 100 μg/mL
ampicillin was inoculated with 1 mL overnight culture and grown at 37°C until $OD_{600}$ ~
0.8. *B. subtilis* constructs were treated similarly, except that the LB broth was
supplemented instead with 10 μg/ml chloramphenicol and 2% (w/v) xylose. For *E.
faecalis* ATCC 49383, 100 mL Bacto tryptic soy broth (Becton, Dickinson and Company,
Reference Number 211825) supplemented with 200 or 2000 μg/mL gentamicin was
inoculated with 2 mL overnight culture and grown at 37°C until $OD_{600}$ ~ 0.8. Serial
dilutions were plated onto LB agar plates supplemented with ampicillin (100 μg/mL),
chloramphenicol (10 μg/mL) and kanamycin (50 μg/mL) for *E. coli*, *B. subtilis* and *E.
faecalis* respectively and grown at 37°C for 16-24 hours to determine colony-forming
units (CFUs) in the original 100 mL cultures. Cells were pelleted at 10 000x*g* for 20
minutes and stored at –20°C.

Cells were resuspended in 3-5 mL lysis buffer and treated with mutanolysin
(0.017 mg/mL) and lysozyme (1.7 mg/mL) for 2 hours, prior to the addition of DNAase
(1.7 mg/mL) and RNAase (1.7 mg/mL) and an additional hour of incubation at 22°C. Cell
lysis was completed by passing the solutions 4-5 times through a French pressure cell at
20 000 psi. Cellular debris was pelleted by centrifugation at 10 000x*g* for 20 minutes, and
the supernatant was dialyzed against 50 mM HEPES-NaOH pH 7.5 and stored at –20°C.

Aliquots of supernatant and standard purified proteins (5 – 1000 ng) were subjected to 15% SDS PAGE and electroblotted onto polyvinylidene fluoride membrane (Millipore Immobilon-P transfer membrane) using standard methods (Towbin *et al.*, 1979). The Western blot was developed using rabbit polyclonal antibodies directed against AAC(6')-APH(2") and goat anti-rabbit antibodies conjugated with horse radish peroxidase (PerkinElmer) according to the protocol outlined by the supplier of the chemiluminescent detection system (Western Lightning Chemiluminesce Reagent Plus, PerkinElmer Life Sciences, Boston, MA). Blots were scanned into digital format with a Typhoon 9200 variable mode imager (Molecular Dynamics, Amersham Pharmacia Biotech) and the visualized bands were quantified using the computer program ImageQuant, supplied with the imager. A plot of pixel volume vs. logarithm of protein amount for the known standard proteins gave a linear slope that was used to determine the amount of protein in the original sample solutions.

**Table 5.1:** Plasmids and Primers used in the Study.

| Plasmid | Primers used to generate | Protein Expressed | Reference |
|---|---|---|---|
| *Plasmids for antibiotic screening in* E.coli | | | |
| pBF9 | | AAC(6')-APH(2") | (Daigle *et al.*, 1999) |
| pBF16 | | APH[175-479] | (Daigle *et al.*, 1999) |
| pKKBFAPH -20 | 5'-CGGAATTCCATATGCATTACTTTGATAATT TC 5'-CCGGAATTCAAGCTTGGATCCTCAATCTTT ATAAGTCCTTTT | APH[195-479] | This work |
| pKKBFAAC | 5'-CAGGTACCCATATGAATATAGTTGAAAATGAA 5'-GAATTCAAGCTTACTAAATTAAATATTTCATGC | AAC[1-194] | This work |
| pKKBFAAC -10 | 5'-CAGGTACCCATATGAATATAGTTGAAAATGAA 5'-GAATTCAAGCTTAGGCATTATCATCATATC | AAC[1-184] | This work |
| pKKBFAAC -20 | 5'- CCAGGTACCCATATGAATATAGTTGAAAATGAA 5'-GAATTCAAGCTTATAAATAACAATCTTCT | AAC[1-174] | This work |
| | | | |
| *Plasmids to generate* B.subtilis | | | |

| integrants | | | |
|---|---|---|---|
| pSWAACAPH | 5'-CCGGAATTCTTAATTAACATTAGGAAGGA GCGTTTCTTTAAATGAATATAGTTGAAAATG 5'-CCGGAATTCAAGCTTGGATCCTCAATCTTT ATAAGTCCTTTT | AAC(6')-APH(2") | This work |
| pSWAAC | 5'-CCGGAATTCTTAATTAACATTAGGAAGGA GCGTTTCTTTAAATGAATATAGTTGAAAATG 5'-CCAAAGCTTGGATCCCTAAATTAAATATTT CATTGC | AAC[1-194] | This work |
| pSWAPH | 5'-CCTGCCCGGGTTAATTAACATTAGGAAGGA GCGTTTCTTTAAATGGAATATAGATATG 5'-CCGGAATTCAAGCTTGGATCCTCAATCTTT ATAAGTCCTTTT | APH[175-479] | This work |
| pDRTF | 5'-GATCCAAGCTTTAGAAGGAGATATACATATG 5'-CAGGATCCATCGATTCATAAATAACAATCTTCT 5'-GATCCATCGATTAGAAGGAGATATACATATG 5'-CAGGATCCAAGCTTTCAATCTTTATAAGTCCTT | AAC[1-174] and APH[175-479] | This work |
| | | | |
| *Plasmids for protein expression and purification* | | | |
| pET15AACAPH | | N-terminal 6-His Tagged Wild-type | (Boehr *et al.*, 2001) |
| pET15AACAPH K190P | 5'-GCCACAAATGTTAAGGCAATGCCATATTTA ATTGAGC 5'-GCTCAATTAAATATGGCATTGCCTTAACAT TTGTGGC | AAC(6')-APH(2")-Lys190Pro mutation | This work |

| pET15AACAPH L192P | 5'-GCCACAAATGTTAAGGCAATGAAATATCC AATTGAGC 5'-GCTCAATTGGATATTTCATTGCCTTAACAT TTGTGGC | AAC(6')-APH(2")-Leu192Pro mutation | This work |
|---|---|---|---|
| pET15AACAPH KLP | 5'-GCCACAAATGTTAAGGCAATGCCATATCCA ATTGAGC 5'-GCTCAATTGGATATGGCATTGCCTTAACAT TTGTGGC | AAC(6')-APH(2")-Lys190Pro, Leu192Pro mutations | This work |
| | | | |
| pET15BFAAC | fragment subcloned from pKKBFAAC | N-terminal 6-His tagged AAC[1-194] | This work |
| pET22BFAAC | fragment subcloned from pKKBFAAC | AAC[1-194] | This work |
| pET22BFAAC -20 | Fragment subcloned from pKKBFAAC-20 | AAC[1-174] | This work |
| pET22BFAPH | | APH[175-479] | (Boehr et al., 2001) |

## 5.3 Results

### 5.3.1 Construction of Minimum Acetyltransferase and Phosphotransferase Domains

Sequence analysis and initial truncation experiments of AAC(6')-APH(2") situated the acetyltransferase and phosphotransferase activities in the N- and C-terminal portions of the protein (Ferretti *et al.*, 1986). Previously, in our attempts to purify AAC(6')-APH(2") from an *E. coli* overexpression host, we noted the synthesis of both full-length AAC(6')-APH(2") and a C-terminal truncated protein, starting at Met175, that possessed only aminoglycoside phosphotransferase activity (Daigle *et al.*, 1999).

To identify the minimum regions of both the acetyltransferase and phosphotransferase domains, we constructed additional plasmids expressing both N- and C-terminal truncated proteins (Table 5.1). Following transformation into *E.coli* XL1 Blue, constructs were screened for growth in media containing aminoglycoside antibiotics (10 μg/mL), including fortimicin which is only inactivated by acetylation (Figure 5.1). Only two constructs provided resistance to aminoglycosides, corresponding to the expression of amino acid residues 1-194 (hereafter designated as AAC[1-194]) and the originally identified C-terminal truncated protein, expressing amino acid residues 175-479 (designated as APH[175-479]). The AAC[1-194] fragment provided resistance to kanamycin A and fortimicin A but not to gentamicin, consistent with aminoglycoside acetyltransferase activity, whereas the APH[175-479] fragment provided resistance to kanamycin A and gentamicin but not to fortimicin A, consistent with aminoglycoside phosphotransferase activity. Constructs expressing amino acid residues 1-174 (designated as AAC[1-174]), 1-184 and 195-479 (designated as APH[195-479]) did not provide

resistance to any of the aminoglycosides tested. This was not the result of lack of protein expression, as SDS PAGE analysis demonstrated similar protein expression as the resistance-providing constructs (data not shown).

| Plasmid | Protein Expressed | Growth In: | | |
| --- | --- | --- | --- | --- |
| | | KanamycinA | Gentamicin | Fortimicin |
| pBF9 | ▐██████████████████▌ 1 — 479 | + | + | + |
| pKKBFAAC -20 | ▐████▌ 1 — 174 | - | - | - |
| pKKBFAAC -10 | ▐█████▌ 1 — 184 | - | - | - |
| pKKBFAAC | ▐██████▌ 1 — 194 | + | - | + |
| pBF16 | ▐██████████▌ 175 — 479 | + | + | - |
| pKKBFAPH –20 | ▐█████████▌ 195 — 479 | - | - | - |

**Figure 5.1:** Antibiotic Screening of *E.coli* XL1 Blue Expressing N- and C-terminal Truncated Versions of AAC(6')-APH(2"). Growth was assayed by inoculating 2 mL Luria Bertani (LB) broth containing 10 µg/mL aminoglycoside antibiotic from a single colony on LB agar (100 µg/mL ampicillin) and incubating for 16-20 hours at 37°C. The identities of the plasmids are listed in Table 5.1.

## 5.3.2 Purification and Steady-State Kinetic Characterization of N- and C-Terminal Truncated Versions of AAC(6')-APH(2")

To characterize the *in vitro* activity of the constructs, the fragments were cloned into pET15b(+) and/or pET22b(+), expressed and purified (Figure 5.2) according to

Section 5.2. APH[175-479] has previously been shown to have similar steady-state kinetic parameters as the phosphotransferase activity of full-length AAC(6')-APH(2") (Boehr *et al.*, 2001) (Table 5.2). AAC[1-194], however, is catalytically impaired compared to full-length enzyme (Table 5.2). There are significant effects for a number of aminoglycoside substrates and acetyl-CoA, where the N-terminal hexahistidine tagged AAC[1-194] (hereafter referred to as His-AAC[1-194]) is more severely affected than non-tagged AAC[1-194]. Neither addition of APH[175-479] and/or GTP into the acetyltransferase assay buffer had any affect on the kinetic parameters for either AAC[1-174], His-AAC[1-194] or AAC[1-194] (data not shown).

## 1   2   3   4   5   6
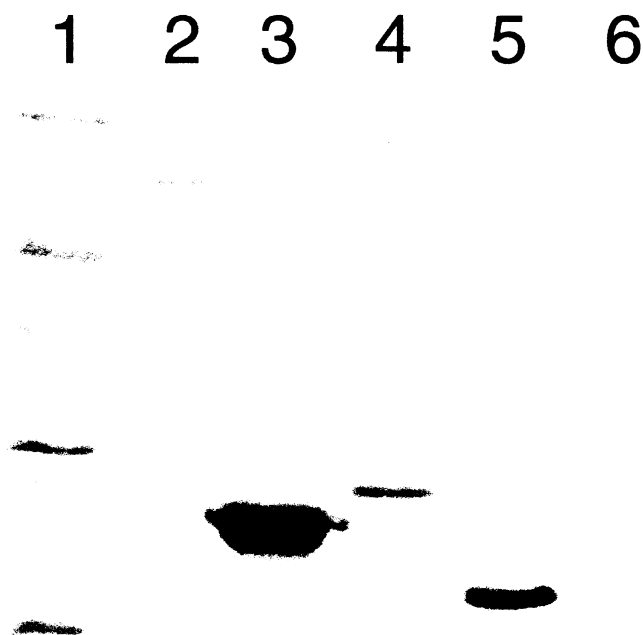
**Figure 5.2:** Purity of Full-length and Truncated Versions of AAC(6')-APH(2"). Assessed by 15% SDS-PAGE. Proteins were visualized using Coomassie brilliant blue stain. Lanes are as follows: *1* standard molecular weight markers (66, 45, 36, 29, 24, 14.2 kDa), *2* N-terminal 6-His tagged AAC(6')-APH(2"), *3* AAC[1-194], *4* N-terminal 6-His tagged AAC[1-194], *5* AAC[1-174], *6* APH[175-479].

**Table 5.2:** Steady-State Kinetic Characterization of N- and C-terminal Truncated Versions of AAC(6')-APH(2").

| Protein | Substrate | $K_M$ (μM) | $k_{cat}$ ($s^{-1}$) | $k_{cat}/K_M$ ($M^{-1}s^{-1}$) | $(k_{cat})^{Full}/(k_{cat})^{Frag.}$ | $(k_{cat}/K_M)^{Full}/(k_{cat}/K_M)^{Frag.}$ |
|---|---|---|---|---|---|---|
| N-terminal 6-His tagged AAC(6')-APH(2") | | | | | | |
| *acetyltransferase* | amikacin | 97.1 +/- 14.9 | 0.272 +/- 0.014 | $2.8 \times 10^3$ | | |
| | butirosin | 60.9 +/- 19.0 | 0.129 +/- 0.012 | $2.1 \times 10^3$ | | |
| | [a]fortimicin A | 25.4 +/- 5.5 | 0.28 +/- 0.04 | $1.1 \times 10^4$ | | |
| | [b]kanamycin A | 31 +/- 3 | 1.7 +/- 0.2 | $5.6 \times 10^4$ | | |
| | neomycin B | 19.8 +/- 5.2 | 0.080 +/- 0.008 | $4.0 \times 10^3$ | | |
| | ribostamicin | 131 +/- 25 | 0.370 +/- 0.039 | $2.8 \times 10^3$ | | |
| | [b]acetyl-CoA | 38 +/- 5 | 1.2 +/- 0.3 | $3.1 \times 10^4$ | | |
| | | | | | | |
| *phosphotransferase* | kanamycin A | 18.3 +/- 4.3 | 0.16 +/- 0.02 | $8.9 \times 10^3$ | | |
| | GTP | 3.74 +/- 0.47 | 0.13 +/- 0.01 | $3.6 \times 10^4$ | | |
| | | | | | | |
| N-terminal 6-His tagged AAC[1-194] | | | | | | |
| | amikacin | 110 +/- 29 | 0.010 +/- 0.001 | $9.4 \times 10^1$ | 26 | 30 |
| | butirosin | 29.2 +/- 12.0 | 0.002 +/- 0.000 | $6.4 \times 10^1$ | 69 | 33 |
| | fortimicin A | 94.0 +/- 5.7 | 0.200 +/- 0.069 | $2.1 \times 10^3$ | 1.4 | 5.2 |
| | kanamycin A | 233 +/- 45 | 0.152 +/- 0.013 | $6.5 \times 10^2$ | 11 | 86 |
| | neomycin B | 42.0 +/- 7.7 | 0.008 +/- 0.001 | $1.8 \times 10^2$ | 10 | 22 |
| | ribostamicin | 28.7 +/- 7.7 | 0.006 +/- 0.001 | $2.1 \times 10^2$ | 61 | 13 |

| | | | | | | |
|---|---|---|---|---|---|---|
| | acetyl-CoA | 247 +/- 52 | 0.188 +/- 0.019 | $7.6 \times 10^2$ | 6.4 | 41 |
| | | | | | | |
| AAC[1-194] | | | | | | |
| | amikacin | 214 +/- 21 | 0.060 +/- 0.003 | $2.8 \times 10^2$ | 4.5 | 10 |
| | butirosin | 383 +/- 47 | 0.013 +/- 0.001 | $3.5 \times 10^1$ | 10 | 61 |
| | fortimicin A | 105 +/- 39 | 1.49 +/- 0.26 | $1.4 \times 10^4$ | 0.19 | 0.78 |
| | kanamycin A | 146 +/- 16 | 0.38 +/- 0.05 | $2.6 \times 10^3$ | 1.8 | 24 |
| | neomycin B | 173 +/- 21 | 0.038 +/- 0.002 | $2.2 \times 10^2$ | 2.1 | 18.3 |
| | ribostamicin | 120 +/- 30 | 0.036 +/- 0.003 | $3.0 \times 10^2$ | 10 | 9.3 |
| | acetyl-CoA | 74.4 +/- 18.3 | 0.341 +/- 0.043 | $4.6 \times 10^3$ | 3.5 | 6.7 |
| | | | | | | |
| APH[175-479] | GTP | 7.87 +/- 1.32 | 0.079 +/- 0.002 | $1.0 \times 10^4$ | 1.7 | 3.6 |

[a] values taken from (Boehr *et al.*, 2003)
[b] values taken from (Boehr *et al.*, 2001)

### 5.3.3 Secondary Structure of Full-Length and Truncated Versions of AAC(6')-APH(2")

Circular dichroism spectra of purified full-length and truncated versions of AAC(6')-APH(2") were determined to assess their secondary structure and folded state (Figure 5.3). Although AAC[1-174] did not possess any measurable *in vitro* activity and it could not confer aminoglycoside resistance when expressed in *E.coli*, it still retained significant secondary structure. In particular, the CD spectrum displayed strong α-helical content, similar to AAC[1-194]. These results suggest that the lack of acetyltransferase activity in AAC[1-174] is not due to complete misfolding of the protein.

**A**
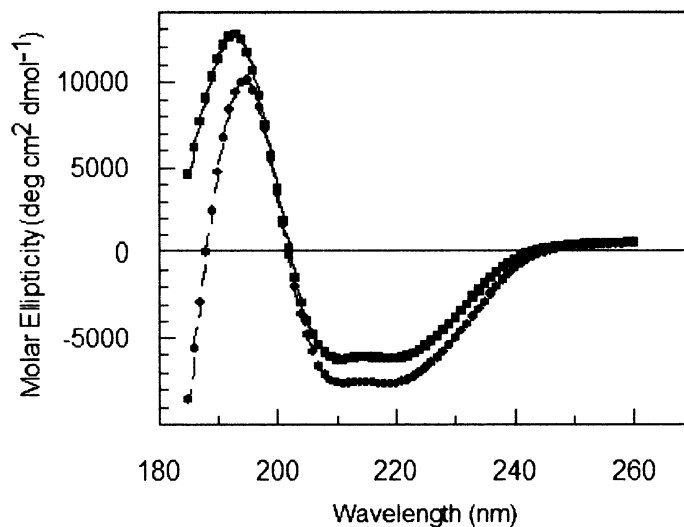


**B**
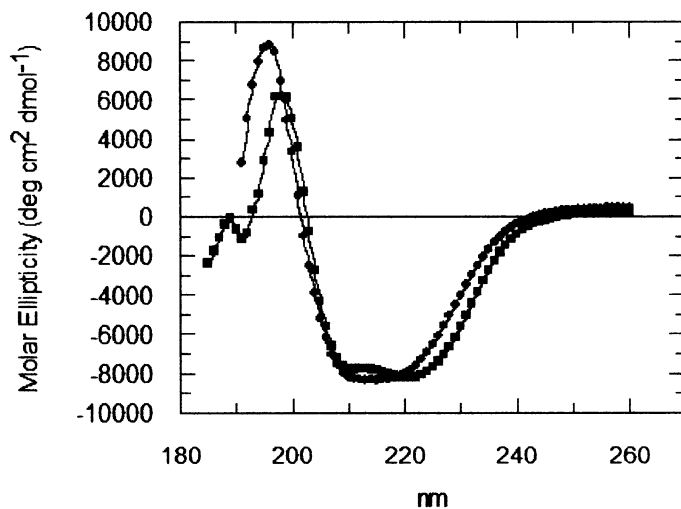


**Figure 5.3:** Secondary Structure Determinations for Full-Length, Mutant and Truncated Versions of AAC(6')-APH(2"). **A** circular dichroism spectra for AAC[1-174] (●) and AAC[1-194] (■). **B** circular dichroism spectra for His-AAC(6')-APH(2") (■) and His-AAC(6')-APH(2") K190P (●).

## 5.3.4 Secondary Structure Predictions for Region Spanning Residues 175-204

Proteolysis and truncation experiments were inconsistent with a flexible loop adjoining the acetyltransferase and phosphotransferase domains of AAC(6')-APH(2"). To determine if the region between the two domains may possess a regular secondary structure, the sequence between residues 175 and 204 was analyzed for potential α-helical or β-structure using *in silico* predictive software (Figure 5.4). All four programs used to analyze the sequence, PSIPRED (Jones, 1999; McGuffin *et al.*, 2000), Prof (Ouali and King, 2000), nnPredict (Kneller *et al.*, 1990) and jpred (Cuff *et al.*, 1998), predict α-helical structure spanning residues 186-196 (Figure 5.4).

```
Program/    175                      185                   195                  204
Algorithm   M  E Y  R  Y D D N A T  N  V K  A  M K Y L I E H  Y F D N F K V D S

PSIPRED     E  E E  E  E C C C C C  C  H H  H  H H H H H H H  H H H H C C C C C
Prof        E  E E  E  C C C C C C  C  H H  H  H H H H H H H  H C C C C C C C C
nnPredict   H  E C  C  C C C C C C  H  H H  H  H H H H H H H  H C C C C C C C C
jpred       H  H C  C  C C C H H H  H  H H  H  H H H H H H H  C C C C C C C C C

Consensus   E/H E E/C E/C C C C C C C C/H H H  H  H H H H H H H  H C C C C C C C C
                                    *  *   *  * * * * * * *  *
```

**Figure 5.4:** Secondary Structure Predictions for AAC(6')-APH(2") Region Spanning Residues 175-204, using the programs PSIPRED (Jones, 1999; McGuffin *et al.*, 2000), Prof (Ouali and King, 2000), nnPredict (Kneller *et al.*, 1990) and jpred (Cuff *et al.*, 1998). C= random coil, E= β-sheet, H= α-helix. * indicates region spanning residues 186-196 which is predicted to be α-helical by all four programs.

## 5.3.5 Mutational Analysis of Potential α-Helix Adjoining Acetyltransferase and Phosphotransferase Domains of AAC(6')-APH(2")

To address the role of the predicted α-helix in the structure and function of AAC(6')-APH(2"), Lys190 and Leu192 in the middle of the helix were mutated to Pro individually and together. These mutations had significant impacts on both the

acetyltransferase and phosphotransferase activities of AAC(6')-APH(2") (Table 5.3). The acetyltransferase activity was more affected than the phosphotransferase activity, where mutation of Leu192 was more deleterious than mutation of Lys190. The kinetic effects were primarily on $k_{cat}$ values, whereas the $K_M$ values were very similar between WT and mutant proteins. These results are not due to complete misfolding of the proteins as the CD spectra of the mutant proteins had similar features to that of wild-type His-AAC(6')-APH(2") (Figure 5.3b). Analysis of the CD spectra by CDNN ver. 2.1 (Bohm *et al.*, 1992; Dalmas *et al.*, 1994) yielded similar results between wild-type and 'helix mutant' proteins (data not shown).

## 5.3.6 Effects of GTP on the Thermal Stability of the AAC and APH Domains

It has been previously noted that GTP can protect both the acetyltransferase and phosphotransferase activities of AAC(6')-APH(2") from thermal inactivation (Martel *et al.*, 1983). We conducted additional thermal inactivation studies on full-length and truncated versions of His-AAC(6')-APH(2") to assess the stability of the individual domains in the absence and presence of the other domain and nucleotide (Figure 5.5A). Our results confirmed that GTP has a protective effect on both the AAC and APH activities of His-AAC(6')-APH(2") (Figure 5.5B). GTP can also protect APH[175-479] from thermal inactivation but not AAC[1-194] (Figure 5.5B). Addition of APH[175-479] into the thermal inactivation broth with AAC[1-194] did not confer any protection to the acetyltransferase activity in the absence or presence of GTP (data not shown). Moreover, the protection provided by GTP to the acetyltransferase activity of His-AAC(6')-

APH(2") Lys190Pro, Leu192Pro decreased substantially compared to wild-type protein

(Figure 5.5B).

**Table 5.3:** Steady-State Kinetic Parameters for His-AAC(6')-APH(2") 'Helix' Mutants.

| Mutation | Substrate | $K_M$ ($\mu$M) | $k_{cat}$ ($s^{-1}$) | $k_{cat}/K_M$ ($M^{-1}s^{-1}$) | $(k_{cat})^{WT}/(k_{cat})^{Mut}$ | $(k_{cat}/K_M)^{WT}/(k_{cat}/K_M)^{Mut}$ |
|---|---|---|---|---|---|---|
| **K190P** | | | | | | |
| *AAC* | kanamycin A | 46.1 +/- 11.5 | 0.214 +/- 0.069 | 4.7 x $10^3$ | 7.9 | 12 |
| | acetyl-CoA | 73.8 +/- 18.4 | 0.126 +/- 0.013 | 1.7 x $10^3$ | 9.6 | 18 |
| | | | | | | |
| *APH* | kanamycin A | 3.28 +/- 0.20 | 0.028 +/- 0.001 | 8.4 x $10^3$ | 5.9 | 1.1 |
| | GTP | 6.38 +/- 2.82 | 0.032 +/- 0.002 | 5.0 x $10^3$ | 4.2 | 7.2 |
| | | | | | | |
| **L192P** | | | | | | |
| *AAC* | kanamycin A | 36.8 +/- 8.9 | 0.025 +/- 0.002 | 6.7 x $10^2$ | 68 | 83 |
| | acetyl-CoA | 21.3 +/- 5.5 | 0.014 +/- 0.001 | 6.4 x $10^2$ | 86 | 49 |
| | | | | | | |
| *APH* | kanamycin A | 0.4 +/- 0.1 | 0.030 +/- 0.001 | 7.4 x $10^4$ | 5.3 | 0.12 |
| | GTP | 3.14 +/- 1.31 | 0.032 +/- 0.002 | 1.0 x $10^4$ | 4.1 | 3.6 |
| | | | | | | |
| **K190P, L192P** | | | | | | |
| *AAC* | kanamycin A | 36.5 +/- 11.3 | 0.012 +/- 0.001 | 3.4 x $10^2$ | 142 | 166 |
| | acetyl-CoA | 45.1 +/- 4.8 | 0.011 +/- 0.004 | 2.4 x $10^2$ | 109 | 130 |
| | | | | | | |
| *APH* | kanamycin A | 2.66 +/- 0.55 | 0.012 +/- 0.001 | 4.5 x $10^3$ | 13 | 2.0 |
| | GTP | 3.55 +/- 0.69 | 0.012 +/- 0.001 | 3.3 x $10^3$ | 11 | 11 |

161

A
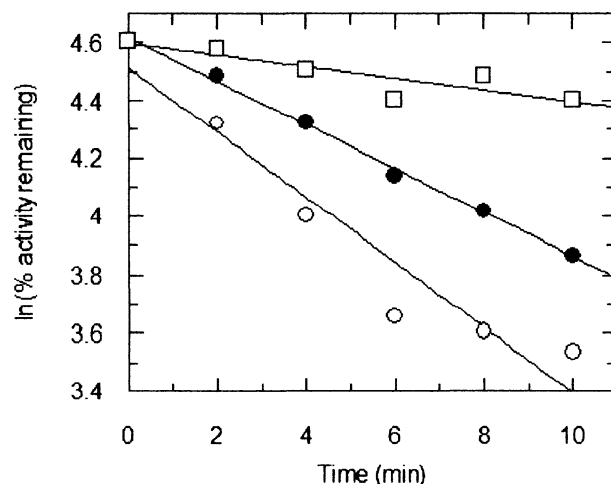


B
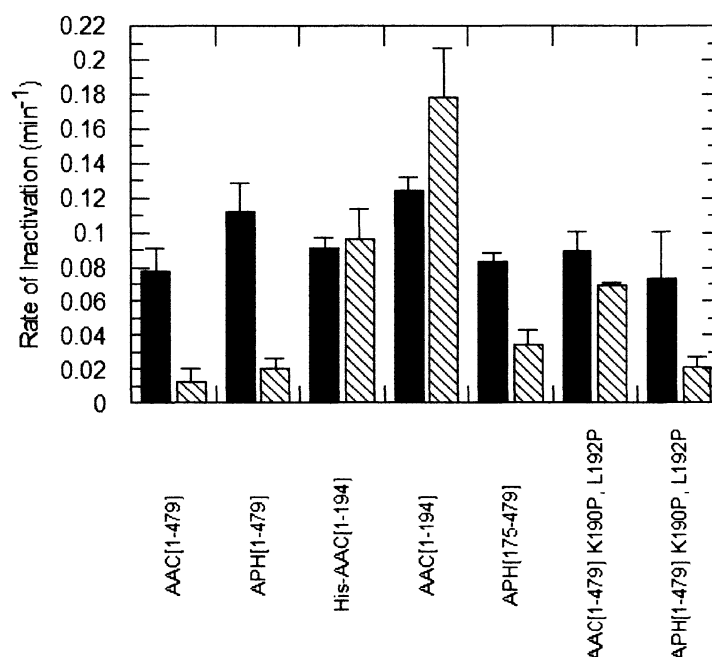


**Figure 5.5:** Thermal Inactivation of Acetyltransferase and Phosphotransferase Activities of Full-Length and Truncated Versions of AAC(6')-APH(2"). Proteins were incubated at 50°C for various time intervals before aliquots were transferred to thermally equilibrated 37°C assay buffer to assess remaining acetyltransferase or phosphotransferase activity. **A** Thermal inactivation of the phosphotransferase activity of His-AAC(6')-APH(2") incubated with no nucleotide (o), 5 mM ATP (●) or 5 mM GTP (□) . **B** The first order decays in enzyme activity were used to determine rate constants of inactivation (solid- no nucleotide, hatched- in presence of 5 mM GTP).

### 5.3.7 Analytical Gel Filtration of Full-length and Truncated Versions of AAC(6')-APH(2")

To assess the oligomeric nature of full-length and truncated versions of AAC(6')-APH(2") and to determine whether the separated domains may interact with one another *in vitro*, the constructs alone and together were subjected to analytical gel filtration (Table 5.4). His-AAC(6')-APH(2") and APH[175-479] elute as monomers, whereas AAC[1-174] and AAC[1-194] elute partially in dimeric form (Table 5.4). After incubation of APH[175-479] with either AAC[1-174] or AAC[1-194], subsequent analysis failed to show a new peak consistent with the association between AAC and APH, although the dimers of AAC could no longer be detected (Table 5.4).

**Table 5.4:** Analytical Gel Filtration of Full-length and Truncated Constructs of AAC(6')-APH(2").

| Protein | [a]Concentration (mg/mL) | Elution Volume (mL) | Area under Curve (mAU*min) | % Total | Apparent $M_r$ | Expected $M_r$ |
|---|---|---|---|---|---|---|
| His-AAC(6')-APH(2") | 5.2 | 12.7 | 562 | 99 | 72 000 | 58 300 |
| | | | | | | |
| AAC[1-174] | 2.0 | 13.5 | 78 | 36 | 50 000 | 42 000 (dimer) |
| | | 14.9 | 140 | 64 | 26 000 | 21 000 (monomer) |
| | | | | | | |
| AAC[1-194] | 5.0 | 13.4 | 99 | 11 | 52 000 | 46 800 (dimer) |
| | | 14.9 | 800 | 89 | 26 000 | 23 400 (monomer) |
| | | | | | | |
| APH[175-479] | 4.8 | 13.9 | 447 | 97 | 42 000 | 35 900 |
| | | | | | | |
| AAC[1-174] +APH[175-479] | 1.0 and 1.4 | 13.9 | 130 | 54 | 42 000 | 35 900 (APH[175-479]) |
| | | 14.7 | 109 | 46 | 28 000 | 21 000 (AAC[1-174]) |
| | | | | | | |
| AAC[1-194] +APH[175-479] | 2.5 and 2.4 | 14.0 | 152 | 23 | 41 000 | 35 900 (APH[175-479]) |
| | | 14.9 | 494 | 76 | 26 000 | 23 400 (AAC[1-194]) |

[a] 100 µL was injected onto a Superdex 200 column (10 x 30 cm, 24 mL bed volume) as described in Section 5.2.

### 5.3.9 Biological Assessment of Domain Interactions in Providing Antibiotic Protection to *E. coli* and *B. subtilis*

To assess the biological role that domain interactions in AAC(6')-APH(2") may play in antibiotic resistance, *B. subtilis* chromosomal integrants were constructed expressing AAC(6')-APH(2"), AAC[1-194], APH[175-479] and AAC[1-174]+APH[175-479] using either the pSWEET (Bhavsar *et al.*, 2001) or the pDR67 system according to Section 5.2. The resistance level of the *B. subtilis* integrants and previous *E. coli* constructs were assessed through minimum inhibitory concentration (MIC) determinations (Table 5.5). Expression of both AAC[1-174] and APH[175-479] simultaneously in *B. subtilis* did not result in resistance to fortimicin A, an antibiotic exclusively detoxified by the acetyltransferase activity, suggesting that APH[175-479] did not have any biological impact on the activity of AAC[1-174] (data not shown). The MIC results also demonstrate that for some aminoglycosides, the acetyltransferase activity is most important for resistance (e.g. fortimicin), while in other cases, the phosphotransferase activity is most important (e.g. gentamicin), and finally, for the remaining antibiotics, both activities make significant contributions towards resistance (e.g. kanamycin A; Table 5.5). These contributions appear to be additive.

**Table 5.5:** Minimum Inhibitory Concentration Determinations for *E.coli* and *B.subtilis* Constructs Expressing Full-Length and Truncated Versions of AAC(6')-APH(2").

| | MIC (μg/mL) | | | | | | | |
|---|---|---|---|---|---|---|---|---|
| | *E.coli* XL1 Blue | | | | *B.subtilis* | | | |
| | AAC(6')-APH(2") | AAC [1-194] | APH [175-479] | control | AAC(6')-APH(2") | AAC [1-194] | APH [175-479] | control |
| amikacin | 32 | 16 | 16 | 1 | 8 | 4 | 8 | <0.25 |
| butirosin | 4 | 4 | <2 | 2 | 1 | 1 | 1 | <0.25 |
| fortimicin A | 160 | 80 | <4 | 2 | 64 | 64 | 1 | <0.25 |
| gentamicin C | 64 | 1 | 64 | <0.25 | 16 | 0.5 | 16 | <0.25 |
| kanamycin A | 500 | 125 | 250 | 2 | 64 | 16 | 32 | <0.25 |
| ribostamicin | 128 | 128 | 4 | 4 | 8 | 8 | 2 | 0.5 |
| tobramycin | 128 | 8 | 64 | 0.5 | 16 | 2 | 8 | <0.25 |

## 5.3.10 Quantitative Western Analysis to Determine Expression Levels in *B.subtilis* and *E. faecalis*

The protein copy numbers in cells carrying the resistance constructs were evaluated by quantitative Western analysis according to Section 5.2. The three *B. subtilis* constructs, expressing AAC(6')-APH(2"), AAC[1-194] and APH[175-479], expressed protein to similar levels (Figure 5.6), indicating that the MIC results are not biased by different expression levels. The growth of *E. faecalis* in different amounts of aminoglycoside did not have an impact on protein expression (Figure 5.6), validating the constitutive nature of AAC(6')-APH(2") expression.

**A**
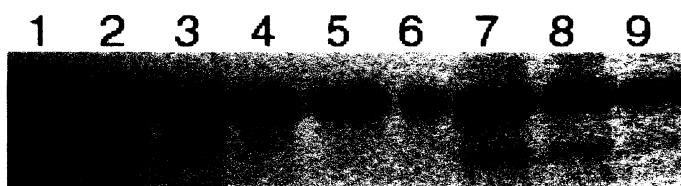


**B**
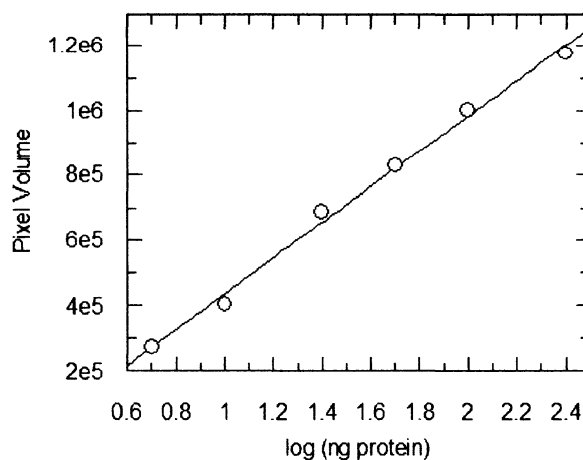


**C**

| Lane | Sample Dilution | Pixel Volume | Protein in Band (ng) | Total protein (μg) | Number of Cells | Protein Copy/Cell |
|------|-----------------|--------------|----------------------|--------------------|-----------------|-------------------|
| 7 | 1500 to 1 | 850 000 | 49.8 | 74.6 | $2.3 \times 10^{10}$ | $3 \times 10^{4}$ |
| 8 | 3000 to 1 | 660 000 | 24.4 | 73.3 | $2.3 \times 10^{10}$ | $3 \times 10^{4}$ |
| 9 | 6000 to 1 | 490 000 | 13.0 | 78.2 | $2.3 \times 10^{10}$ | $3 \times 10^{4}$ |

**D**

| Construct | Protein Copy/Cell |
|-----------|-------------------|
| *B. subtilis* | |
| W/ AAC(6')-APH(2") | $1 \times 10^{4}$ |
| W/ AAC[1-194] | $2 \times 10^{4}$ |
| W/ APH[175-479] | $2 \times 10^{4}$ |
| | |
| *E. faecalis* | |
| - grown in 200 μg/mL gentamicin | $3 \times 10^{4}$ |

| - grown in 2000 µg/mL gentamicin | $3 \times 10^4$ |
| --- | --- |

**Figure 5.6:** Quantification of Protein Expression in *B. subtilis* and *E. faecalis*. Cultures (100 mL) were grown and treated according to Section 5.2. **A** Sample Western blot to determine expression of AAC(6')-APH(2") in *E. faecalis* ATCC 49383 when grown in 200 µg/mL gentamicin. Standard lanes with purified AAC(6')-APH(2"): *1* 250 ng, *2* 100 ng, *3* 50 ng, *4* 25 ng, *5* 10 ng, *6* 5 ng; and sample lanes with different dilutions taken from supernatant of lysed cells: *7* 1500:1, *8* 3000:1, *9* 4500:1. **B** Standard curve describing the association between amount of protein and pixel volume as determined by ImageQuant. Each construct was run with its own set of standard proteins to account for experiment-to-experiment variation. **C** Calculations to determine protein copy number/cell for *E. faecalis* grown in 200 µg/mL gentamicin. **D** Summarized list describing the protein copy number/cell for *B. subtilis* integrants and *E. faecalis* ATCC 49383 grown in different amounts of aminoglycoside.

## 5.4 Discussion

The enzyme AAC(6')-APH(2") is a critical aminoglycoside resistance determinant in Gram-positive pathogens, including *Staphylococcus* and *Enterococcus*, where it is able to inactivate nearly all clinically-relevant aminoglycoside antibiotics (Culebras and Martinez, 1999). It is a bifunctional enzyme, consisting of a N-terminal acetyltransferase and C-terminal phosphotransferase domains, and is thought to have arisen from a gene fusion event between an *aac* and an *aph* (Ferretti *et al.*, 1986). The juxtaposition of two different aminoglycoside modifying activities may have important consequences in terms of antibiotic resistance. One thought is that the ability of AAC(6')-APH(2") to doubly modify (6'-acetylation, 2"-phosphorylation) aminoglycosides leads to greater detoxification of the antibiotic and further decreases the host's susceptibility to the harmful effects of the antibiotic. Thus, a thorough understanding of the protein and its resistance patterns requires a determination of the importance of domain-domain interactions in enzyme function and how this relates to the phenotypic read-out of antibiotic resistance.

To begin analysis, we generated minimal protein segments that expressed either acetyltransferase or phosphotransferase activity. These protein fragments, AAC[1-194] and APH[175-479], were able to modify aminoglycosides *in vitro* and consequently, provide resistance to aminoglycoside substrates appropriate for each activity when expressed in *E. coli* and *B. subtilis*. The active fragments share a short peptide linkage in common, encompassing residues 175-194 that is predicted to be α-helical by *in silico* secondary structure prediction software. This region is not predicted to form part of either the acetyltransferase nor the phosphotransferase active site (Ferretti *et al.*, 1986). This region is likely required for proper structure for both domains and involved in mediating and/or potentiating structural interactions between the two domains of AAC(6')-APH(2").

The AAC domain requires the APH domain for full activity, as it is catalytically impaired *in vitro* when expressed as a N-terminal truncated protein. The thermostabilities of each domain are impacted by the presence of the other domain, especially when GTP is added in thermal inactivation studies. GTP protects both the AAC and APH activities from thermal inactivation, despite the fact that GTP is not a ligand for the AAC domain. The effect of GTP must be mediated through the APH to the AAC domain, considering that GTP does not protect AAC[1-194]. Moreover, when the linkage between the AAC and APH domains is disturbed, by mutation of Lys190 and Leu192 to Pro, GTP protection is diminished.

The mutation of Lys190 and Leu192 to Pro, an effect that would disturb the α-helical nature of the linkage region, also negatively affects the activities of both AAC and

APH. The side chain of Lys190 is not critical to APH function considering that mutation of this residue to Ala had no effect on the activity of APH[175-479] (Chapter 3). This residue is likely solvent exposed in the C-terminal truncated protein since it is susceptible to modification by wortmannin (Chapter 3). In this case, the absence of the AAC domain would reveal the 'linker region' to solvent and potential covalent modifiers.

Thus, the AAC and APH domains make important interactions that are required for proper structure and thermostability, however, there is no evidence that there are functional interactions between the two domains (e.g. substrate channeling). The cofactors of either domain do not affect the kinetics of the other domain and there is no absolute requirement of phosphorylation or acetylation of aminoglycoside prior to the modification catalyzed by the other activity (Azucena *et al.*, 1997; Daigle *et al.*, 1999; Martel *et al.*, 1983). Furthermore, when expressed in either *E. coli* or *B. subtilis*, the fragments only give additive resistance, in terms of MIC, with respect to the full-length enzyme. This may not be surprising as 2"-phosphoryl, 6'-acetylkanamycin A has similar affinity for a model 16S rRNA as does 2"-phosphorylkanamycin A (Llano-Sotelo *et al.*, 2002); that is, there is no added benefit in acetylation following phosphorylation of the antibiotic at least in terms of decreasing the thermodynamic interaction between drug and rRNA target. There may be other 'kinetic' considerations such as the presence of bacterial sugar deacetylases and phosphotases which would inadvertently "re-toxify" aminoglycosides that makes dual modification of antibiotic advantageous for the bacteria.

The results with AAC(6')-APH(2") parallel the results seen with AAC(6')-Im and APH(2")-Id, two monofunctional enzymes found expressed together in *E. faecalis*

and *E. coli* (Chow *et al.*, 2001). In this case, resistance was also additive when AAC(6')-Im and APH(2")-Ib were expressed together in *E. coli* (Chow *et al.*, 2001), and not synergistic as one would expect if there were functional interactions between the two resistance enzymes. Instead, the presence of two different classes of modifying enzyme broadens the range of aminoglycosides that can be detoxified, and the absolute level of resistance to individual antibiotics is only impacted slightly.

These results have important implications in inhibitor design strategies for AAC(6')-APH(2"). The most commonly used aminoglycoside is gentamicin that is detoxified primarily through the APH activity, and thus, inhibitors against APH(2") will be more critical for returning aminoglycoside efficacy. However, other clinically important aminoglycosides, such as amikacin and kanamycin A, are inactivated by both AAC and APH activities, and overcoming resistance to these antibiotics will require the design of inhibitors for both domains of AAC(6')-APH(2"). The best targets for inhibitors will be the active sites of the domains, but there may also be a unique opportunity to design compounds that can disrupt the domain-domain interactions in AAC(6')-APH(2") given their importance in maintaining proper structure and function in the resistance protein. This could effectively negatively impact both activities simultaneously. More structural information on this protein will be required to assess the feasibility of this approach.

Antibiotic modifying enzymes can become resistant to inhibitors through mutation of important protein contacts and again complicate antimicrobial treatment, as demonstrated by inhibitor-resistant β-lactamases (Livermore, 1995). Targeting multiple

sites on AAC(6')-APH(2") would make it more difficult for newer versions to evolve that

do not respond to the inhibitors. The crystal structure of AAC(6')-APH(2") will reveal

the validity of this approach and further bring to light the intimate linkages between the

domains of this important antibiotic resistance enzyme.


## 5.5 References

**Azucena, E., Grapsas, I. and Mobashery, S. 1997.** Properties of a bifunctional bacterial antibiotic resistance enzyme that catalyzes ATP-dependent 2"-phosphorylation and acetyl-CoA dependent 6'-acetylation of aminoglycosides. *J Am Chem Soc.* 119: 2317 - 2318.

**Bhavsar, A.P., Zhao, X. and Brown, E.D. 2001.** Development and characterization of a xylose-dependent system for expression of cloned genes in *Bacillus subtilis*: conditional complementation of a teichoic acid mutant. *Appl Environ Microbiol.* 67: 403-410.

**Boehr, D.D., Jenkins, S.I. and Wright, G.D. 2003.** The Molecular Basis of the Expansive Substrate Specificity of the Antibiotic Resistance Enzyme Aminoglycoside Acetyltransferase-6'- Aminoglycoside Phosphotransferase-2". The Role of Asp-99 as an active site base important for acetyl transfer. *J Biol Chem.* 278: 12873-12880.

**Boehr, D.D., Lane, W.S. and Wright, G.D. 2001.** Active site labeling of the gentamicin resistance enzyme AAC(6')- APH(2") by the lipid kinase inhibitor wortmannin. *Chem Biol.* 8: 791-800.

**Bohm, G., Muhr, R. and Jaenicke, R. 1992.** Quantitative analysis of protein far UV circular dichroism spectra by neural networks. *Protein Eng.* 5: 191-195.

**Chow, J.W., Kak, V., You, I., Kao, S.J., Petrin, J., Clewell, D.B., Lerner, S.A., Miller, G.H. and Shaw, K.J. 2001.** Aminoglycoside resistance genes aph(2")-Ib and aac(6')-Im detected together in strains of both *Escherichia coli* and *Enterococcus faecium*. *Antimicrob Agents Chemother.* 45: 2691-2694.

**Cuff, J.A., Clamp, M.E., Siddiqui, A.S., Finlay, M. and Barton, G.J. 1998.** Jpred: A consensus secondary structure prediction server. *Bioinformatics.* 14: 892-893.

**Culebras, E. and Martinez, J.L. 1999.** Aminoglycoside resistance mediated by the bifunctional enzyme 6'-N-aminoglycoside acetyltransferase-2"-O-aminoglycoside phosphotransferase. *Front Biosci.* 4: D1-8.

**Daigle, D.M., Hughes, D.W. and Wright, G.D. 1999.** Prodigious substrate specificity of AAC(6')-APH(2"), an aminoglycoside antibiotic resistance determinant in enterococci and staphylococci. *Chem Biol.* 6: 99-110.

**Dalmas, B., Hunter, G.J. and Bannister, W.H. 1994.** Prediction of protein secondary structure from circular dichroism spectra using artificial neural network techniques. *Biochem Mol Biol Int.* 34: 17-26.

**Ferretti, J.J., Gilmore, K.S. and Courvalin, P. 1986.** Nucleotide sequence analysis of the gene specifying the bifunctional 6'-aminoglycoside acetyltransferase 2"-aminoglycoside phosphotransferase enzyme in *Streptococcus faecalis* and identification and cloning of gene regions specifying the two activities. *J Bacteriol.* 167: 631-638.

**Jones, D.T. 1999.** Protein secondary structure prediction based on position-specific scoring matrices. *J Mol Biol.* 292: 195-202.

**Kneller, D.G., Cohen, F.E. and Langridge, R. 1990.** Improvements in protein secondary structure prediction by an enhanced neural network. *J Mol Biol.* 214: 171-182.

**Leatherbarrow, R.J. 2000.** Grafit. . Erithacus Software, Staines.

**Livermore, D.M. 1995.** beta-Lactamases in laboratory and clinical resistance. *Clin Microbiol Rev.* 8: 557-584.

**Llano-Sotelo, B., Azucena, E.F., Kotra, L.P., Mobashery, S. and Chow, C.S. 2002.** Aminoglycosides Modified by Resistance Enzymes Display Diminished Binding to the Bacterial Ribosomal Aminoacyl-tRNA Site. *Chem Biol.* 9: 455-463.

**Martel, A., Masson, M., Moreau, N. and Le Goffic, F. 1983.** Kinetic studies of aminoglycoside acetyltransferase and phosphotransferase from *Staphylococcus aureus* RPAL. Relationship between the two activities. *Eur J Biochem.* 133: 515-521.

**McGuffin, L.J., Bryson, K. and Jones, D.T. 2000.** *Bioinformatics.* 16: 404-405.

**Miller, G.H., Sabatelli, F.J., Hare, R.S., Glupczynski, Y., Mackey, P., Shlaes, D., Shimizu, K. and Shaw, K.J. 1997.** The most frequent aminoglycoside resistance mechanisms--changes with time and geographic area: a reflection of aminoglycoside usage patterns? Aminoglycoside Resistance Study Groups. *Clin Infect Dis.* 24 Suppl 1: S46-62.

**Ouali, M. and King, R.D. 2000.** Cascaded multiple classifiers for secondary structure prediction. *Prot Sci.* 9: 1162-1176.

Rouch, D.A., Byrne, M.E., Kong, Y.C. and Skurray, R.A. 1987. The aacA-aphD gentamicin and kanamycin resistance determinant of Tn4001 from *Staphylococcus aureus:* expression and nucleotide sequence analysis. *J Gen Microbiol.* 133: 3039-3052.

Towbin, H., Staehelin, T. and Gordon, J. 1979. Electrophoretic transfer of proteins from polyacrylamide gels to nitrocellulose sheets: procedure and some applications. *Proc Natl Acad Sci U S A.* 76: 4350-4354.

# Chapter 6.

## Broad-Spectrum Peptide Inhibitors of Aminoglycoside Phosphotransferases and Acetyltransferases

Antimicrobial peptides were supplied by Drs. M. Bains and R.E. Hancock. Remaining peptides were synthesized by Dr. K. Koteva. Assays and characterization of AAC(6')-Ii was performed by K.-a. Draker. Assays and characterization with APH(3')-IIIa and AAC(6')-APH(2") was performed by myself.

Note: I have included the results with AAC(6')-Ii to demonstrate the larger implications of this work, that is, the ability to generate inhibitors that have cross-reactivity across the classes of aminoglycoside resistance enzymes.

## 6.1 Introduction

Overcoming aminoglycoside resistance requires the development of new antibiotics that are impervious to modification by the enzymes, or in an alternative approach, the use of an aminoglycoside alongside an inhibitor directed against the inactivating enzymes. Although antibiotics have been developed that resist modification by some inactivating enzymes, the large number and differing regiospecificities of group transfer presented by aminoglycoside modifying enzymes virtually guarantees that a new aminoglycoside will not be effective against all resistance mechanisms. Broad-spectrum inhibitors directed against more than one class of modifying enzyme would therefore be highly desirable and would allow the rescue of aminoglycoside antibiotic activity, analogous to the employment of β-lactamase inhibitors to overcome penicillin resistance (Livermore, 1995).

The three-dimensional structures of representative members of all three classes of aminoglycoside modifying enzymes have directed our efforts to identify inhibitors active against resistance enzymes. For example, the aminoglycoside phosphotransferase APH(3')-IIIa was shown to be structurally homologous to ePKs (Hon *et al.*, 1997), prompting a screen of protein kinase inhibitors from which many compounds were determined to inhibit APHs (Daigle *et al.*, 1997). The AACs and ANTs also have eukaryotic homologs, and in particular, AAC(3)-Ia (Wolf *et al.*, 1998) and AAC(6')-Ii (Wybenga-Groot *et al.*, 1999) belong to the large GCN5-related N-acetyltransferase superfamily, which includes the eukaryotic histone acetyltransferases GCN5 and Hat1. These structural studies have correlated well with functional studies that have shown that

APHs (Daigle *et al.*, 1999b) and AACs (Wybenga-Groot *et al.*, 1999) can phosphorylate

and acetylate peptides, respectively. In general, positively charged peptides are favored,

likely owing to the prevalence of negatively charged residues in the active site pockets of

aminoglycoside modifying enzymes (Figure 6.1). The anionic depression present in the

resistance enzymes is thought to attract positively charged antibiotics and act as an

electronic scaffold for the efficient binding of a variety of aminoglycoside structures.

Given this common binding site feature, positively charged molecules could be

developed that interfere with this interaction with aminoglycosides and lead to broad-

spectrum inhibition of resistance activity.
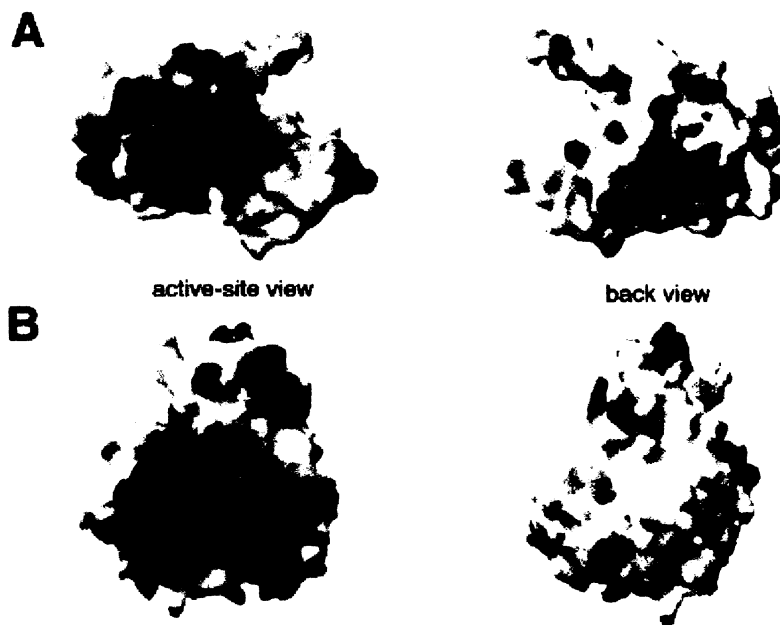


**Figure 6.1:** The Common Anionic Depression Found in the Active Sites of Aminoglycoside Resistance Enzymes. (A) Electrostatic surface potential map of the aminoglycoside acetyltransferase AAC(6')-Ii (PDB 1B87). Red and blue indicate the regions of the enzyme with the greatest electronegative and electropositive characters, respectively. (B) Electrostatic surface potential map of the aminoglycoside phosphotransferase APH(3')-IIIa (PDB 1J71), with colors denoted as in (A). Figure generated using DeepView (Guex and Peitsch, 1997).

Given that aminoglycoside resistance enzymes share this common binding strategy and that many of them also bind peptides and proteins, we hypothesized that cationic peptides could serve as lead molecules in the development of a universal aminoglycoside resistance inhibitor. Cationic peptides are also good starting points for these studies, as many of them have antimicrobial activity themselves (Sitaram and Nagaraj, 2002). While the site of action for some of these peptides appears to be the bacterial cytoplasmic membrane, there is evidence for penetration of others into the cytoplasm where aminoglycoside resistance enzymes are active (Matsuzaki *et al.*, 1997; Wu *et al.*, 1999).

In this Chapter, we have screened a variety of cationic antimicrobial peptides against three well-characterized aminoglycoside resistance enzymes, APH(3')-IIIa, AAC(6')-Ii, and AAC(6')-APH(2"). APH(3')-IIIa (Kan[R]) and AAC(6')-APH(2") (Gent[R]) are two of the most common and important resistance determinants in Gram-positive bacterial pathogens (Miller *et al.*, 1997), whereas AAC(6')-Ii is a chromosomally encoded determinant found in the difficult-to-treat *Enterococcus faecium* that lends low-level intrinsic resistance to many aminoglycosides and obviates aminoglycoside/penicillin synergy in these organisms (Costa *et al.*, 1993). We have identified cationic peptide inhibitors of both aminoglycoside phosphotransferases and aminoglycoside acetyltransferases that show similar affinity for binding to the enzymes as natural substrates. Moreover, the bovine antimicrobial peptide indolicidin and its analogs were shown to inhibit enzymes belonging to both the aminoglycoside phosphotransferase and aminoglycoside acetyltransferase classes of resistance enzymes.

These compounds represent the first broad-spectrum inhibitors of aminoglycoside modifying enzymes.

## 6.2 Materials and Methods

### 6.2.1 Chemicals

Antimicrobial peptides were synthesized at the University of British Columbia's Nucleic Acid and Protein Sequencing Facility using N-(9-fluorenyl)methoxy carbonyl (Fmoc) chemistry and were purified by reversed phase high-pressure liquid chromatography. The peptide purity was confirmed by mass spectrometry. APH(3')-IIIa (McKay et al., 1994), AAC(6')-APH(2") (Boehr et al., 2001; Daigle et al., 1999a), and AAC(6')-Ii (Wright and Ladak, 1997) were purified as previously described.

### 6.2.2 APH and AAC Kinetic Assays

APH and AAC assays were described in Chapters 2 and 3. Kinetic parameters for those cationic peptides behaving as AAC(6')-Ii substrates were determined using $[1-^{14}C]$ acetyl-CoA and a phosphocellulose binding assay described previously (Wybenga-Groot et al., 1999). Reaction mixtures typically contained 25 mM HEPES (pH 7.5), 2 mM EDTA, 0.10 μCi $[1-^{14}C]$acetyl-CoA, and 40 pmoles pure AAC(6')-Ii with varying concentrations of poly-L-lysine (as positive control) or cationic peptide and were allowed to proceed for 45 min.

For the phosphotransferase assays, ATP was fixed at 1000 μM and kanamycin A was fixed at 100 μM when measuring the steady-state kinetic parameters for

aminoglycoside substrate and ATP, respectively. For the acetyltransferase assays, acetyl-

CoA was held at 100 μM when measuring the steady-state kinetic parameters for the

cationic peptides. Results are reported +/- standard error.

### 6.2.3 IC$_{50}$ Determinations

IC$_{50}$ values for enzyme inhibition by various cationic peptides were determined

for APH(3')-IIIa, APH(2'')-Ia, AAC(6')-Ie, and AAC(6')-Ii using the spectrophotometric

kinetic assays described. Initial velocities in the presence of increasing concentrations of

cationic peptides and appropriate concentrations of substrates were fit to the four

parameter equation 6.2 using Grafit 4.0 software (Leatherbarrow, 2000):

$$y = \frac{Range}{1 + \left(\dfrac{x}{IC_{50}}\right)^{s}} + Background$$

(Eq. 6.2)

where *Range* is the fitted uninhibited rates minus background values, *y* is the enzyme

rate, *x* is the inhibitor concentration and *s* is a slope factor.

### 6.2.4 $K_i$ Determinations for the Indolicidin Analogs

To determine $K_i s$, steady-state kinetic parameters were determined in the presence

of increasing amounts of peptide inhibitors and the data was fit to either a noncompetitive

pattern (equation 6.3), a mixed pattern (equation 6.4), or a competitive pattern (equation

6.5) using Grafit 4.0 (Leatherbarrow, 2000):

$$v = \frac{V_{max} \cdot [S] \cdot \dfrac{1}{1+[I]/K_i}}{K_m + [S]}$$

(Eq. 6.3)

$$v = \frac{V_{max} \cdot [S]}{K_m\left(1 + \dfrac{[I]}{K_i}\right) + \left(1 + \dfrac{[I]}{K_i'}\right)[S]}$$

(Eq. 6.4)

$$v = \frac{V_{max} \cdot [S]}{K_m\left(1 + \dfrac{[I]}{K_i}\right) + [S]}$$

(Eq. 6.5)

## 6.2.5 Synthesis of Indolicidin-Based Peptides

All peptides were prepared by solid-phase peptide synthesis (0.5 mmol scale, 2-(1H-benzotriazole-1-yl)-1,1,3,3,-tetramethyluronium

terafluoroborate/hydroxybenzotriazole/diisopropylethylamine,          alternated          by

dicyclohexylcarbodiimide/hydroxybenzotriazole activation) on Wang resin derivatized

with appropriate C-terminal amino acid using 9-fluorenylmethoxy carbonyl-protected

monomers. Side chain protecting groups used were *tert*. butoxycarbonyl for Lys and Trp,

2,2,4,6,7-pentamethyldihydro-benzofuran-5-sulfonyl for Arg. The peptides were cleaved

from the resin using 0.1% $H_2O$ in trifluoroacetic acid for 2 hr at room temperature.

Reverse phase (C18) MPLC purification (20%–60% acetonitrile in 0.05%TFA/$H_2O$) over

2 hr afforded the peptides in more than 99% purity (by analytical HPLC) as a white solid.

The identity of all peptide products were verified by electrospray mass spectrometry at

the    McMaster    Regional    Centre    for    Mass    Spectrometry.

## 6.3 Results and Discussion

### 6.3.1 Antimicrobial Peptides Inhibit Aminoglycoside Resistance Enzymes

Several structural classes of cationic peptides were screened against three aminoglycoside modifying enzymes representing two classes of aminoglycoside resistance enzymes, the APHs and the AACs, which are most prevalent in Gram-positive pathogens (Table 6.1). Most of these peptides, except protegrin 1 and gramicidin S, are predicted to be unstructured in free solution and only adopt the structures described in Table 6.1 upon interaction with membranes (Friedrich *et al.*, 2001).

The two aminoglycoside acetyltransferases, AAC(6')-Ii and AAC(6')-Ie (the acetyltransferase activity associated with the bifunctional enzyme AAC(6')-APH(2")), showed different peptide affinities (Table 6.1). Neither indolicidin nor its analogs, CP11CN or CP10A, appeared to inhibit AAC(6')-Ie, whereas these peptides were good inhibitors of AAC(6')-Ii. On the other hand, the α-helical-forming peptides CP29 and CP2600 effectively inhibited AAC(6')-Ie, but did not have an effect against AAC(6')-Ii. CP10A appeared to be the best inhibitor of AAC(6')-Ii, whereas gramicidin S, a bacterium-derived cyclic decapeptide, was the best inhibitor of AAC(6')-Ie.

For the most part, the two aminoglycoside phosphotransferases surveyed, APH(3')-IIIa and APH(2")-Ia (the kinase activity of the bifunctional AAC(6')-APH(2") enzyme), had similar peptide inhibitor profiles (Table 6.1). The β-hairpin-structured

peptide protegrin (PG1) appeared to be the best inhibitor of the aminoglycoside

phosphotransferases, and indolicidin and its analog, CP10A, had efficient inhibitory

activity against both enzymes. CP11CN weakly inhibited APH(3')-IIIa but did not show

any activity against APH(2")-Ia, suggesting a limited selectivity between the

aminoglycoside                                                          phosphotransferases.

**Table 6.1:** Cationic Antimicrobial Peptides that Inhibit the Aminoglycoside Antibiotic Resistance Enzymes AAC(6')-Ii, AAC(6')-APH(2"), and APH(3')-IIIa).

| Peptide[a] | Sequence[b] | Charge at pH 7 | Structure | $IC_{50}$ $(\mu M)^c$ | | | |
|---|---|---|---|---|---|---|---|
| | | | | AAC(6')-Ii[c] | AAC(6')-Ie | APH(2")-Ia | APH(3')-IIIa |
| CP29 | KWKSFIKKLTTAVKKVLTTGLPALIS | +6 | α-helical | -[d] | 21 ± 9 | - | - |
| CP2600 | KWKSFIKKLTSAAKKVTTAAKPLTK | +7 | α-helical | - | 38 ± 9 | - | - |
| CM3 | KWKKFIKSLTKAAKTVVKTAKKPLIV | +9 | α-helical | 24 ± 1 | - | - | - |
| Indolicidin | ILPWKWPWWPWRR-NH₂ | +4 | Extended | 13 ± 1 | - | 64 ± 5 | 11 ± 2 |
| CP11CN | ILKKWPWWPWRRK-NH₂ | +6 | Extended | 23 ± 4 | - | - | 51 ±10 |
| CP10A | ILAWKWAWWAWRR-NH₂ | +4 | α-helical | 4.4 ± 0.2 | - | 36 ± 6 | 11 ± 1 |
| PG1 | RGGRLCYCRRRFCVCVGR | +6 | β-hairpin | - | - | 20 ± 4 | 5.2 ± 0.3 |
| Gramicidin S | (cyclic) LF$^d$PVOLF$^d$PVO | +2 | β-sheet | - | 14 ± 2 | - | - |

[a] In addition to these peptides, the following α-helical peptides were screened against one or more aminoglycoside modifying enzymes: CP26, CEME, CEMA, CPα1, and CPα2, but did not show any significant inhibitory activity

[b] For gramicidin S, the superscript [d] indicates D enantiomer and O is the one letter code for ornithine. All other amino acid residues are described by their one letter code.

[c] For the aminoglycoside acetyltransferases, the $IC_{50}$s for AAC(6')-Ii and AAC(6')-Ie were determined in the presence of 50 μM acetyl-CoA and 50 μM kanamycin A, and 100 μM acetyl-CoA and 40 μM kanamycin A, respectively, using the aminoglycoside acetyltransferase assay described in Section 6.2. For the aminoglycoside phosphotransferases, the $IC_{50}$s were determined in the presence of 1000 μM ATP and 100 μM kanamycin A, using the kinase assay described in Experimental Procedures.

[d] dashes indicate that there was no inhibitory activity for this peptide against this enzyme target

The best peptide inhibitors were not necessarily those with the greatest positive charge, demonstrating that inhibitory peptides make specific amino acid contacts with the enzymes and their interaction is not exclusively dictated by ionic interactions. Indolicidin and its analog, CP10A, were especially effective in inhibiting the resistance enzymes with $IC_{50}$s in the low to mid-micromolar range for three of the four enzyme activities (Table 6.1). The more highly charged indolicidin analog CP11CN was only effective against AAC(6')-Ii and APH(3')-IIIa, although it was a significantly weaker inhibitor of APH(3')-IIIa compared to CP10A and indolicidin.

### 6.3.2 Indolicidin Analogs Inhibit Aminoglycoside Phosphotransferases and Aminoglycoside Acetyltransferases through Different Modes of Action

As indolicidin and its analog CP10A were able to inhibit both APHs and AAC(6')-Ii, we compared the mode of action between the two classes to gain insight into the structural requirements for efficient inhibition by these compounds. Toward the first goal, we determined the inhibition patterns with respect to AAC(6')-Ii and the two APH enzymes.

With AAC(6')-Ii, CP10A demonstrated a competitive inhibition pattern with respect to the aminoglycoside substrate kanamycin A (Figure 6.2A) and a noncompetitive pattern with respect to acetyl-CoA (Figure 6.2B). This classical pattern of inhibition suggests that CP10A binds at or near the aminoglycoside-binding pocket and does not make any interactions with the acetyl-CoA binding pocket (Table 6.2). In contrast, a more complex situation arises in inhibition patterns determined with the aminoglycoside

phosphotransferases, APH(3')-IIIa and APH(2")-Ia, where the peptide inhibitors demonstrated noncompetitive patterns with respect to both aminoglycoside (Figure 6.2C) and ATP (Figure 6.2D, Table 6.2). These results suggest that the peptide inhibitors have multiple binding modes to the APH class of resistance enzyme. The inhibition patterns demonstrate that the peptides bind both to free enzyme and to enzyme-substrate complexes, and also suggests that the peptides do not bind simply to either the aminoglycoside binding site or the ATP binding pocket, but influence both sites directly or indirectly.

**Table 6.2:** $K_i$ Determinations for Indolicidin and Its Analogs with the Aminoglycoside Resistance Enzymes.

| Enzyme - Inhibitor | Variable Substrate | Pattern | $K_{is}$ ($\mu$M) | $K_{ii}$ ($\mu$M) |
|---|---|---|---|---|
| **APH(2")-Ia** | | | | |
| - indolocidin | kanamycin A | non-competitive | 22.1 ± 1.7 | 22.1 ± 1.7 |
| | ATP | non-competitive | 23.8 ± 3.4 | 23.8 ± 3.4 |
| - CP10A | kanamycin A | non-competitive | 10.1 ± 0.8 | 10.1 ± 0.8 |
| | ATP | non-competitive | 7.66 ± 0.61 | 7.66 ± 0.61 |
| **APH(3')-IIIa** | | | | |
| - indolocidin | kanamycin A | non-competitive | 14.6 ± 2.1 | 14.6 ± 2.1 |
| | ATP | non-competitive | 10.3 ± 1.4 | 10.3 ± 1.4 |
| - CP10A | kanamycin A | non-competitive | 30.5 ± 4.6 | 30.5 ± 4.6 |
| | ATP | non-competitive | 13.8 ± 1.1 | 13.8 ± 1.1 |
| - CP11CN | kanamycin A | non-competitive | 51.2 ± 5.2 | 51.2 ± 5.2 |
| | ATP | non-competitive | 73.0 ± 28.2 | 73.0 ± 28.2 |
| **AAC(6')-Ii** | | | | |
| -indolocidin | ribostamicin | competitive | 4.23 ± 0.96 | |
| | acetyl-CoA | non-competitive | 38.0 ± 1.7 | 38.0 ± 1.7 |
| - CP10A | kanamycin B | competitive | 2.41 ± 0.60 | |
| | acetyl-CoA | mixed | 4.76 ± 1.33 | 31.7 ± 8.3 |
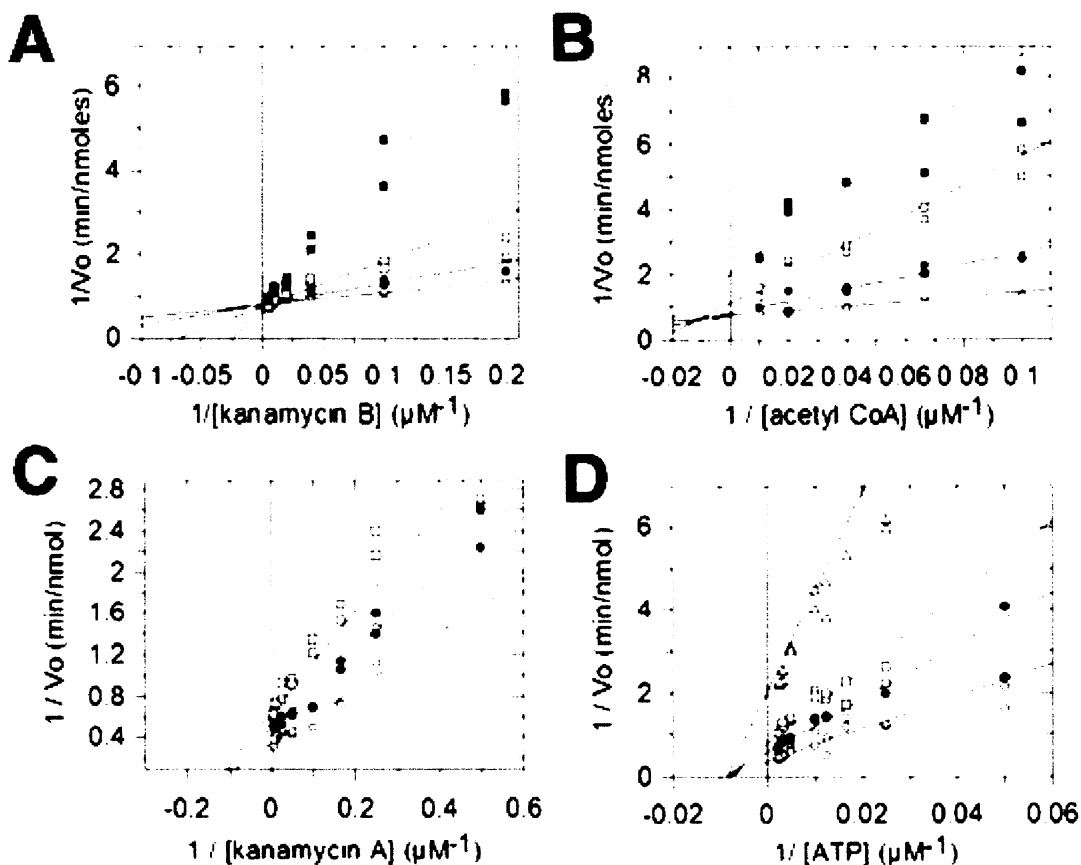
Figure 6.2: The Inhibition Patterns of Aminoglycoside Acetyltransferases and Phosphotransferases with the Peptide CP10A (A) Inhibition of AAC(6')-Ii with kanamycin B as the variable substrate and acetyl-CoA as the saturating substrate. The concentrations of CP10A are as follows: 0 (O ), 5 (●), 10 (□), and 20 (■) μM. (B) Inhibition of AAC(6')-Ii with acetyl-CoA as the variable substrate and kanamycin B as the saturating substrate. The concentrations of CP10A are as follows: 0 (O ), 10 (●), 20 (□), and 40 (■) μM. (C) Inhibition of APH(2")-Ia with kanamycin A as the variable substrate and ATP as the saturating substrate. The concentrations of CP10A are as follows: 0 (O ), 5 (●), and 10 (□) μM. (D) Inhibition of APH(2")-Ia with ATP as the variable substrate and kanamycin A as the saturating substrate. The concentrations of CP10A are as follows: 0 (O ), 5 (●), 10 (□), and 40 (△) μM.

### 6.3.3 Structure-Activity Relationships of Indolicidin Analog CP10A

The indolicidin analog CP10A demonstrated similar affinity as aminoglycoside substrates, with $K_i$s in the mid to low micromolar range, to both AAC and APH classes of antibiotic resistance enzymes (Table 6.3). Our initial hypothesis was that these peptides would inhibit the aminoglycoside resistance enzymes by binding primarily through electrostatic interactions. Consistent with this hypothesis, increasing the salt concentration had a negative impact on $IC_{50}$ for CP10A with both AAC(6')-Ii (Figure 6.3A) and APH(3')-IIIa (Figure 6.3B).

To gain further insight into the important interactions between the peptide and the enzymes, we assayed the resistance enzymes against a number of fragments of CP10A. A peptide consisting of the six N-terminal residues of CP10A (GW15) did not inhibit either APH(3')-IIIa or AAC(6')-Ii; however, a peptide composed of the five C-terminal residues (GW11) was able to weakly inhibit APH(3')-IIIa (Table 6.3). This suggests that the most important binding interaction to APH(3')-IIIa occurs with the C-terminal proportion of CP10A. However, inhibition was significantly increased as additional residues were added onto the N terminus, where the addition of hydrophobic residues had the largest impact on changes in $IC_{50}$ (Table 6.3). This result suggests that hydrophobic interactions and van der Waals forces also play important roles in the interactions between peptide and resistance enzyme.
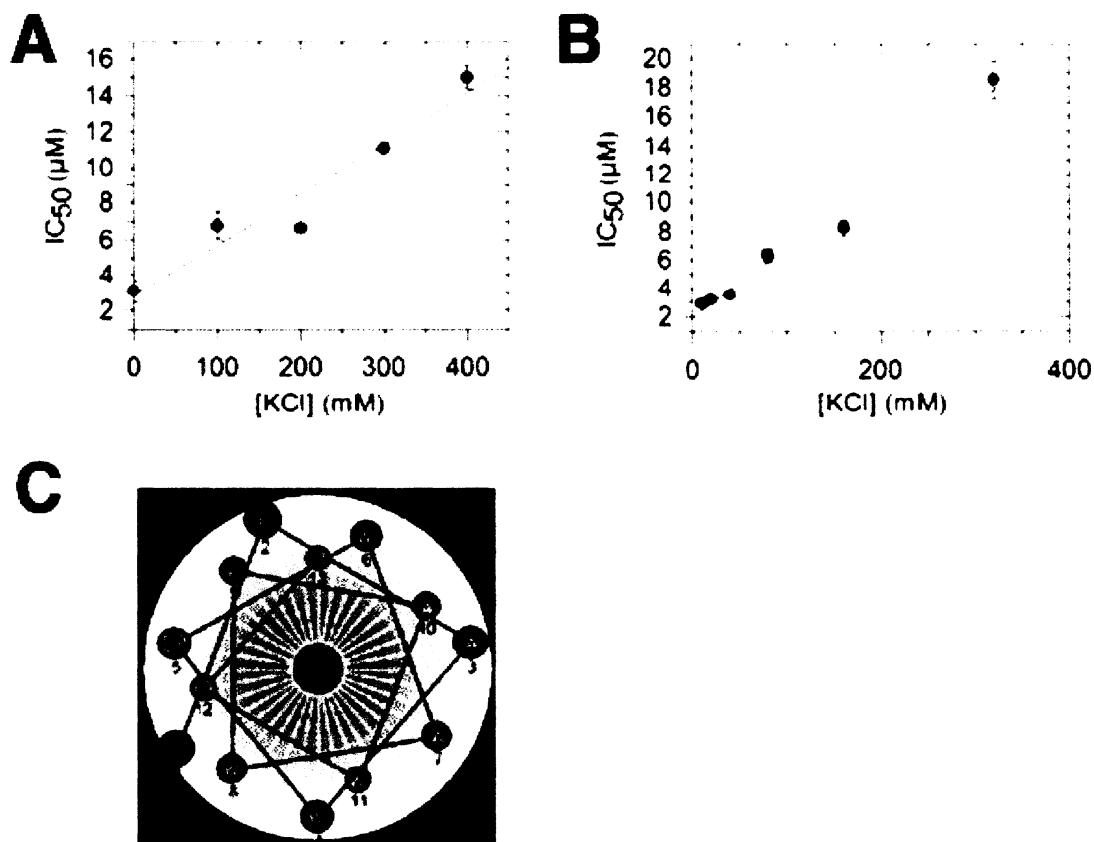
**Figure 6.3:** The Nature of the Interactions between the Peptide CP10A and the Aminoglycoside Resistance Enzymes AAC(6')-Ii and APH(3')-IIIa. (A) Effect of salt on the inhibitory activity of CP10A on AAC(6')-Ii. $IC_{50}$ were determined in the presence of 50 $\mu$M acetyl-CoA and 50 $\mu$M kanamycin A. (B) Effect of salt on the inhibitory activity of CP10A on APH(3')-IIIa. $IC_{50}$ were determined in the presence of 100 $\mu$M ATP and 60 $\mu$M kanamycin A. (C) Helical wheel diagram for CP10A. CP10A has the ability to form an amphipathic helix with positive charged amino acid residues on one face and primarily hydrophobic amino acid residues on the other face. The propensity for $\alpha$-helical formation increases in the presence of negatively charged lipids. This secondary structure may be important for the peptide's interactions with the negatively charged surface patches of aminoglycoside resistance enzymes.

**Table 6.3:** Structure-Activity Relationship for the Peptide CP10A with APH(3')-IIIa and AAC(6')-Ii.

| Peptide | Sequence | IC$_{50}$ ($\mu$M)$^a$ | |
|---|---|---|---|
| | | APH(3')-IIIa | AAC(6')-Ii |
| | | | |
| CP10A | ILAWKWAWWAWRR | 8.5 ± 0.7 | 4.4 ± 0.2 |
| GW22 | LAWKWAWWAWRR | 22 ± 1 | 10 ± 2 |
| GW21 | AWKWAWWAWRR | 16 ± 1 | 13 ± 1 |
| GW20 | WKWAWWAWRR | 31 ± 3 | 17 ± 3 |
| GW19 | KWAWWAWRR | 79 ± 7 | No inhibition |
| GW18 | WAWWAWRR | 55 ± 6 | No inhibition |
| GW17 | AWWAWRR | > 100 | No inhibition |
| GW16 | WWAWRR | > 100 | No inhibition |
| GW11 | WAWRR | ~400 | No inhibition |
| GW15 | ILAWKA | No inhibition | No inhibition |
| | | | |
| GW27 | ILAWAWKWWAWRR | 9.0 ± 1.4 | 10 ± 1 |
| GW28 | ILAWKWAWWARWR | 5.0 ± 0.5 | 5.8 ± 1.0 |

$^a$ determined in the presence of 100 $\mu$M ATP and 60 $\mu$M kanamycin A for APH(3')-IIIa, and 50 $\mu$M acetyl-CoA and 50 $\mu$M kanamycin A for AAC(6')-Ii.

With either APH(3')-IIIa or AAC(6')-Ii, maximum inhibition occurred only with full-length CP10A (Table 6.3). CP10A is predicted to adopt an amphipathic helix structure with one face primarily hydrophobic and the other positively charged (Figure 6.3C). To determine the potential importance of this secondary structure and the placement of positively charged amino acid residues in the peptide, we tested the resistance enzymes against peptides GW27, which exchanges residues 5 and 7 in CP10A, and GW28, which exchanges residues 11 and 12 in CP10A. These peptides have the same amino acid composition and charge as CP10A, but with disrupted amphipathic properties. GW28 was a slightly better inhibitor of APH(3')-IIIa than was CP10A; however, CP10A was still the best inhibitor of AAC(6')-Ii where GW27 was 2.3-fold less

potent in inhibiting the enzyme than CP10A (Table 6.3). Considering these relatively

minor effects on inhibition, the positioning of the positively charged amino acid residues

has little impact on inhibitory activity against the resistance enzymes. This is not

completely unexpected, as there are a number of negatively charged residues in the

resistance enzymes that could interact with the positively charged amino acid residues in

the peptides, depending on the nature of the peptide. This is encouraging as it suggests

that there is enough flexibility in the peptide-resistance enzyme interaction such that the

peptides have the ability to attenuate a broad range of resistance activity by adopting the

most energetically favorable conformations dependent upon the available interactions in

the different enzymes.


While there is evidence to suggest that some cationic peptides do enter the cell

(Matsuzaki *et al.*, 1997; Wu *et al.*, 1999), none of the peptides we examined in this study

showed synergistic antimicrobial properties with aminoglycosides in organisms harboring

resistance genes (data not shown).


## 6.4 References

**Boehr, D.D., Lane, W.S. and Wright, G.D. 2001.** Active site labeling of the gentamicin resistance enzyme AAC(6')- APH(2") by the lipid kinase inhibitor wortmannin. *Chem Biol.* 8: 791-800.

**Costa, Y., Galimand, M., Leclercq, R., Duval, J. and Courvalin, P. 1993.** Characterization of the chromosomal aac(6')-Ii gene specific for *Enterococcus faecium. Antimicrob Agents Chemother.* 37: 1896-1903.

**Daigle, D.M., Hughes, D.W. and Wright, G.D. 1999a.** Prodigious substrate specificity of AAC(6')-APH(2"), an aminoglycoside antibiotic resistance determinant in enterococci and staphylococci. *Chem Biol.* 6: 99-110.

Daigle, D.M., McKay, G.A., Thompson, P.R. and Wright, G.D. 1999b. Aminoglycoside antibiotic phosphotransferases are also serine protein kinases. *Chem Biol.* 6: 11-18.

Daigle, D.M., McKay, G.A. and Wright, G.D. 1997. Inhibition of aminoglycoside antibiotic resistance enzymes by protein kinase inhibitors. *J Biol Chem.* 272: 24755-24758.

Friedrich, C.L., Rozek, A., Patrzykat, A. and Hancock, R.E. 2001. Structure and mechanism of action of an indolicidin peptide derivative with improved activity against gram-positive bacteria. *J Biol Chem.* 276: 24015-24022.

Guex, N. and Peitsch, M.C. 1997. SWISS-MODEL and the Swiss-Pdbviewer. An environment for comparative protein modeling. *Electrophoresis*, 18: 2714-2723.

Hon, W.C., McKay, G.A., Thompson, P.R., Sweet, R.M., Yang, D.S., Wright, G.D. and Berghuis, A.M. 1997. Structure of an enzyme required for aminoglycoside antibiotic resistance reveals homology to eukaryotic protein kinases. *Cell.* 89: 887-895.

Leatherbarrow, R.J. 2000. Grafit. . Erithacus Software, Staines.

Livermore, D.M. 1995. beta-Lactamases in laboratory and clinical resistance. *Clin Microbiol Rev.* 8: 557-584.

Matsuzaki, K., Yoneyama, S. and Miyajima, K. 1997. Pore formation and translocation of melittin. *Biophys J.* 73: 831-838.

McKay, G.A., Thompson, P.R. and Wright, G.D. 1994. Broad spectrum aminoglycoside phosphotransferase type III from *Enterococcus*: overexpression, purification, and substrate specificity. *Biochemistry.* 33: 6936-6944.

Miller, G.H., Sabatelli, F.J., Hare, R.S., Glupczynski, Y., Mackey, P., Shlaes, D., Shimizu, K. and Shaw, K.J. 1997. The most frequent aminoglycoside resistance mechanisms--changes with time and geographic area: a reflection of aminoglycoside usage patterns? Aminoglycoside Resistance Study Groups. *Clin Infect Dis.* 24 Suppl 1: S46-62.

Sitaram, N. and Nagaraj, R. 2002. The therapeutic potential of host-defense antimicrobial peptides. *Curr Drug Targets.* 3: 259-267.

Wolf, E., Vassilev, A., Makino, Y., Sali, A., Nakatani, Y. and Burley, S.K. 1998. Crystal structure of a GCN5-related N-acetyltransferase: *Serratia marcescens* aminoglycoside 3-N-acetyltransferase. *Cell.* 94: 439-449.

**Wright, G.D. and Ladak, P. 1997.** Overexpression and characterization of the chromosomal aminoglycoside 6'-N-acetyltransferase from *Enterococcus faecium*. *Antimicrob Agents Chemother*. 41: 956-960.

**Wu, M., Maier, E., Benz, R. and Hancock, R.E. 1999.** Mechanism of interaction of different classes of cationic antimicrobial peptides with planar bilayers and with the cytoplasmic membrane of Escherichia coli. *Biochemistry*. 38: 7235-7242.

**Wybenga-Groot, L.E., Draker, K., Wright, G.D. and Berghuis, A.M. 1999.** Crystal structure of an aminoglycoside 6'-N-acetyltransferase: defining the GCN5-related N-acetyltransferase superfamily fold. *Structure Fold Des*. 7: 497-507.

# Chapter 7.

# Conclusions and Future Directions

Figure 7.2A and B were generated by Dr. James R. Cox. All other work was performed by myself.

## 7.1 Recap

Resistance to the aminoglycoside antibiotics is most often the result of inactivating enzymes that modify the drugs such that they can no longer bind to their target, the prokaryotic ribosome (Azucena and Mobashery, 2001; Wright, 1999). Two of the most prevalent resistance enzymes in Gram-positive pathogens are APH(3')-IIIa and AAC(6')-Ie-APH(2")-Ia (Miller *et al.*, 1997). APH(3')-IIIa is the best studied aminoglycoside kinase with a number of functional, structural and inhibitors studies completed, whereas there is much less known about AAC(6')-APH(2").

In this thesis, the chemical mechanism of APH(3')-IIIa has been further elucidated and compared to studies performed with APH(2")-Ia (Chapter 2) (Boehr *et al.*, 2001b; Thompson *et al.*, 2002). The mechanisms of phosphoryl transfer for both APHs are consistent with a dissociative-type mechanism, where base catalysis and abstraction of the hydroxyl proton is less important in the formation of an exploded transition-state. This has important implications for inhibitor design, considering that compounds that mimic the elongated transition-state should be potent inhibitors of APH resistance activity. There is also the opportunity to target Lys44 (APH(3')-IIIa numbering) in the ATP binding pocket for covalent modification, although different APHs have different sensitivities to the irreversible inhibitors FSBA and wortmannin (Chapter 3) (Boehr *et al.*, 2001a).

In contrast, the molecular mechanism for AAC(6')-Ie appears to be more associative, where base catalysis by Asp99 is critical (Chapter 4) (Boehr *et al.*, 2003c). This residue is also susceptible to covalent modification and can act as an important

anchoring site for inhibitors of AAC(6')-Ie (Boehr *et al.*, 2003c). The generality of base catalysis among the AACs is not known presently. Thus, inactivation of other AACs, and other GNAT family members, through covalent modification of the active site base may or may not be a possible strategy.

The studies in this thesis are the foundation upon which a greater understanding of these critical resistance enzymes can be built. The goal now is to design compounds that can inhibit APH(3')-IIIa and AAC(6')-APH(2"), and find new paths to returning efficacy to the aminoglycoside antibiotics.

## 7.2 Implications for Enzyme-Catalyzed Acetylation and Phosphorylation Reactions

Aminoglycoside kinases and acetyltransferases belong to larger protein families, and hence the results here have broader implications. The results with APH(3')-IIIa and APH(2")-Ia agree with the results obtained with ePKs that suggest that this family of kinases operate through a dissociative-like transition-state (Adams, 2001; Hengge *et al.*, 1995; Kim and Cole, 1997; Kim and Cole, 1998; Knowles, 1980), similar to what is observed in the uncatalyzed solution reactions (Herschlag and Jencks, 1989a; Herschlag and Jencks, 1989b; Kirby and Varvoglis, 1967). Thus, the chemical pathway to phosphorylation in these cases does not change when the reaction is enzyme-catalyzed. The important residues implicated in ePK and APH catalysis are also the same (Adams, 2001; Boehr *et al.*, 2001b), which is not surprising as these residues are the only ones that are absolutely conserved between ePKs and APHs. The structures of ePKs and APHs are very similar, despite this lack of sequence conservation, and yet, similar residues are positioned almost identically to catalyze phosphorylation (Hon *et al.*, 1997).

Catalysis among the GNAT superfamily, in contrast to the ePK/APH family of enzymes, is much more varied, where base catalysis may or may not be important depending on the substrate to be acetylated. Although the acetylation reactions appear to be through direct-transfer mechanisms in all of the enzyme members studied (Dyda *et al.*, 2000), the transition states are likely to be very different, where some enzymes stabilize associative-like transition states (AAC(6')-Ie included) (Langer *et al.*, 2001; Scheibner *et al.*, 2002; Tanner *et al.*, 1999) whereas others may utilize a dissociative-like transition state (e.g. AAC(6')-Ii; Draker, K.-a. and Wright, G. D., unpublished observations). Sequence conservation is also low among GNAT family members where there does not appear to be any absolutely conserved residues that are important in catalysis (Dyda *et al.*, 2000). Instead, the formation of an acetyl-CoA binding pocket appears to be the most critical factor underlying the structural similarities among family members, and the specifics of catalysis differ from enzyme to enzyme.

The molecular reasons for maintaining similar structures in the GNAT and ePK/APH superfamilies are thus quite different. In the ePK/APH superfamily, structure is preserved to provide identical chemical scaffolds for catalyzing analogous reactions, whereas the structures of GNAT family members supply only similar binding pockets for substrates. These differences suggest that both ground-state and excited-state considerations are important for maintaining evolutionary conserved structures.

## 7.3 Broad-Range Inhibitors of Aminoglycoside Modifying Enzymes

Cationic peptides have been identified that can inhibit both AAC and APH functionalities, however, these peptides, including indolicidin, are not effective in

reversing aminoglycoside resistance *in vivo* (Chapter 6) (Boehr *et al.*, 2003a). This is most likely related to the affinity that the peptides have for the resistance enzymes and/or their ability to cross the bacterial cell membrane. First, the peptides have only moderate affinity for the resistance enzymes, with $K_i$s in the low micromolar range, less potent than the nanomolar range inhibitors that are usually desired to exert a biological effect, and second, the peptides are positively charged and it is not yet clear if they can penetrate into the bacterial cytoplasm where the resistance enzymes are located (Matsuzaki *et al.*, 1997; Wu *et al.*, 1999). Furthermore, although the peptide inhibitors show traditional, competitive-type inhibition for AAC(6')-Ii, they show more complex patterns for APH(2")-Ia and APH(3')-IIIa, complicating the further development of these inhibitors. These patterns for the APHs may indicate multiple binding modes for the peptides, which would likely limit the ability to increase the potency of these inhibitors. Modification of the peptides may enhance one binding mode at the expense of sacrificing the binding efficiency for another binding mode, resulting in a zero net change to the overall affinity. On the other hand, the noncompetitive kinetic patterns may indicate binding to allosteric sites on the APHs and may suggest an alternate site to target on APHs. Structures of the aminoglycoside resistance enzymes in complex with these peptides will clear up these issues.

It has been shown that APH(3')-IIIa and APH(2")-Ia have different inhibitor sensitivities (Chapter 3) (Boehr *et al.*, 2001a; Daigle *et al.*, 1997), and it has already been noted that it may be difficult to design compounds that can potently inhibit both of these important resistance enzymes. There are also differences among the AACs. For example,

among the AAC(6')s, this subclass can be further divided into three major groups based on primary sequence homology (Shmara *et al.*, 2001). This division based on structure also has mechanistic collieries: AAC(6')-Ie, belonging to one group, uses an active site base in its chemical mechanism (Boehr *et al.*, 2003c), while the chemical mechanism for AAC(6')-Ii, belonging to another subgroup, is very different (Draker, K.-a. and Wright, G.D., unpublished observations). Furthermore, AAC(6')-Ie cannot acetylate peptides while AAC(6')-Ii can, and their inhibitor sensitivies are vastly different (Boehr *et al.*, 2003a). Thus, finding an inhibitor for all of the APHs or finding an inhibitor for all of the AACs is not likely, and finding an inhibitor that can affect all three classes of resistance enzyme to a significant biological level is not reasonable. In the absence of a general aminoglycoside resistance enzyme inhibitor, focus should be on inhibiting single, specific enzymes.

## 7.4 Bisubstrate Inhibitors of Aminoglycoside Kinases and Acetyltransferases

The APHs catalyze the direct transfer of the $\gamma$-phosphate of ATP to hydroxyls around the aminoglycoside structure, where catalysis likely operates through a dissociative-mechanism. A potent bisubstrate inhibitor of insulin receptor kinase has already been designed based on a dissociative-mechanism (Parang *et al.*, 2001) and this may be a possible approach for APH(3')-IIIa and APH(2")-Ia.

Bisubstrate inhibitors have previously been designed based on the tethering of neamine to adenosine through varying linker lengths (Liu *et al.*, 2000). Bisubstrate inhibitors have also been synthesized where H-9, a protein kinase inhibitor that binds competitively with respect to ATP, is attached to neamine moieties, however, the

inhibition patterns were inconsistent with simultaneous occupation of both the ATP and aminoglycoside binding pockets for APH(3')-IIIa (Thompson, 1999). In an alternative approach, spear-headed by Dr. Frank LaRonde, we can use 'click-chemistry' (Kolb *et al.*, 2001) to find the optimal distance between moieties binding to the ATP and aminoglycoside binding sites (Figure 7.1). This approach is not dependent on differentiating between associative or dissociative mechanisms of catalysis, and the results, themselves, may give insight into the nature of the transition-state by indicating the optimal chain length between the cofactor and aminoglycoside moieties.

Bisubstrate inhibitors have also been reported for an AAC (Williams and Northrop, 1979a). Other inhibitors can be designed by tethering appropriate cofactor and aminoglycoside mimics to create highly specific, potent inhibitors of aminoglycoside resistance enzymes.
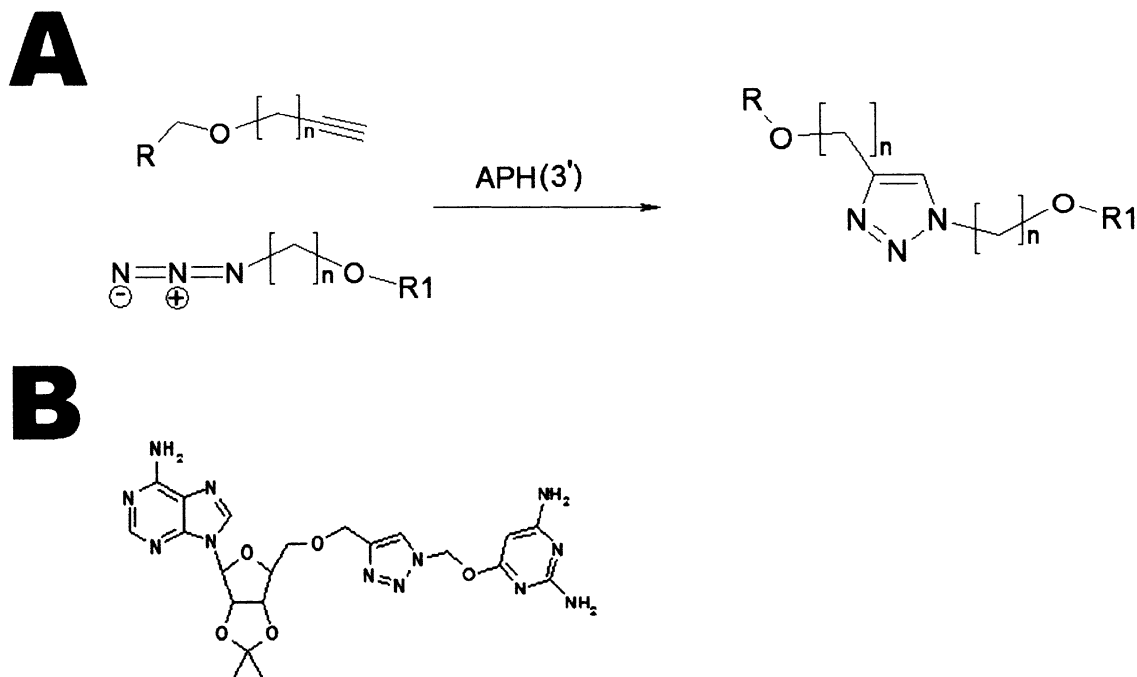
**Figure 7.1:** Dynamic Combinatorial Chemistry as a Method to Finding Bisubstrate Inhibitors of APHs. *A* The 1,3-dipolar cycloaddition reaction only occurs to a significant extent at room temperature when the two components are juxtaposed. The active site of APH(3')-IIIa can serve as the template to which the constituents bind, where product generated can then be measured through mass spectral techniques. *B* A proposed outcome of the experiment in *A*, where an adenosine analog and an aminoglycoside "mimic" are joined.

## 7.5 Optimizing Inhibitors for the ATP-binding pocket of APH(3')-IIIa

High throughput screening may be able to find lead compounds that can be further developed into potent inhibitors, or that can serve as cofactor or aminoglycoside analogs. A more rational approach can also be followed in the design of ATP mimics. The best inhibitors of protein kinases are directed towards the ATP-binding pocket, including clinically approved compounds (Bishop *et al.*, 2001; Habeck, 2002; Toledo *et al.*, 1999), and similarly, taking advantage of the interactions in the ATP-binding pockets

of APHs should provide the affinity required to elicit the desired biological effect. The ATP mimic can subsequently be linked to an aminoglycoside mimic to increase the specificity, as mentioned above.

In this endeavor, it appears that ATP binding is electrostatically based (Figure 7.2) (Boehr *et al.*, 2002). Isothermal titration calorimetry can be used not only to determine the affinity of an interaction but also to elucidate what types of forces are governing the interaction (Ladbury and Chowdhry, 1996). In this way, we can understand what interactions are most important and consequently, act to increase these interactions through the design of novel compounds (Holdgate, 2001). This may also be important in designing compounds that will specifically inhibit APHs and yet have no substantial effect against host ePKs. Adenine analogues and ITC have been used to begin to illuminate these important interactions, including the revealing of new interactions that can be utilized in the design of novel inhibitors of APH(3')-IIIa (Figure 7.2).

**C**

| Compound | $K_d$ ($\mu M$) | $\Delta G$ (kcal/mol) | $\Delta H$ (kcal/mol) | $-T\Delta S$ (kcal/mol) |
|---|---|---|---|---|
| adenosine | 11.0 ± 0.1 | -6.88 ± 0.01 | -17.46 = 0.07 | -10.58 = 0.08 |
| 8-bromoadenosine | 2.43 ± 0.11 | -7.78 ± 0.02 | -11.81 ± 0.02 | +4.03 ± 0.05 |
| 2-chloroadenosine | 4.72 ± 0.09 | -7.38 ± 0.01 | -11.80 ± 0.30 | +4.42 ± 0.35 |
| 7-deazaadenosine | 38.2 ± 1.9 | -6.13 ± 0.03 | 13.58 = 0.26 | -7.45 = 0.13 |
| 3-deazaadenosine | 56.3 ± 0.2 | -5.89 ± 0.01 | -15.58 ± 0.02 | +9.69 ± 0.03 |
| 1-deazaadenosine | ---- | ---- | ---- | ---- |
| purine riboside | 727 | -4.35 ± 0.94 | -8.08 ± 1.75 | +3.73 ± 0.81 |
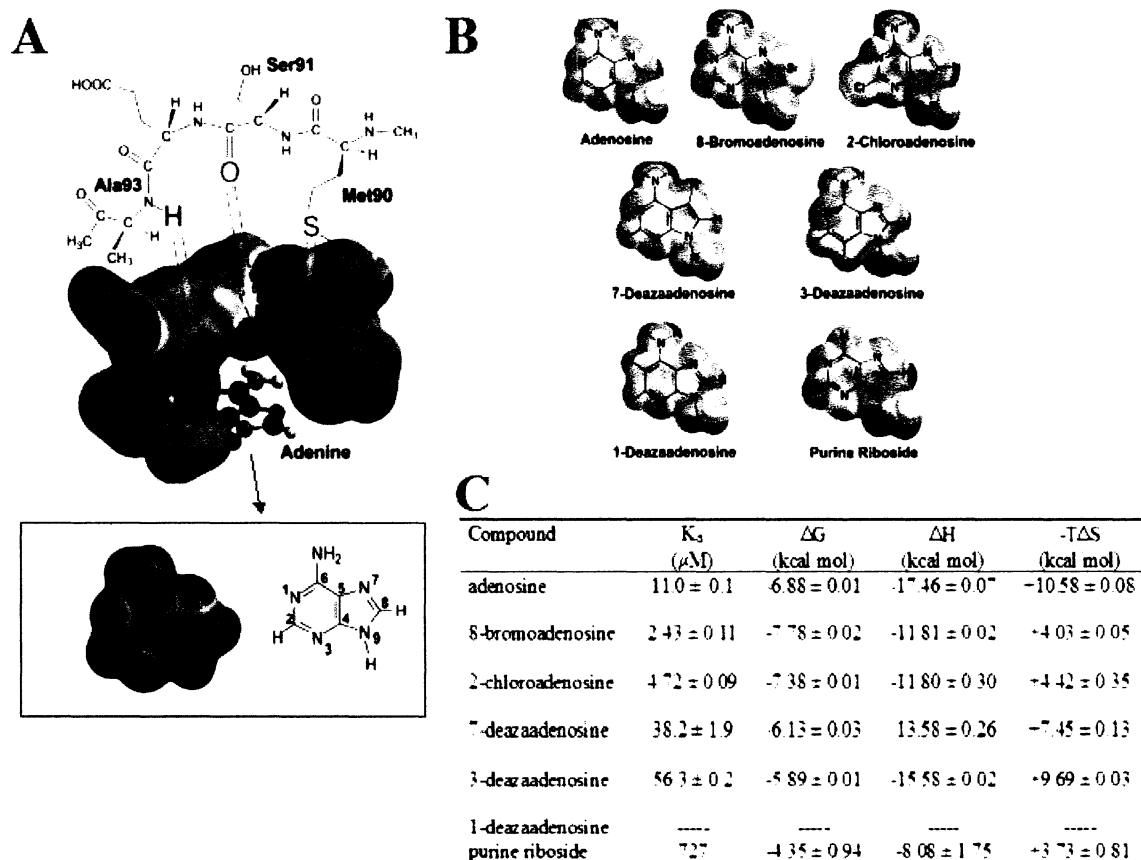
**Figure 7.2:** Electrostatic Considerations in the Binding of Adenosine Derivatives to APH(3')-IIIa. *A* Electrostatic complementarity between the nucleotide binding pocket of APH(3')-IIIa and adenine, highlighting important H-bonds between protein and ligand. The violet ball is attached to N9 of adenine. *B* Electrostatic maps of adenosine derivatives. *C* Isothermal titration data describing the binding of the adenosine derivatives to APH(3')-IIIa obtained at 303 K, using similar conditions as described in Chapter 2. Disruption of contacts highlighted in *A* compromises ligand binding (i.e. 7-deazaadenosine, 3-deazaadenosine, 1-deazaadenosine and purine riboside show lowered binding affinity). Novel interactions may be available by derivatisizing positions 8 and 2, considering that 8-bromoadenosine and 2-chloroadenosine show enhanced binding. A complete thermodynamic profile provides a more in-depth structure-activity relationship.

## 7.6 Reversible and Irreversible Inhibitors of Aminoglycoside Resistance Enzymes

Other than the inhibitors described in this thesis, there are number of inhibitors already described for the aminoglycoside modifying enzymes (Figure 7.3), including both

reversible and irreversible modulators (Boehr *et al.*, 2003a; Boehr *et al.*, 2003c; Boehr *et al.*, 2001a; Daigle *et al.*, 1997; Liu *et al.*, 2000; McKay *et al.*, 1994; Roestamadji *et al.*, 1995; Roestamadji and Mobashery, 1998; Sucheck *et al.*, 2000; Williams and Northrop, 1979b). For aminoglycoside resistance enzymes, irreversible inhibitors may be the best approach with a complete shut down of the resistance mechanism such that the antibiotics can act freely without any interference from the resistance enzymes. The challenge here is to design molecules that are chemically unreactive yet provide irreversible inhibition to specific aminoglycoside resistance enzymes.
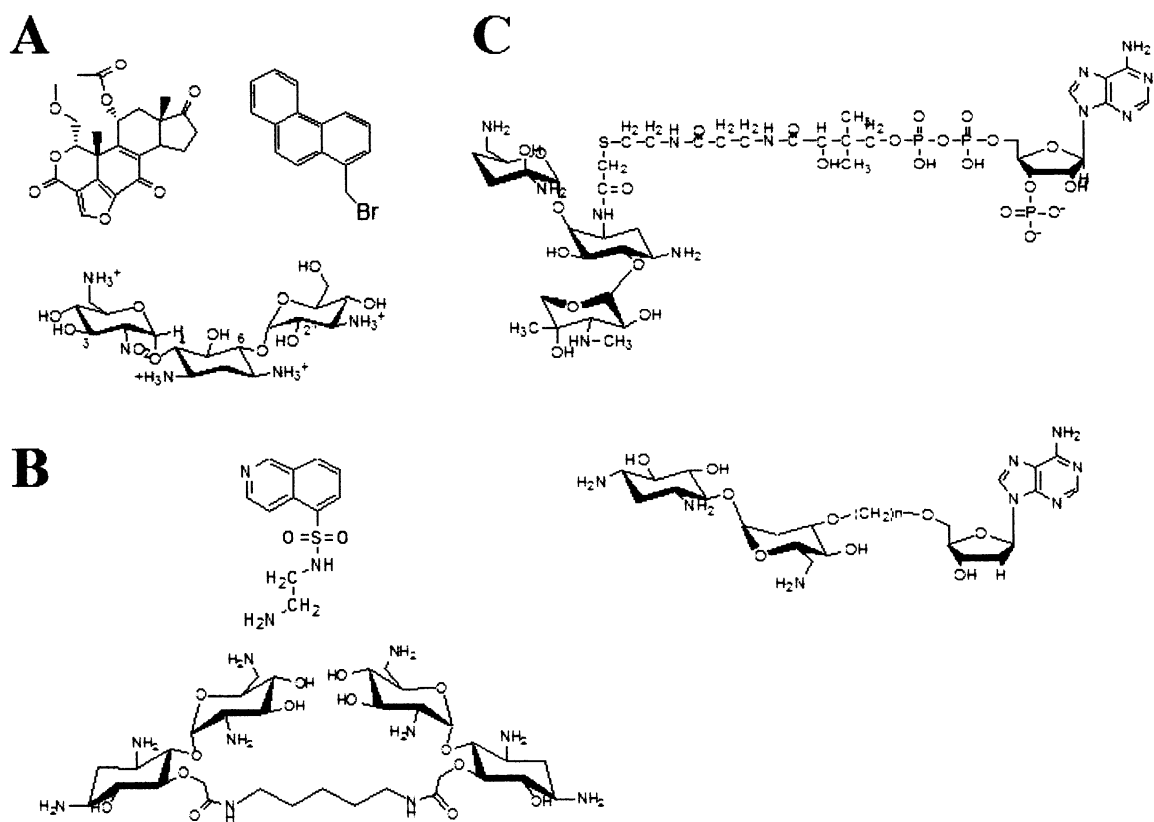


**Figure 7.3:** Selected Inhibitors of Aminoglycoside Phosphotransferases and Acetyltransferases, including *A* irreversible, *B* ATP/aminoglycoside mimics and *C* bisubstrate inhibitors.

In the β-lactam field, the clinically used inhibitors are covalent modifiers of β-lactamases (Livermore, 1995). A number of residues in aminoglycoside resistance enzymes have proven susceptible to covalent modification, both in the cofactor and aminoglycoside binding sites (Boehr *et al.*, 2003c; Boehr *et al.*, 2001a; McKay *et al.*, 1994; Roestamadji *et al.*, 1995; Roestamadji and Mobashery, 1998). The absolutely conserved Lys (Lys44 in APH(3')-IIIa) is a prime candidate for the APHs, although it was shown that different APHs have different inactivator sensitivities. Asp99 in AAC(6')-APH(2") also appears to be a choice target residue.

For reversible inhibitors, there are also important interactions that would act to increase potency and/or selectivity. To increase specificity for the APH(3') enzymes, Tyr42 (or its Phe equivalent) is an important residue, where the best inhibitors would likely have electrostatic complementarily to the ATP binding pocket (Figure 7.2) (Boehr *et al.*, 2002). The backbone amide of Met26 is also an important interaction, as it appears that this interaction is important in transition state stabilization (Thompson *et al.*, 2002). By targeting this interaction, the complex would most resemble the predicted transition state, thus harnessing the vast amount of binding energy available.

As mentioned in Chapter 5, there is also an opportunity for targeting the domain interface in AAC(6')-APH(2"), such that a single compound can inhibit both activities of this critical enzyme. Upon mutation of Lys190, in the region adjoining the two domains, both AAC and APH activities are diminished (Chapter 5). This residue is also susceptible to covalent modification by wortmannin, at least when the APH domain is expressed as a separate protein (i.e. APH[175-479]) (Boehr *et al.*, 2001a). However, wortmannin has no

effect on the activity of the AAC domain of the full-length protein, and it is not known if wortmannin can modify Lys190 when the entire protein is intact. The association binding energy between the AAC and APH domains is also not known, which is a critical consideration when designing an approach to disturb protein-protein interactions.

## 7.7 New Approaches and Novel Antibiotics

In the absence of broad-spectrum inhibitors of aminoglycoside modifying enzymes, selective, potent, specific inhibitors are the best option. However, with the large diversity of resistance enzymes available, the application of specific inhibitors may only result in the selection of alternative resistance enzymes that are insensitive to the employed inhibitors. Another approach that has shown success is the design of new antibiotics that are not modified by resistance enzymes. This approach was used in the design of semisynthetic aminoglycosides such as netilmicin that resist modification by certain aminoglycoside resistance enzymes (Kabins *et al.*, 1976; Miller *et al.*, 1976).

The crystal structure of the prokaryotic ribosome bound with known antibiotics provides opportunities for structure-based drug design that can be applied to discover novel antibiotics that resist modification of the known resistance enzymes (Brodersen *et al.*, 2000; Bower *et al.*, 2003; Carter *et al.*, 2000; Schlunzen *et al.*, 2001). This is especially beneficial for aminoglycosides as their use has been limited, owing to problems with their bioavailability and toxicity (Boehr *et al.*, 2003b). Mobashery has recently applied this approach to discover neamine derivatives that remain potent antibiotics *in vitro* but resist modification by APH(3')-Ia and AAC(6')-APH(2") (Haddad *et al.*, 2002; Russell *et al.*, 2003). Mobashery's approach relied on virtual screening,

whereas a different study has used NMR to detect low affinity binders (Yu *et al.*, 2003). There is also the option of using more traditional high-throughput screening using a model oligonucleotide of the 16S rRNA that is fluorescently labeled (Haddad *et al.*, 2002; Llano-Sotelo *et al.*, 2002). These techniques may yield compounds that are not only better antibiotics that resist enzyme-catalyzed modification, but they may also have better pharmacology that would increase their clinical value.

## 7.8 Future Use of Antibiotics

Regardless of whether inhibitors against aminoglycoside resistance enzymes and/or entirely new antibiotics are applied to the resistance problem, a more rigorous and careful approach must be undertaken regarding antibiotics. Antibiotics are used throughout our ecosystem, not only in medicine, but also in agriculture, animal husbandry, even to more exotic practices, such as in apiculture and fish farms (Levy, 1992). The presence of all of these antibiotics in the environment necessarily selects for resistance determinants. These determinants have likely always existed, and the saturation of the environment with antibiotics has only worked to select for a greater abundance of these mechanisms.

It is becoming accepted that antibiotic use outside of medicine has significant impacts on medical applications (Levy, 1992; Shnayerson and Plotkin, 2002). It is recognized by many that the use of antibiotic growth promoters, or the subtherapeutic chronic use of antibiotics, has a severe negative consequence in selecting for resistance mechanisms and may help to complicate treatment of bacterial infections in humans (Shnayerson and Plotkin, 2002). It is encouraging that many countries have already

banned the use of antibiotics that are used in human therapy as growth promoters (Shnayerson and Plotkin, 2002).

Physicians, patients and consumers also have critical roles to play. Antibiotics should only be prescribed and asked for when there is appropriate need. Although antibiotic use is highly regulated in developed countries, less rigorous approaches are applied in the developing world, where antibiotics may be available to the general public without doctor approval (Levy, 1992). Inappropriate use, including amounts that are too high or too low, or dosage times that are too short or too long, leads to the further development of resistance (Levy, 1992). Bacteria do not respect international borders, and one country's antibiotic resistance problems can eventually be every country's antibiotic resistance problem. To curtail resistance, guidelines need to be in place and followed by all countries, including both developed and developing nations.

Alternatives to antibiotics, such as newer vaccines, may help to alleviate the problems associated with antibiotic resistance, but they are unlikely to be a complete solution in the near future (Shnayerson and Plotkin, 2002). Newer antibiotics or inhibitors of resistance mechanisms will also not solve the problem in the long term. New resistance mechanisms, or mechanisms not susceptible to inhibition, may evolve in the absence of more judicious measures. The rate at which resistance arises is increasing, where an antibiotic introduced to the clinic may select for a resistance mechanism in two or three years (Levy, 1992). A combination of more managed use of antibiotics, less dependence on antibiotics, and a greater containment of resistant bacteria is as important as the introduction of new antibiotics or inhibitors of resistance mechanisms.

Antibiotics may be the single most important discovery of human medicine and it

is critical to protect these invaluable resources. Changes are needed at all levels, from

practitioner to consumer, to ensure we keep these products safe and effective. These

changes must occur alongside continued development of newer antimicrobials and

methods to overcome and/or control resistance. We have used antibiotics very

successfully over the past fifty years to increase life expectancy and the quality of life,

and it will require every effort, from basic to clinical science, to continue the successful

use of these life-preserving compounds.


## 7.9 References

**Adams, J.A. 2001.** Kinetic and catalytic mechanisms of protein kinases. *Chem Rev.* 101:
2271-2290.

**Azucena, E. and Mobashery, S. 2001.** Aminoglycoside-modifying enzymes:
mechanisms of catalytic processes and inhibition. *Drug Resist Updat.* 4: 106-117.

**Bishop, A.C., Buzko, O. and Shokat, K.M. 2001.** Magic bullets for protein kinases.
*Trends Cell Biol.* 11: 167-172.

**Boehr, D.D., Draker, K., Koteva, K., Bains, M., Hancock, R.E. and Wright, G.D.
2003a.** Broad-spectrum Peptide inhibitors of aminoglycoside antibiotic resistance
enzymes. *Chem Biol.* 10: 189-196.

**Boehr, D.D., Draker, K.-a. and Wright, G.D. 2003b.** Aminoglycosides and
aminocyclitols. In Finch, R.G., Greenwood, D., Norrby, S.R. and Whitley, R.J. (eds.),
*Antibiotic and Chemotherapy: Anti-infective agents and their use in therapy.* Churchill
Livingstone, Edinburgh, pp. 155-184.

**Boehr, D.D., Farley, A.R., Wright, G.D. and Cox, J.R. 2002.** Analysis of the pi-pi
stacking interactions between the aminoglycoside antibiotic kinase APH(3')-IIIa and its
nucleotide ligands. *Chem Biol.* 9: 1209-1217.

**Boehr, D.D., Jenkins, S.I. and Wright, G.D. 2003c.** The molecular basis of the
expansive substrate specificity of the antibiotic resistance enzyme aminoglycoside

acetyltransferase-6'- aminoglycoside phosphotransferase-2". The role of Asp-99 as an active site base important for acetyl transfer. *J Biol Chem*. 278: 12873-12880.

**Boehr, D.D., Lane, W.S. and Wright, G.D. 2001a.** Active site labeling of the gentamicin resistance enzyme AAC(6')- APH(2") by the lipid kinase inhibitor wortmannin. *Chem Biol*. 8: 791-800.

**Boehr, D.D., Thompson, P.R. and Wright, G.D. 2001b.** Molecular mechanism of aminoglycoside antibiotic kinase APH(3')-IIIa: roles of conserved active site residues. *J Biol Chem*. 276: 23929-23936.

**Bower, J., Drysdale, M., Hebdon, R., Jordan, A., Lentzen, G., Matassova, N., Murchie, A., Powles, J. and Roughley, S. 2003.** Structure-based design of agents targeting the bacterial ribosome. *Bioorg Med Chem Lett*. 13: 2455-2458.

**Brodersen, D.E., Clemons, W.M., Jr., Carter, A.P., Morgan-Warren, R.J., Wimberly, B.T. and Ramakrishnan, V. 2000.** The structural basis for the action of the antibiotics tetracycline, pactamycin, and hygromycin B on the 30S ribosomal subunit. *Cell*. 103: 1143-1154.

**Carter, A.P., Clemons, W.M., Brodersen, D.E., Morgan-Warren, R.J., Wimberly, B.T. and Ramakrishnan, V. 2000.** Functional insights from the structure of the 30S ribosomal subunit and its interactions with antibiotics. *Nature*. 407: 340-348.

**Daigle, D.M., McKay, G.A. and Wright, G.D. 1997.** Inhibition of aminoglycoside antibiotic resistance enzymes by protein kinase inhibitors. *J Biol Chem*. 272: 24755-24758.

**Dyda, F., Klein, D.C. and Hickman, A.B. 2000.** GCN5-related N-acetyltransferases: a structural overview. *Annu Rev Biophys Biomol Struct*. 29: 81-103.

**Habeck, M. 2002.** FDA licences imatinib mesylate for CML. *Lancet Oncol*. 3: 6.

**Haddad, J., Kotra, L.P., Llano-Sotelo, B., Kim, C., Azucena, E.F., Jr., Liu, M., Vakulenko, S.B., Chow, C.S. and Mobashery, S. 2002.** Design of novel antibiotics that bind to the ribosomal acyltransfer site. *J Am Chem Soc*. 124: 3229-3237.

**Hengge, A.C., Sowa, G.A., Wu, L. and Zhang, Z.Y. 1995.** Nature of the transition state of the protein-tyrosine phosphatase- catalyzed reaction. *Biochemistry*. 34: 13982-13987.

**Herschlag, D. and Jencks, M.P. 1989a.** Phosphoryl transfer to anionic oxygen nucleophiles. Nature of the transition state and electrostatic repulsions. *J. Am. Chem. Soc*. 111: 7587-7596.

**Herschlag, D. and Jencks, W.P. 1989b.** Evidence that metaphosphate monoanion is not an intermediate in solvolysis reactions in aqueous solution. *J. Am. Chem. Soc.* 111: 7679-7586.

**Holdgate, G.A. 2001.** Making cool drugs hot: isothermal titration calorimetry as a tool to study binding energetics. *Biotechniques.* 31: 164-166.

**Hon, W.C., McKay, G.A., Thompson, P.R., Sweet, R.M., Yang, D.S., Wright, G.D. and Berghuis, A.M. 1997.** Structure of an enzyme required for aminoglycoside antibiotic resistance reveals homology to eukaryotic protein kinases. *Cell.* 89: 887-895.

**Kabins, S.A., Nathan, C. and Cohen, S. 1976.** In vitro comparison of netilmicin, a semisynthetic derivative of sisomicin, and four other aminoglycoside antibiotics. *Antimicrob Agents Chemother.* 10: 139-145.

**Kim, K. and Cole, P.A. 1997.** Measurement of a Bronsted nucleophilic coefficient and insights into the transition state for a protein tyrosine kinase. *J. Am. Chem. Soc.* 119: 11096-11097.

**Kim, K. and Cole, P.A. 1998.** Kinetic analysis of a protein tyrosine reaction transition state in the forward and reverse directions. *J. Am. Chem. Soc.* 120: 6851-6858.

**Kirby, A.J. and Varvoglis, A.G. 1967.** The reactivity of phosphate esters. Monoester hydrolysis. *J. Am. Chem. Soc.* 89: 415-423.

**Knowles, J.R. 1980.** Enzyme-catalyzed phosphoryl transfer reactions. *Annu Rev Biochem.* 49: 877-919.

**Kolb, H.C., Finn, M.G. and Sharpless, K.B. 2001.** Click chemistry: Diverse chemical function from a few good reactions. *Angew Chem Int Ed Engl.* 40: 2004-2021.

**Ladbury, J.E. and Chowdhry, B.Z. 1996.** Sensing the heat: the application of isothermal titration calorimetry to thermodynamic studies of biomolecular interactions. *Chem Biol.* 3: 791-801.

**Langer, M.R., Tanner, K.G. and Denu, J.M. 2001.** Mutational analysis of conserved residues in the GCN5 family of histone acetyltransferases. *J Biol Chem.* 276: 31321-31331.

**Levy, S.B. 1992.** The Antibiotic Paradox: How miracle drugs are destroying the miracle. Plenum Press, New York.

211

Liu, M., Haddad, J., Azucena, E., Kotra, L.P., Kirzhner, M. and Mobashery, S. 2000. Tethered bisubstrate derivatives as probes for mechanism and as inhibitors of aminoglycoside 3'-phosphotransferases. *J Org Chem*. 65: 7422-7431.

Livermore, D.M. 1995. beta-Lactamases in laboratory and clinical resistance. *Clin Microbiol Rev*. 8: 557-584.

Llano-Sotelo, B., Azucena, E.F., Kotra, L.P., Mobashery, S. and Chow, C.S. 2002. Aminoglycosides modified by resistance enzymes display diminished binding to the bacterial ribosomal aminoacyl-tRNA site. *Chem Biol*. 9: 455-463.

Matsuzaki, K., Yoneyama, S. and Miyajima, K. 1997. Pore formation and translocation of melittin. *Biophys J*. 73: 831-838.

McKay, G.A., Robinson, R.A., Lane, W.S. and Wright, G.D. 1994. Active-site labeling of an aminoglycoside antibiotic phosphotransferase (APH(3')-IIIa). *Biochemistry*. 33: 14115-14120.

Miller, G.H., Arcieri, G., Weinstein, M.J. and Waitz, J.A. 1976. Biological activity of netilmicin, a broad-spectrum semisynthetic aminoglycoside antibiotic. *Antimicrob Agents Chemother*. 10: 827-836.

Miller, G.H., Sabatelli, F.J., Hare, R.S., Glupczynski, Y., Mackey, P., Shlaes, D., Shimizu, K. and Shaw, K.J. 1997. The most frequent aminoglycoside resistance mechanisms--changes with time and geographic area: a reflection of aminoglycoside usage patterns? Aminoglycoside Resistance Study Groups. *Clin Infect Dis*. 24 Suppl 1: S46-62.

Parang, K., Till, J.H., Ablooglu, A.J., Kohanski, R.A., Hubbard, S.R. and Cole, P.A. 2001. Mechanism-based design of a protein kinase inhibitor. *Nat Struct Biol*. 8: 37-41.

Roestamadji, J., Grapsas, I. and Mobashery, S. 1995. Mechanism-based inactivation of bacterial aminoglycoside 3'-phosphotransferases. *J Am Chem Soc*. 117: 80-84.

Roestamadji, J. and Mobashery, S. 1998. The use of neamine as a molecular template: inactivation of bacterial antibiotic resistance enzyme aminoglycoside 3'-phosphotransferase type IIa. *Bioorg Med Chem Lett*. 8: 3483-3486.

Russell, R.J., Murray, J.B., Lentzen, G., Haddad, J. and Mobashery, S. 2003. The complex of a designer antibiotic with a model aminoacyl site of the 30S ribosomal subunit revealed by X-ray crystallography. *J Am Chem Soc*. 125: 3410-3411.

Scheibner, K.A., De Angelis, J., Burley, S.K. and Cole, P.A. 2002. Investigation of the roles of catalytic residues in serotonin N-acetyltransferase. *J Biol Chem.* 277: 18118-18126.

Schlunzen, F., Zarivach, R., Harms, J., Bashan, A., Tocilj, A., Albrecht, R., Yonath, A. and Franceschi, F. 2001. Structural basis for the interaction of antibiotics with the peptidyl transferase centre in eubacteria. *Nature.* 413: 814-821.

Shmara, A., Weinsetel, N., Dery, K.J., Chavideh, R. and Tolmasky, M.E. 2001. Systematic analysis of a conserved region of the aminoglycoside 6'-N-acetyltransferase type Ib. *Antimicrob Agents Chemother.* 45: 3287-3292.

Shnayerson, M. and Plotkin, M.J. 2002. The Killers Within: The deadly rise of drug-resistant bacteria. Little, Brown & Company, New York.

Sucheck, S.J., Wong, A.W., Koeller, K.M., Boehr, D.D., Draker, K.-a., Sears, P., Wright, G.D. and Wong, C.-H. 2000. Design of bifunctional antibiotics that target bacterial rRNA and inhibit resistance-causing enzymes. *J Am Chem Soc.* 122: 5230-5231.

Tanner, K.G., Trievel, R.C., Kuo, M.H., Howard, R.M., Berger, S.L., Allis, C.D., Marmorstein, R. and Denu, J.M. 1999. Catalytic mechanism and function of invariant glutamic acid 173 from the histone acetyltransferase GCN5 transcriptional coactivator. *J Biol Chem.* 274: 18157-18160.

Thompson, P.R. 1999. Characterization of the catalytic mechanisms of two aminoglycoside phosphotransferases: APH(3')-IIIa from *Enterococcus faecalis* and APH(9)-Ia from Legionella *pneumophila.* Biochemistry. McMaster University, Hamilton, Ontario, pp. 1-305.

Thompson, P.R., Boehr, D.D., Berghuis, A.M. and Wright, G.D. 2002. Mechanism of aminoglycoside antibiotic kinase APH(3')-IIIa: role of the nucleotide positioning loop. *Biochemistry.* 41: 7001-7007.

Toledo, L.M., Lydon, N.B. and Elbaum, D. 1999. The structure-based design of ATP-site directed protein kinase inhibitors. *Curr Med Chem.* 6: 775-805.

Williams, J.W. and Northrop, D.B. 1979a. Synthesis of a tight-binding, multisubstrate analog inhibitor of gentamicin acetyltransferase I. *J Antibiot (Tokyo).* 32: 1147-1154.

Wright, G.D. 1999. Aminoglycoside-modifying enzymes. *Curr Opin Microbiol.* 2: 499-503.

**Wu, M., Maier, E., Benz, R. and Hancock, R.E. 1999.** Mechanism of interaction of different classes of cationic antimicrobial peptides with planar bilayers and with the cytoplasmic membrane of *Escherichia coli. Biochemistry.* 38: 7235-7242.

**Yu, L., Oost, T.K., Schkeryantz, J.M., Yang, J., Janowick, D. and Fesik, S.W. 2003.** Discovery of aminoglycoside mimetics by NMR-based screening of *Escherichia coli* A-site RNA. *J Am Chem Soc.* 125: 4444-4450.